The Tip60 chromatin remodeling complex is required for maintenance and polarity of *Drosophila* neural stem cells

Dissertation

for the award of the degree

"Doctor rerum naturalium" (Dr. rer. nat.)

Division of Mathematics and Natural Sciences

of the Georg-August-University Göttingen

submitted by

Katja Rust

from Hanover

Göttingen, 2016

Members of the Thesis Committee

Prof. Dr. Andreas Wodarz	Institute I of Anatomy
(Referee and Thesis Supervisor)	Department of Molecular Cell Biology
	University of Cologne
Prof. Dr. Tomas Pieler	University Medical Center
(Co-Referee)	Department of Developmental Biochemistry
	Georg-August-University, Göttingen
PD Dr. Halyna Shcherbata	Max Planck Institute for Biophysical Chemistry
	Gene Expression and Signaling
	Göttingen

Further Members of the Examination Board

Prof. Dr. Matthias Dobbelstein	University Medical Center
	Institute for Molecular Oncology
	Georg-August-University, Göttingen
Dr. Roland Dosch	University Medical Center
	Deparment of Developmental Biochemistry
	Georg-August-University, Göttingen
Prof. Dr. Ernst Wimmer	Johann-Friedrich-Blumenbach-Institute of Zoology and Anthropology
	Department of Developmental Biology
	Georg-August-University, Göttingen

Date of the oral examination: 18th November 2016

Affidavit

I hereby declare that I prepared the thesis “The Tip60 chromatin remodeling complex is required for maintenance and polarity of *Drosophila* neural stem cells” on my own and with no other sources and aids than quoted.

Katja Rust

Göttingen, September 30th, 2016

Table of contents

Abstract

Stem cells are self-renewing cells which produce differentiating offspring during development and tissue homeostasis. Appropriate regulation of stem cell division is highly important to ensure maintenance of the stem cell and prevent overproliferation and tumor formation. A widely used model in stem cell research is the *Drosophila* neural stem cell, which divides asymmetrically. Hereby, the underlying polarity network is highly conserved.

In this study I investigate the role of Domino, the *Drosophila* homolog of mammalian p400, in *Drosophila* larval neural stem cells. Domino is the ATPase subunit of the Tip60 chromatin remodeling complex, which is conserved in eucaryotes. Like its homolog p400 and several members of the Tip60 complex, Domino has been implicated in the maintenance of stem cells in *Drosophila* and mammals. Several transcription factors have been described to interact with the Tip60 complex in mammalian stem cells, including the cell cycle regulator Myc. However, the exact mechanism of Tip60 complex function in stem cells and how the interaction with the various transcription factors regulates stem cell behaviour has not been fully unraveled.

Knockdown studies of *domino* and other Tip60 members revealed that the Tip60 complex in a specific subunit composition is required to maintain *Drosophila* neural stem cells. Systematic analyses of potential Tip60 complex cofactors moreover reveal a role for Myc in *Drosophila* neural stem cell self-renewal. Subsequent investigations show that the Myc/Tip60 network ensures appropriate asymmetric neural stem cell division and prevents Prospero dependent premature differentiation.

Using next generation sequencing I found that Domino regulates the expression of genes which regulate neuroblast fate. Further analyses reveal a role of the Tip60 complex in histone modification in *Drosophila* neural stem cells. Taken together, this suggests that as in mammals Myc recruits the Tip60 complex to target promoters for the regulation of gene expression. Remarkably, the proto-oncogene p53 and the p21 homolog Dacapo, a p53-responsive gene and cell cycle regulator, were found to be regulated by Domino. This

points to the p53-pathway as a potential novel target of the Myc/Tip60 network in stem cells.

The function of Myc and the Tip60 complex in *Drosophila* neural stem cells is remarkably similar to the role of the Myc/Tip60 pathway in mammalian pluripotent stem cells. Thus, the gene regulatory network for stem cell self-renewal in *Drosophila* is highly conserved. Therefore, this study contributes to the general understanding of how Myc and the Tip60 complex maintain the stem cell state.

1. Introduction

Drosophila neuroblasts (NBs) are a population of self-renewing cells, which asymmetrically divide to produce differentiated offspring cells to establish the nervous system. Many key players of polarity and proliferation are conserved in *Drosophila* and mammals (Wodarz and Näthke, 2007). Additionally, the vast availibility and feasibility of genetic manipulation in *Drosophila* has led to the establishment of the NB as a powerful tool to study asymmetric cell division and stem cell behavior (del Valle Rodríguez et al., 2012).

1.1. Drosophila neurogenesis

Neurogenesis in mammals and *Drosophila* is linked to gastrulation when the three germ layers are formed. In both cases neural stem cells (NSCs) are descendants of epithelial cells. While in mammals a contiguous region of the epithelium is determined to become the neural plate and then forms the neural tube, in *Drosophila* single epithelial cells acquire NSC fate. Importantly, in both a correct specification of the epithelium is indispensable for appropriate neurogenesis (Hartenstein and Wodarz, 2013).

1.1.1. The embryonic epithelium: Parent tissue of the *Drosophila* neuroblast

In *Drosophila* the embryonic epithelium is established during cellularization. The first 13 nuclear divisions are syncytial and in the end of these the nuclei have arranged at the plasma membrane (Mazumdar and Mazumdar, 2002). The migration to the plasma membrane coincides with nuclear shape changes. In earlier stages when zygotic transcription is shut off, nuclei are round and small with uniform chromatin. Upon relocation to the plasma membrane nuclei elongate and the microtubule network induces grove formation, which changes the chromatin dynamics and is believed to contribute to the formation of a chromatin state that allows zygotic gene expression (Brandt et al., 2006; Hampoelz et al., 2011) .

The plasma membrane at this stage already shows polarization, forming an apical- and a basolateral-like domain over each nucleus (Lye and Sanson, 2011). The plasma membrane invaginates in a process comparable to cytokinesis. A furrow canal forms at which the

actomyosin network interacts with septins and anillins, guiding the membrane stalks. In the end of cellularization the actomyosin ring contracts, sealing the single cells. During membrane invagination the first type of junctions, so called basal adherens junctions (AJs), form apical to the furrow canal (Tepass et al., 2001). AJs form cell-cell contacts and consist of complexes of cadherin, in *Drosophila* E-cadherin is encoded by the gene *shotgun (shg),* and α- and β-catenin, the latter of which is called Armadillo in *Drosophila* (Harris, 2012). The basal AJs disappear, which is required for the formation of AJs at the apical membrane part in a spot-like pattern (spot AJs). These are formed by the accumulation of cadherin and catenins into a complex and the subsequent recruitment into spot AJs by the Par-3 homolog Bazooka (Baz) (Grawe et al., 1996; McGill et al., 2009; Müller and Wieschaus, 1996). Formation of spot AJs thus requires a distinct localization of the scaffold protein Baz for correct positioning. At this point of epithelium formation, cells are polarized with an apical membrane domain above the spot AJs facing the embryo outside and a basolateral domain. However, a mature *zonula adherens* (ZA) and the basement membrane are not present. Also, the epithelium does not yet secrete cuticle (Lye and Sanson, 2011). The further establishment of polarity and refinement of AJs is tightly regulated by a complex protein network out of which many key players are highly conserved across the animal kingdom. Spot AJs require a subapically localized protein complex of Crumbs (Crb), a transmembrane protein, and Stardust (Std), a guanylate-kinase and intracellular binding partner of Crb, to form a belt-like structure, the ZA (Grawe et al., 1996; Müller and Wieschaus, 1996; Tepass, 1996). Intracellularly, the ZA is linked to the actin cytoskeleton, which is therefore organized by cell-cell contacts (Tepass et al., 2001).

The membrane region apical to the ZA is called subapical region and harbors many important polarity regulators including the Crb-Std complex. Another protein complex found at the subapical region is the highly conserved Par-complex consisting of Baz, the atypical protein kinase (aPKC), a serine-threonine kinase and the aPKC-regulatory protein Par-6 (Tepass, 2012). Baz initially recruits aPKC and Par-6 to the subapical region, is then phosphorylated by aPKC and localizes to the AJ region where it interacts with AJ proteins (Harris and Peifer, 2004; Harris and Peifer, 2005; Morais-de-Sá et al., 2010). Phosphorylation of Baz by aPKC also weakens the interaction between Baz and Std

thereby allowing the formation of the Crb-Std complex (Krahn et al., 2010; Walther and Pichaud, 2010).

aPKC targets include not only apically localized proteins like Baz, but also Lgl (Lethal (2) giant larvae) and Par-1. Lgl and Par-1 phosphorylation by aPKC restricts them to the basolateral side (Betschinger et al., 2003; Hurov et al., 2004). Par-1 in turn is a kinase that phosphorylates Baz and prevents localization of Baz to the basolateral membrane and the assembly of basolateral Par complexes (Benton and St Johnston, 2003; Krahn et al., 2009). Lgl localizes with a group of basolateral tumor suppressor proteins, Discs large (Dlg) and Scribble (Scrib). This group is required for the establishment of septate junctions at the lateral domain. These junctions function similar to mammalian tight junctions (Su et al., 2013) (Figure 1).

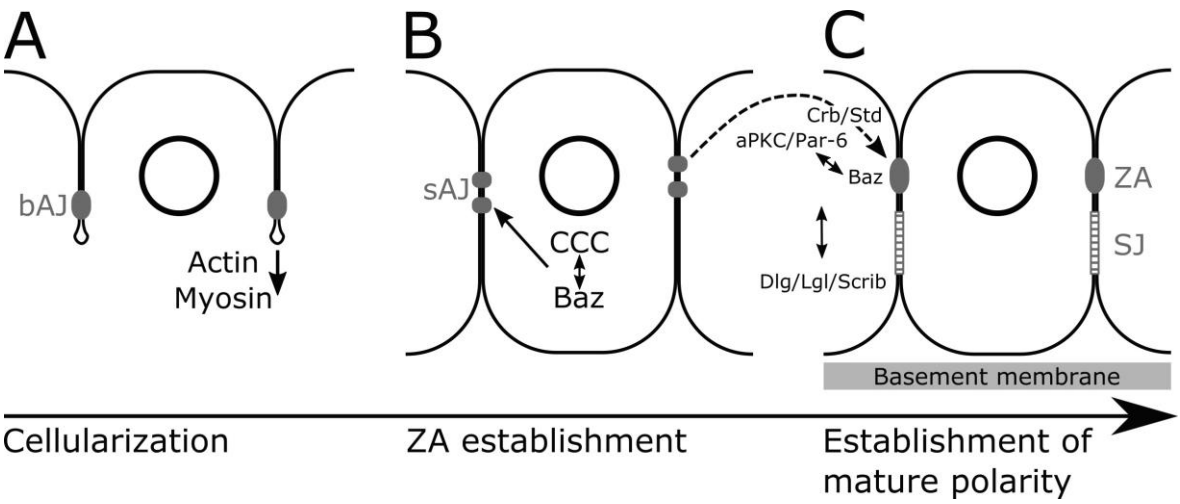

Figure 1: Establishment of epithelial polarity

A simplified view of embryonic epithelium formation. (A): During cellularization the membrane forms furrow canals and invaginates driven by the actomyosin network. Basal adherens junctions (bAJ) form apical to the furrow canal. (B): bAJs disappear after cellularization is completed. Cadherin-Catenin complexes (CCC) form which are recruited into spot adherens junctions (sAJ) by Baz. (C): sAJs are refined into a mature *zonula adherens* (ZA) belt by the Crb/Std complex, which is localized at the subapical region. Baz interacts with aPKC and Par-6 in the Par complex and recruits its interactors to the subapical region. Later Baz localizes to the ZA region. Apical complexes interact with each other and the basolateral Dlg/Lgl/Scrib group to establish polarity. The Dlg/Lgl/Scrib group is also required to form septate junctions (SJ). Finally, the epithelium secretes the basement membrane and cuticle (not shown).

Proteins of the polarity network do not only interact with each other and junctional proteins, but are also linked to cytoskeletal proteins and are required for various processes including cell proliferation, growth and cell death (Wodarz and Näthke, 2007). Importantly, the interactions of the polarity network need to be stable for example for the establishment of cell-cell contacts, but must nevertheless be very dynamic to allow for cell shape changes, for example during morphogenetic movements like germband extension and retraction, or dorsal closure, where the epithelium stretches over the extraembryonic amnioserosa (Tepass, 2012). Another highly dynamic process that is influenced by the polarity network is cell division. Epithelial cells orient their spindle apparatus parallel to the epithelial cell layer, resulting in symmetric division. This is influenced by the polarity network, which provides cues for the appropriate localization of Gαi, Partner of Inscuteable (Pins) and Mushroom bodies defective (Mud). This tripartite complex interacts with dynein to orient the spindle apparatus (Bergstralh et al., 2013). Importantly, epithelial cells do not increase their size during embryonic stages and therefore become smaller with each division (Lye and Sanson, 2011).

1.1.2. Neural stem cells in *Drosophila* development

Drosophila NBs are specified during embryogenesis by a process called lateral inhibition and delaminate from the epithelium in five waves. Morphogenesis and pattern formation in the embryo is tightly controlled by a gene expression cascade which results in the expression of proneural genes in cell clusters of the neurectoderm. These proneural clusters express several basic Helic-loop-helix (bHLH) transcription factors from the Achaete Scute-Complex (AS-C), like Achaete, Scute and Lethal of scute, and the Enhancer of Split-Complex (E(spl)-C), importantly Enhancer of Split and the WD40 repeat protein Groucho. These gene clusters influence each other's expression via Notch-Delta signaling. AS-C activates the expression of the transmembrane protein Delta, which interacts with its receptor Notch of neighboring cells. Upon interaction with Delta, Notch is cleaved and the intracellular domain locates to the nucleus where it interacts with Supressor of Hairless to activate the expression of E(spl)-C. E(spl)-C in turn repress AS-C genes, which then cannot induce Delta expression. Initially, the expression of AS-C and E(spl)-C genes is equal in all cells. By stochastic imbalance one cell in a proneural cluster gains higher

expression of AS-C, leading to active Notch signaling in neighbouring cells which express the E(spl)-C. The AS-C positive cell delaminates from the epithelial tissue and acquires NB fate while the surrounding E(spl)-C positive cells maintain epithelial cell fate (Hartenstein and Wodarz, 2013).

NBs divide to establish the embryonic nervous system by giving rise to a daughter cell called ganglion mother cell (GMC) in each division which further divides to establish two fully differentiated neurons or glia. How a NB influences the specific fate of the GMC is especially well understood in NBs delaminating in the first wave. These NBs first express the temporal transcription factor Hunchback, which is also expressed in the GMC after division and influences the fates of the differentiated cells. Over time the NB sequentially changes the expression of the temporal transcription factor in a specific timewise order: Hunchback is the first transcription factor expressed, Krüppel, Pou-domain proteins 1/2, Castor and Grainyhead expression follow. The transcription factors in this cascade cross-regulate each other, allowing the sequential expression and enabling the establishment of specific neural fates to produce a functional embryonic nervous system (Maurange, 2012).

Embryonic NBs undergo apoptosis or enter quiescence at the end of embryogenesis. The timing of the end of embryonic neurogenesis is controlled by the temporal transcription factor cascade. The cell fate choice between cell cycle exit and apoptotic cell death additionally requires spatial information from Hox gene expression (Cenci and Gould, 2005; Tsuji et al., 2008).

Quiescent NBs are reactivated in the larval brain dependent on the nutritional status during L1 or L2 larval instar. The fat body signals to glial cells which secrete insulin-like peptides to activate the phosphatidylinositol-3 kinase (PI3K) pathway in NBs to trigger cell cycle re-entry (Chell and Brand, 2010; Sousa-Nunes et al., 2011). Interestingly, the temporal transcription factor cascade is continued in larval NBs and extended by Castor and Seven up expression finally leading to Grainyhead expressing NBs (Maurange et al., 2008).

Most larval NBs are refered to as type I NBs and divide similarly to embryonic NBs, each time producing a GMC, which divides once more (type I NBs). Additionally, the larval central brain harbors eight type II NBs per hemisphere which divide in a slightly different

pattern, giving rise to a Mira expressing intermediate neural precursor which transiently amplifies to give rise to larger neural lineages (Bello et al., 2008; Boone and Doe, 2008). Type I and II NBs differ from each other by the expression of Asense and Earmuff and in their response to Notch signaling (Bowman et al., 2008; Weng et al., 2010). While Notch signaling is vital for type II NBs, inhibition of Notch signaling has little effect on type I NBs (Song and Lu, 2011). Besides the central brain type I and II NBs, an additional population of NBs is present in the optic lobe. These optic lobe NBs are specified from the neurectoderm in the optic placodes during larval stages and differ from the bigger central brain NBs in size and position (Figure 2) (Saini and Reichert, 2012).

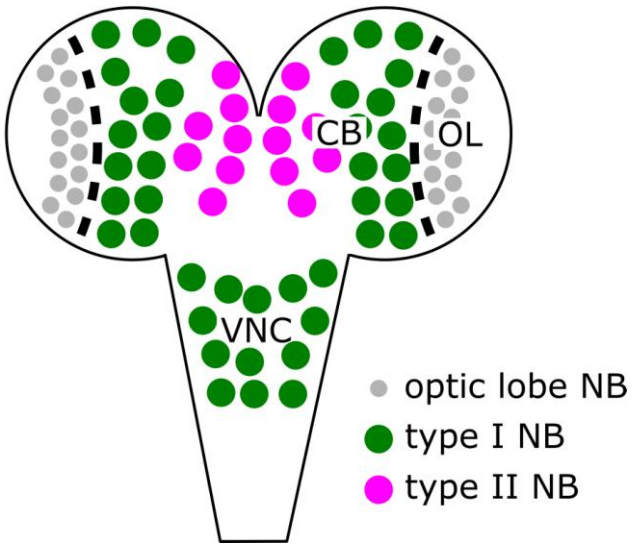

Figure 2: Neuroblasts in the L3 larval brain

The L3 larval brain harbors three different types of NBs. Optic lobe NBs are comparably small, originate from the optic placodes and reside in the optic lobe (OL). Two types of central brain (CB) NBs are present. Type I NBs can be found in the CB region of the brain lobes and the ventral nerve cord (VNC). 8 type II NBs are present in the dorsoposterior and medioposterior regions in each brain hemisphere.

1.1.3. Neuroblast polarity and asymmetric division

NBs, the NSCs of *Drosophila*, are directly specified from epithelial cells after the establishment of epithelial polarity in embryonic stage 8 – 11. Remarkably, NBs inherit polarity from their parent epithelial tissue and many polarity regulators act similarly in the epithelium and the NB (Hartenstein and Wodarz, 2013). Like in the epithelium the Par

complex plays a key role in NB polarity. After delamination from the epithelium the Par complex, consisting of Baz, aPKC and Par-6, localizes apically in the NB (Petronczki and Knoblich, 2001; Wodarz et al., 1999; Wodarz et al., 2000).

Here it interacts with a complex of proteins regulating spindle apparatus orientation: Baz recruits Inscuteable (Insc) to the apical cortex, which binds to Pins and the associated G-protein Gαi (Parmentier, 2000; Schaefer et al., 2000; Schober et al., 1999; Wodarz et al., 1999; Yu et al., 2000). By the interaction with Mud the Insc-complex and the Par-complex act together to reorient the spindle apparatus, which first forms parallel in the first NB division like in the epithelium (Kaltschmidt et al., 2000; Kraut et al., 1996; Rebollo et al., 2009; Schaefer et al., 2000). The apically localized Mud interacts with astral microtubules and pulls one centrosome to the apical side of the NB, thereby aligning the spindle apparatus and the division axis on the apico-basal axis, allowing the NB to divide asymmetrically (Bowman et al., 2006; Izumi et al., 2006; Siller et al., 2006). Interestingly, recent work has shown that Tre1, a G-protein coupled receptor expressed in NBs, receives an unknown signal from the epithelium and interacts with Pins to orient NB spindle polarity (Yoshiura et al., 2012). This further underpins the importance of an intact epithelium for correct NB division.

NB polarity is crucial for appropriate neurogenesis and maintenance of the stem cell. It is therefore not surprising that an additional pathway exists which can rescue spindle orientation in the absence of Insc. In that case the interaction of Mud with Dlg and Kinesin heavy chain-73 orients the spindle (Siegrist and Doe, 2005).

The daughter NB centrosome remains apical after division and in comparison to the mother centrosome accumulates more pericentriolar material and acts as a microtubule organizing center. This is crucial for the division into two daughter cells with distinct sizes: One bigger apical daughter cell, the NB, and a smaller basal daughter cell, the GMC (Januschke et al., 2011; Januschke et al., 2013; Rebollo et al., 2007; Rusan and Peifer, 2007). The centrosome is crucial for the establishment of NB polarity in subsequent NB divisions by recruiting the Par complex to the apical cortex of mitotic NBs (Januschke and Gonzalez, 2010).

aPKC kinase activity plays an important role in NB polarity similarly like in the epithelium. In the NB aPKC activity is linked to the cell cycle by the mitotic kinases Aurora A which

phosphorylates Par-6 thus releasing its inhibitory activity on aPKC and allowing the formation of the Par complex (Wirtz-Peitz et al., 2008). Additionally, the Polo kinase, a cell cycle regulator, controls aPKC localization (Wang et al., 2007). Like in the epithelium aPKC phosphorylates and thereby inactivates Lgl, which co-localizes with Dlg and Scrib and promotes actomyosin-dependent basal localization of target proteins (Albertson and Doe, 2003; Betschinger et al., 2003; Betschinger et al., 2005). Basally localized targets include Miranda (Mira) and Partner of Numb (Pon), both of which are adaptor proteins for basally localized cell fate determinants (Ohshiro et al., 2000; Peng et al., 2000). Pon is a basally localized adaptor for Numb, an inhibitor of Notch signaling that acts via binding of the Notch intracellular domain and by promoting Notch endocytosis thereby inhibiting the self renewing activity of Notch in the GMC daughter (Lu et al., 1998; Skeath and Doe, 1998; Spana and Doe, 1996). Mira is an adaptor protein for GMC-fate determinants and itself an aPKC target. The aPKC-mediated Mira phosphorylation additionally restricts Mira and its bound targets to the basal NB cortex (Atwood and Prehoda, 2009). Mira-binding partners include Prospero (Pros), a transcription factor which is held cytoplasmic by Mira in the NB (Fuerstenberg et al., 1998; Ikeshima-Kataoka et al., 1997). Upon division Pros is inherited by the GMC and released to enter the nucleus where it inhibits gene expression of self renewal genes and activates the cellular program for neural differentiation (Choksi et al., 2006; Chu-Lagraff et al., 1991; Doe et al., 1991; Matsuzaki et al., 1992; Vaessin et al., 1991). Another Mira binding partner is Brain tumor (Brat), a translational regulator which acts redundantly with Pros in neural differentiation (Bello et al., 2006; Lee et al., 2006b). Additionally, Mira controls the localization of Staufen which localizes mRNAs, including Pros mRNA, to the basal side of the NB during division (Broadus et al., 1998; Fuerstenberg et al., 1998).

The polarized localization of cell fate determinants and the spindle apparatus enables the NB to asymmetrically divide into a large NB daughter cell which inherits apically localized stem cell factors, and a basally forming smaller GMC daughter cell to which factors that restrict self renewal and promote neurogenesis are segregated. The GMC divides once more to give rise to two differentiated neurons or glia (Figure 3).

Misregulation of NB asymmetric division may result in loss of the stem cell or overproliferation thus giving rise to tumors (Knoblich, 2010). This has been demonstrated

in *Drosophila* by the emergence of brain tumors upon gain of function of apical determinants, by aPKC mislocalization, or loss of function of basally localized tumor supressors like Brat or Lgl (Bello et al., 2006; Lee et al., 2006a; Manfruelli et al., 1996). Misbalance of asymmetric to symmetric cell division is also widely discussed as a potential mechanism of human tumor formation (Li et al., 2014). In neuroblastoma, for example, enhanced symmetric cell division was shown to lead to more aggressive tumors (Izumi and Kaneko, 2012). Therefore, and because a remarkably high number of proteins required for NB polarity are conserved in mammals, the *Drosophila* NB has emerged as a model to study asymmetric cell division

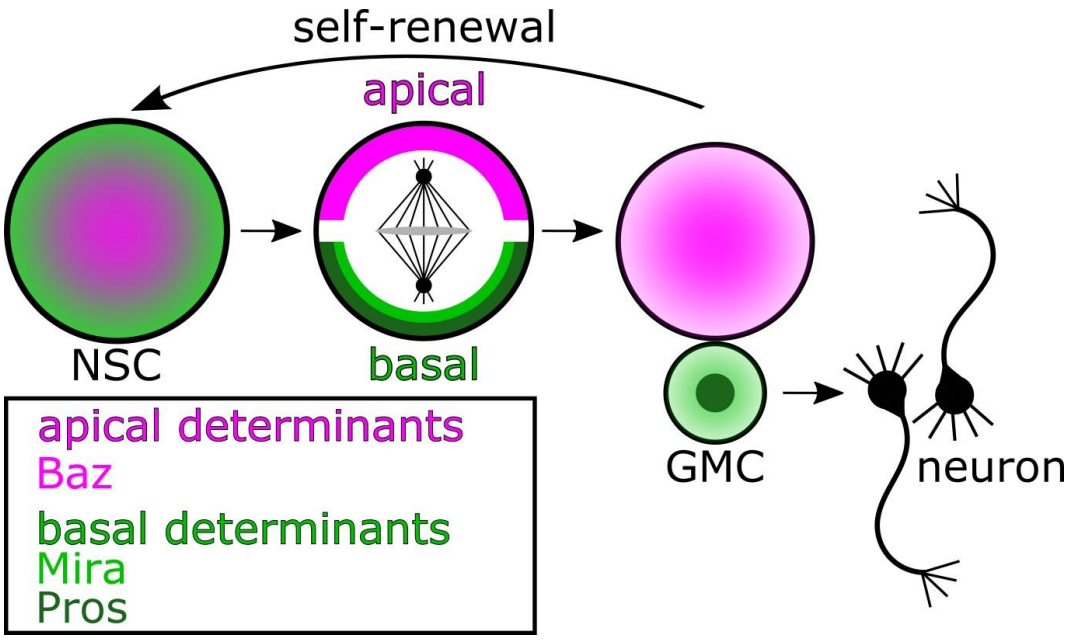

Figure 3: Asymmetric neuroblast division

Stem cell maintenance of the *Drosophila* NB relies on asymmetric cell division, which is regulated by polarized localization of cell fate determinants to the apical (magenta) and basal (green) side of the NB. Polarity determinants are required to orient the spindle apparatus, which is polarized to give rise to a bigger apical NB and a smaller basal GMC. The NB inherits apical determinants like Baz while basally localized determinants like Mira and Pros segregate into the GMC. Mira is an adaptor for the transcription factor Pros and keeps it cytoplasmic in the NB. In the GMC Mira is degraded and Pros can enter the nucleus to repress genes for self-renewal and activate genes for neural differentiation. The GMC divides once more and gives rise to two differentiated neurons or glial cells.

1.1.4. *Drosophila* neuroblasts terminate neurogenesis

Drosophila NBs do not persist until adulthood. Termination of neurogenesis has been shown to differ between central brain NB populations. Abdominal NBs in the ventral nerve cord undergo apoptotic cell death in early L3 stage by the concerted action of the temporal transcription factor Grainyhead and the Hox gene Abdominal-A (Bello et al., 2003; Maurange et al., 2008). Also the NBs that establish the mushroom body, the center for learning and memory in the *Drosophila* brain, undergo apoptosis yet are maintained until late pupal stages. Here apoptosis is induced by Foxo, which can enter the nucleus upon reduced PI3K signaling initially leading to a reduction of cellular growth and proliferation rates and later apoptotic cell death. In case of a failure of the apoptotic program Foxo can induce autophagic cell death in mushroom body NBs ensuring them to terminate neurogenesis (Siegrist et al., 2010). Most central brain NBs, however, undergo termination of neurogenesis by cell cycle exit early during pupal stage which again requires the temporal transcription factor cascade as well as input from Hedgehog signaling (Chai et al., 2013; Maurange et al., 2008).

While larval NBs grow back to their original size after each cell division, the ecdysone pulse during metamorphosis induces pupal NBs to uncouple cell cycle and cell growth. Moreover, the energy metabolism switches from glycolysis to oxidative phosphorylation (Homem et al., 2014). Consequently, pupal NBs divide slower and become smaller after every division. When the NB has almost reached the size of a GMC, Pros enters the NB nucleus in interphase, which precedes one final NB division (Maurange et al., 2008).

Although NBs terminate neurogenesis, the adult *Drosophila* brain exhibits proliferative potential, which is especially induced upon brain damage. These proliferating cells are distinct from larval NBs as they often express glial markers (Fernández-Hernández et al., 2013; von Trotha et al., 2009). Although the origin of mitotic cells in the adult brain remains ambiguous, these cells provide a promising model to study the response to brain damage.

1.2. *Drosophila* intestinal stem cells

Another stem cell population in *Drosophila* has recently been described to utilize the Par complex to divide asymmetrically: The intestinal stem cell (ISC), which gives rise to differentiated cells in the midgut. In the past decade, *Drosophila* ISCs were established as a widely used model to study cancer development, tissue homeostasis and response to tissue damage due to a high conservation of signaling pathways and cellular function between the *Drosophila* and mammalian gut (Jiang and Edgar, 2011).

The *Drosophila* gut is established during embryogenesis and maintained through larval stages. The larval midgut harbors a population of so-called adult midgut precursos (AMPs), which possess stem-cell potential. AMPs are present as single cells in early larval stages and expand their pool by symmetric division (Micchelli et al., 2011). Later during larval development, AMPs undergo one asymmetric division and produce peripheral cells in a process that requires Notch signaling. The peripheral cells surround the AMPs like a sheath and provide niche function to maintain the AMPs in an undifferentiated state via decapentaplegic (bone morphogenic protein 2/4 homolog) signaling. The AMPs afterwards divide symmetrically and give rise to cell clusters, the imaginal midgut islands. During metamorphosis the surrounding peripheral cell undergoes cell death allowing the AMPs to produce differentiated cells and establish the adult gut. AMPs are the progenitor cells of the adult ISC, thus are referred to as pupal ISCs during metamorphosis (Mathur et al., 2010). During the pupal establishment of the adult gut and for adult midgut homeostasis ISCs have to self-renew while they produce differentiated daughter cells. The two main types are enterocytes (ECs), large, polyploid cells that absorb nutrients, and enteroendocrine cells (EEs), which secrete hormones. To allow the establishment of a differentiated cell as well as self-renewal, ISCs divide asymmetrically, which was recently shown to be regulated by the Par complex (Goulas et al., 2012; Guo and Ohlstein, 2015). In the pupal midgut the decision of the cell fate that the differentiating cell will acquire is dependent on the ISC. Pupal ISCs that express Pros, which is held cytoplasmic in the ISC by Mira, divide asymmetrically dependent on the Par complex and produce an apical ISC which inherits the Par proteins, and a basal EE-mother cell (EMC) which inherits Pros. In the EMC Pros now enters the nucleus after Mira degradation. Both ISC and EMC subsequently divide once more, giving rise to two ISCs or EEs respectively. Here, the EMC

division is again asymmetric with one EE inheriting the Par complex and one Par negative EE (Figure 4 A). This asymmetry appears to regulate asymmetric Notch signaling in the EEs, which is required for appropriate EE specification. Pros negative pupal ISCs also divide asymmetrically with the Par complex being localized to the apical side. However, the cell that inherits the Par complex, the enteroblast (EB), differentiates into an EC while the ISC self-renews on the basal side (Figure 4 B). In addition to Pros expression, Notch signaling influences the cell fate choice between EE (low Notch activity) and EC (high Notch activity) (Guo and Ohlstein, 2015).

After the establishment of the adult midgut during metamorphosis ISCs are maintained and required for homeostasis of the adult midgut. Like in the pupal gut, ISCs can divide asymmetrically dependent on the Par complex and produce EB cells (Goulas et al., 2012). In the adult midgut EEs and ECs are both produced by differentiation of EBs. These produce EEs when the ISC expresses low Delta levels thus leading to low Notch activity in the EB, and ECs when the ISC expresses high Delta levels (Ohlstein and Spradling, 2007).

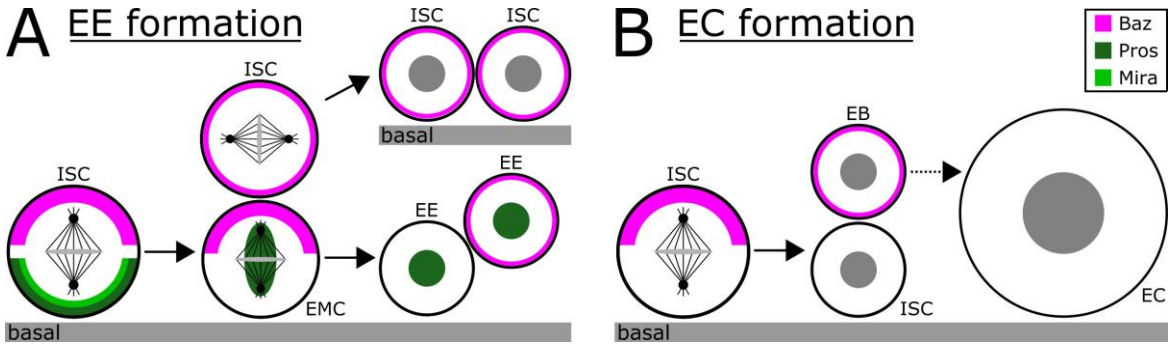

Figure 4: Intestinal stem cell division in the pupal midgut

Notch signaling and Pros expression influence EE and EC formation in the pupal gut. (A): Low Notch activity and Pros positive ISCs lead to EE production. ISCs express the Par complex (including Baz), which localizes apically, and Pros, which is localized basally by Mira interaction. Asymmetric division produces two similarly sized daughter cells. The apical ISC which divides symmetrically once, produces two ISCs which are recruited back to the basal side of the midgut epithelium. The basal EMC inherits Pros, which localizes to the nucleus upon Mira degradation. The EMC re-expresses the Par complex and divides asymmetrically to produce EEs of which one inherits the Par proteins and expresses Delta while the second does not. This asymmetry between EEs is required for appropriate EE fate. (B): High Notch activity and Pros absence in ISC lead to EC formation. Here, ISCs divide asymmetrically to produce one apical Par-inheriting EB, which differentiates into an EC, and a basal ISC.

Notch signaling does not only influence the cell fate but is further required in AMPs as well as ISCs to maintain the stem cells (Guo and Ohlstein, 2015; Ohlstein and Spradling, 2007; Takashima et al., 2011). Additionally, ISC proliferation and differentiation of daughter cells is regulated by various signaling pathways and by cell-intrinsic as well as cell-nonautonomous mechanisms. ISCs have been shown to respond to different cell types inside and outside the midgut as well as to cell population imbalance. This contributes to the regulation of proliferation rates and the switch between asymmetric division for the production of differentiated cells, and symmetric division to replenish the ISC population (Li and Jasper, 2016). Besides substantial recent advances in understanding the molecular mechanisms underlying ISC behaviour much remains to be learned to fully resolve the complex regulatory mechanisms in midgut development and homeostasis.

1.3. The Tip60 chromatin remodeling complex

The eukaryotic genome is associated with nucleosomes, octamers consisting of H2A/H2B and H3/H4 dimers which wrap around 147 bp of DNA. DNA with associated histones is defined as chromatin and this packaging allows eukaryotic cells to organize, compact and stabilize the genome. To make the DNA accessible for replication, transcription and DNA repair and for the regulation of these processes, nucleosomes have to be shifted or restructured, removed or loaded to the DNA. The molecular machines accomplishing these tasks are called chromatin remodeling complexes: Multimeric protein complexes that require ATP. The catalytic subunits of these complexes are ATPases, which utilize a Swi2/Snf2-type ATPase domain consisting of an ATP-binding domain (DExx-domain) and a helicase domain (HELICc-domain). Dependent on additional domains, chromatin remodeler ATPases are grouped into four distinct families: SWI/SNF, ISWI, CHD and INO80 (Lessard and Crabtree, 2010).

In this study, I investigated the function of *Drosophila* Domino (Dom), an INO80-type ATPase. Dom is conserved in eukaryotes from yeast (Dom homologs are Swr1 and Eaf1) to human (human homologs are p400 and SRCAP) and the associated chromatin remodeling complexes are likewise conserved in subunit composition and molecular as well as cellular functions (Yamada, 2012).

Yeast homologs of Dom are present in two distinct complexes: Swr1 is the ATPase of the Swr1-chromatin remodeling complex; Eaf1 associates with the NuA4-complex. The Swr1-complex exchanges H2A/H2B dimers with dimers containing the H2A variant Htz1 and H2B in an ATP-dependent manner (Kobor et al., 2004; Krogan et al., 2003; Mizuguchi et al., 2004). Eaf1, although a Dom homolog, does not possess ATPase function and the NuA4-complex does not have ATP-dependent chromatin remodeling function. Rather, the catalytic function of the NuA4-complex relies on the histone acetyltransferase (HAT) Esa1, which acetylates H2A, Htz1 and H4 *in vivo* (Altaf et al., 2010; Clarke et al., 1999; Keogh et al., 2006; Zhang et al., 2004).

In human and the fly the functions of the Swr1- and NuA4-complex are merged in one ATPase- and HAT-containing complex, called Tip60 complex (Yamada, 2012). The HAT homolog of Esa1 is Tip60 and the *Drosophila* Tip60 complex contains Dom, while the Dom-homolog in the human Tip60 complex is called p400 (Fuchs et al., 2001; Kusch et al., 2004). Additionally, humans further have the SRCAP ATP-dependent chromatin remodeling complex containing the Swr1/Dom-homolog SRCAP. The SRCAP complex does not contain HAT activity and has been proposed to be also present in *Drosophila,* containing Dom as ATPase subunit (Cai et al., 2006; Johnston et al., 1999a). However, besides the absence of the Tip60 HAT, subunit composition is not well investigated in *Drosophila* (Eissenberg et al., 2005). The components of the *Drosophila* Tip60 complex as well as the subunits of the evolutionarily conserved complexes in human and yeast are better documented. Table 1 shows that many subunits are part of not only one but both evolutionarily related complexes in human (Tip60- and SRCAP-complex) and yeast (NuA4- and Swr1-complex).

Table 1: *Drosophila* Tip60-components and conservation in human and yeast

The Tip60 complex is evolutionarily conserved in eukaryotes and has most likely evolved as a fusion of the yeast NuA4 and Swr1 complexes. The Tip60 complex contains HAT- and ATPase-activity, while the SRCAP complex in human solely relies on ATPase function.

Drosophila	*Homo sapiens*		Yeast		Molecular function
Tip60 complex	Tip60 complex	SRCAP-complex	NuA4-complex	Swr1-complex	
Domino	P400	SRCAP	Eaf1	Swr1	Histone-tail binding/ ATP-dependent helicase
Tip60	Tip60	-	Esa1	-	HAT activity
Act87E	Actin	Arp6	-	Arp6	Positive regulation of ATPase activity, actin related
Bap55	BAF53a	BAF53a	Arp4	Arp4	Phospho-H2A-variant-dependent DNA recruitment upon DNA damage
Brd8	Brd8	-	-	Bdf1	Binding to acetylated histones, transcriptional coactivator
DMAP1	DMAP1	DMAP1	Eaf2	Eaf2	Histone-tail binding
Eaf6	hEaf6	-	-	-	unknown
E(Pc)	EPC1	-	Epl1	-	Protein-interaction within complex, regulation of HAT activity
Gas41	Gas41	-	Yaf9	Yaf9	Transcriptional activation, nuclear matrix interaction
Ing3	Ing3	-	Yng2	-	H3K4me3 binding
MrgBP	MrgBP	-	Eaf7	-	MRG15-binding, potential DNA-binding
MRG15	MRG15	-	Eaf3	-	H3K36me2/3 binding
Nipped-A	TRRAP	-	Tra1	-	Adaptor, Scaffold
Pontin	Tip49	Tip49	-	Tip49A	ATP-dependent helicase (unclear), scaffold
Reptin	Tip48	Tip48	-	Tip49B	ATP-dependent helicase (unclear), scaffold
YL-1	YL-1	YL-1	-	Vps72	H2A-variant binding

Additionally, many subunits function in unrelated chromatin or HAT-complexes, interact with other proteins (eg. transcription factors) or function in smaller complexes, which contain only a few subunits of the full complex. Moreover, specific interactors of the Tip60 complex have been shown to alter the subunit composition (Boudreault et al., 2003; Cheng and Côté, 2014; Fuchs et al., 2001; Jha and Dutta, 2009; Jin et al., 2005; Mitchell et al., 2008; Park et al., 2002; Rountree et al., 2000; Saksouk et al., 2009; Ullah et al., 2008). Besides, some components are partially functionally redundant in the Tip60 complex (Brd8 and Gas41), making it challenging to dissect which processes require which complex, subunits or additional interactors (Bianchi et al., 2004). Surprisingly, findings of a recent study support the presence of a p400 complex which functions independently of the Tip60 HAT to incorporate the H3 variant H3.3 into promoters of actively expressed genes, further underlining the biochemical variation of the Tip60 complex (Pradhan et al., 2016).

In the present study, I focus on the function of Dom in the Tip60 chromatin remodeling complex. The Tip60 complex has various molecular functions:

- ATP-dependent exchange of H2A/H2B dimers with H2Av-H2B dimers
- Helicase function
- Histone acetyltransferase activity on H2A, H2Av and H4
- Acetyltransferase activity on non-histone substrates

Several functions of the Tip60 complex are executed via depositing or modifying non-canonical H2A variants. H2Av is the only H2A variant in *Drosophila* and functions homologous to mammalian H2A.X and H2A.Z (Baldi and Becker, 2013). H2Av can be incorporated into DNA by all Dom isoforms (Börner and Becker, 2016). Like H2A.X, H2Av is phosphorylated upon DNA double strand breaks to signal to the DNA repair machinery and grant an easily accessible DNA conformation (Kusch et al., 2004). H2A.Z and H2Av are required for heterochromatin formation and both prevent spreading of heterochromatin at boundaries to euchromatin (Fu et al., 2008; Meneghini et al., 2003; Rong, 2008). Further, both H2A variants are enriched at the transcription start site of promoter regions of actively transcribed genes (Mavrich et al., 2008; Nekrasov et al., 2012). This facilitates gene expression, as H2Av-containing nucleosomes are less stable. Thus, the transcriptional machinery can access the DNA easier (Abbott et al., 2001; Jin and

Felsenfeld, 2007). However, H2A.Z is also linked to repression of gene expression (Gévry et al., 2007).

In addition to the ATPase activity of Dom, the HAT-activity of the Tip60 complex is the second catalytical function. The Tip60 complex is named after the HAT catalytical subunit Tip60 which acetylates H2A, H2Av and H4 as histone-targets *in vivo* (Keogh et al., 2006; Kusch et al., 2004; Mitchell et al., 2008; Mizuguchi et al., 2004). Histone acetylation occurs on the ε-amino group of lysines, which can lead to the recruitment of bromodomain containing epigenetic readers. Furthermore, it brings a negative charge to the basic histones, which weakens the interactions with the negatively charged DNA backbone. Therefore, histone acetylation is associated with processes that require an open chromatin formation, like replication, transcription or DNA repair (Clapier and Cairns, 2009; van Attikum and Gasser, 2005). Interestingly, Tip60 also acetylates several non-histone targets, including various transcription factors, to regulate stability or activity (Judes et al., 2015).

Many components of the Tip60 complex are amplified or overexpressed in human neuroblastoma, glioblastoma and colorectal cancer, while loss of function is mostly lethal, leading to impaired cell growth, cell cycle arrest or cell death as well as genome instability (Yamada, 2012). In addition, recent research has connected p400 and Tip60 as well as several other Tip60 subunits to maintenance of stem cells (Chen et al., 2011; Chen et al., 2013; Fazzio et al., 2008a; Fazzio et al., 2008b; Fujii et al., 2010; Lu et al., 2015; Ravens et al., 2015). In *Drosophila* especially Dom is known to function in stem cell maintenance (Börner and Becker, 2016; Morillo Prado et al., 2013; Neumüller et al., 2011; Xi and Xie, 2005; Yan et al., 2014).

1.3.1. Domino: A chromatin remodeler ATPase

dom (CG9696) has been isolated in a screen for regulators of hematopoiesis. Lymph glands of larvae homozygous for a *dom* mutation are melanized and turn black, making the white larvae look like Domino tokens. Thus the authors named the identified gene *domino* (Braun et al., 1997; Braun et al., 1998). Like its homologs, *dom* is a vital gene that binds to DNA and can be recruited via interaction with H3K4me3 (Fazzio et al., 2008b; Kusch et al., 2014; Ueda et al., 2007). *dom* null mutation is early larval lethal and cell

clones induced with null mutant alleles were not recovered (Ruhf et al., 2001). *dom* contains 18 exons and is encoded on chromosome 2R (Figure 5 A). Alternative splicing produces four different isoforms dom-RA, RE, RD and RG, which all share the first four exons (Figure 5 B). The resulting proteins encode ATPases from the Swi2/Snf2-type, which contain a DExx-domain for ATP-binding (in this case the DEXDx-subtype), and a HELICc-helicase domain. Dom proteins contain a long insertion between these domains, which specifies them as members of the INO80-family, also termed split-ATPases. As other INO80 family members, Dom proteins contain a helicase SANT domain (HSA), which is believed to interact with Actin-related protein subunits in the chromatin remodeler complex. Additionally, several coiled-coil motifs can be identified (Figure 5 C).

The larger isoforms Dom-PA, PD and PG contain a C-terminal myb/SANT-like DNA binding domain, found in the c-Myb family of transcriptional activators and poly-glutamine (poly-Q) stretches (Clapier and Cairns, 2009).

The smaller isoform Dom-PE (previously annotated as Dom-PB) has a unique C-terminus, which is conserved only in three closely related *Drosophila* species *D. simulans, D. willis* and *D. buskii*. This C-terminal domain was identified as a potential Baz-interacting domain in a Yeast two-hybrid screen previously conducted in our lab (Egger-Adam, 2005).

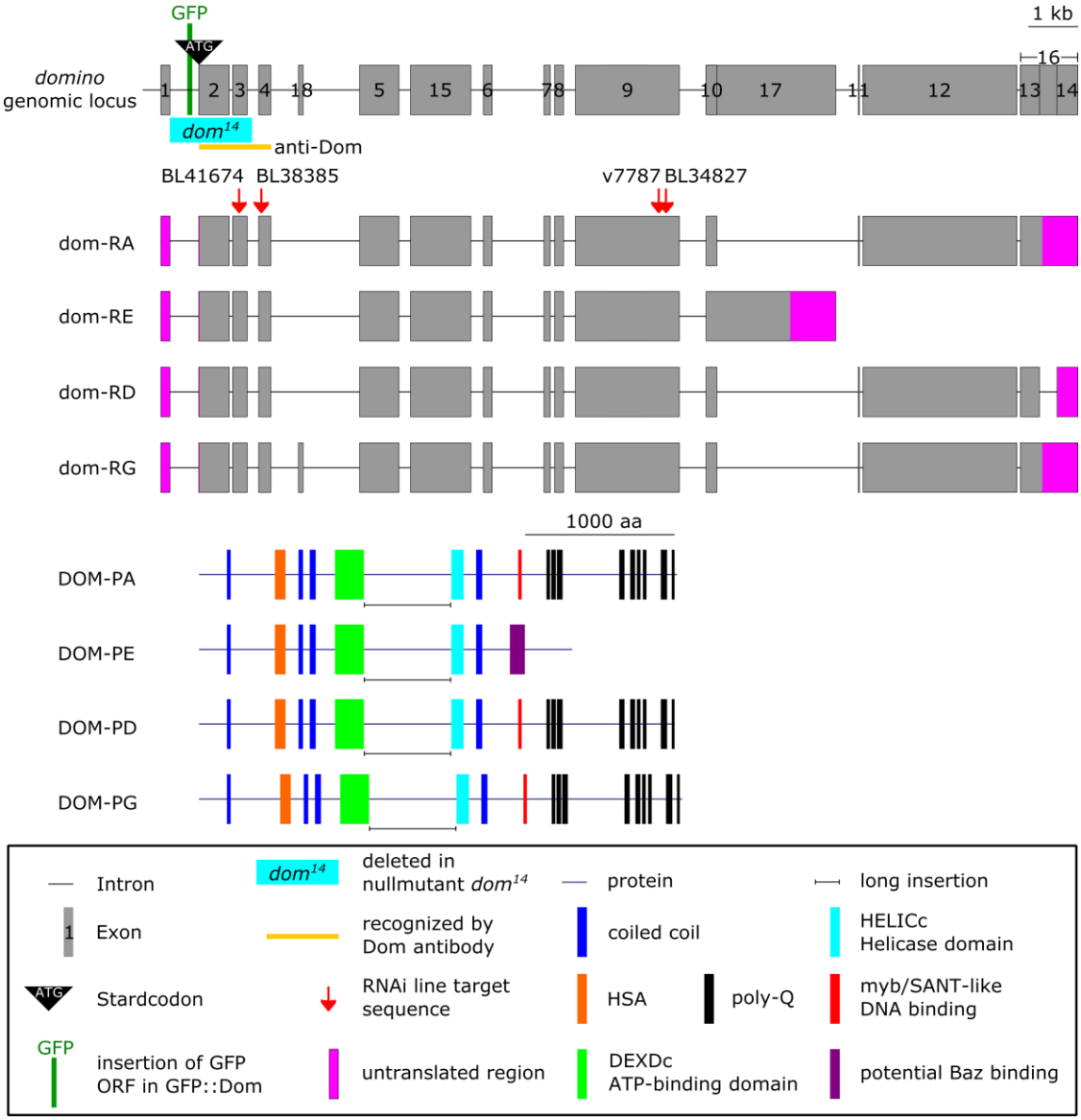

Figure 5: The *domino* gene locus and encoded transcripts and protein isoforms.

*dom (*CG9696*)* encodes four transcripts and proteins. (A): Exon and introns of *dom*. The startcodon is located in exon 2 and is removed by the null mutation *dom*^{14}. The GFP open reading frame (ORF) in the GFP-Dom trap line (BA00164) is inserted before the start codon and might be translated from an alternative start codon (CTG) two codons before the GFP insertion. The antibody detecting Dom is directed against the protein sequence resulting from exons 2 – 4, which are shared by all isoforms A, D, E, G (B): All isoforms are targeted by dom-RNAi lines used. (C): Dom proteins encode chromatin remodelers of the split-ATPase family, characterized by an ATPase domain (DEXDc) and a helicase domain (HELICc) separated by a long insertion. Dom also contains a helicase/SANT-domain (HSA) and four coiled coil motifs. A myb/SANT-like DNA-binding domain and several poly-Q stretches are found in the larger isoforms A,D and G. Isoform E (previously DomB) has a unique C-terminus found in our yeast two-hybrid screen as a potential Baz-binding site (Egger-Adam, 2005).

The human homologs of Dom are p400 and SRCAP. p400 and SRCAP function as ATPase subunits of the Tip60 complex and the SRCAP-complex, respectively (Fuchs et al., 2001; Johnston et al., 1999a). While p400 misregulation is connected to tumorigenesis, SRCAP mutation is found to cause a rare disease, the Floating-Harbor syndrome, which leads to dysmorphia and mental retardation (Kehrer et al., 2014; Mattera et al., 2009; Nagasaki et al., 2014). In *Drosophila* both ATPase subunits are encoded by *dom*. It has been proposed that the DomA isoform functions as p400-homolog in the Tip60 complex and the isoform DomE functions as SRCAP-homolog (Börner and Becker, 2016; Eissenberg et al., 2005; Kusch et al., 2004). As SRCAP-homolog, Dom functions as an activator of the Notch signaling pathway (Eissenberg et al., 2005). Mutations in *dom*, like mutations in the Tip60-subunit Nipped-A or in mammalian TRRAP, have been shown to modulate Notch signaling phenotypes upon mutation of *Notch* or *mastermind (mam)* (Gause et al., 2006; Hall et al., 2004; Kwon et al., 2013). The intracellular domain of Notch interacts with Mastermind to activate the expression of Notch-responsive genes. Dom is a co-activator of Notch-responsive gene expression and further modifies the Notch pathway by negatively regulating Notch mRNA expression levels. It has been proposed that Dom recruits the HAT CBP (expressed by *nejire*) to regulate Notch targets. This mechanism was supposed to be independent of Tip60 and therefore might be a function of the SRCAP-complex (Eissenberg et al., 2005). Also the Tip60 subunit Nipped-A modulates Notch singaling in *Drosophila* (Eissenberg et al., 2005; Gause et al., 2006). However, in mouse Nipped-A can positively regulate Notch signaling independent of Tip60 and Dom within a distinct complex, SAGA, which contains the Gcn5 HAT (Kurooka and Honjo, 2000). In mammals the Tip60 HAT negatively regulates Notch signaling upon UV-irradiation, by acetylation of Notch (Kim et al., 2007). Although the functions of Dom, Nipped-A and also Tip60 in Notch signaling are well established, it is unclear whether the SRCAP complex, the Tip60 complex or a sub-complex acts in Notch regulation.

The function of Dom in Notch signaling and the ambiguity of participating complexes underline how important it is to study chromatin remodeling complexes as a whole instead of having only a restricted view on single subunits. Recent studies have connected Dom to the regulation of alternative splicing and the microRNA pathway (Pressman et al., 2012). However, the lack of data about Dom interacting proteins makes it speculative

which complexes are involved. Likewise, the importance of Dom or the homolog p400 in the Tip60 complex is well established in various processes. The specific function is thereby dependent on the cellular context, the cellular state and different interacting proteins.

1.3.2. Specific interactors define Tip60 complex functions

The Tip60 complex has diverse functions which are well conserved. Some functions, like the role in DNA repair, are relevant for all cell types. The importance in the regulation of the cell cycle is especially required in dividing cells but independent of the cell type (Yamada, 2012). In addition, a cell type specific function of Tip60 in the nervous system connects the HAT to regulation of neural gene expression (Lorbeck et al., 2011). Interestingly, Tip60 functions together with the Alzheimer's disease amyloid precursor protein (APP) to regulate gene expression (Cao and Südhof, 2001; Słomnicki and Leśniak, 2008). Data from *Drosophila* indicate a role in axonal transport and regulation of the sleep rhythm (Pirooznia et al., 2012). Another study connected the Tip60 complex to dendritic targeting in neurons (Tea and Luo, 2011).

1.3.2.1. The Tip60 complex in the p53 pathway and DNA repair

The involvement of the Tip60 complex in repair of DNA double strand breaks is a good example of a function, which is dependent on the cellular state. Further, the response to DNA damage illustrates the dynamics of the Tip60 complex, as some functions are executed by the whole Tip60 complex while others depend on single subunits. Figure 6 summarizes the functions of the Tip60 complex in DNA repair.

p400 has been shown to protect cells from DNA damage by regulation of reactive oxygen species (ROS) metabolism (Mattera et al., 2010). When DNA double strand breaks occur, the Tip60 HAT is required to acetylate ATM (ataxia telangiectasia mutated), a protein kinase which upon acetylation by Tip60 gets autophosphorylated and can phosphorylate and activate effector proteins (Sun et al., 2005). An important target of ATM is H2A.X (Burma et al., 2001). After H2A.X phosphorylation near the DNA double strand breaks the resulting γH2A.X recruits proteins for DNA repair (Podhorecka et al., 2010). In yeast upon DNA damage phosphorylated H2A has been shown to recruit the Tip60 homologous NuA4

complex by interaction with the Bap55-homolog Arp4 (Downs et al., 2004). At the site of DNA damage the Tip60 complex hyperacetylates H4 and relaxes the DNA compaction by nucleosome remodeling as well as H2A.Z incorporation, thereby facilitating the DNA access for the DNA repair machinery (Squatrito et al., 2006). In *Drosophila* the Tip60 complex is further required to remove phosphorylated H2Av, the *Drosophila* γH2A.X counterpart, after successful DNA repair (Kusch et al., 2004).

Another well-studied target of ATM is the p53 transcription factor (Banin et al., 1998; Canman et al., 1998; Maya et al., 2001). Phosphorylation of p53 enables p53 target gene expression, which in turn can be regulated by the Tip60 complex (Gévry et al., 2007). p53 activates gene expression for cell cycle checkpoint and DNA repair, thereby promoting cellular survival (Beckerman and Prives, 2010). Depending on the cell cycle phase, cells can activate homologous recombination (HR) which relies on a homologous DNA region for DNA repair, or non-homologous end joining (NHEJ) which brings DNA double strand breaks together and might lead to deletions (Branzei and Foiani, 2008). Notably, NHEJ relies on the interaction of a dimer of Ku70 and Ku80 and in mammals, surprisingly, the interaction with Par-3 (Fang et al., 2007). The choice between the DNA repair pathways is partly directed by p400 (Taty-Taty et al., 2015). Upon unsuccessful DNA damage repair and under high stress levels, p53 is capable of inducing apoptosis by a distinct set of target genes (Riley et al., 2008). The choice between cell cycle arrest by activation of the checkpoint and apoptosis relies on Tip60 dependent acetylation of p53 at lysine 120, which alters the affinity of p53 for target gene promoters (Tang et al., 2006). Depending on the cellular context p53 can alternatively also trigger cellular senescence by promoting cell cycle exit via high activation of p21 expression. p21 is a cyclin-dependent kinase inhibitor that promotes G1 arrest (Muñoz-Espín and Serrano, 2014).

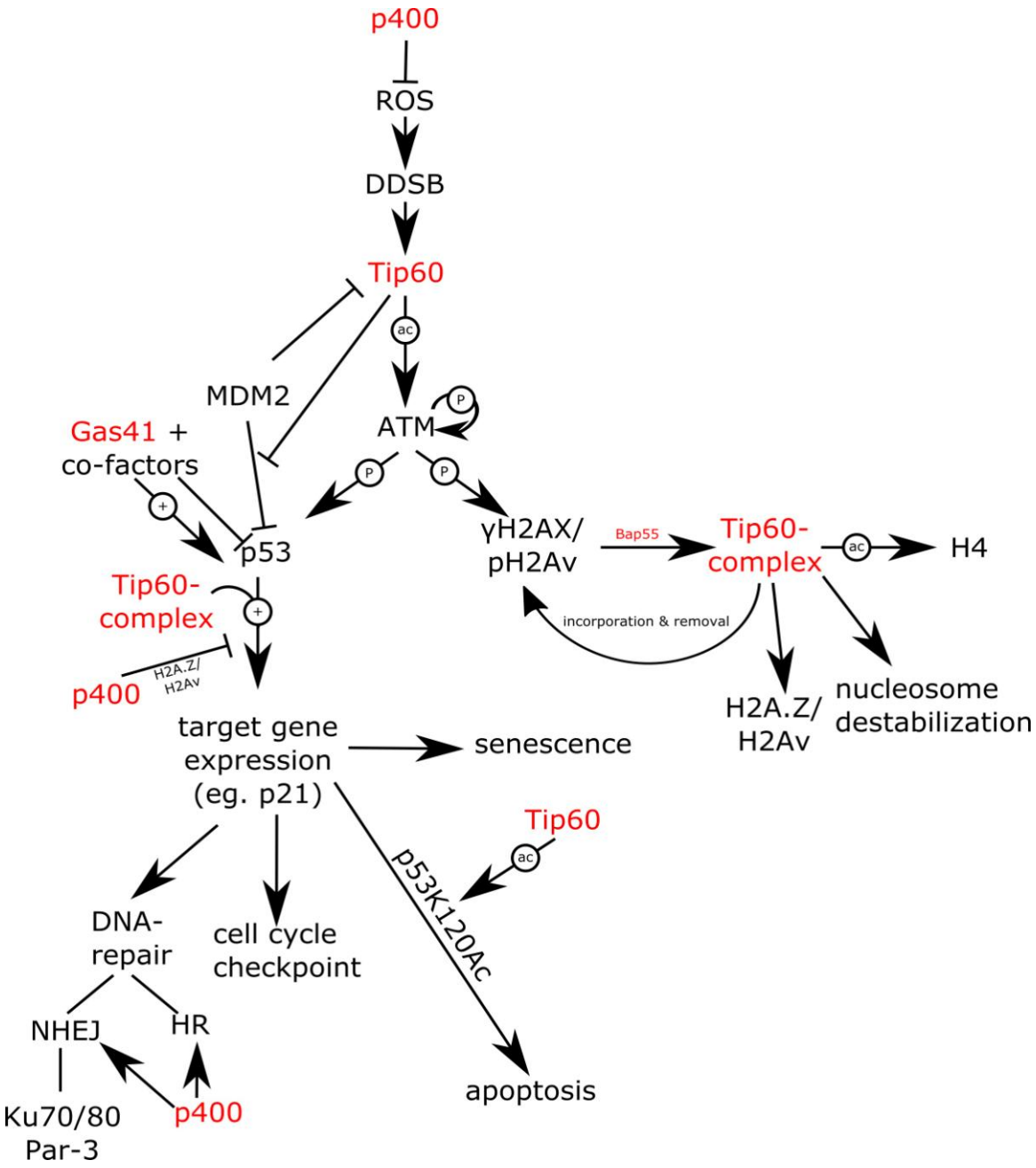

Figure 6: Tip60 complex members in DNA damage response

Subunits of the Tip60 complex (red) function together and independently at various levels of the DNA damage response. p400 restricts DNA damage by regulating ROS metabolism. Activation of the DNA damage response relies on the Tip60 HAT. The Tip60 complex facilitates access of the DNA repairs machinery by various mechanisms to γH2A.X positive DNA regions. p53 stability, activity and target gene specificity is regulated at multiple levels by Tip60 complex subunits. p400 directly influences DNA repair and influences the choice between HR and NHEJ, the latter of which requires Ku70/80 dimers and Par-3.

Interestingly, subunits of the Tip60 complex have been shown to interact with p53 independent on transcriptional regulation. Gas41, a Tip60 complex member, can act independently of the Tip60 complex on p53 by destabilizing the transcription factor and repressing p53 mediated transcription (Llanos et al., 2006; Park and Roeder, 2006; Park et al., 2011). The Tip60 HAT stabilizes p53 by interfering with MDM2, an E3 ligase which targets p53 for proteasomal decay and inhibits its DNA binding domain (Legube et al., 2004). Notably, the Tip60 HAT is co-regulated with p53 as it is also a MDM2 target protein (Legube et al., 2002).

Additionally, Tip60 complex members regulate p53-mediated transcription, which is especially well investigated for p21 expression. In unstressed cells p400 negatively regulates p21 expression by deposition of H2A.Z into the p21 promoter region in a Tip60 independent complex (Chan et al., 2005; Gévry et al., 2007; Park et al., 2010; Tyteca et al., 2006). Interestingly, in aging cell p400 is downregulated to induce p21 mediated cellular senescence (Lee et al., 2012). Also upon DNA damage H2A.Z is removed from the p21 promoter and the Tip60 complex acts as a p53 coactivator of p21 expression (Legube et al., 2004; Tyteca et al., 2006). In the absence of DNA damage p400 acts in the Tip60 complex to repress the HAT activity of Tip60 to repress p21 expression, thus p400 has a dual role in p21 transcriptional regulation (Park et al., 2010). These findings demonstrate the contrasting functions of p400 and Tip60 in regulation of p21 expression. The antagonistic functions of p400 in the p53 pathway might also explain why tumor cells often exhibit a p400/Tip60 misbalance with Tip60 being downregulated in comparison to p400 (Mattera et al., 2009).

1.3.2.2. Cell cycle regulation by the Tip60 complex

The regulation of the cell cycle is closely coupled to DNA repair to ensure appropriate segregation of the chromosomes. The Tip60 complex interacts with several key regulators of cell cycle progression, including the Retinoblastoma (Rb)-Elongation factor 2 (E2F) pathway (Sapountzi et al., 2006). This pathway is well conserved in *Drosophila* and consists of the Rb protein and activator E2Fs (E2F1 in *Drosophila*) and repressor E2Fs (E2F2 in *Drosophila*). Rb represses activator E2Fs by direct interaction and by repression of target genes and gets phosphorylated and degraded upon cell cycle entry. The release

of the Rb inhibitory effect on activator E2Fs activates expression of S-phase cell cycle genes. This in turn is counteracted by repressor E2Fs during G2-phase, which thereby support cell cycle progression (Gheghiani and Gavet, 2016).

Dom and the Tip60 complex apparently act in two ways on activator E2F-mediated target gene expression. A study in *Drosophila* found that Dom represses E2F1 target gene expression most probably via H2Av incorporation, while experiments conducted in mammalian cell culture showed that the Tip60 complex activates gene expression by histone acetylation upon recruitment of E2F1 to target gene promoters (Lu et al., 2007; Taubert et al., 2004). Furthermore, the Tip60 HAT acetylates at E2F1 in mammalian cells to promote stabilization of the transcription factor (Van Den Broeck et al., 2012).

On of the target genes positively regulated by E2F and the Tip60 complex is *myc* (Kramps et al., 2004). Myc, a proto-oncogene regulating cell growth and proliferation, in turn stimulates activator E2F transcription and target gene expression by recruiting activator E2Fs to their target promoters to induce cell cycle entry (Gheghiani and Gavet, 2016). Myc is a sequence specific transcription factor known to regulate genes for cell cycle progression and cellular metabolism (Bretones et al., 2015). Myc recruits the Tip60 complex to target promoters and activate gene expression by means of histone acetylation (Frank et al., 2003). Myc has been shown to interact with specific Tip60 subunits, including Tip60, p400, TRRAP, Tip48, Tip49, BAF53 and the actin related subunit (Frank et al., 2003; Fuchs et al., 2001; McMahon et al., 1998; Park et al., 2002; Wood et al., 2000). Interestingly, the Tip60 subunit E(Pc) was shown to not be present in the Myc interacting complex, indicating that only a sub-Tip60 complex interacts with Myc (Fuchs et al., 2001). Although the interaction between Myc and the Tip60 complex is well established in mammals it is still unclear whether this interaction is conserved in *Drosophila*.

Activation of gene expression by sequence specific DNA binding appears to be the major function of Myc, however it can also regulate gene expression by several mechanisms. A well-understood example is the effect of Myc on the p21 promoter, which is regulated by Myc in multiple ways. For example, Myc forms a complex with the transcription factor Miz-1 to recruit a DNA methyltransferase to the p21 promoter and repress p21 expression by DNA methylation (Brenner et al., 2005; Seoane et al., 2002). Myc also

sequesters the transcription factor Sp1/Sp3, which has a positive effect on p21 expression (Gartel et al., 2001). Furthermore, it recruits the Tip60 complex, potentially without HAT activity, to induce H2A.Z incorporation thereby repressing p21 expression (Gévry et al., 2007).

Besides effects on target gene expression, Myc and the Tip60 complex regulate each other mutually. Myc positively regulates p400 levels in human cancer cell lines at least in part by ensuring correct p400 mRNA splicing (Chan et al., 2005; Koh et al., 2015). The Tip60 HAT acetylates Myc, which inhibits poly-ubiquitination and thus stabilizes Myc (Patel et al., 2004).

1.3.2.3. Multiple cofactors for a Tip60 complex transcriptional network in stem cells

Several Tip60 members have been linked to stem cell maintenance in mouse and *Drosophila* stem cells (Table 2) (Börner and Becker, 2016; Chen et al., 2011; Fazzio et al., 2008a; Fazzio et al., 2008b; Lu et al., 2015; Morillo Prado et al., 2013; Neumüller et al., 2011; Xi and Xie, 2005; Yan et al., 2014). In stem cells the Tip60 complex appears to regulate gene expression both in an activatory as well as inhibitory manner (Fazzio et al., 2008a; Fazzio et al., 2008b; Ravens et al., 2015). Both catalytical functions, histone acetylation and H2A variant incorporation, were supposed to be required (Börner and Becker, 2016; Morillo Prado et al., 2013; Ravens et al., 2015).

Table 2: Tip60 complex subunits implicated in stem cell maintenance

CSC = cyst stem cell, ESC = embryonic stem cell, GSC = germline stem cell, NB = neuroblast, NSC = neural stem cell, SSC = somatic stem cell

Tip60 subunit	Maintenance of stem cell types
P400/Domino	Mouse ESCs, *Drosophila* SSC, GSC, CSC, NB
Tip60	Mouse ESCs
BAF53a	Mouse ESC
DMAP1	Mouse ESC
Gas41	Mouse ESC
Mrg15	Mouse NSC
Tip48	Mouse ESC
Tip49	Mouse ESC
TRRAP	Mouse ESC

In mouse embryonic stem cells (ESCs) a variety of different interactors and regulators of the Tip60 complex has been described. A recent report has linked Myc to the regulation of transcription in mouse ESCs. Here, gene expression was reported to be activated upon Myc dependent recruitment of the Tip60 complex to target promoters and subsequent histone acetylation (Ravens et al., 2015). Additionally, the Tip60 complex was reported to interact with the stem cell factors Nanog and potentially Sox2 (Fazzio et al., 2008a; Lu et al., 2015).

The histone mark H3K4me3 is a posttranslational histone modification on histone 3 which is connected to active gene expression and found on bivalent promoters, which are repressed but primed for activation (Vastenhouw and Schier, 2012). Set1-family methyltransferases were shown to methylate H3K4 and the subsequent H3K4me3 recruits the Tip60 complex to promoter regions in ESCs, which appears to be conserved in *Drosophila* (Fazzio et al., 2008a; Kusch et al., 2014).

On repressed Tip60 complex target genes, HDAC6, a histone deacetylase, functions as an upstream regulator of Tip60 complex target gene expression in ESCs (Chen et al., 2013). The requirement of H2A.Z on Polycomb Group (PcG)-regulated promoters in ESCs further underlines the importances of the gene repressive function of the Tip60 complex, as PcG genes are required to maintain a repressed chromatin state (Creyghton et al., 2008). Although a direct interaction between PcG and the Tip60 complex in ESCs has not been investigated, several studies in *Drosophila* link Dom and the Tip60 members Reptin, Pontin and E(Pc) (Enhancer of Polycomb) to PcG-dependent gene regulation (Diop et al., 2008; Qi et al., 2006; Ruhf et al., 2001; Sato et al., 1983; Sinclair et al., 1998).

Besides mouse ESCs, several other stem cell populations require Tip60 complex members. In mouse NSCs MRG15 prevents the accumulation of active p53. In the absence of MRG15 the ectopic expression of the p53 target gene p21 limits proliferation (Chen et al., 2011). In *Drosophila* the importance of the Tip60 complex in stem cells is poorly investigated. Several stem cell populations including stem cells in the male and female germline as well as NBs require Dom for their maintenance (Börner and Becker, 2016; Morillo Prado et al., 2013; Neumüller et al., 2011; Xi and Xie, 2005; Yan et al., 2014). However, no studies have analyzed the executing chromatin remodeling complexes or interacting transcription

factors. Recent studies have highlighted the importance of H2Av incorporation by Dom in germline cells (Börner and Becker, 2016; Morillo Prado et al., 2013).

1.4. The roles of the transcription factor Myc in stem cells

Myc, in human encoded by three genes with overlapping function L-, N- and c-Myc, is a sequence specific transcription factor and dimerizes with its partner Max to bind to the E-box sequence in target promoters to activate their expression (Kress et al., 2015). Myc is known to recruit the Tip60 complex to target promoters to stimulate histone acetylation and thereby transcription (Frank et al., 2003). However, Myc is also able to repress gene expression by various mechanisms, including the stimulation of H2A.Z incorporation by p400 (Gévry et al., 2007). The role of Myc is well established in regulation of the cell cycle and cellular growth as well as tumorigenesis. Despite, Myc has been described to be important for several types of mammalian stem cells but its function is surprisingly variable dependent on the type of stem cell (Murphy et al., 2005).

In human hematopoietic stem cells c-Myc expression is required for the ability of the stem cells to leave the niche and differentiate (Baena et al., 2007; Dubois et al., 2008; Wilson et al., 2004). In addition, data from cell culture indicate a role for c-Myc in hematopoietic stem cell self-renewal (Satoh et al., 2004). Moreover, the combined action of c- and N-Myc is required to prevent apoptosis of hematopoietic stem cells (Laurenti et al., 2008).

In contrast, c-Myc prevents differentiation in human keratinocytes (Gandarillas and Watt, 1997). Likewise, in mouse epidermal stem cells c-Myc overactivation leads to loss of the stem cells by differentiation. Additionally, here c-Myc levels further dictate the fate of the differentiating offspring cells (Arnold and Watt, 2001; Berta et al., 2010; Waikel et al., 2001). Mouse NSCs require N-Myc for proliferation and inhibition of premature differentiation and N-Myc is involved in determining neuronal versus glial fate (Knoepfler et al., 2002; Nagao et al., 2008). Moreover, mammary stem cells require c-Myc for self-renewal (Moumen et al., 2012). In erythroblasts, c-Myc does not influence differentiation but prevents apoptosis (Dubois et al., 2008). To summarize, Myc has diverse functions in mammalian stem cells and can induce or prevent differentiation, regulate cell fate and stem cell maintenance dependent on the cellular context.

Remarkably, c-Myc is one of the factors supporting induction pluripotency (Takahashi and Yamanaka, 2006). The exact mechanism of c-Myc function in induction of pluripotency is still under investigation and hypotheses have considered cell cycle entry, regulation of microRNAs and epigenetic reprogramming to allow dedifferentiation (Knoepfler, 2008; Lin et al., 2009). The latter might be at least in part executed by the Tip60 complex, which would make the Tip60 complex an interesting candidate in regulating the spontaneous differentiation of ESCs upon co-depletion of *N*- and *c-myc* (Lin et al., 2009; Ravens et al., 2015; Varlakhanova et al., 2010).

In *Drosophila* Myc is encoded by only one gene also known as *diminutive* and believed to function homologous to c-Myc. Here, the role of Myc in stem cells is similarly ambiguous as in mammalian stem cells (Quinn et al., 2013). Knockdown of *myc* in adult ISCs reduces proliferation, but only when induced over a long time period, and does not influence ISC maintenance (Ren et al., 2013). While knockdown of *myc* reduces germline stem cell proliferation in the testis and leads to a loss of the stem cells, *myc* knockdown in the female germline stem cell was not found to affect stem cell maintenance (Jin et al., 2008; Siddall et al., 2009). However, endogenous downregulation of *myc* in female germline stem cells is required for differentiation and exit from the stem cell niche by competition between germline stem cells expressing high and low Myc levels (Jin et al., 2008). In the larval nervous system Myc is expressed in NBs and downregulated by Brat in offspring cells, which inhibits Myc-induced overproliferation. NB tumors upon *brat* depletion are most probably driven by a failure in *myc* downregulation, thus Myc was postulated to maintain NB self-renewal and to prevent premature differentiation (Betschinger et al., 2006).

Together, Myc function in mammalian and *Drosophila* stem cells highly relies on the cellular context and shows fundamentally different modes of action dependent on the stem cell type. To date, it is not well understood which factors define Myc function and unraveling these factors might be a great benefit for potential treatment strategies of Myc driven tumors.

1.5. Scope of the thesis

Stem cell research is an expanding field contributing significantly to the development of stem cell therapies and providing insight into how cancer cells might immortalize and circumvent restriction of proliferation. Several recent studies have highlighted the importance of chromatin remodeling complexes in cancer, stem cells and differentiation (Chen and Dent, 2014; Meshorer, 2007; Nair and Kumar, 2012). Chromatin remodelers operate on diverse cellular functions, like DNA repair, genome maintenance and transcriptional regulation. Unraveling which functions of chromatin remodelers are required for specific cell types, like stem cells, and which cofactors regulate these processes remains challenging due to the vast variety of interactors and regulated processes (Clapier and Cairns, 2009). The Tip60 complex has been investigated with growing interest, due to its implication in stem cell maintenance and tumorigenesis (Yamada, 2012). The diversity of Tip60 interactors in stem cells sets the complex as a potential key regulator of self-renewal (Chen et al., 2013; Fazzio et al., 2008a; Lu et al., 2015; Ravens et al., 2015). However, it remains unclear whether the Tip60 complex functions similarly in all stem cells, how subunits vary between functions and which cofactors play key roles in Tip60 directed stem cell maintenance.

This study seeks to investigate the role of Dom, the Tip60 complex ATPase subunit, in maintenance of *Drosophila* stem cells. As Dom was initially identified as a potential Baz interactor, I focus on the NB population as proxy for asymmetrically dividing stem cells. To unravel the Dom associated chromatin remodeling complex and elucidate whether Dom functions as a p400 or SRCAP homolog in *Drosophila* stem cell maintenance, additional subunits and the importance of the Tip60 HAT are considered. I aim to resolve the mechanism by which Dom maintains NBs and therefore potentially other stem cell populations and examine potential cofactors required in this process.

2. Materials and Methods

2.1. Materials

2.1.1. Chemicals, enzymes and kits

Chemicals, reagents, enzymes and kits were purchased from one of the following companies: AppliChem GmbH, Becton Dickinson GmbH, Bioline, Bio-Rad, Carl Roth GmbH, GE Healthcare, Genecraft, Gibco/BRL Life Technologies, Macherey Nagel, Merck Chemicals GmbH, Perbio Science, Roche Diagnostics, Sigma-Aldrich, ThermoFisher Scientific.

2.1.2. Antibodies

2.1.2.1. Primary antibodies

Primary antibodies used in this study are listed. IF = Immunofluorescence, WB = Western blotting, DSHB = Developmental Studies Hybridoma Bank.

Antigen	Host	Application	Dilution	Reference/Source
aPKC	Rabbit	IF	1:1000	Santa Cruz sc-216
Baz	Rabbit	IF	1:1000	Wodarz et al. 2000
β-Tub	Mouse	IF	1:50	DSHB (E7)
β-Gal	Mouse	IF	1:20	DSHB (JIE7)
Crb	Mouse	IF	1:20	DSHB (Cq4)
Dlg	Mouse	IF	1:20	DSHB (4F3)
Dom (SAC523)	Rabbit	IF	1:400	This study
FasIII	Mouse	IF	1:20	DSHB (7G10)
GFP	Mouse	IF	1:1000	Invitrogen A11120
GFP	Rabbit	IF/WB	1:1000	Invitrogen A11122
H4K8Ac	Rabbit	IF	1:2000	Abcam ab15823
Mira	Guinea pig	IF	1:1000	Halbsgut et al. 2011
Pros	Mouse	IF	1:50	DSHB (MR1A)
pH3	Mouse	IF	1:1000	Cell Signaling #97068
pH3	Rabbit	IF	1:500	Millipore #06-570
Repo	Mouse	IF	1:5	DSHB (8D12)

2.1.2.2. Secondary antibodies

For Western blotting (WB) and immunofluorescence (IF) the following secondary antibodies were used:

Antigen Ig	Host	Conjugate	Application	Dilution	Source
Rabbit	Goat	HRP	WB	1:10000	Dianova, 111-035-144
Mouse	Goat	AF488	IF	1:200	Invitrogen, A11029
Mouse	Goat	AF555	IF	1:200	Invitrogen, A21424
Mouse	Goat	AF647	IF	1:200	Invitrogen, A21236
Guinea pig	Goat	AF488	IF	1:200	Invitrogen, A11073
Guinea pig	Goat	AF555	IF	1:200	Invitrogen, A21435
Guinea pig	Goat	AF647	IF	1:200	Invitrogen, A21450
Rabbit	Goat	AF488	IF	1:200	Invitrogen, A11008
Rabbit	Donkey	Cy3	IF	1:200	Dianova, 711-165-152
Rabbit	Goat	AF647	IF	1:200	Invitrogen, A21450

2.1.3. Fly stocks

The following fly stocks have been used in this study. Balancer fly lines have been ordered from Bloomington Drosophila Stock Center or were present in the AG Wodarz stock collection. BL = Bloomington Drosophila Stock Center, V = Vienna Drosophila RNAi Center. For additional fly stocks see Appendix Table S 1.

Stock	Genotype	Description	Source/Reference
Wild type fly line			
w^{1118}	*w^{1118}*	white eyes	BL5905
Gal4 driver lines			
act::Gal4	*act::Gal4/TM6B (Dfd::YFP)*	Ubiquitous driver	BL4414
insc::Gal4	*UAS::dcrII,insc::Gal4*	AMP and NB specific driver	Neumüller et al., 2011
insc::Gal4, UAS::CD8-GFP	*UAS::dcrII,insc::Gal4, UAS-CD8::GFP/CyO*	GFP marked AMP and NB specific driver	Neumüller et al., 2011
en::Gal4, UAS::CD8-GFP	*en::Gal4, UAS::CD8-GFP*	Gal4 and GFP expression in posterior parts of each embryonic segment and imaginal discs	Wodarz stock collection
UAS::Gal4	*UAS::Gal4;UAS::Gal4; UAS::Gal4*	To amplify Gal4 driven expression	BL5940

Stock	Genotype	Description	Source/Reference
Dom fly lines			
dom^{14}	*dom^{14},FRT42B/ CyO(twi::GFP)*	*dom* null mutant	Ruhf et al., 2001
dom^{k08108}	*dom^{k08108}/ CyO(twi::GFP)*	*dom* mutant allele and β-Gal reporter	Braun et al., 1997
UAS::DomA	*UAS::DomA*	Dom overexpression	BL64261, BL64262
UAS::DomB	*UAS-DomB/ CyO(twi::GFP)*	Dom overexpression	BL64263
UAS::DomB; UAS::Gal4	*UAS::DomB; UAS::Gal4*	Dom overexpression, boosted via Gal4 expression	BL64263
UAS::dcrII; UAS::dom-RNAi	*UAS::dcrII; UAS::dom-RNAi*	dom-RNAi line, dcrII expression for higher efficiency of RNAi	V7787
UAS::dom-RNAi	*UAS::dom-RNAi*	dom-RNAi lines	V7787, BL34827, BL38385, BL41674
UAS::DomB; UAS::dom-RNAi	*UAS::DomB/ CyO(twi::GFP); UAS::dom-RNAi*	dom-RNAi line with DomB overexpression	BL64263, V7787
GFP-Dom	*dom::GFP-Dom*	Expressed N-terminally GFP tagged Dom under the endogenous *dom* promoter	Buszczak et al., 2007 (BA00164)
Df(2R)AA21	*Df(2R)AA21/ CyO(twi::GFP)*	Deficiency removing *dom* gene	BL3447
Df(2R)BSC821	*Df(2R)BSC821/ CyO(twi::GFP)*	Deficiency removing *dom* gene	BL27582
dom duplication	*Dp(2;3)CH321-01P07,M(CH321-01p07)ZH-86Fb*	Duplication including *dom* inserted on III	BL34492
Fly lines for the manipulation of Tip60 complex members			
UAS::Brd8-RNAi	*UAS::Brd8-RNAi*	Brd8-RNAis	V104879
UAS::DMAP1-RNAi	*UAS::DMAP1-RNAi*	DMAP1-RNAi	V103734
UAS::MrgBP-RNAi	*UAS::MrgBP-RNAi*	MrgBP-RNAis	V41402
UAS::Nipped-A-RNAi	*UAS::Nipped-A-RNAi*	Nipped-A-RNAis	V52487,
UAS::rept-RNAi	*UAS::rept-RNAi*	rept-RNAis	V19021
UAS::pont-RNAi	*UAS::pont-RNAi*	pont-RNAi	v105408
UAS::Tip60	*UAS::Tip60*	Tip60 overexpression	Lorbeck et al., 2011
UAS::Tip60-RNAi	*UAS::Tip60-RNAi*	Tip60-RNAi	Zhu et al., 2007

Stock	Genotype	Description	Source/Reference
Fly lines for H2Av knockdown			
UAS-H2Av-RNAi	*UAS-H2Av-RNAi*	UAS-H2Av-RNAi	V12768, V110598, BL28966
UAS-H2Av-RNAi	*UAS-H2Av-RNAi/ TM6B*	UAS-H2Av-RNAi	BL34844
Fly lines for the investigation of apoptosis			
UAS::P35	*UAS::P35*	Expresses the apoptotic inhibitor P35	BL5072
UAS::P35; UAS::dom-RNAi	*UAS::P35; UAS::dom-RNAi*	Dom-RNAi expressed with P35	BL5072, V7787
UAS::rpr	*UAS::rpr*	Expresses the apoptosis inducer Rpr	BL5823
H99	*Df(3L)H99/ TM6(Ubi::GFP)*	Triple for rpr, hid and grim, abolishes the induction of most apoptotic events	BL1576
Dom14;H99	*Dom14,FRT42B/ CyO(twi::GFP); Df(3L)H99/ TM6(Ubi::GFP)*	Dom null mutant in which apoptosis cannot be induced by rpr, hid, grim	Generated from *dom*^{14} (Ruhf et al., 2001) and BL1576
Fly lines for MARCM analysis			
MARCM driver line	*hs::flp,elav::Gal4, UAS::CD8-GFP; FRTG13,tub::Gal80*	MARCM line for the induction of mitotic, GFP positive cell clones on chromosome II	Wodarz stock collection
FRTG13		FRT on chromosome II for control MARCM clones	BL1956
Fly lines for the manipulation of potential Dom/Tip60 complex interactors			
UAS::CBP	*UAS::CBP-V5*	Overexpression of V5-tagged CBP	BL32573
UAS::CBP^{F2161A}	*UAS::CBP*^{F2161A}*-V5*	Expresses HAT deficient V5-tagged CBP	BL32574
UAS::CBP^{F2161A}*, UAS::CBP-RNAi*	*UAS::CBP*^{dF2161A}*-V5, UAS::CBP-RNAi*	Expresses HAT deficient V5-tagged CBP together with CBP-RNAi	BL32579
UAS::CBP-RNAi	*UAS::CBP-RNAi*	CBP-RNAi	V46534, V102885, V105115, BL27724, BL31728, BL32576, BL32577, BL37489
UAS::myc	*UAS::myc*	Myc overexpression	BL9674

Stock	Genotype	Description	Source/Reference
UAS::myc-RNAi	*UAS::myc-RNAi*	myc-RNAi	V2947, V2948, V106066, BL25783, BL25784, BL36123 (strong),
UAS::myc-RNAi	*UAS::myc-RNAi/ CyO(twi::GFP)*	myc-RNAi	BL43962
UAS::myc-RNAi	*UAS::myc-RNAi/ Sm6-TM6B*	myc-RNAi (weak)	BL51454
UAS::p53	*UAS::p53/TM6B*	Overexpression of p53	BL8418
UAS::p53	*UAS::p53/Sm6-TM6B*	Overexpression of p53	BL6584
UAS::p53^{R155H}	*UAS::p53^{R155H}/ CyO(twi::GFP)*	Expresses p53 with defective DNA binding domain	BL8419
UAS::p53^{H159N}	*UAS::p53^{H159N}*	Expresses p53 with defective DNA binding domain	BL8420, BL8421, BL8422
UAS::p53-RNAi	*UAS::p53-RNAi*	p53-RNAi	V10692, V38235, V45138, V45139, V103001, BL29351, BL41720
UAS::p53-RNAi	*UAS::p53-RNAi/TM6B*	p53-RNAi	BL36814
UAS::p53-RNAi	*UAS::p53-RNAi/ CyO(twi::GFP)*	p53-RNAi	BL41638
Fly lines for manipulation of potential Dom interactors together with *dom*			
UAS::Tip60; UAS::dom-RNAi	*UAS::Tip60; UAS::dom-RNAi/TM6B*	Overexpression of Tip60 and *dom* knockdown	Tip60: Lorbeck et al., 2011 dom: V7787
UAS::DomB; UAS-p53	*UAS::DomB; UAS-p53/ Sm6-TM6B*	Overexpression of DomB and p53	p53: BL8418 dom: BL64263
UAS::p53^{R155H}; UAS::dom-RNAi	*UAS::p53^{R155H}; UAS::dom-RNAi/ TM6B*	Expression of DNA binding deficient p53 in *dom* knockdown	p53: BL8419 dom: V7787
UAS::p53^{H159N}; UAS::dom-RNAi	*UAS::p53^{H159N}; UAS::dom-RNAi/ Sm6-TM6B*	Expression of DNA binding deficient p53 in *dom* knockdown	p53: BL8420 dom: V7787
UAS::p53-RNAi; UAS::dom-RNAi	*UAS::p53-RNAi; UAS::dom-RNAi/TM6B*	Knockdown of *p53* and *dom*	p53: BL41638, V38235, V45139, V103001 dom: V7787
UAS::myc; UAS::dom-RNAi	*UAS::myc; UAS::dom-RNAi/TM6B*	Overexpression of Myc and knockdown of *dom*	myc: BL9674 dom: V7787
UAS::DomB; UAS-myc-RNAi	*UAS::DomB; UAS-myc-RNAi/ Sm6-TM6B(ubi::GFP)*	Overexpression of DomB, knockdown of *myc*	myc: BL36123 dom: BL64263

Stock	Genotype	Description	Source/Reference
Other fly lines			
act::GFP	*Mega/FM7(act::GFP); sp/CyO*	Ubiquitous GFP expression	Wodarz stock collection

2.1.4. Oligonucleotides

Primer	Sequence (5' – 3')	Application
DomGatefor	CACCATGAATGAAGGTAATTCAGCA	Cloning of *dom* fragment for antibody production against N-terminus, forward primer
DomAbNterm+Stop	ACCTTGTTGCGTTAGCTGGACGATAA	Cloning of *dom* fragment for antibody production against N-terminus, reverse primer

2.1.5. Vectors

Vector	Description	Source
pENTR/D-TOPO	Gateway entry vector, kanamycin resistance	Invitrogen
pGGWA	Expression vector for GST fused proteins	Busso et al., 2005

2.1.6. Bacterial strains

E. coli strain	Genotype	Application
DH5α	*Φ80lacZΔM15, ΔlacZYA-argF)U169, deoR, recA1, endA1, hsdR17(rk-, mk+), phoA, supE44, λ-, thi-1, gyrA96, relA1*	Amplification of plasmid DNA
XL1-Blue	*endA1, gyrA96(nalR), thi-1, recA1,relA1,lac, glnV44, F'[Tn10 proAB+lacIq Δ(lacZ)M15], hsdR17(rk-, mk+)*	Amplification of plasmid DNA
BL21-DE3	*fhuA2 [lon] ompT gal (λ DE3) [dcm] ΔhsdS λ DE3 = λ sBamHIo ΔEcoRI-B int::(lacI::PlacUV5::T7 gene1) i21 Δnin5*	Protein expression for antibody production
TOP10	*FÅL[lacIq, Tn10(TetR)]mcrAΔ (mrrhsdRMS-mcrBC) Φ80lacZΔM15, ΔlacX74, recA1, araD139, Δ(araleu), 7697 galUgalKrpsL (StrR) endA1 nupG*	Cloning of PCR fragments into pENTR vector

2.1.7. Buffer and reagent recipes

Tris-HCl (1 M):

Component	Amount	Final concentration
Tris base	157.6 g	1 M
HCl		Set to required pH
Final volume (ddH_2O)	1 L	

2.1.7.1. Recipes for molecular biology methods

500 mM EDTA pH 8: Autoclave before use.

Component	Amount	Final concentration
EDTA	93 g	500 mM
NaOH		Set pH to 8
Final volume (ddH_2O)	500 mL	

500 mM EGTA pH 8: Autoclave before use.

Component	Amount	Final concentration
EGTA	95 g	500 mM
NaOH		Set pH to 8
Final volume (ddH_2O)	500 mL	

LB antibiotic plates: Agar plates for selection of bacteria with antibiotic resistance. Autoclave directly after adding water. Cool down until hand warm (50 °C) and add antibiotics in the required concentration (50 µg/mL kanamycin, 100 µg/mL ampicillin). Pour into petridishes and store lid down at 4 °C.

Component	Amount
Trypton	4 g
Yeast extract	2 g
NaCl	4 g
Agar Agar	65 g
Final volume (ddH_2O)	400 mL

LB medium: Medium for raising bacteria. Autoclave immediately.

Component	Amount
Trypton	10 g
Yeast extract	5 g
NaCl	5 g
Final volume (ddH_2O)	1 L

50x TAE: Buffer for running agarose gels. Dilute to 1x before use.

Component	Stock	Amount	Final concentration
Tris base		242.28 g	2 M
EDTA pH 8	0.5 M	100 mL	50 mM
Acetic acid			Set pH to 7.4
Final volume (ddH_2O)	1 L		

TE buffer pH 8.0:

Component	Stock	Amount	Final concentration
Tris-HCl pH 8	1 M	1 mL	10 mM
EDTA pH 8	500 mM	10 µL	0.5 mM
Final volume (ddH_2O)	10 mL		

SOC medium: Bacterial culture medium for plasmid transformation. pH should be 7.0. Autoclave and freeze aliquots at –20 °C.

Component	Stock	Amount	Final concentration
Trypton	-	4 g	2%
Yeast extract	-	1 g	0.5%
NaCl	1 M	1.7 mL	8.5 mM
KCl	1 M	0.5 mL	2.5 mM
$MgCl_2$	1 M	2 mL	10 mM
Glucose	1 M	4 mL	20 mM
Final volume (ddH_2O)	200 mL		

S1 Mini prep buffer: For plasmid purification in small scale. pH should be 8.0. Can be prepared and kept in larger amounts without adding RNase A. With RNase store at 4 °C.

Component	Stock	Amount	Final concentration
Tris-HCl pH 8.0	1 M	5 mL	50 mM
EDTA pH 8.0	500 mM	2 mL	10 mM
RNase A	10 mg/mL	1 mL	100 µg/mL
Final volume (ddH_2O)	1 L		

S2 Mini prep buffer: For plasmid purification in small scale.

Component	Stock	Amount	Final concentration
NaOH	1 M	200 mL	200 mM
SDS	20%	50 mL	1%
Final volume (ddH_2O)	1 L		

S3 Mini prep buffer: For plasmid purification in small scale. pH should be 5.1. Store at 4 °C.

Component	Amount	Final concentration
KAc	274.82 g	2.8 M
Final volume (ddH_2O)	1 L	

2x YT: E coli culture medium for protein purification.

Component	Amount
Tryptone peptone	16 g
Yeast extract	5 g
NaCl	5 g
Final volume (ddH_2O)	1 L

2.1.7.2. Recipes for biochemical methods

Protein purification buffer: Buffer for lysis, wash and elution for GST-tagged protein purification.

Component	Stock	Amount	Final concentration
Tris-HCl pH 8	1 M	50 mL	50 mM
NaCl		5.71 g	10 mM
EDTA pH 8	500 mM	200 µL	1 mM
EGTA pH 8	500 mM	200 µL	1 mM
Final volume (ddH_2O)	1 L		
Add immediately before use:			
Aprotinin			2 µg/mL
Leupeptin			2 µg/mL
Pefabloc			200 µg/mL
Pepstatin			2 µg/mL
DTT			5 mM

For lysis: Add 0.005 g lysozyme per 1 g of pellet.

For wash: Use as described.

For elution: Add glutathione in a final concentration of 20 mM.

2x SDS loading dye: For loading of protein samples on polyacrylamid gels.

Component	Stock	Amount	Final concentration
Bromophenolblue	1%	2 mL	0.2%
β-mercaptoethanol		140 µL	200 mM
Glycerol	100%	2 mL	20%
SDS	100%	400 µL	4%
Tris-HCl pH 6.8	1 M	1 mL	100 mM
Final volume (ddH_2O)	10 mL		

10x SDS running buffer: Stock for running SDS gels. Dilute to 1x with ddH_2O before use.

Component	Stock	Amount	Final concentration
Glycin		144.13 g	192 mM
Tris base		30.28 g	250 mM
SDS	10%	100 mL	1%
Final volume (ddH_2O)	1 L		

SDS PAGE: For separation of proteins based on their size by gel electrophoresis.

Separation gel: Mix the following chemicals in the indicated order and pour gel between glass plates for preparing an SDS gel. For larger proteins select a high percentage, for small proteins use preferably a smaller percentage of acrylamide.

Component	for 7.5%	for 10%	for 12.5%
30% Acrylamide/BIS (29:1)	1.9 mL	2.5 mL	3.1 mL
1 M Tris-HCl pH 8.8	2.8 mL	2.8 mL	2.8 mL
20% SDS	38 µL	38 µL	38 µL
ddH_2O	2.7 mL	2.1 mL	1.5 mL
10% APS	30 µL	30 µL	30 µL
TEMED	8 µL	8 µL	8 µL

Cover the gel with isopropanol until hardened to assure a flat edge between the gels. Remove isopropanol before pouring the stacking gel.

Stacking gel: Put comb between glass plates after pouring the stacking gel.

Component	Amount
30% Acrylamid/BIS (29:1)	310 µL
1 M Tris-HCl pH 6.8	235 µL
20% SDS	10 µL
ddH_2O	1.3 mL
10% APS	10 µL
TEMED	5 µL

20x TBS: Stock for Western blot washing buffer.

Component	Stock	Amount	Final concentration
Tris-HCl pH 8.0	1 M	400 mL	400 mM
NaCl		175.32 g	3 M
Final volume (ddH_2O)	1 L		

TBST: Western blot washing buffer.

Component	Stock	Amount	Final concentration
TBS stock	20x	50 mL	1x
Tween-20	10%	2 mL	0.1%
Final volume (ddH_2O)	1 L		

TNT buffer: Buffer for protein lysate preparation for SDS gel electrophoresis. Store at 4 °C.

Component	Stock	Amount	Final concentration
NaCl	1 M	30 mL	150 mM
Tris-HCl pH 8.0	1 M	10 mL	50 mM
Triton X-100	100%	2 mL	1%
Final volume (ddH_2O)	200 mL		

10x Western buffer: 10x stock solution for running wet blots (transfer buffer).

Component	Amount	Final concentration
Tris base	30.29 g	250 mM
Glycine	144.13 g	192 mM
Final volume (ddH_2O)	1 L	

1x Western buffer: Wet blot buffer (transfer buffer).

Component	Stock	Amount	Final concentration
10x Western buffer	10x	100 mL	1x
Methanol	99.9%	200 mL	20%
Final volume (ddH_2O)	1 L		

Western blot blocking buffer

Component	Stock	Amount	Final concentration
TBS	20x	12.5 mL	1x
Tween-20	10%	2.5 mL	0.1%
Skim milk powder		7.5 g	3%
BSA		2.5 g	1%
Final volume (ddH_2O)	250 mL		

2.1.7.3. Recipes for histology and cell culture

Apple agar plates: For egg deposition.

Component	Amount
Agar-agar	20 g
Sugar	8.5 g
Fill up to 500 mL with H_2O	
Apple juice	170 mL
Cook in microwave until the agar is in solution, allow to cool down to 60 °C	
10% Nipagin in ethanol	10 mL
Pour into big or small petri dishes, store at 4 °C, lid down	

CTX: Buffer required for TUNEL procedure. Store at 4 °C.

Component	Stock	Amount	Final concentration
Na_3Citrate		14.71 g	100 mM
Triton X-100	10%	0.5 mL	0.1%
Final volume (ddH_2O)	50 mL		

Hoyers medium: For cuticle preparations of embryos. Mix 1:1 with lactic acid before use.

Component	Amount
Gum arabic	30 g
Stir overnight in 50 mL ddH_2O	
Chloral hydrate	200 g
Add slowly while stirring until dissolved:	
Glycerol	20 g
Centrifuge for 15 min at 11000 rpm to remove debris	

KCM: Washing buffer for polytene chromosome preparations.

Component	Stock	Amount	Final concentration
KCl	1 M	120 mL	120 mM
NaCl	1 M	20 mL	20 mM
Tris-HCl pH 8.0	1 M	10 mL	10 mM
EDTA pH 8	500 mM	10 mL	0.5 mM
Triton X-100	100%	1 mL	0.1%
Final volume (ddH_2O)	1 L		

Lead citrate: For EM-contrasting.

Component	Amount	Final concentration
$Pb(NO_3)_2$	1.33 g	134 mM
$Na_3(C_6H_5O_7)$x2 H_2O	1.76 g	200 mM
Final volume (ddH_2O)	30 mL	

- Shake vigorously for 1 min, a white precipitate forms, wait shortly
- Shake for 30 min
- Add 6 – 8 mL of 1 N NaOH in drops until the solution is clear
- Add volume up to 50 mL with ddH_2O (pH should be 12.0)
- Leave bottle open only as short as possible: Incubation with CO_2 produces lead carbonate precipitate

Modified Rinaldini solution: Cell Culture Buffer.

Component	Amount	Final concentration
NaCl	800 mg	136.9 mM
$NaHCO_3$	100 mg	11.9 mM
Glucose	100 mg	5.6 mM
KCl	20 mg	2.7 mM
NaH_2PO_4	5 mg	4.2 mM
Final volume (ddH_2O)	100 mL	

Mowiol: For mounting of samples for light and confocal microscopy.

Component	Amount
Mowiol	5 g
1x PBS	20 mL
Glycerol	10 mL

10x PBS: Autoclave and dilute with ddH_2O to 1x before use. To prepare 1x PBST add Tween-20 (for PBSTw) or Triton X-100 (for PBSTx) in the required amount.

Component	Amount	Final concentration
NaCl	80 g	140 mM
KCl	2 g	10 mM
Na_2HPO_4 x 2 H_2O	14.4g	6.4 mM
KH_2PO_4	2 g	2 mM
NaOH		Set pH to 7.4
Final volume (ddH_2O)	1 L	

Toluidine blue staining solution: Staining of semithin sections.

Chemical/ Buffer	Required amount	Final concentration
Solution A		
Toluidine blue	0.2 g	0.2%
Final volume (ddH_2O)	100 mL	
Solution B (filtrated)		
Sodium tetraborate	0.5 g	1%
Methylene blue	0.5 g	1%
Final volume (ddH_2O)	50 mL	
Mix final solution before use and sterile filter it:		
Solution A Solution B	5 mL 5 mL	0.01% Toluidine blue 0.05% Sodium tetraborate 0.05% Methylene blue
Final volume (ddH_2O)	100 mL	

Phosphatebuffer: 0.1 M PO_4 pH 7.2 after Sørensen. Buffer required for preparation of EM and semithin-histological specimen preparation.

Component	Stock	Amount	Final concentration
Na_2HPO_4	0.2 M (autoclaved)	36 mL	0.1 M total PO_4
NaH_2PO_4	0.2 M (autoclaved)	14 mL	
Final volume (ddH_2O)	100 mL		

2.1.7.4. Recipes for fly work

10% Nipagin:

Chemical/ Buffer	Stock	Required amount	Final concentration
Ethanol	99%	700 mL	70%
Nipagin ($C_8H_8O_3$)		100 g	10%
Final volume (ddH_2O)	1 L		

Standard medium: For fly keeping (Ashburner, 1989).

- Heat 9.5 L water, add Agar Agar (50 g), brewer's yeast (168 g), soy flour (95 g)
- Mix until foam forms
- Add the following components one by one and mix in between: 450 g malt extract, 400 g treacle, 712 g polenta
- Cook for 45 min
- Cool down to 60 °C then add 45 mL propionic acid and 150 mL 10% nipagin

2.1.8. Microscope and imaging systems

Axioimager:	Carl Zeiss Jena GmbH
Binocular Stemi 2000:	Carl Zeiss Jena GmbH
Fluorescence Binocular:	Leica MZ 16 FA
LSM 510 Meta:	Carl Zeiss Jena GmbH
LSM 880 (with Airyscan):	Carl Zeiss Jena GmbH
FV1000 confocal microscope:	Olympus
X-Ray developer:	Tenetal Roentogen
EM 109:	Carl Zeiss Jena GmbH
EM 912:	Carl Zeiss Jena GmbH

2.1.9. Other systems

Western blot detector:	Tenetal Roentogen
FACSVantage SE:	Becton Dickinson Biosciences
Mastercycler gradient 5331:	Eppendorf
Centrifuge Z446 K:	Hermle
Centrifuge Z216 M:	Hermle
Centrifuge 5417 R:	Eppendorf
Incubation shaker Minitron:	Infors HT
Cooled incubator 3201:	Rubarth Apparate GmBH (Rumed)
Incubator B6:	Heraeus
BioPhotometer 6131:	Eppendorf
NanoDrop 2000:	ThermoFisher Scientific
TapeStation:	Agilent Technologies, Inc. 2014
Sonopuls UW 2070:	Bandelin

2.1.10. Software

LSM 5 Image Browser:	Carl Zeiss Jena GmBH
Zen black:	Carl Zeiss Jena GmBH
FIJI:	Schindelin et al., 2012
Inkscape:	Free Software Foundation, Inc.
DNA sequence analysis:	DNA-Star Lasergene V7

2.2. Methods

2.2.1. Molecular biology methods

2.2.1.1. mRNA extraction

mRNA was extracted from an overnight egg deposition from w^{1118} flies in order to reverse transcribe it to cDNA for cloning purposes. For mRNA extraction the Milteny Biotec µMACS kit was used according to the manufacturer's instructions. In short the tissue was homogenized in 1 mL lysis buffer and transferred to the column in a centrifuge tube and then centrifuged for 3 min at 13000 g. The cleared flowthrough lysate was incubated with

25 µL Oligo(dT) micro beads and subsequently added to a rinsed MACS column placed in a magnetic MACS separator which retains the magnetic Oligo(dT) beads and bound mRNA. The MACS column was rinsed once each with lysate buffer, wash buffer and pre-heated elution buffer. The final elution was done with 50 µL pre-heated elution buffer to a RNase-free microtube. Concentrations were measured with a photometer and RNA was stored at -80 °C.

2.2.1.2. cDNA production

cDNA was reverse transcribed from mRNA using the First Strand cDNA Synthesis Kit (ThermoFisher Scientific) according to the enclosed instructions. 400 ng of mRNA was mixed with 10 µL 10x dsDNase buffer and dsDNase each on ice in an RNase free tube and then added up with RNase free water to 10 µL. The solution was heated for 2 min at 37 °C prior to adding 100 pmol oligo$(dT)_{18}$ primer and 1 µL 10 mM dNTP Mix. The volume was made up to 15 µL with RNase free water. 4 µL 5x RT Buffer and 1 µL Maxima H Minus Enzyme Mix were added. After mixing, the solution was incubated for 30 min at 50 °C and the reaction was terminated by 5 min incubation at 85 °C. cDNA was stored at -20 °C.

2.2.1.3. Polymerase chain reaction

For the amplification of specific DNA fragments a polymerease chain reaction (PCR) was performed (Saiki et al., 1985). The following ingredients were mixed in a PCR tube:

cDNA	2 µL
Forward primer (10 µM)	0.8 µL
Reverse primer (10 µM)	0.8 µL
dNTPs (25 mM each)	0.2 µL
10x polymerase buffer	2 µL
Polymerase	0.5 µL
ddH_2O	ad 20 µL

The PCR reaction was then subjected to a PCR program to allow *in vitro* DNA amplification.

Time	Temperature	Purpose	
5 min	95 °C	Initial denaturation	
30 s	95 °C	Denaturation	⎫ 35 cycles
30 s	50 – 65 °C (primer specific)	Annealing	⎪
90 s/kb (Pfu) 60 s/kb (Taq)	72 °C	Elongation	⎭
5 min	72 °C	Final elongation	

The annealing temperature was selected based on the primer specific melting temperature, elongation time depended on the length of the desired DNA fragment. PCR products were confirmed by agarose gel electrophoresis.

2.2.1.4. Agarose gel electrophoresis

Agarose gel electrophoresis was performed to separate DNA fragments based on their size based on the fact that negatively charged DNA migrates towards the cathode in an electric field (Schwartz and Cantor, 1984). Agarose gels (1% w/v agarose, 40 mM Tris, 10 mM EDTA, 0.5 µg/mL ethidium bromide) were overlaid with TAE buffer. The sample was mixed with 1/6 volume of DNA loading buffer (Fermentas) prior to loading. For discrimination of fragment size, GeneRuler 1kB DNA ladder (Fermentas) was loaded to a separate pocket. The gel was run at 120 V for 20 – 30 min. DNA bands were visualized using ethidium bromide under UV light.

2.2.1.5. DNA extraction from agarose gels

To obtain DNA fragments of specific sizes from a mixture of DNA fragments the DNA was subjected to agarose gel electrophoresis and the band of the desired size was cut out. DNA was extracted using NucleoSpin Extract II Kit (Macherey-Nagel). In short, the agarose gel piece was molten in NTI buffer, loaded to a column and centrifuged shortly to remove excess liquid and the column was then washed twice with 700 µL NT3 buffer. After an additional centrifugation step for drying of the column, 20 µL pre-heated NE elution buffer were added and DNA was eluted by centrifugation into a fresh microtube.

2.2.1.6. Gateway cloning and transformation of *Escherichia coli*

DNA fragments were cloned into the pENTR/D-TOPO vector (Invitrogen, K240020):

2 µL	PCR product / gel extraction
0.5 µL	Salt solution
0.5 µL	pENTR/D-TOPO vector

The mixture was incubated for 7 min at RT and then transformed to 50 µL chemocompetent Top10 *E. coli* cells by incubation on ice for 30 s. After 30 s heatshock at 42 °C, 250 µL pre-warmed SOC medium was added and the cells were allowed to grow for 1 h at 37 °C. Cells were plated on pre-warmed kanamycin containing LB agar plates. Bacteria were grown overnight at 37 °C and plasmid DNA was purified (2.2.1.7).

To clone DNA fragments contained in pENTR vectors into destination vectors for tagging of the construct, a clonase reaction was perfomed:

100 ng	pENTR vector containing validated DNA fragment
75 ng	Destination vector
1 µL	Clonase II
ad up to 5 µL	TE buffer pH 8.0

The reaction was incubated for 1 h at 25 °C and terminated by Proteinase K digest (0.5 µL) for 10 min at 37 °C. The reaction was transformed to chemocompetent *E. coli* (*XL1blue* or *DH5α*) as described before and clones were allowed to grow on ampicillin containing LB agar plates overnight at 37 °C before plasmid DNA purification.

2.2.1.7. Plasmid DNA purification

Single *E. coli* clones from an LB agar plate or few µL from a glycerol stock were cultured in antibiotic containing LB medium (depending on the plasmid) overnight at 37 °C. On the following day 1.5 mL culture were centrifuged for 3 min at 13000 rpm at RT. The supernatant was discarded and the bacteria lysed by adding 200 µL S1 buffer. 200 µL S2 buffer were added, the solution was mixed and incubated for 5 min at RT. 200 µL S3 buffer were mixed with the solution prior to centrifugation for 20 min at 13000 rpm at 4 °C. The supernatant was incubated in a new microtube with 400 µL isopropanol for DNA precipitation. After 30 min centrifugation at 13000 rpm at 4 °C the pellet was washed

with icecold 70 °C ethanol and again centrifuged for 5 min. The supernatant was discared and the pellet was dried at RT before resuspension in 20 µL ddH_2O.

For larger plasmid DNA amounts with higher purity the NucleoBond PC 100 (Macherey Nagel) was used according to the manufacturer's instructions. The purification method used here relies on the same principle but allows the clarification of the lysate over a column.

2.2.1.8. Preparation of glycerol stocks

For longterm storage of *E. coli* stocks 800 µL from an overnight *E. coli* LB culture were mixed with 200 µL 99% glycerol in a cryotube. The stocks were snapfrozen in liquid nitrogen and stored at -80 °C.

2.2.1.9. Validation of cloning products

To validate plasmids the DNA was digested with restriction enzymes for 1 h at 37 °C and the DNA fragments were inspected for correct size by agarose gel electrophoresis.

3 µL	Plasmid DNA
1 µL	10x restriction enzyme buffer
0.3 µL	Restriction enzyme
5.7 µL	ddH_2O

Correct plasmids were sequenced using the BigDye Terminator v3.1 kit (ThermoFisher Scientific).

0.5 µL	Plasmid DNA
1.5 µL	Seqbuffer
1.5 µL	SeqMix
0.8 µL	Sequencing primer (10 µM)
5.7 µL	ddH_2O

The mixture was subjected to a PCR program as shown in 2.2.1.3. DNA was precipitated by adding 1 µL of 125 mM EDTA, 1 µL 3 M NaAc and 50 µL 100% ethanol. After incubation for 5 min at RT the sample was centrifuged for 15 min at 13000 rpm and the pellet was washed with 70% ethanol. After air-drying the DNA was dissolved in 15 µL HiDi (Applied Biosystems). Sanger sequencing was performed by the in-house sequencing service in the Department of Developmental Biochemistry, GZMB, Göttingen.

2.2.2. Biochemical methods

2.2.2.1. Preparation of protein lysate

Protein lysate has been prepared from ovaries dissected in PBS and kept on ice until dissections were finished. The tissue was transferred into the homogenization buffer TNT containing the peptidase blockers pepstatin, aprotinin, leupeptin (2 µg/mL each) and pefabloc (200 µg/ml). The tissue was grinded and incubated for 20 min on ice with shaking. To obtain the protein lysate, the homogenate was centrifuged for 10 min 4 °C at 13000 rpm. The middle phase containing the protein was then used as protein lysate for Western blotting. For this, the lysate was mixed with equal amounts of 2x SDS loading buffer and heated for 5 min at 95°C to denature the proteins.

2.2.2.2. SDS-polyacrylamide gel electrophoresis

The SDS-polyacrylamide gel electrophoresis is a method to separate proteins based on their size. The negatively charged SDS binds to the proteins such that all proteins have a negative charge. In an electrical field they will thus run towards the cathode. In the SDS-polyacrylamide gel electrophoresis this migration happens in a gel containing polyacrylamide. In this polyacrylamide mesh smaller proteins migrate faster while larger proteins migrate slower (Laemmli, 1970).

For SDS gels, the BioRad system was used. Gels were placed into electrophoresis chamber containing 1x SDS running buffer. The protein samples and a protein ruler for size comparison were loaded into the gel pockets and the gel was run for circa 45 min at 200V.

2.2.2.3. Western blot

A Western blot is used to detect proteins with specific antibodies (Burnette, 1981). For this, the proteins were first separated via SDS-polyacrylamide gel electrophoresis and then transferred horizontally onto a nitrocellulose membrane by the use of an electrical field using the BioRad system. The blot was assembled in the following order: 2x Whatman, nitrocellulose membrane, SDS gel, 2x Whatman and then placed into the electrophoresis chamber with 1x Western buffer. The transfer was performed for 1 h with 100V at 4°C. Here the proteins, which are negatively charged due to the SDS, run towards

the nitrocellulose membrane, which is placed on the cathode side of the blot. After disassembly of the blot the transfer was confirmed with Ponceau staining of the nitrocellulose membrane.

The membrane was rinsed with TBST to remove the Ponceau and blocked for 30 min with Western blot blocking buffer to prevent unspecific binding of the antibodies. Afterwards, the membrane was incubated overnight at 4 °C with the primary antibody in Western blot blocking buffer under shaking.

On the following day the membrane was washed three times for 10 min with TBST with shaking. The secondary HRP-coupled antibody was diluted in Western blot blocking buffer and the membrane was incubated for 2 h at RT under shaking. After three times 10 min washing steps with TBST, the protein detection was performed using Pierce ECL Western Blotting Substrate. Here, the enzymatic activity of the HRP is used to chemically convert luminol and light is produced as a byproduct. This light was detected using X-Ray developing films (Fuji) and developing them with a Western blot developer.

2.2.2.4. Purification of GST-fusion proteins for antibody production

For the production of an antibody directed against the N-terminus of Dom, a GST-tagged fusion protein was purified from *BL21-DE3 E. coli* cells containing the DomAbN-term+Stop-pGGWA vector. Cloning procedures to obtain the DomAbN-term+Stop-pGGWA vector were kindly conducted by Mona Honemann-Capito. 200 µL chemocompetent *E. coli* cells were transformed as described in 2.2.1.6. A successfully transformed and confirmed clone was used for an overnight 50 mL LB culture containing 100 µg/mL ampicillin. From this, a 1 L 2x YT culture (with 100 µg/mL ampicillin) was grown to OD_{600} = 0.7. Protein expression was then induced by adding 20 mL 100% ethanol and 1 mL 0.5 M IPTG. The culture was incubated overnight at 16 °C. On the following day the culture was centrifuged for 15 min at 4 °C at 500 rpm and the pellet was snapfrozen in liquid nitrogen and then frozen for 2 – 12 h at -80 °C. The pellet was resuspended in 50 mL protein purification lysis buffer and mixed for 30 min on ice. After sonification (80%, cycle 7, 4 x 1 min with 15 s breaks) Triton X-100 was added in a final concentration of 1%. After 30 min incubation on ice the sample was centrifuged for 45 min at 4 °C and 16000 rpm. The supernatant was incubated with 1 mL pre-washed glutathione beads for 1 h at 4

°C. After centrifugation for 5 min at 500 rpm the beads were washed 4 times with 15 mL protein purification wash buffer. Ten elution steps were performed, each by adding 1 mL protein purification elution buffer. For each step the sample was incubated for 5 min at RT. The procedure was controlled by SDS gel electrophoresis and subsequent comassie staining of samples from each step of the protocol. A polyclonal antibody was produced in guinea pig by Eurogentec.

2.2.2.5. Coomassie staining

To stain proteins in a polyacrylamide gel, the gel was washed with ddH_2O and stained with 1:5 diluted Brilliant Blue R Concentrate (Sigma Aldrich) for 1 h at RT. After rinsing the gel with ddH_2O it was destained in 10% v/v acetic acid and 20% v/v ethanol. Protein bands appear blue in the polyacrylamide gel.

2.2.3. Histology and cell culture

2.2.3.1. Embryo fixation for immunostaining and TUNEL staining

Flies of the appropriate genotype were allowed to deposit eggs on an apple agar plate overnight at 25 °C. Embryos were carefully loosened from the plate using water and a brush and afterwards dechorionated for 3 min by adding equal amounts of sodium hypochlorite. After washing the embryos with water they were transferred into a glass vial containing 3 mL of heptane. For conventional immunofluorescence staining the embryos were fixated by adding PBS with 4% formaldehyde and incubated for 20 min on a rocker. For tubulin staining embryos were instead strong-fixed by adding 2.675 mL 37% formaldehyde and 300 µL 0.5 M EGTA pH 8 and then incubated for 5 min.

The fixation solution was replaced by 3 mL methanol and the embryos were vigorously shaken to remove the vitelline membrane until they sunk down into the methanol. The embryos were transferred into a 1.5 mL microtube and washed thrice with methanol. They were then stored at -20 °C or directly used for immunostaining.

2.2.3.2. Fixation of tissue for immunostaining

For immunostaining, larval, pupal and adult tissue was dissected using Dumont No 5 forceps in PBS and kept on ice until the fixation was started. Importantly, for staining of basally localized proteins in the NBs, the brains were kept on RT to prevent degradation of the microtubule network. After dissection the tissue was transferred either into a 1.5 mL microtube or, in case of very fragile tissue, into a dissection glass and fixed for 20 min at RT in a PBS with 4% formaldehyde under shaking.

2.2.3.3. Immunostaining

The tissue or embryos were washed thrice for 10 min at RT on a rocker. Generally, PBSTw containing 0.1% Tween-20 was used, in case of staining postembryonic gut PBSTx containing 0.1% Triton X-100 was used for the entire staining procedure. The tissue was permeabilized to assure the entry of the antibodies and blocked to prevent unspecific binding. The time and solution used for this step was dependent on the stained tissue:

Tissue	Blocking Solution	Blocking Time (min)
Embryos	PBSTw + 5% NHS	30
Postembryonic brain	PBSTx (1% Triton X-100) + 5% NHS	60
Imaginal discs	PBSTw + 5% NHS	30
Ovary	PBSTw + 5% NHS	30
Postembryonic gut	PBSTx + 5% NHS	30

After blocking, the tissue was incubated with the primary antibodies in the respective washing buffer containing 5% NHS. Primary antibody incubation was done overnight at 4 °C under shaking. On the next day, the tissue was washed three times in the respective washing buffer before incubation with the secondary antibody was started. The secondary fluorophor-coupled antibodies were diluted in washing buffer with 5% NHS and the tissue was incubated for 2 h at RT with shaking.

Subsequently, the specimen was washed once for 20 min in washing buffer containing either Hoechst 33342 (Hoechst) or DAPI. After washing twice for 10 min the tissue was mounted. Gut tissue was mounted in VectaShield and sealed with nail polish. All other tissue was mounted in mowiol. Larval and adult brain was mounted between two coverslips in mowiol to enable turning of the sample. The mounted brain sample was fixed on a slide by applying a small drop of water underneath the coverslips.

2.2.3.4. Polytene chromosome squashes

For investigation of DNA-binding proteins, polytene chromosome squashes were prepared using salivary glands of well-fed L3 larvae. Salivary glands were dissected in PBSTx containing 0.1% Triton X-100 and fixed for 30 to 60 s in PBSTx (0.1% Triton X-100) pH 7.5 containing 4% formaldehyde in a dissection glass. A drop of 50% acetic acid and 4% formaldehyde was given onto a poly-L-lysine coated superfrost slide. The salivary glands were transferred into the drop for 2 min for further fixation and spreading of the chromatin and then squashed by covering the drop with a coverslip and applying firm pressure with the thumb. The slide was cooled in liquid nitrogen and the coverslip was removed using a razor blade. The tissue was dehydrated for at least 10 min in 80% ethanol. The squashes could also be stored in 80% ethanol for up to one week.

For immunostaining the polytene squashes were rehydrated by first incubating them for 10 min in 40% ethanol and then 10 min in PBS at RT. Blocking was done for 1 h at RT in PBSTx containing 0.5% Triton X-100 and 2% BSA. Primary antibody incubation was done in a wet chamber overnight at 4 °C in KCM with 2% BSA. On the following day the squashes were washed for 15 min at RT in KCM and then incubated for 1 h in a wet chamber with the secondary fluorophor-coupled antibodies and DAPI or Hoechst in KCM with 2% BSA. After washing for 15 min with KCM the polytene squashes were mounted in mowiol.

2.2.3.5. Immunostaining of *Drosophila* cells

Fluorescence activated sorted cells were put on poly-L-lysine coated coverslips and placed into 24-well plate for 30-40 min at 25 °C to allow the cells to settle down. The medium was removed and cells were fixed with 4% formaldehyde for 15 min at RT. The cells were washed three times for 2 min with PBS and then blocked in PBSTx (0.2% Tween-20) with 5% NHS for 30 min at RT. After rinsing once with PBSTx the cells were incubated overnight at 4 °C with the primary antibodies dissolved in PBSTx containing 5% NHS. The cells were washed twice with PBSTx for 2 min and then incubated with the secondary fluorophor-coupled antibodies and Hoechst in PBSTx with 5% NHS for 1 h at RT. Following three times washing for 2 min in PBSTx the cells were mounted in VectaShield and sealed with nail polish.

2.2.3.6. TUNEL reaction

A TUNEL (terminal deoxynucleotidyl transferase-mediated dUTP nick end labeling) was performed on embryos to investigate apoptotic cell death after Wang et al. (1999). The embryos were immunostained as described above (2.2.3.1) until the incubation with the secondary antibody was finished. However, for TUNEL staining PBTx (0.3% Triton X-100) was used. The embryos were washed for 5 min and additionally fixated for 15 min in 4% formaldehyde. The formaldehyde was removed in two subsequent washing steps with PBTx for 10 min each. The buffer was then replaced with CTX and the embryos were again washed for 5 min and then heated at 65 °C in CTX for 30 min. After removing the buffer by a 5 min washing step with PBTx the embryos were washed twice with 100 µL TUNEL dilution buffer for 5 min (*In Situ* Cell Death Detection Kit, TMR Red from Roche). 30 µL of the TUNEL labeling solution were then added and the embryos were incubated for 5 min. Subsequently, the TUNEL reaction was performed by adding previously mixed 5 µL TUNEL enzyme and 45 µL TUNEL labeling solution. The embryos were incubated for 3 h at 37 °C. Afterwards embryos were washed and simultaneously stained with Hoechst for 20 min in PTX. After additional two washing steps for 10 min embryos were mounted in Mowiol.

2.2.3.7. Cuticle preparation from embryos

For wild type embryos an overnight egg deposition was used. For embryonic lethal mutants an overnight egg deposition was incubated for 48 h at 25 °C. During this time period, fresh yeast paste was repeatedly placed to the middle of the plate and discarded after a while to remove larvae.

Embryos were transferred to a net using water and a brush and washed several times with water. Sodium hypochlorite was added and embryos were dechorionated for 3 min and afterwards washed several times with water. The embryos were transferred to a drop of 50% Hoyers medium and 50% lactic acid on a slide and mounted with a coverslip. The slides were incubated overnight at 60 °C and then sealed with nail polish.

2.2.3.8. *Ex vivo* live imaging of whole mount L3 brains

Live imaging procedure was conducted according to Pampalona et al. (2015). For live imaging young L3 larvae were selected, washed once in Schneider's medium with 1 mg/mL glucose and then dissected in this medium. Per brain a 2 µL drop of fibrinogen solution (10 mg/mL fibrinogen, Sigma F3879-1G, in Schneider's medium with 1 mg/mL glucose, dissolved under shaking at 37 °C) was given on a FluoroDish (WPI FD35-100). The brains were oriented in the drop and the liquid spread using dissection forceps to prevent floating of the brain. 0.5 µL Thrombin (GE Healthcare 27-0846-01, 0.5 U in sterile PBS) were added to initiate clot formation. After coagulation for 10 min in the dark, the clot was washed once with Schneider's medium with 1 mg/mL glucose and then covered with the medium. Brains were analyzed by confocal imaging for up to 3 h. For this, a z-stack (≥ 20% overlap between the z-levels) through the ventral part of the brain lobe was taken every 2 min to ensure the imaging of NB divisions and the resulting daughter cells.

2.2.3.9. Sample preparation for semithin-histological sections and electron microscopy

Flies were allowed to deposit eggs on apple agar plates for 1 h at 25 °C and embryos were further incubated at 25 °C until they reached the desired stage (10 h 30 min for stage 13). Embryos were then washed and incubated with sodium hypochlorite for 3 min to achieve dechorionisation. After washing and carefully drying the embryos were fixed in 5% glutaraldehyde:

<u>Fixation solution I</u>

- 2 mL heptane
- 250 µL phosphate buffer
- 250 µL 50% glutaraldehyde

After 20 min heptane was removed, embryos were transferred to a coverslide with double-sided adhesive tape and overlaid with phosphate buffer to prevent drying out. The vitelline membrane was mechanically removed with a preparation needle. Embryos were washed with phosphate buffer several times and subsequently fixed in 1% osmium and 2% glutaraldehyde for 30 min in the dark.

Fixation solution II (mixed 1:1 shortly before use):

- 0.5 mL 4% osmium mixed with 0.5 mL phosphate buffer
- 0.1 mL 50% glutaraldehyde mixed with 1.15 mL phosphate buffer

After several phosphate buffer washing steps embryos were additionally fixed in 2% osmium (in phosphate buffer) for 1 h in the dark and on ice. Before subsequent procedures, embryos were first washed several times with phosphate buffer and then with ddH_2O. To dehydrate the fixed embryos, they were incubated in an ascending alcohol series:

- 30%, 50%, 70%, 90%, 96% for 5 min on ice each
- 100% dry ethanol 2 x for 10 min at RT
- 100% dry acetone 2 x for 10 min at RT

Embryos were incubated overnight at 4 °C in a mixture with equal parts of araldite (Sigma) and acetone. On the following day embryos were transferred to a dissection dish and acetone was allowed to evaporate for 1.5 h under the fumehood. Embryos were put into fresh araldite in an embedding form. After polymerization of the araldite at 65 °C for 1 – 2 days and trimming of dispensable araldite the samples were primed for cutting with the ultracut microtome.

2.2.3.9.1. Semithin-histological sections

For semithin-histological sections samples, 1 µM cuts were prepared and stained with toluidine blue staining solution for 2 min on a heating plate. Samples were analyzed by light microscopy with the Axioimager.

2.2.3.9.2. Ultrathin sections for electron microscopy

For electron microscopy, samples were cut to 50 – 100 nm and placed on electron microscopy grids. Contrasting was done after Reynolds (1963) with uranylacetate and lead citrate. Sections were incubated for 3 – 5 min in a drop of uranylacetate (2% in ddH_2O) and washed in several drops of ddH_2O. Subsequently, sections were incubated for 3 – 5 min in lead citrate drops (NaOH drops near the lead citrate drops prevents sodium carbonate precipitates). After several washes with ddH_2O sections were analyzed with EM109 transmission electron microscope at 80 kV.

2.2.4. Fly work

Drosophila fly lines were maintained at 18 °C in plastic vials containing fly food. Flies were anesthetized with CO_2 and sorted with a binocular. For crosses flies were incubated at 25 °C.

2.2.4.1. The Gal4-UAS system

The Gal4-UAS system is a binary system that was adapted from yeast. It utilizes the yeast transcription factor Gal4, which binds to a specific promoter sequences called upstream activating sequence (UAS) and activates expression of downstream gene products. In *Drosophila* this system is widely used for ectopic gene expression, timely controlled manipulation of gene expression and reporter expression (Brand and Perrimon, 1993). Since yeast preferably grows at 37 °C, optimal activation of the Gal4-UAS system is achieved at higher temperatures. To attain maximal expression of target genes in *Drosophila*, fly crosses in which the Gal4-UAS system was used were raised at 29 °C, a temperature at which the flies grow without heat shock. In cases in which target gene expression was lethal at 29 °C crosses were reared at 25 °C.

2.2.4.2. Mosaic analysis with a repressible cell marker

The mosaic analysis with a repressible cell marker (MARCM) method is an elegant method to induce mitotic cell clone positively marked with GFP (Lee and Luo, 1999; Lee and Luo, 2001). It combines two systems.

The Gal4-UAS system (Brand and Perrimon, 1993). Gal4 is expressed under a tissue specific promoter (here *elav* for expression in NBs) and used to express a UAS-responsive reporter (here CD8-GFP, a membrane tethered GFP). Gal4 is inhibited by Gal80, which is ubiquitously expressed under the *tubulin*-promoter.

The Flp-FRT system (Golic and Lindquist, 1989; Xu and Rubin, 1993). The Flippase (Flp) is expressed under a heat shock promoter. After induction it binds to the flippase recognition target (FRT) DNA sequence and can lead to recombination between two FRT-sites.

For the induction of homozygous cell clones the mutant allele on a FRT chromosome is brought into the MARCM genetic background and is placed *in trans* to the Gal80 construct. After the heatshow the Flp can lead to recombination in mitotic cells in which

the DNA is condensed. The combination of the two chromosomes FRT-mutant and FRT-Gal80 leads to a twin-spot clone: One cell inherits two copies of Gal80, the other clone inherits two copies of the mutant allele and loses Gal80, which leads to the expression of GFP. For control clones, a FRT chromosome without any mutations is used.

For the induction of MARCM clones in L3 NBs, crosses were held at 25 °C. Flies were allowed to deposit eggs for 1 day and the resulting embryos were heat shocked on the following two days for 1 h 25 min at 37 °C. Dissection and staining of L3 larval brains was performed after another 3 days.

2.2.5. Statistical analysis

For statistical analysis Excel (Microsoft office package 2008) was used. Replicate number was at least 5 and I used the student's T-test for the calculation of p-values.

2.2.5.1. Calculation of neuroblast numbers

For determination of NB numbers, prepupal brains were consulted. In contrast to the L3 instar, the prepupal stage is very short, which reduces sample variances, and NBs are maintained. Brains with the neural marker *insc*::CD8-GFP were stained for the NB marker Mira as described above (2.2.3.2, 2.2.3.3). Z-stacks were taken with a confocal microscope (with ≥ 20% overlap between the z-levels) through the ventral part of the central brain. NBs in the central brain region were identified by position (not in the optic lobe) and Mira expression and further confirmed with GFP expression. Counting was performed manually with Zeiss software (LSM image browser or Zen black).

2.2.5.2. Calculation of cell size

Cell sizes were measured either on live imaged L3 larval brains in which neural membranes were marked with CD8-GFP (imaged as described in 2.2.3.8) or on immunostained L3 brains (for NBs Mira was used as marker, airyscan z-stacks with ≥ 35% overlap between the z-levels were taken). Using Zen black (Zeiss) the ends on both sides of the cell in z-dimension were identified and taken as diameter (d1). Additionally, the stack with the maximal area of the cell (signifying the middle of the cell) was used to set two diameters perpendicular to each other for the maximal and minimal diameter (d2

and d3). The average of the three diameters was used for further calculation. Please note that recent publications described NB sizes in radius. To enable better comparison, cell sizes are therefore presented as radii (diameter divided by two).

2.2.6. Next generation sequencing

2.2.6.1. *Drosophila* lines used for RNA-sequencing

For the transcriptome-wide analysis, I used L3 larval neural brain cells. The *insc::Gal4* driver line was utilized to drive the expression of CD8-GFP in neural cells. This *insc::Gal4, UAS::CD8-GFP* was crossed to *UAS::dom-RNAi* (v7787) for the knockdown of *dom* in neural cell lineages. As this dom-RNAi is in the w^{11118} background, the w^{1118} allele was crossed to the same driver for a wild type control. Crosses were reared at 25 °C and for both resulting lines samples were prepared in triplicates. GFP-expressing larval brains were dissected in complete Schneider's medium (10% FBS) and kept on ice in modified Rinaldini buffer until the end of dissections (maximum duration up to 1 h). Brains were then washed once with modified Rinaldini buffer and subsequently incubated for 1 h at 30 °C in complete Schneider's medium with 1 mg/mL collagenase and papain each. In between, the samples were gently mixed twice to ensure homogeneous incubation. The dissociation buffer was carefully removed and the specimen was washed once with 500 µL modified Rinaldini buffer to which 200 µL complete Schneider's cell culture medium were added. To obtain a single cell suspension the tissue was then first homogenized by gentle pipetting. After making the volume up to 1 mL using complete Schneider's cell culture medium the solution was filtered through a 50 µm filter (CellTrics, Partec).

2.2.6.2. Fluorescence activated cell sorting

For fluorescence activated cell sorting (FACS) 1 µL of 1 mg/mL propodium iodide was added to the single cell suspension for sorting of viable cells. For each sort a GFP negative single cell solution (insc>Gal4) was prepared in similar fashion. This GFP-negative sample was used to discriminate the GFP-positive cell population in the desired sample. Cells were sorted on a FACSVantage SE (Becton Dickinson Biosciences) together with Christoph Göttlinger, University of Cologne, Institute for Genetics.

2.2.6.3. RNA isolation for next generation sequencing

Sorted cells were centrifuged (5 min at 1000 g, 4 °C), resuspended in 360 µL TRIzol and homogenized by pipetting. After 15 min incubation at RT, 72 µL chloroform were added, followed by vigorous shaking for 30 sec and incubation for 3 min at RT. The mixture was centrifuged at 12000 g for 20 min at 4 °C and the aqueous upper phase transferred into a fresh tube. For precipitation 180 µL isopropyl alcohol were added. For a better detection of the RNA precipitate 1 µL GlycoBlue was used additionally. After vortexing for 15 sec the samples were incubated overnight at -80 °C to allow precipitation of RNA. On the next day the samples were centrifuged at 12000 g for 30 min at 4 °C. The supernatant was removed and the RNA pellet washed twice with 0.5 mL of 75% ethanol and centrifuged for 10 min each. The RNA was dried at 37 °C for 5 min and dissolved in 20 µL RNase-free water. Purity and concentration were measured by NanoDrop and TapeStation (CCG).

2.2.6.4. Library preparation and next generation sequencing

RNA was delivered to the Cologne Center for Genomics (CCG) for library preparation and next generation sequencing. The Illumina TruSeq RNA Preparation Kit was used for library preparation according to the manufacturer's protocol. The resultant unstranded paired-end 100 bp mRNA libraries were multiplexed and run on Illumina HiSeq2000 generating a total of 160 million reads and thus ≈ 91 fold genome coverage.

2.2.6.5. Bioinformatic analysis of RNA-sequencing data

We obtained data in the FASTA-format and used these for further bioinformatic analysis (Dr. Manu Tiwari, University of Cologne, Anatomy I, Molecular Cell Biology). Quality control was performed with FastQC (v0.11.2, Andrews, Babraham Bioinfomatics). After quality of all samples was confirmed, reads were mapped to the *Drosophila* genome (FB6.05) with STAR (v2.3.0e) (Dobin et al., 2013). The resulting SAM files were converted to BAM files with samtools (v0.1.19) (Li, 2011a; Li, 2011b; Li et al., 2009a) and viewed with the integrative genome viewer (Robinson et al., 2011; Thorvaldsdóttir et al., 2012). Counts were called using Htseq (v0.6.1) (Anders et al., 2015). For normalization and calculation of differential expression, Deseq2 (1.14.0 Bioconductor package 2.14) (Gentleman et al., 2004) in R (v3.1.1, R Core Team, 2014) was used. Genes were considered to be differentially expressed at a false discovery rate (FDR) of ≤ 0.05.

3. Results

3.1. Domino is required for *Drosophila* embryonic development

3.1.1. Domino is expressed ubiquitously during oogenesis and embryogenesis

In order to study the role of Dom in embryonic NSCs, I initially sought to investigate the expression of Dom in early *Drosophila* development and especially the nervous system. For this I utilized a fly line expressing a GFP-Dom fusion protein at the *dom* gene locus and under the endogenous *dom* promoter, thus reflecting the endogenous expression and localization of Dom (Buszczak et al., 2007). The GFP open reading frame lacks start and stop codons and is inserted in an intronic region upstream to the *dom* start codon. By sequence analysis I identified an alternative start codon (CTG) two codons upstream in frame with the GFP open reading frame which potentially initiates the expression of the GFP-Dom fusion protein. The resulting GFP-Dom fusion protein would contain two additional N-terminal amino acids prior to the GFP. The splice donor of the inserted GFP sequence enables splicing to the adjacent intron in frame with the start codon of the *dom* open reading frame. The start codon is located in the beginning of the adjacent intron, resulting in the expression of a GFP-Dom protein with few additional amino acids linking the two open reading frames.

To confirm the expression of a fusion protein and exclude the expression of untagged GFP I performed Western blot analysis. I used ovary lysate, which appears to have high amounts of GFP-Dom protein as determined in preceding experiments (Figure 7 A). The *dom* gene locus encodes four different protein isoforms DomA, DomD, DomE and DomG, which have molecular weights of 352, 350, 275 and 357 kDA respectively (Figure 5). The isoforms DomA and DomE are both expressed during oogenesis (Börner and Becker, 2016). Thus, I expected to identify at least two GFP bands running higher than the biggest marker band of 170 kDA in the *GFP-Dom* lysate. One band representing the smaller GFP-tagged DomE isoform, and a second band containing the GFP-tagged larger isoform DomA and potentially also DomD and G. The larger isoforms would most probably be indistinguishable due to their similar size. An antibody directed against GFP detects a single band clearly over 170 kDa in *GFP-Dom* lysate, which is absent in w^{1118} lysate and

lysate containing untagged GFP (expressed under the ubiquitous *actin* promoter). This band most probably represents the GFP-Dom protein. The absence of a second GFP-Dom band might be due to technical difficulties, like entry of the large protein into the polyacrylamide gel, or due to low expression levels.

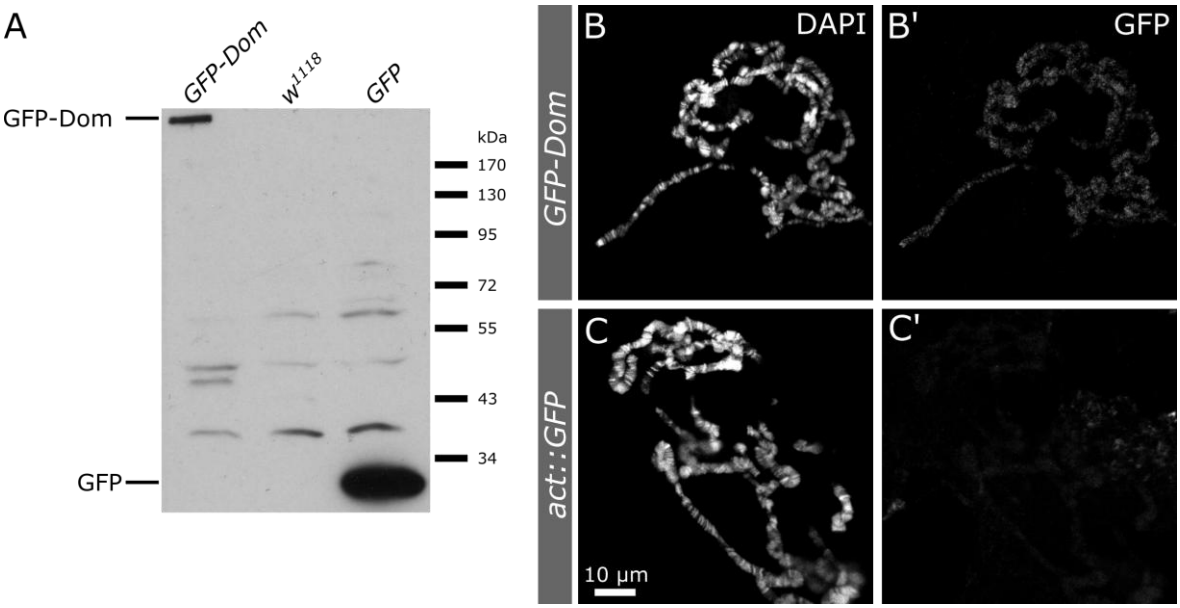

Figure 7: The *GFP-Dom* trap line expresses a GFP fusion protein that binds to polytene chromosomes
(A): Western blot from ovary lysate of the *GFP-Dom* gene trap line, a w^{1118} control and a ubiquitously (*act* promoter driven) GFP-expressing line. A GFP antibody detects untagged GFP (26.9 kDA) in the GFP control but not in *GFP-Dom* or w^{1118}. The GFP-Dom fusion proteins have an expected size of roughly between 300 and 390 kDa, dependent on the Dom isoform. A single GFP-Dom band is detected clearly over 170 kDa. (B and C): Polytene chromosome preparations of the *GFP-Dom* line and a ubiquitously GFP-expressing line. The GFP signal is visible at the DNA only in the *GFP-Dom* line (B'). The microscope pictures were taken with the same settings.

I could not detect untagged GFP (26.9 kDa) in the *GFP-Dom* sample, although the GFP antibody detects several bands between 35 and 80 kDa, which are most probably unspecific as they are also detected in both control samples. A single band at 45 kDa is present in the *GFP-Dom* lysate that I could not detect in the control samples. This band either reflects a degradation product of the GFP-Dom protein or is also unspecific, but runs too high to represent untagged GFP (Figure 7 A).

Homozygous mutation of *dom* is early larval lethal, hence the viability of the homozygous *GFP-Dom* fly line indicates that the fusion protein is functional (Ruhf et al., 2001). Importantly, Dom is a chromatin remodeler protein which binds to DNA (Eissenberg et al., 2005; Ruhf et al., 2001). Thus, to further confirm the functionality of the GFP-Dom fusion protein, I studied its DNA-binding abilities in polytene chromosome preparations (Figure 7 B). GFP staining can be detected at the DNA in the *GFP-Dom* fusion line but not in a control line expressing GFP (Figure 7 C), indicating that the fusion protein is capable of binding DNA.

To investigate the expression of Dom in early *Drosophila* development I analyzed the expression of GFP-Dom in ovaries and embryos by confocal microscopy. GFP-Dom can be detected in all nuclei of ovaries and embryos throughout oogenesis and embryogenesis (Figure 8).

To furthermore confirm the expression of Dom in the *Drosophila* embryo, I immunostained GFP-Dom embryos with an antibody directed against all isoforms of Dom produced in this study (Figure 9). The Dom antibody signal overlaps with the GFP-Dom staining. Although, I could also detect some background staining, visible as spots, which do not colocalize with the GFP-Dom signal (Figure 9 B').

Both, the GFP-Dom signal and the Dom staining confirm the expression of Dom in embryonic NBs positive for Baz (Figure 9 C) and the overlying epithelium (Figure 9 B). This finding could further be underpinned using the reporter line dom^{k08108} (Figure S 1). Dom is nuclear unless the nuclear envelope has broken down during cell division. Dom staining of polytene chromosomes further validates that Dom binds to DNA and mostly localizes to the euchromatic regions, which are not or weakly stained by Hoechst (Figure 9 D).

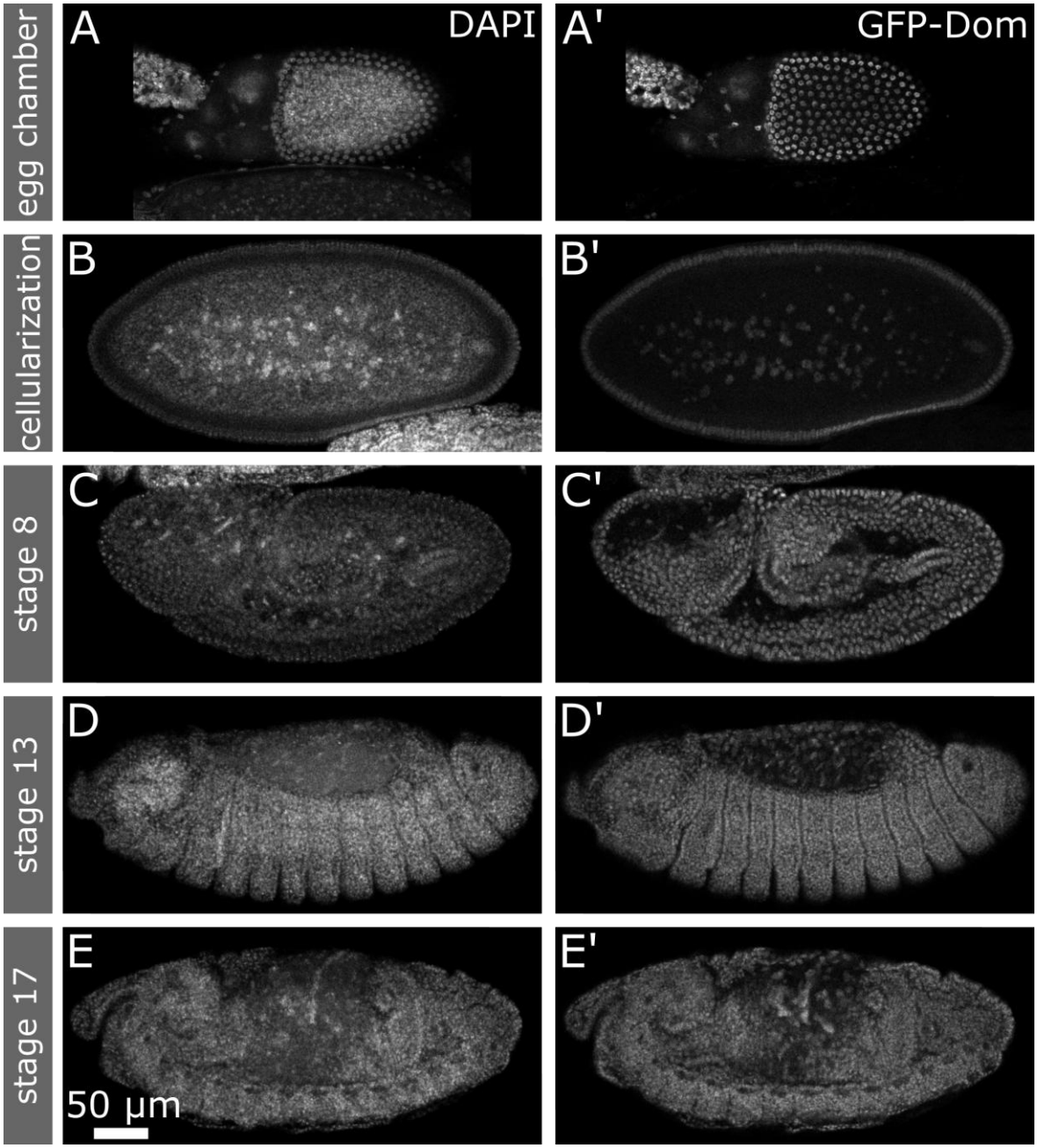

Figure 8: Domino expression in ovary and embryo

Confocal microscopy pictures of GFP-Dom ovary and embryos. GFP-Dom is expressed in ovary cells (A) and throughout embryogenesis (B – E). The fusion protein localizes to nuclei.

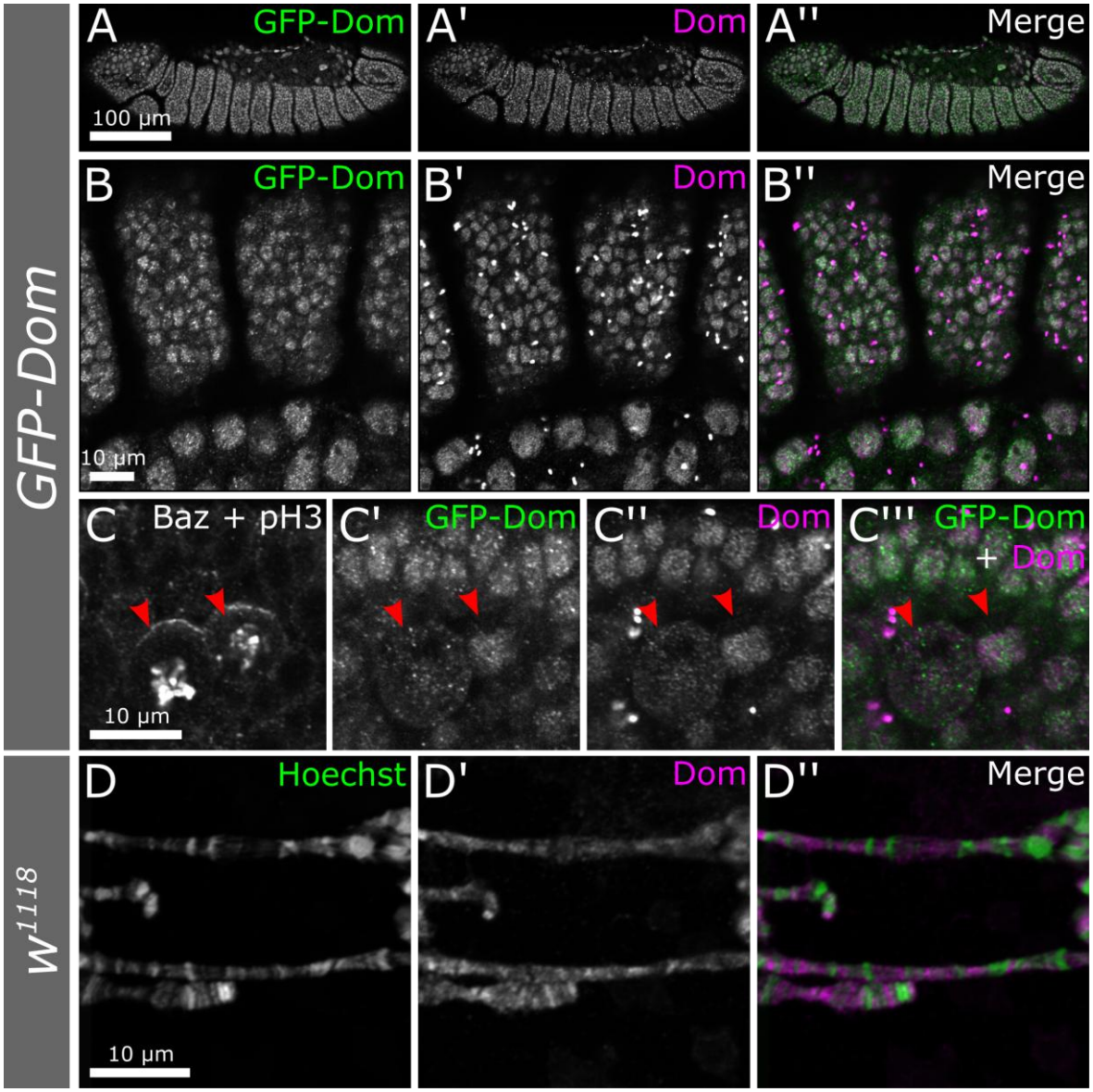

Figure 9: Domino is expressed in embryonic neuroblasts and binds to polytene chromosomes in euchromatic regions

Confocal microscopy pictures of a stage 13 *GFP-Dom* embryo (A – C). Dom staining (A', B', C'') overlaps with the GFP-Dom signal (A, B, C') in all analyzed nuclei, although some background staining is visible. Dom is expressed in the epithelium (B) and in underlying NBs (C, arrow), which are positive for Baz. Dom localizes to the nucleus but is also visible in the cytoplasm after nuclear envelope breakdown. pH3 stains mitotic nuclei. (D) shows polytene chromosome preparations stained for Dom. The Dom staining is strong in Hoechst negative euchromatic regions.

3.1.2. Neuroblasts in *domino* null mutants are misoriented

To study the function of Dom in embryonic NSCs I used the previously published *dom* null allele *dom*^{14}, which is a deletion comprising the start codon (Figure 5) and early larval lethal (Ruhf et al., 2001). We validated the deletion by Sanger sequencing (Hong Nhung Ngyuen, M.Sc Student, University Medical Center Cologne, Anatomy I, Molecular Cell Biology, see Nguyen, 2016) and by Dom antibody staining of mutant embryos (Figure 10 B), which are almost completely negative for Dom staining. Furthermore, a duplication spanning the *dom* genomic locus and some few neighboring genes (BL34492) can rescue *dom*^{14} mutants to viability and fertility. Embryos containing one or two copies of *dom* were identified by the strength of mesodermal expression of GFP under the *twist* promoter (strong GFP for embryos lacking the *dom* mutant allele). These embryos, in contrast to *dom*^{14} mutants of the same stage, show ubiquitous nuclear Dom staining (Figure 10 A). Ruhf et al. (2001) have suggested the supply of maternal Dom to enable zygotic mutants to survive until L1 larval stage. Thus, the weak Dom staining in mutant embryos is likely the remaining maternally supplied Dom protein.

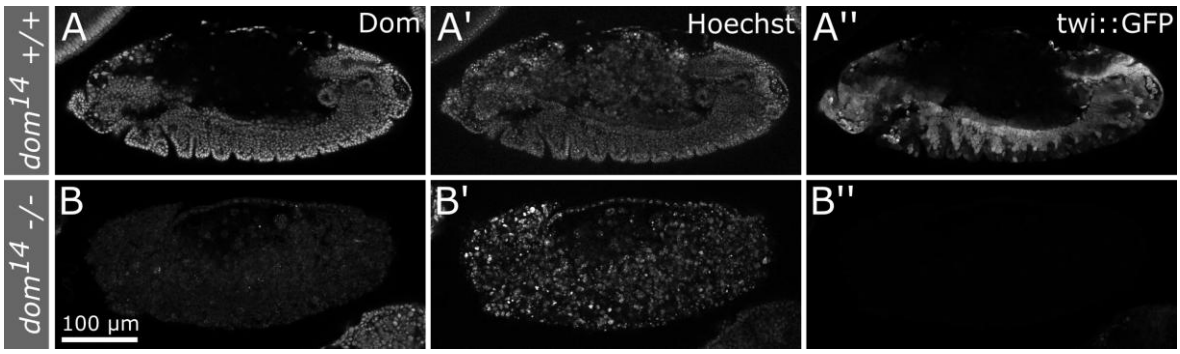

Figure 10: *dom14* mutant embryos are negative for Domino staining

Dom antibody staining on heterozygous (A) and homozygous (B) *dom*^{14} mutant stage 13 embryos. Homozygous mutant embryos were identified by absence of GFP expression under the mesodermal promoter *twist* (*twi*). GFP positive control embryos are positive for Dom staining (A'), *dom*^{14} homozygous mutants are negative for Dom staining (B'). Confocal microscopy pictures were taken with the same settings.

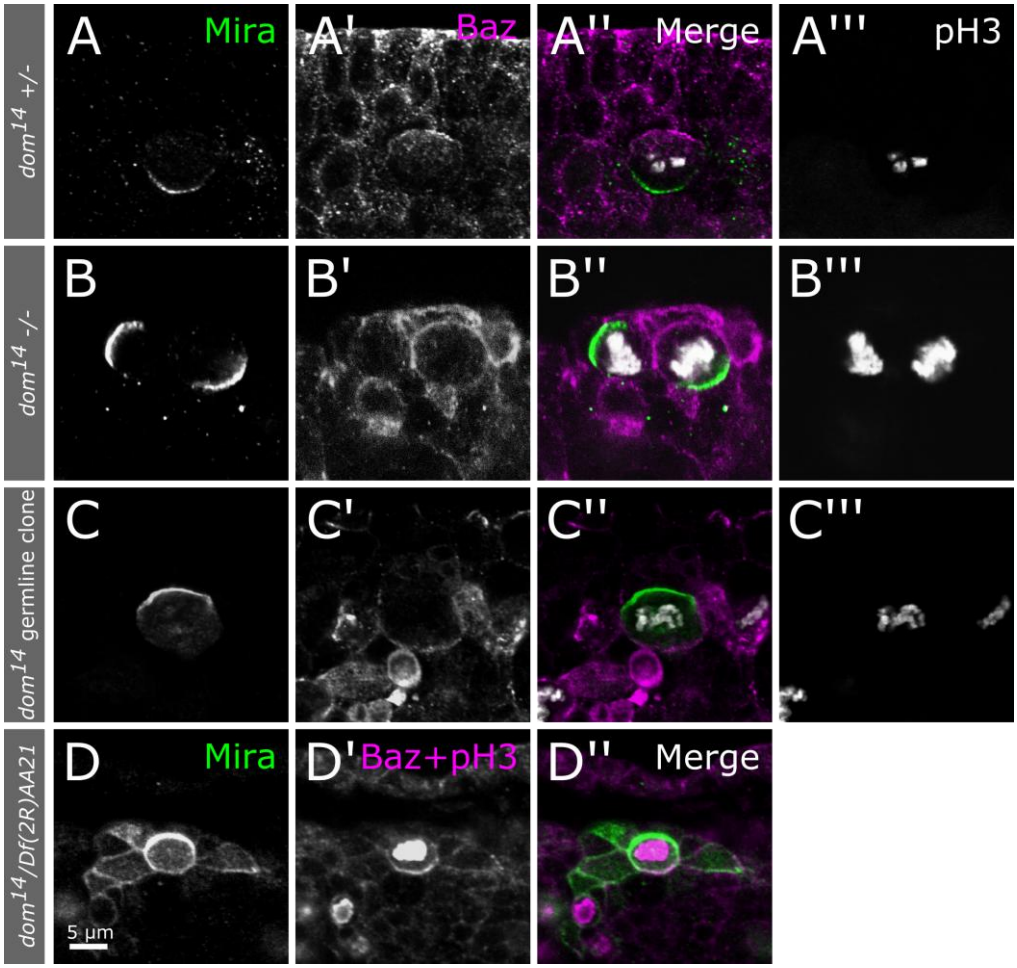

Figure 11: Neuroblast orientation is disturbed in *domino* null mutants

Confocal microscopy pictures of dividing NBs in embryos of stage 13 (A-C) or stage 15 (D). Apical is always up. pH3 marks the nuclei of mitotic cells. (A): In a heterozygous control the apical marker Baz and basal marker Mira are visible as crescents at the apical or basal side of the dividing NB, respectively. (B-D): In zygotic (B) and germline (C) *dom* null mutants and in transheterozygotes with a deficiency removing the *dom* gene (D) crescents of both polarity markers are visible in mitotic NBs but the orientation of the localization axis is disturbed.

To examine whether *dom* is required for embryonic NBs I stained dom^{14} zygotic and maternal) mutants for the NB marker Mira, and Baz, a protein which is also expressed in NBs. In both zygotic as well as maternal mutant embryos I could identify NBs, demonstrating that embryonic NSCs are specified and maintained in *dom* mutants. In mitotic NBs positive for phospho-Histone 3 (pH3) Baz localizes on the apical NB cortex facing the epithelium, while Mira localizes on the opposite basal cortex (Figure 11 A). The localization of Baz and Mira to opposing sides of the NB is well visible also in *dom* mutants

(Figure 11 B and C). However, the sides to which the polarity markers localize are random, signifying that *dom* mutant NBs have correct polarity but disturbed cellular orientation (see also Master's Thesis Katja Rust, 2013). The same phenotype can be observed in *dom*^{14} mutants transheterozygous over deficient chromosomes lacking the *dom* gene (Df(2R)AA21 and Df(2R)BSC821), confirming that the phenotype is dependent on *dom* mutation (Figure 11 D and data not shown).

NBs orient their spindle apparatus based on the localization of polarity determinants like Baz, Insc or Pins to produce one bigger NB daughter cell which inherits apical determinants and one smaller GMC daughter cell which inherits basally localized components. Thus, the spindle apparatus in wild type NBs always orients on the apico-basal axis (Figure 12 A, References). I questioned whether the spindle apparatus orientation in *dom*^{14} NBs with disturbed cell orientation is still coupled to the localization of polarity markers (Figure 12 B) or detached from the cell-intrinsic axis (Figure 12 C).

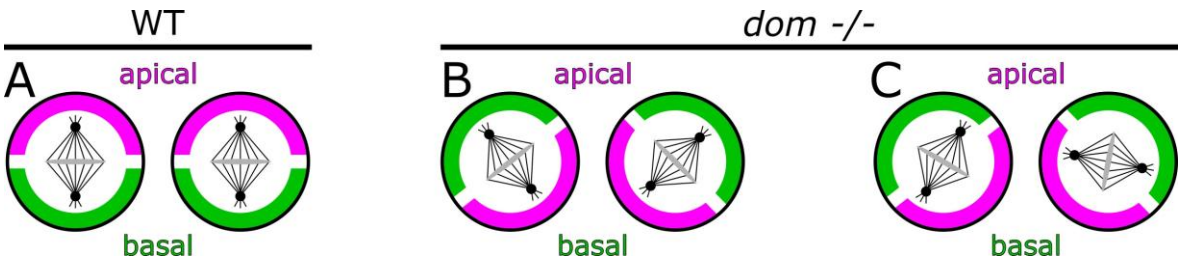

Figure 12: Do neuroblasts in *domino* mutant embryos have correct spindle orientation?

(A): Wild type NBs display apical to basal localization of polarity determinants and spindle apparatus during mitosis. In *dom* mutant NBs orientation of apical and basal determinant localization is disturbed. However, it is unclear whether the spindle apparatus orients according to polarity determinants (B) or randomly (C).

To answer this question, I stained *dom*^{14} mutant embryos for the NB marker and basal determinant Mira and analyzed the spindle apparatus orientation by staining against β-Tub in pH3 positive, dividing NBs. Confocal microscopy unravels that the spindle apparatus orients perpendicular to the Mira localization side of the NB. Also, the metaphase plane stained by pH3 and Hoechst displays correct orientation considering the Mira localization (Figure 13). Together, these results reveal that *dom* mutant NBs are misoriented but polarity determinants and the spindle apparatus are aligned within the NB.

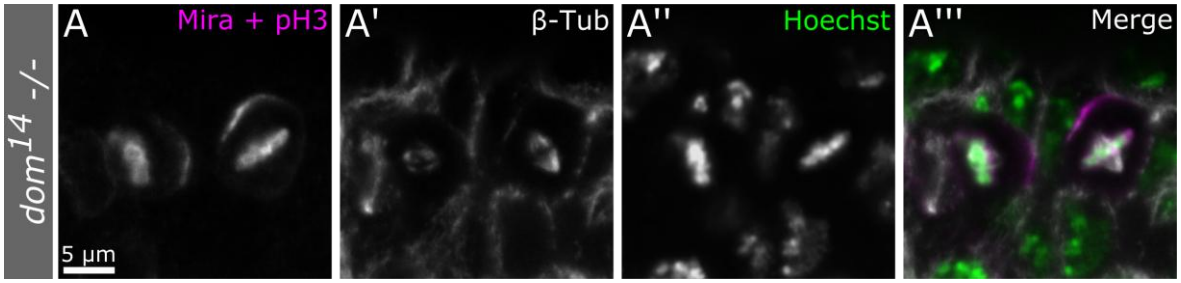

Figure 13: The spindle apparatus in *dom*^{14} mutant neuroblasts orients along the cell-intrinsic axis

dom^{14} mutant stage 13 embryos have been strong fixed for β-Tubulin (β-Tub) staining to analyze the spindle apparatus of dividing (pH3 positive) NBs (Mira positive) by confocal microscopy. Apical is up. Mira and pH3 were co-stained as the signals are distinguishable by subcellular localization. Although NB orientation is incorrect, the spindle apparatus orients according to the NB intrinsic axis.

3.1.3. Embryonic epithelial morphology is disturbed in *domino* mutants

It is a well-established fact that embryonic NB orientation requires the overlying epithelium (Yoshiura et al., 2012). Therefore, the results obtained thus far prompted me to further examine the epithelium in *dom* mutants, considering that the NB misorientation phenotype could depend on epithelial defects rather than being NB cell-autonomous. I stained *dom*^{14} mutant embryos and control embryos of stage 13 for the polarity markers Crb, Baz, and Dlg. Maximum intensity projections (projection of a z-stack) of whole embryos stained against Crb illustrate that *dom* mutants have severe morphological defects (Figure 14 B). While embryos with at least one *dom* gene copy are segmented and start to develop the tracheal system, homozygous *dom*^{14} mutant embryos show poorly established segmentation borders and only rudiments of a tracheal system. The overview as well as magnifications of the epithelium clearly show that *dom*^{14} mutant embryos have less but bigger epithelial cells. Moreover, the epithelium is unorganized and polarity markers are mislocalized (Figure 14 H, J). This holds also true at the leading edge during dorsal closure (Figure 14 D, F).

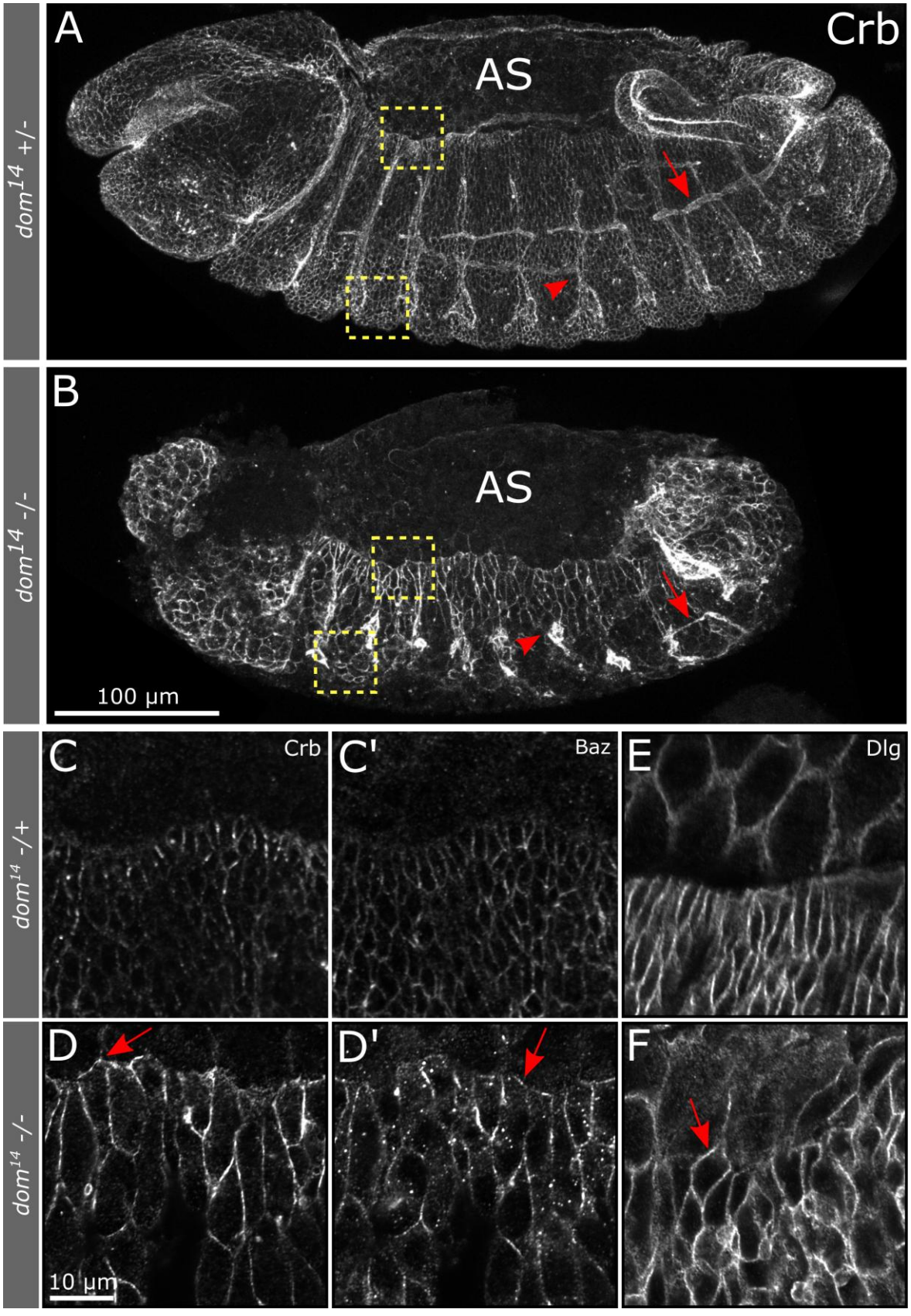
A
Crb
AS
dom14 +/-
B
AS
dom14 -/-
100 µm
C
Crb
C'
Baz
E
Dlg
dom14 -/+
D
D'
F
dom14 -/-
10 µm

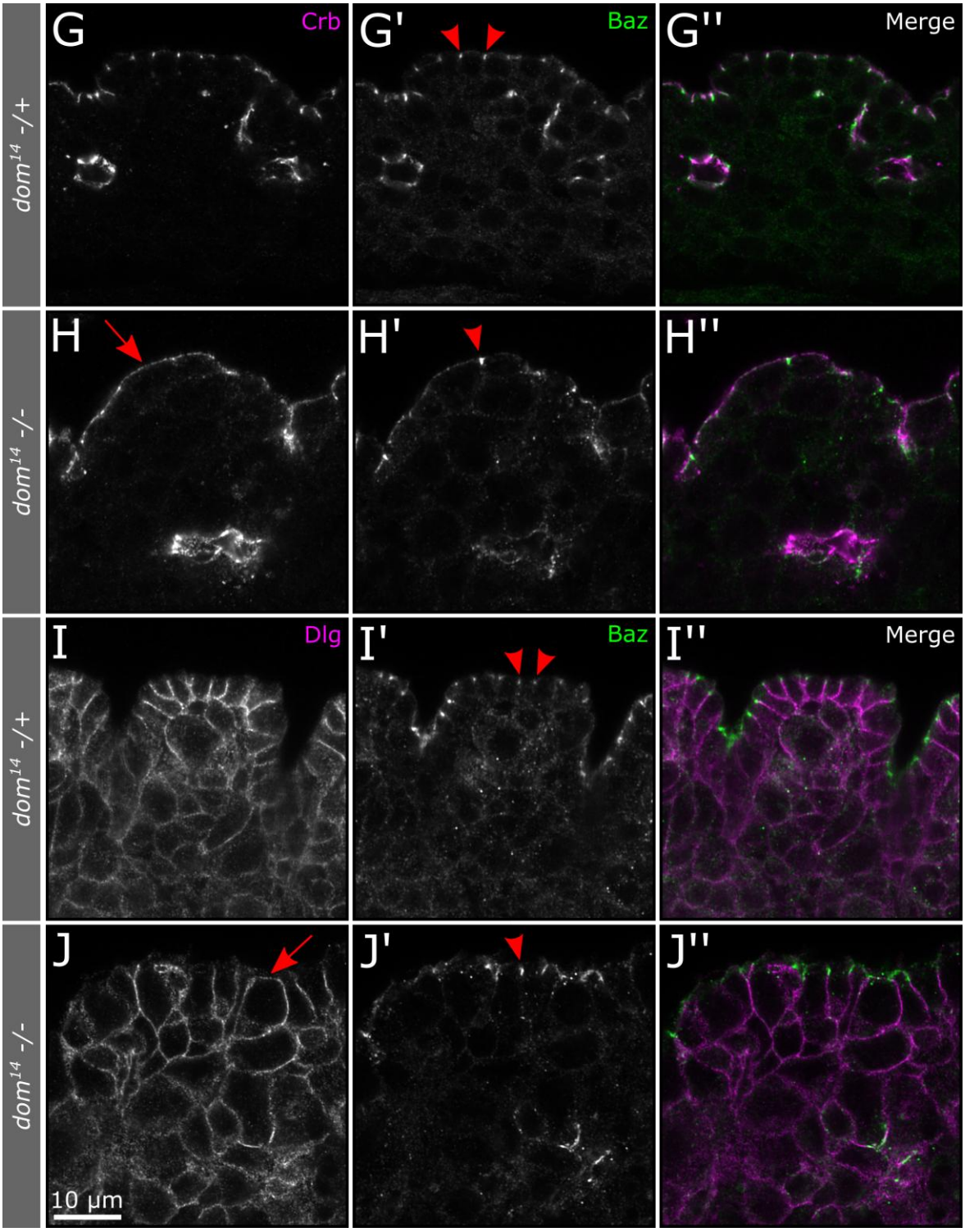
G
Crb
G'
Baz
G''
Merge
dom14 -/+
H
H'
H''
dom14 -/-
I
Dlg
I'
Baz
I''
Merge
dom14 -/+
J
J'
J''
dom14 -/-
10 µm

Figure 14: Epithelial morphology is disturbed in *domino* null mutant embryos

Stage 13 embryos heterozygous (+/-) or homozygous (-/-) for *dom*^{14} are shown. (A,B): Maximum intensity projections with Crb staining. Anterior is left, dorsal is up. Arrowheads in A and B point at segment invaginations, arrows at the tracheal system. AS = amnioserosa. Squares indicate positions of magnifications shown in C-F (upper squares) and G-J (lower squares). (C – F): Airyscan pictures of the leading edge at the onset of dorsal closure. (C – F): Crb, Baz and Dlg are restriced from the leading edge in heterozygous *dom*^{14} embryos (C, C', E) but not in homozygous embryos (arrows in D, D' and F). (G-J): Airyscan pictures oriented apical up. Cross sections through the epithelium of one segment are shown. Arrowheads point at Baz positive AJs, visible as spots. Crb localizes slightly apical to Baz. (G). *dom*^{14} mutants occasionally fail to localize Crb and Baz in a spot-like pattern, Crb is often not restricted from the apical membrane (arrow). Dlg localizes laterally in wild type epithelial cells (I). *dom*^{14} mutants partly show apical Dlg staining (J, arrow).

To gain further insight into the morphological defects of *dom*^{14} null mutants we prepared histological semithin-sections of stage 13 embryos (sample preparation by Ferdinand Grawe, University Medical Center Cologne, Anatomy I, Molecular Cell Biology). Wild type embryos (*w*^{1118}) show developmentally normal amounts of dead cells and well-established segmentation borders. In contrast, *dom*^{14} mutants show more dead cells, the epithelium is uneven and segmentation borders are not well detectable (Figure 15).

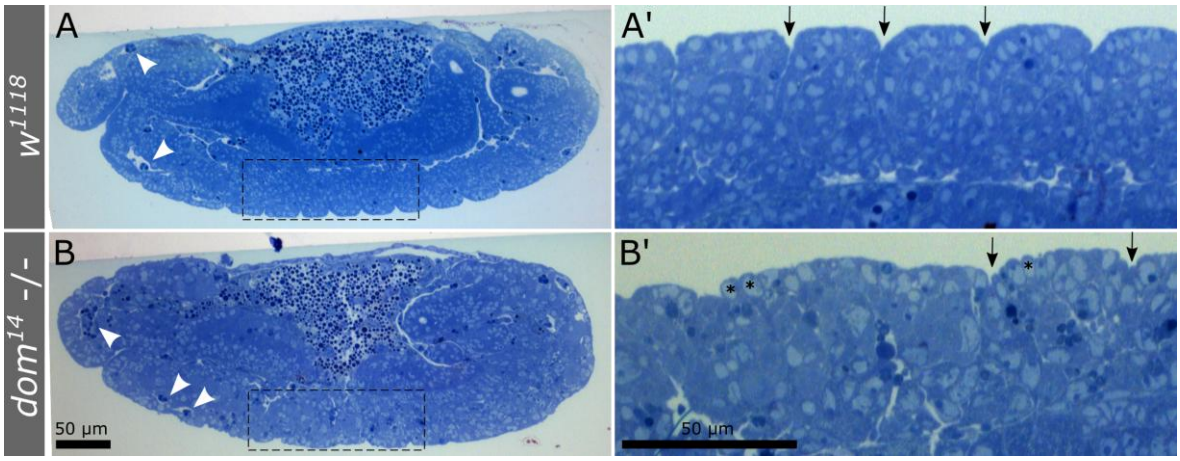

Figure 15: *dom*^{14} mutants show epithelial defects

Histological semithin-sections of a wild type (w^{1118}) embryo and a *dom*^{14} embryo (*dom*^{14} -/-). Sample preparation by Ferdinand Grawe. The overview pictures (A, B) show stage 13 embryos oriented with anterior side to the left and dorsal side up. Arrowheads mark dead cells. The wild type control shows developmental normal amount of dead cells while the *dom* mutant shows more cell death. Squares mark the magnified views in A' and B'. Magnifications are shown with apical side up. Segment borders are marked with arrow. In the *dom*^{14} mutant single epithelial cells round up (asterisk) making the epithelium uneven.

Taken together, the results reveal that *dom*^{14} mutant embryos display severe epithelial defects. Mutants for polarity determinants like *crb, shg* (E-Cadherin) or *baz* show similar epithelial defects, rendering the epithelium unable to produce a continuous cuticle (Grawe et al., 1996; Tepass et al., 1996; Wodarz et al., 2000). To investigate if this is also the case for *dom*^{14} mutants I prepared embryonic cuticles (with the help of Ferdinand Grawe).

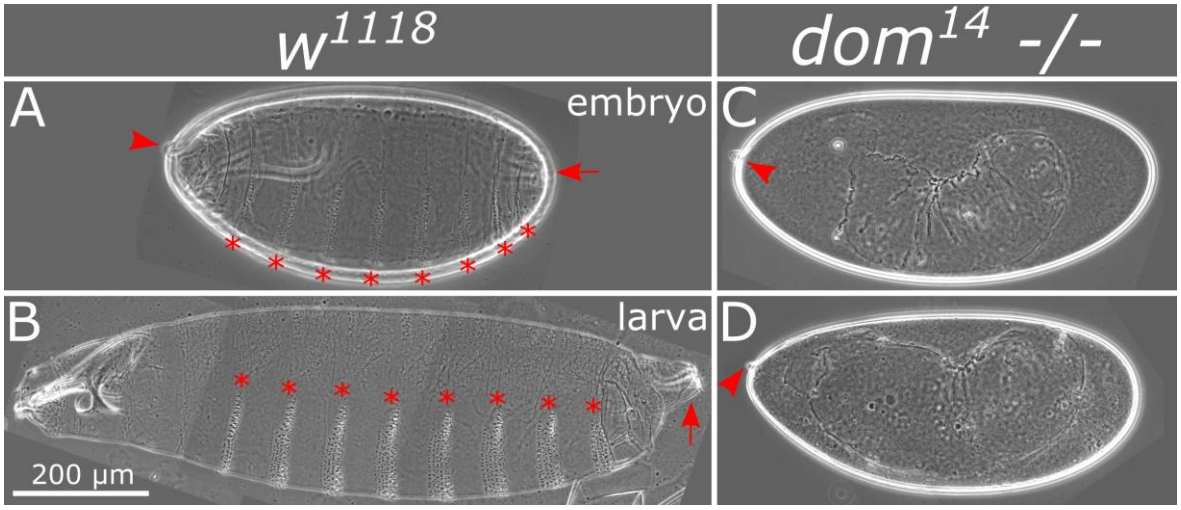

Figure 16: *domino* null mutants do not produce continuous cuticles

Cuticle preparations of *dom*^{14} mutant (*dom*^{14} -/-, C, D) in comparison to a wild type control (*w*^{1118}, A, B). Anterior is left, dorsal is up. (A) shows an embryonic cuticle, (B) shows a larval cuticle. Arrowheads point at micropyles, arrows at posterior spiracles. Asterisks mark abdominal denticle belts. Wild type cuticles show denticle belts, an anterior mouth skeleton and a continuous cuticle. *Dom*^{14} cuticles do not show denticle belts or mouth skeletons and contain huge holes, especially in the head region and at the dorsal side.

Wild type L1 larvae possess denticle belts, a mouth skeleton and posterior spiracles (Figure 16 B). In contrast, late stage wild type embryonic cuticles show a vitelline membrane with the anterior micropyle. Within the vitelline membrane, late stage embryos form a continuous cuticle with mouth skeleton, denticle belts and posterior spiracles, structures that are also seen in L1 larvae (Figure 16 A, B). Although *dom*^{14} embryos were allowed to develop for 48 h, after which which wild type larvae have already hatched, most cuticles are embryonic as demonstrated by the presence of a vitelline membrane. The cuticles within the vitelline membranes are not continuous with anterior and dorsal holes.

Structures required for the larval stage, like the mouth skeleton and denticle belts, are not formed (Figure 16 C, D). Previous studies have shown that *dom*^{14} mutants are able to survive until L1 stage, however L1 larvae were reported to be infrequent (Ruhf et al., 2001). In accordance with this, cuticles from later stages were only very rarely found.

3.1.4. *domino* mutation leads to nuclear fragmentation

To examine whether *dom* mutant embryos are able to form the ZA and maintain AJs, we prepared *dom*^{14} and *w*^{1118} embryos for transmission electron microscopy (together with Ferdinand Grawe). In accordance with results from immunofluorescence staining and semithin-histological staining we detected cells exiting the epithelial tissue. Remarkably, although we found cells with incorrect position, AJs could still be identified (Figure 17 A, B). In addition, comparing nuclei of wild type embryonic epithelial cells with *dom*^{14} nuclei it became obvious that *dom* mutant nuclei were severely fragmented with membrane stacks protruding into the nuclei (Figure 17 C, D).

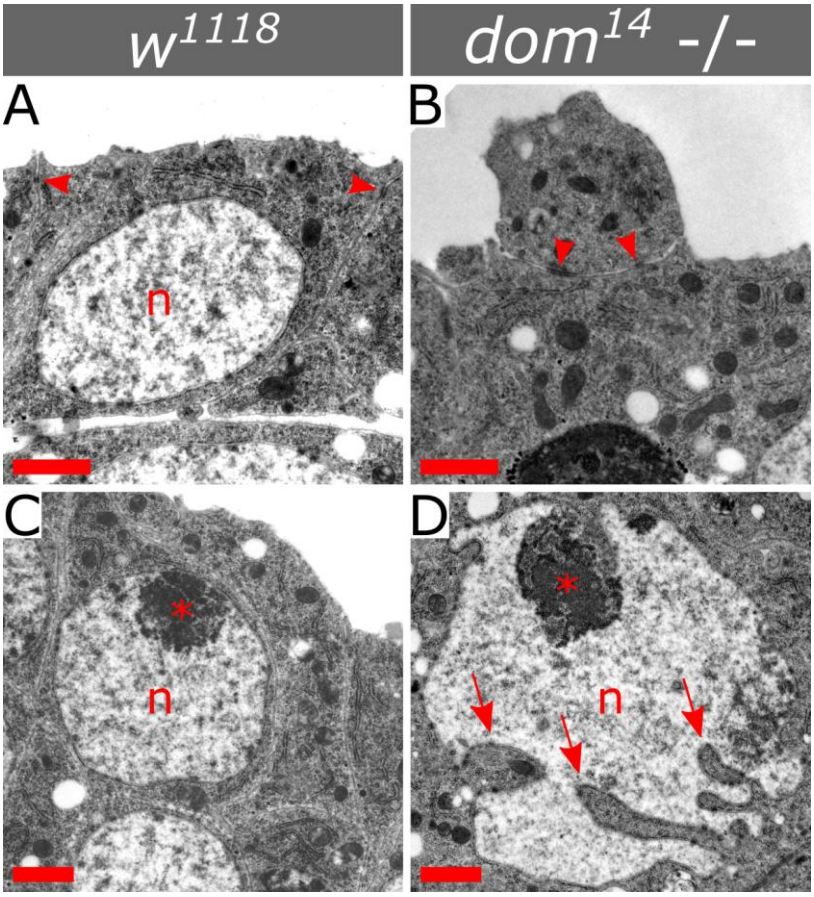

Figure 17: *dom14* mutants show fragmentation of nuclei

Transmission electron microscopy pictures of stage 13 wild type (w^{1118}) and *dom* mutant (dom^{14}) embryos. (A) Wild type embryonic epithelium shows two apically localized AJs from the ZA belt (arrowheads). (B): dom^{14} cells leaving the tissue are visible overlying epithelial cells. These cells still form AJs to neighbouring cells (arrowheads). (C): Wild type epithelial nuclei (n) are round in shape. Asterisks mark nucleoli. (D): dom^{14} epithelial nuclei show invagination of membrane stacks (arrows) and are fragmented. Scalebars = 1 µm.

3.1.5. *domino* mutation does not induce apoptosis in the *Drosophila* embryo

Histological semithin-sections and electron microscopy data of *dom* mutants showed that dom^{14} mutants have more dead cells than the wild type (Figure 15). Comparing Hoechst-stained nuclei of the mutant with the wild type elucidates abnormal nuclei in the *dom* null mutant (Figure 10 A', B'). During apoptotic cell death nuclei condense and DNA gets fragmented making the nuclei appear bright in Hoechst or DAPI staining (Cobb, 2013). Mammalian homologs of Dom and Tip60 have been implicated in apoptosis induction upon DNA double strand breaks (Ikura et al., 2000; Tyteca et al., 2006). Therefore, I asked whether the absence of Dom in the *Drosophila* embryo could induce apoptosis.

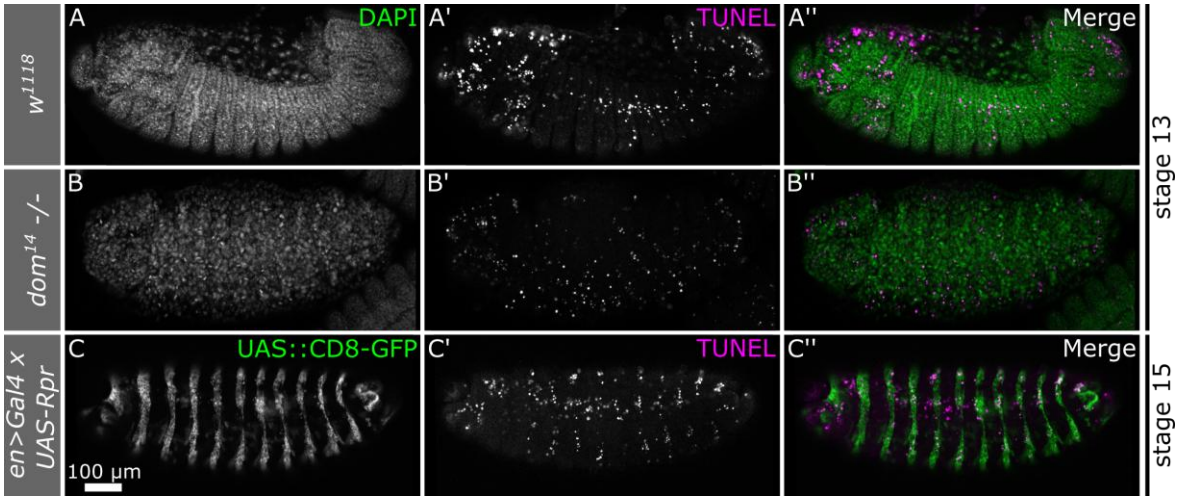

Figure 18: *dom*^{14} mutants do not show enhanced apoptotic cell death

TUNEL staining of stage 13 (A and B) and stage 15 (C) embryos. Anterior is left. Please note that A and C are shown in the lateral view (dorsal up) while in B the embryo is slightly shifted towards the ventral side. Overexpression of the apoptotic inducer Rpr in *en::Gal4* positive stripes leads to additional TUNEL positive cells (C'). The wild type shown in A displays developmental normal amount of apoptotic cells especially in the head and the ventral cord region. The *dom*^{14} mutant shows apoptotic cells in the ventral trunk and the head region.

I used the TUNEL assay to visualize apoptotic cells in *dom*^{14} mutant embryos (Figure 18). A potent activator of apoptosis Reaper (Rpr) was overexpressed in stripes using the *engrailed* (*en*) promoter. TUNEL positive nuclei in these stripes confirmed that the assay worked. Wild type embryos of the analyzed stage 13 show developmental normal amount of apoptotic cells in the head region and the ventral trunk (White et al., 1994). In comparison, *dom*^{14} mutants also display developmental normal amount of apoptotic cells if not less.

The chromosomal deletion *H99* removes three genes *rpr*, *hid* and *grim* essential for apoptotic induction and homozygous *H99* represses most cell death (White et al., 1994). To confirm that the observed *dom*^{14} phenotype is not dependent on apoptosis, I combined the *dom* null mutant with the *H99* deficiency. *H99* homozygous embryos show normal NB orientation. *H99* homozygous deficiency fails to rescue the NB misorientation phenotype of the *dom*^{14} null mutant (Figure 19). Thus, NBs misoriented in *dom*^{14} mutants do not show this phenotype due to apoptosis.

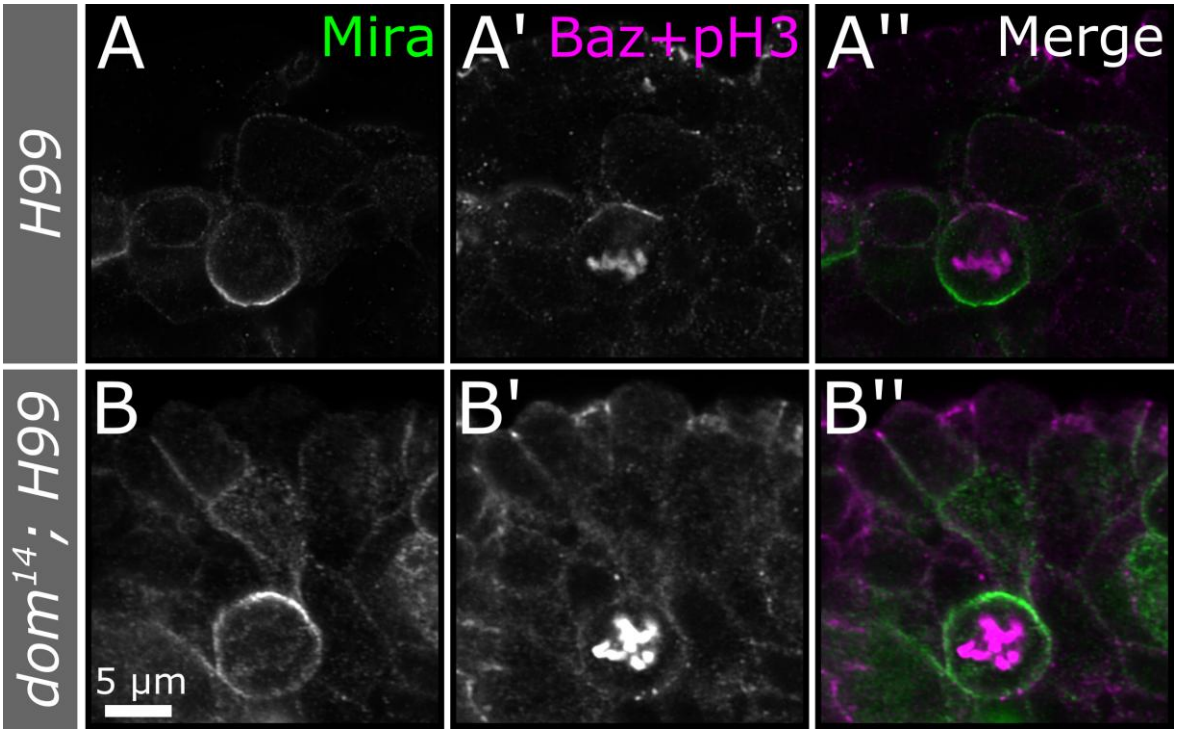

Figure 19: Blocked apoptosis does not rescue *dom*^{14} neuroblast misorientation

The *H99* allele, a deficiency removing the three apoptotic inducers *rpr*, *hid* and *grim* was combined with the null allele *dom*^{14}. (A): In *H99* mutants the NB division is oriented along the apico-basal axis. (B): The *dom*^{14} null allele misorients NBs also in the *H99* background. Airyscan pictures were taken in stage 13 embryos.

Taken together, the results show that the embryonic phenotype displayed by *dom* null mutants is independent of induction of apoptotic cell death. If anything, less apoptotic cell death was observed. This rather points to a role of Dom in apoptotic induction, like the mammalian homolog p400 (Ikura et al., 2000; Tyteca et al., 2006).

3.2. Domino controls *Drosophila* imaginal disc development

Besides the embryonic epidermis, the imaginal disc epithelium is one of the best-studied primary epithelia in the fruit fly (Beira and Paro, 2016). Since *dom* mutant embryos have severe epithelial defects, the question arises whether *dom* is also required for other epithelia in *Drosophila.* However, *dom* null mutants are early larval lethal and Flp/FRT-mediated mitotic homozygous clones have been reported to not be recovered with several *dom* alleles (Ruhf et al., 2001). In order to nonetheless study the function of *dom* beyond embryonic development, I performed RNA Interference (RNAi)-mediated

knockdown of *dom*. An elegant approach to study the imaginal disc epithelium is, to manipulate the gene of interest in only one part of the imaginal disc, such having an unaltered control cell population within the same tissue. This can be achieved by using the *engrailed* promoter to drive the expression of target constructs. The *engrailed* promoter is active in the posterior compartment of the imaginal disc, which was visualized by the reporter CD8-GFP, a membrane-tethered GFP (Figure 20 A). Expression of an RNA probe targeting the dom-RNA for degradation spares only a thin layer of the posterior compartment (Figure 20 B). Please note, that knockdown of *dom* in the well-studied wing disc deformed the tissue severely, making it challenging to distinguish the wing disc from other spatially close imaginal discs. To ensure that tissue with similar fate is compared, I therefore decided to focus on the analysis of leg discs, which can be easily identified by their position in the larva.

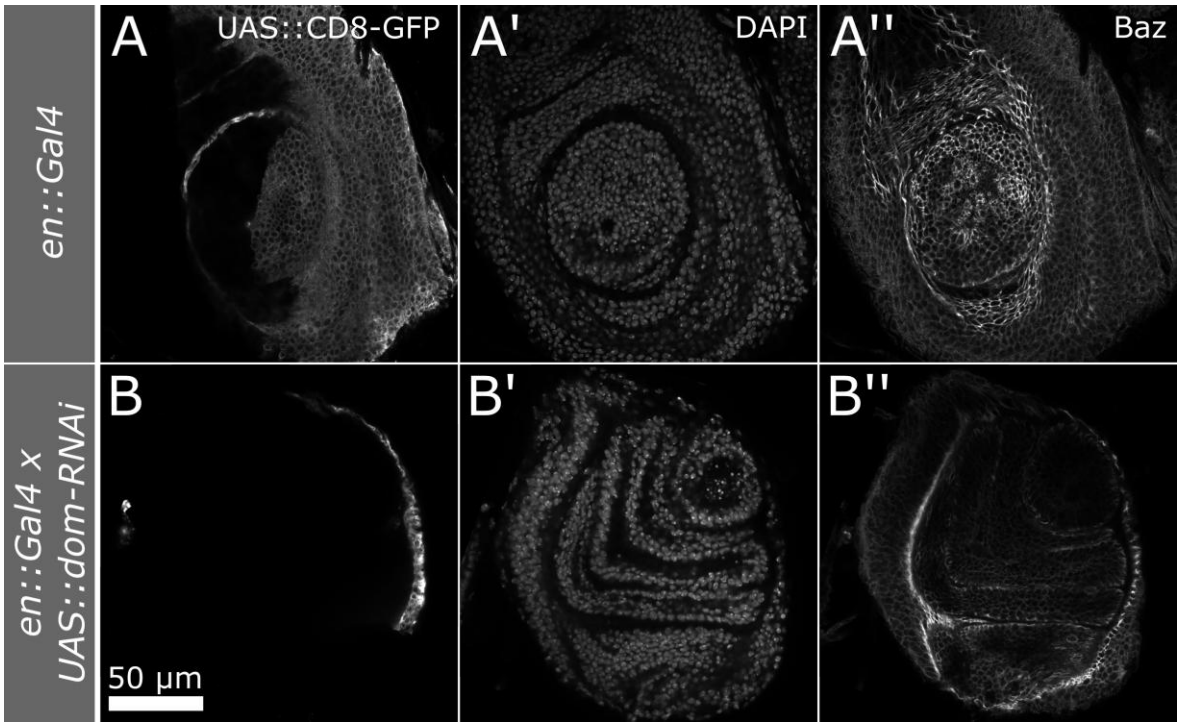

Figure 20: *domino* knockdown affects imaginal disc epithelial cells

Confocal microscopy pictures of L3 leg imaginal discs are shown. Dorsal is up, anterior is to the left. *en::Gal4* drives the expression of UAS constructs in the posterior compartment of the discs and is marked by CD8-GFP expression. In the control sample the posterior compartment accounts for roughly half of the imaginal disc (A), while *dom* knockdown (*UAS::dom-RNAi* v7787) reduces the posterior compartment to only a few cells (B).

All knockout and knockdown studies conveyed so far show that *dom* is indispensable for *Drosophila* development. Therefore, I speculated that upregulation of Dom could also influence *Drosophila* development. Three overexpression lines are available for Dom: Two different DomA UAS-lines and one DomB UAS-line. DomB refers to an earlier annotation of the DomE isoform in which 10 amino acids are different but all conserved domains are unchanged, suggesting that the proteins would fulfill the same function. To validate the overexpression of Dom in these lines we expressed the constructs in stripes under the *engrailed* promoter and detected Dom expression levels with the Dom antibody, which recognizes all annotated isoforms. I could not detect any overexpression of Dom with both DomA overexpression lines (Figure S 2) and thus excluded them for further experiments. Overexpression of DomB in the embryo and the wing imaginal disc, in contrast, is detectable by Dom antibody staining (Figure 21 B',Figure 22 B').

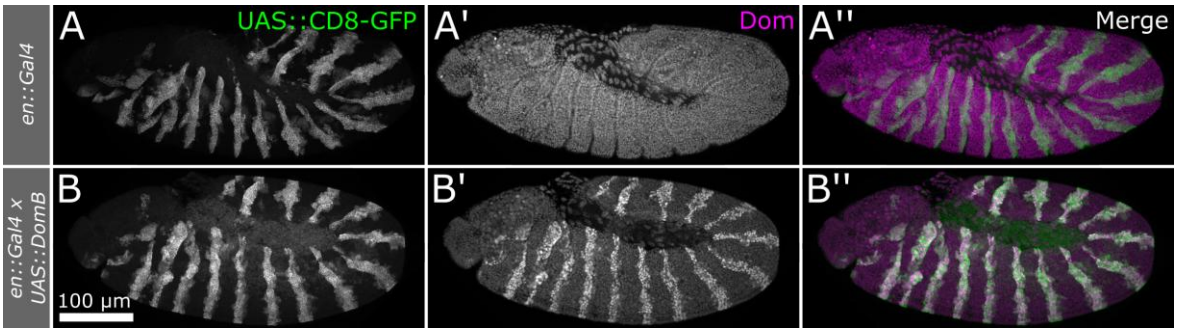

Figure 21: DominoB can be overexpressed with a Gal4 driver

Confocal microscopy pictures of stage 13 embryos oriented anterior to the left and dorsal up. The *en* driver was used to overexpress DomB and *en* positive cells are marked with CD8-GFP. (A): In the control Dom is uniformly expressed in all nuclei of the embryo (A'). (B): Upon DomB overexpression in *en* positive cells, the affected cells show higher levels of Dom staining (B'). Please note that Dom staining was visualized with different microscope settings to adjust to the bright Dom staining upon DomB overexpression.

I analyzed NB polarity and epithelial morphology in DomB overexpressing embryos, yet both cell types appear unaffected (data not shown). Overexpression of DomB in wing imaginal discs on the other hand, severely affected the wing disc morphology (Figure 22). Overexpression was again confirmed by Dom antibody staining. While the endogenous Dom expression is present in most nuclei (Figure 22 A') of the wing disc DomB

overexpression results in a strong nuclear signal in cells in the posterior compartment (Figure 22 B'). To summarize, Dom is likely required in very specific amounts for a normal imaginal disc development.

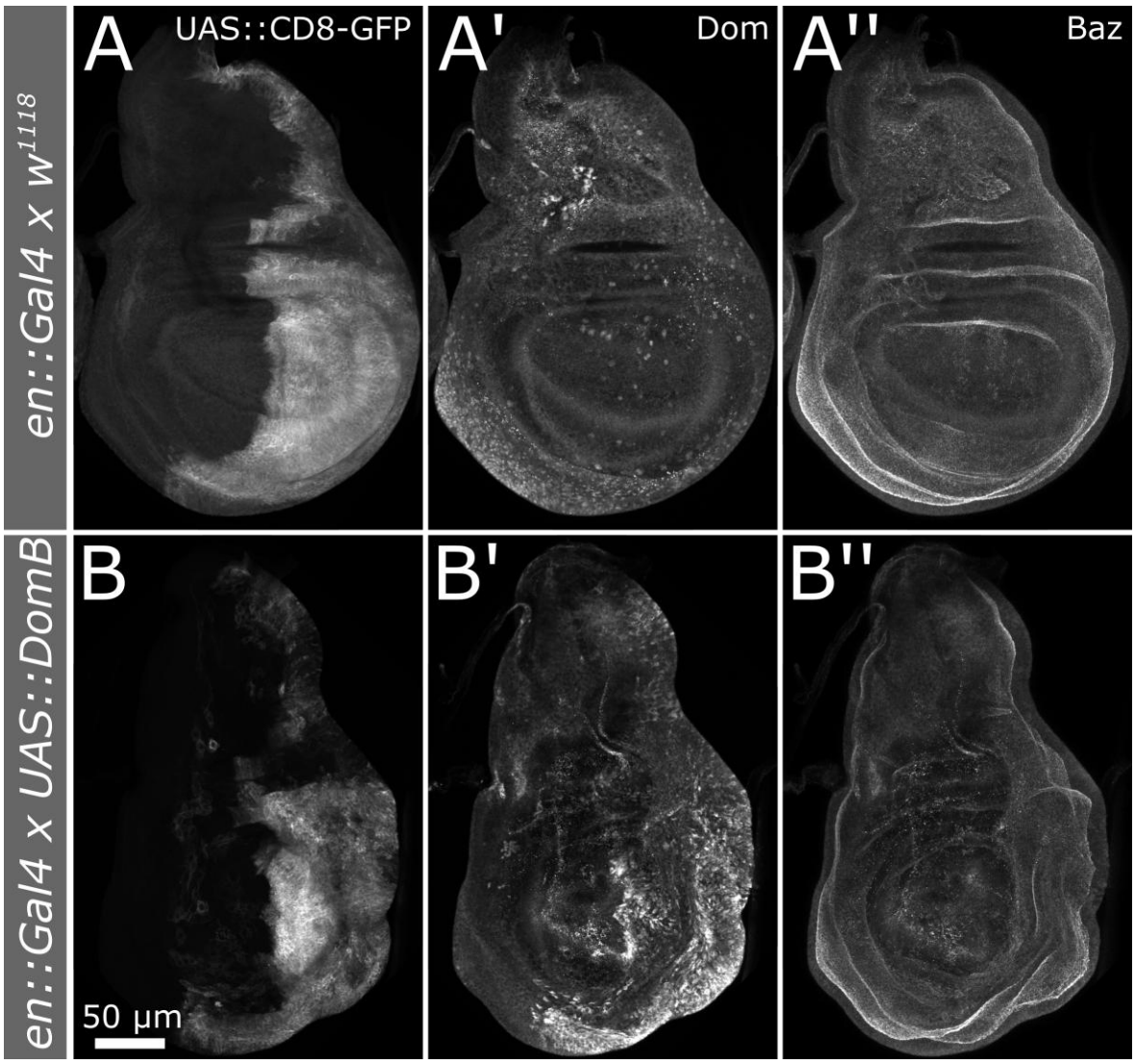

Figure 22: Overexpression of DominoB in the posterior wing disc compartment affects disc morphology
Maximum intensity projections of L3 wing discs shown with anterior to the left and dorsal up. *en::Gal4* was used to drive the expression of DomB in the posterior compartment of the imaginal disc, which is further marked by CD8-GFP and comprises roughly half of the control wing disc (A). Endogenous Dom expression is visible in most nuclei (A'). (B): Upon DomB overexpression the posterior compartment appears slightly smaller and deformed (B). DomB overexpressing cells are strongly stained by Dom antibody staining (B').

3.3. Domino and the Tip60 complex regulate larval neuroblast division

Several NB populations are important for *Drosophila* development: Embryonic NBs produce the embryonic nervous system, larval central brain NBs continue neurogenesis of the central nervous system and optic lobe NBs produce the visual system (Saini and Reichert, 2012). Besides the embryonic NBs, especially the larval central brain NBs are well understood and several sophisticated tools and methods exist to study their behavior. To better understand the role of *dom* in NSCs I decided to investigate *dom* function in larval central brain NBs.

3.3.1. Domino is expressed in the larval central brain

The primary question to be answered for studying *dom* function in larval central brain NBs was to identify in which cell types Dom is expressed. Using the GFP-Dom gene trap line I found that Dom is ubiquitously expressed in all nuclei of the larval central brain (Figure 23). GFP-Dom stains Mira positive NBs as well as Pros positive daughter cells undergoing neurogenesis (Figure 23 A, B). Further, Repo positive glial cells are also positive for Dom. Interestingly, co-staining of Dom with the transcriptional activator Repo showed co-localization of the proteins especially in the nuclear regions stained only weakly for Hoechst (Yuasa et al., 2003) (Figure 23 C).

Like in the embryonic NB Dom is nuclear until nuclear envelope breakdown has occurred during NB division. Dom antibody staining additionally validated the Dom expression in larval NBs. However, the antibody unfortunately produces a rather strong cytoplasmic background staining in larval NBs, which cannot be seen in the GFP-Dom staining (Figure 23 D).

The expression of the larger isoforms DomA, D and G is restricted to a subset of cells in the optic lobe as well as the ventral nerve cord in the larval brain while DomE expression is ubiquitous. Importantly, expression of the three larger isoforms was not reported in those brain regions in which the NBs reside (Ruhf et al., 2001). Thus, DomE appears to be the isoform expressed in larval brain NBs.

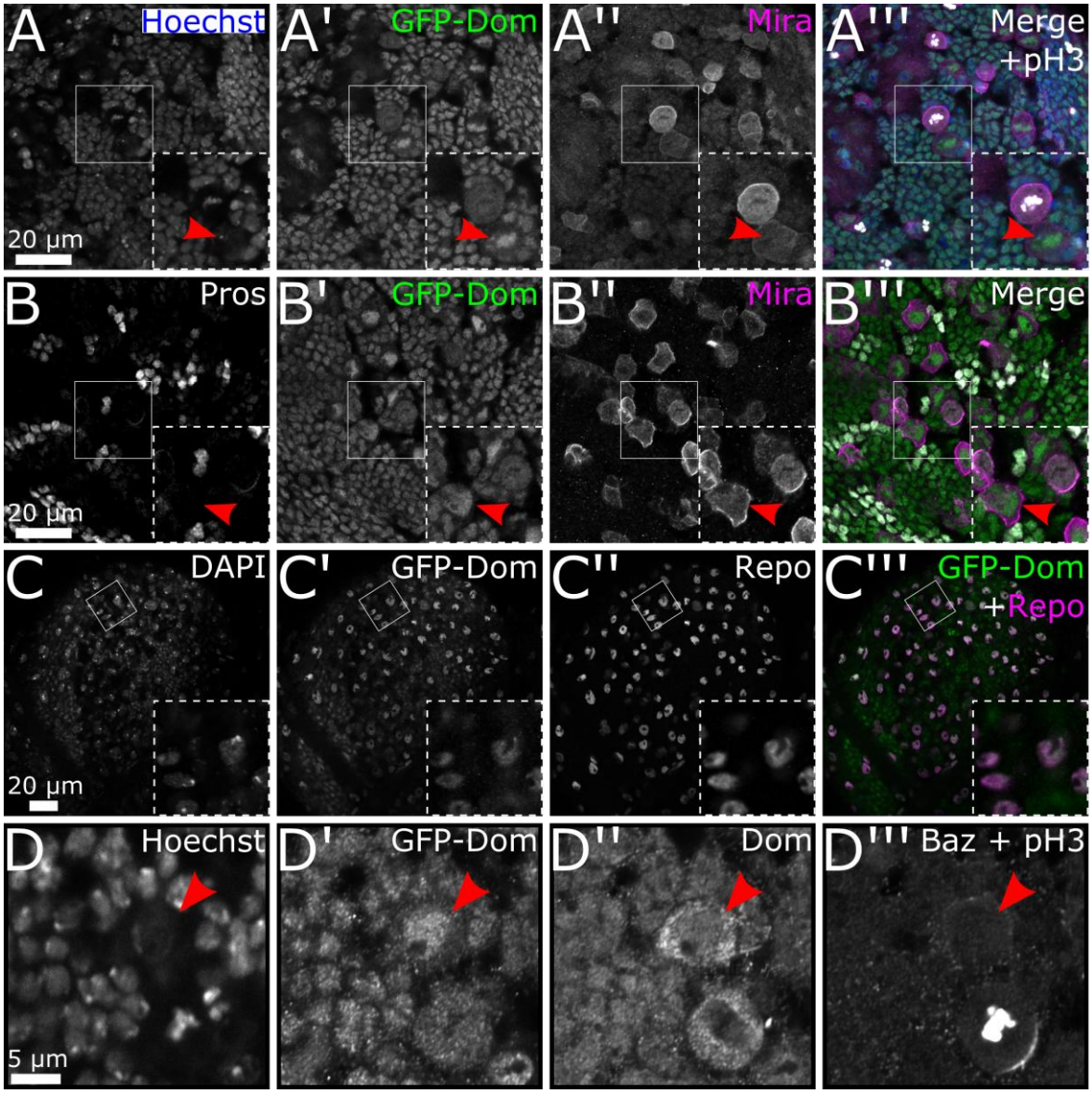

Figure 23: Domino is expressed in all cells of the larval central brain

Confocal microscopy pictures of *GFP-Dom* L3 larval brains showing the expression of Dom in different populations of larval brain cells. Arrowheads point at interphase NB nuclei. (A): GFP-Dom is expressed in Mira positive NBs and remains nuclear until breakdown of the nuclear envelope in pH3 positive dividing NBs. (B): Nuclei of NB offspring cells undergoing neurogenesis are positive for Pros as well as GFP-Dom. (C): Nuclei of glial cells are marked by Repo. Its staining overlaps with GFP-Dom. (D): Dom antibody stains nuclei of Baz expressing NBs, however, shows a strong cytoplasmic background staining.

3.3.2. Domino and the Tip60 complex are required for neural cell lineages

dom null mutants are early larval lethal and Flp/FRT-mediated homozygous *dom* mutant clones have been reported to disappear regardless of the stage of induction (Ruhf et al., 2001). I therefore decided to study *dom* loss of function in the larval NB utilizing RNAi and a Gal4 driver line specific for neural cell lineages, called *insc::Gal4*. *Insc* (*inscuteable*) is expressed in NBs. Gal4 and constructs under the UAS-promoter are, however, inherited by daughter cells. Thus, the *insc::Gal4* driver also influences especially the younger NB offspring cells. I tested several other NB specific driver lines including *ase::Gal4*, *sca::Gal4*, *wor::Gal4*, *elav::Gal4* and *pros::Gal4*, which generally led to similar results, but found *insc::Gal4* to be the strongest inducer.

Knockdown of *dom* with the *insc* driver with several *dom*-RNAi lines resulted in a general decrease of neural cells in comparison to a wild type control (Figure 24, see also M.Sc. Thesis Katja Rust, 2013) and is pupal lethal. Moreover, *dom* knockdown affects the GFP reporter such, that the fluorescence is much higher upon *dom* knockdown. Consequently, the microscope settings have to be adjusted during sample analysis, making the optic lobe appear GFP negative upon *dom* knockown (Figure 24 C – F) in comparison to the control (Figure 24 B). The strongest effect was achieved with the v7787 *dom*-RNAi line (Figure 24 C). Thus, in further experiments this RNAi line was used.

To confirm that indeed *dom* is targeted by the *dom*-RNAi lines, I stained *dom*-RNAi expressing larval brains with the Dom antibody. Nuclear Dom staining, which is present in the wild type control is absent upon *dom* knockdown (Figure 25). Only the cytoplasmic staining, which appears to be background as it does not overlap with the GFP-Dom staining (3.3.1), remains. Importantly, NB nuclei also lack Dom staining.

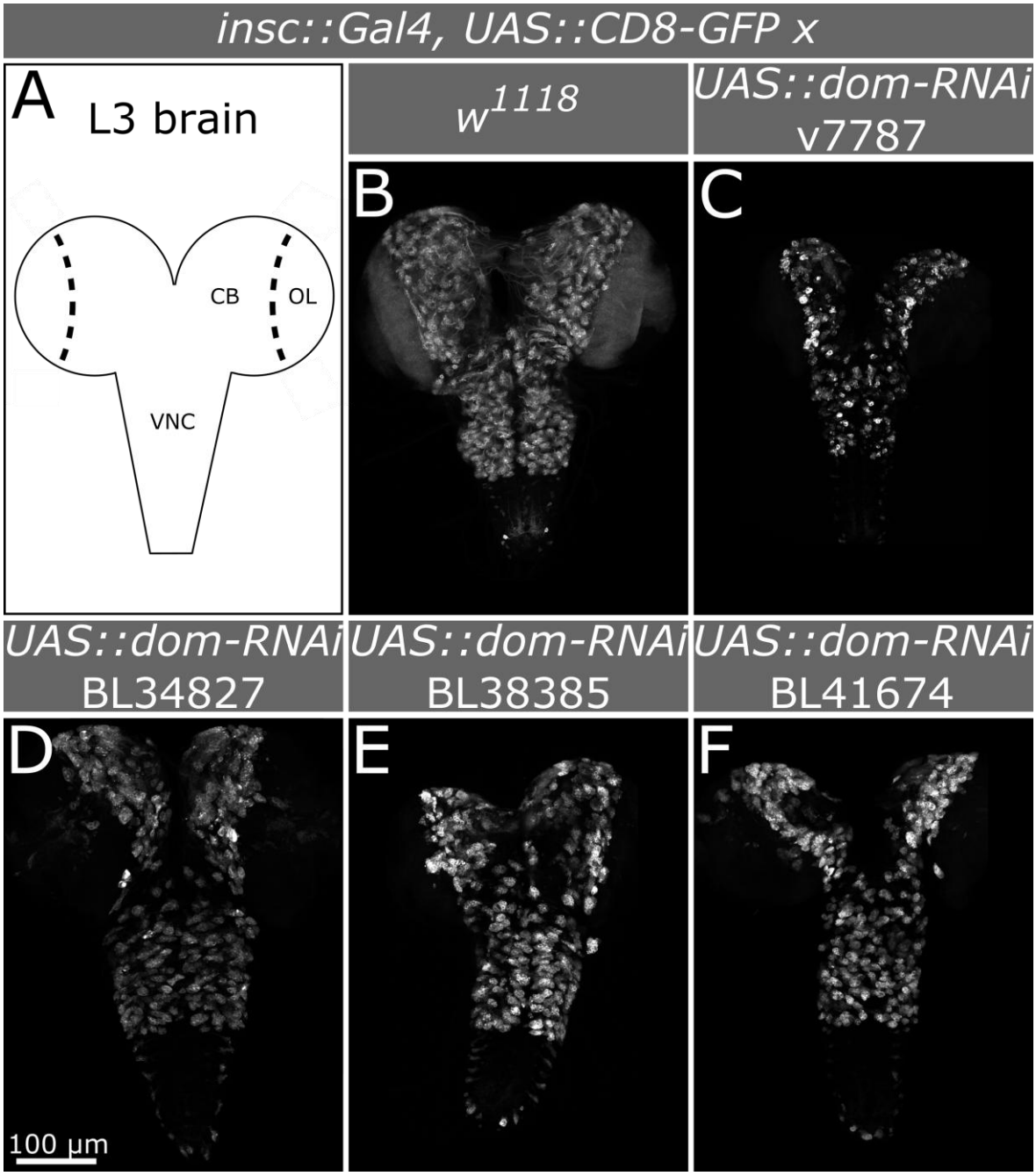

Figure 24: *domino* knockdown in larval neural lineages decreases the number of cells

Maximum intensity projections of larval brains. The *insc* driver was used to induce CD8-GFP marker expression. (B): In the wild type the optic lobe (OL) is slightly positive for GFP, while neural lineages in central brain (CB) and ventral nerve cord (VNC) are highly positive for CD8-GFP. (C – F): Several *dom*-RNAi lines lead to higher GFP expression, which makes the optic lobe appear GFP negative. *dom* knockdown reduces the number of GFP marked cells in the central brain and ventral nerve cord.

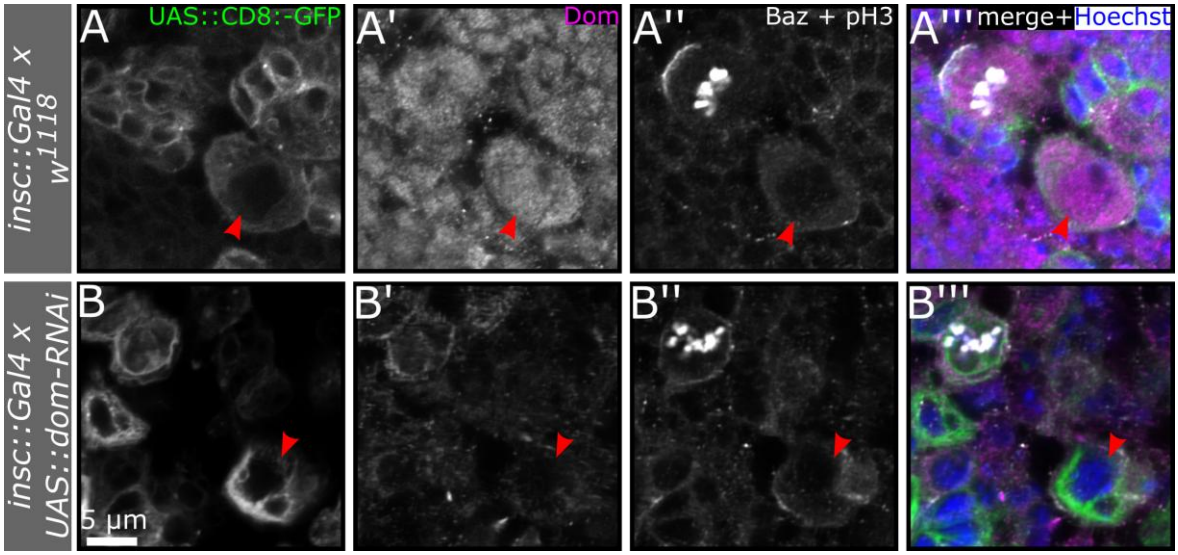

Figure 25: Domino antibody staining is absent upon *domino* knockdown by RNAi

L3 larval brains in which neural lineages are marked by CD8-GFP were stained for Dom. Baz marks NBs. Airyscan pictures show that wild type NB nuclei (A, arrowhead) are positive for Dom staining, while NB nuclei with *dom* knockdown are negative for Dom (B, arrowhead). Both wild type and *dom*-RNAi NBs show cytoplasmic Dom background staining.

Since knockdown of *dom* severely affects neural cells I aimed to investigate the effects of Dom upregulation. Overexpression of DomB (to date annotated as DomE) in larval neural cells is phenotypically normal compared to the wild type control (Figure 26 A, B). Remarkably, co-overexpression of DomB with *dom* knockdown by RNAi is able to partially rescue the cell loss phenotype observed in *dom*-RNAi alone (Figure 26 C, D). A full rescue was not expected as the probe expressed in *dom*-RNAi also targets the domB-RNA. Therefore, this result confirms that the knockdown of *dom* is responsible for the reduction of neural cells and suggests that DomE is the isoform required in larval NBs.

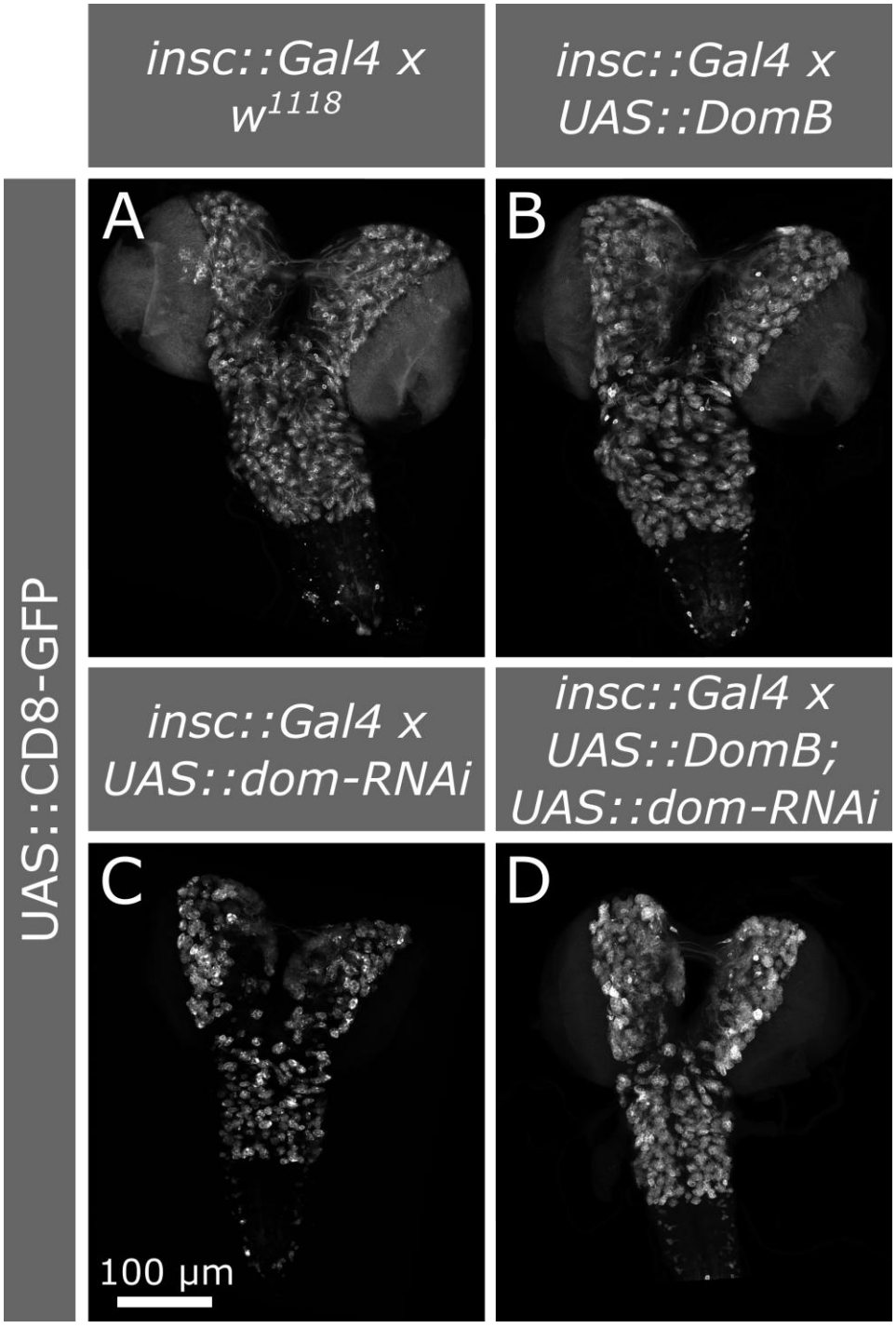

Figure 26: DominoB overexpression in the larval brain is phenotypically normal and partially rescues *domino* knockdown

Maximum intensity projections of L3 larval brains marked with CD8-GFP under the insc-promoter. DomB overexpression (B) resembles the wild type control (A). Combination of DomB overexpression with knockdown of *dom* by RNAi partially rescues the phenotype (D) as more cells are GFP marked than in the *dom* knockdown alone (C).

Flp/FRT-mediated mitotic clones homozygous for *dom* null alleles have been claimed to disappear such that they cannot be studied (Ruhf et al., 2001). Nonetheless, more sophisticated methods for the induction of mitotic cell clones have been developed. The convential Flp/FRT-method produces a homozygous GFP negative mutant cell clone and a homozygous GFP positive wild type twin spot clone in a heterozygous GFP positive background. In this setup the desired GFP negative clone is hard to identify (Xu and Rubin, 1993). The MARCM method produces homozygous GFP positive cell clones in an unmarked heterozygous background (Lee and Luo, 1999; Lee and Luo, 2001). I therefore attempted to induce homozygous dom^{14} MARCM clones using a genetic setup that allows clone induction solely in larval NBs. Please note that I analyzed MARCM clones in the ventral brain lobe and the ventral nerve cord to exclude type II NB clones from the analysis (Boone and Doe, 2008). Figure 27 shows wild type control MARCM clones with one Mira labeled NB founder cell per clone in comparison to a dom^{14} MARCM clone. dom^{14} MARCM clones are much smaller compared to wild type MARCM clones induced at the same time point (compare M.Sc. Thesis Katja Rust, 2013). Although the genetic background did not allow for the induction of clones in cells other than NBs, I found dom^{14} MARCM clones without a Mira positive mother cell, which was never the case in control clones (data not shown). This indicates that NBs get lost in homozygous dom^{14} clones. As the dom^{14} clone frequency was rather small, I decided to quantify NB numbers using *dom*-RNAi.

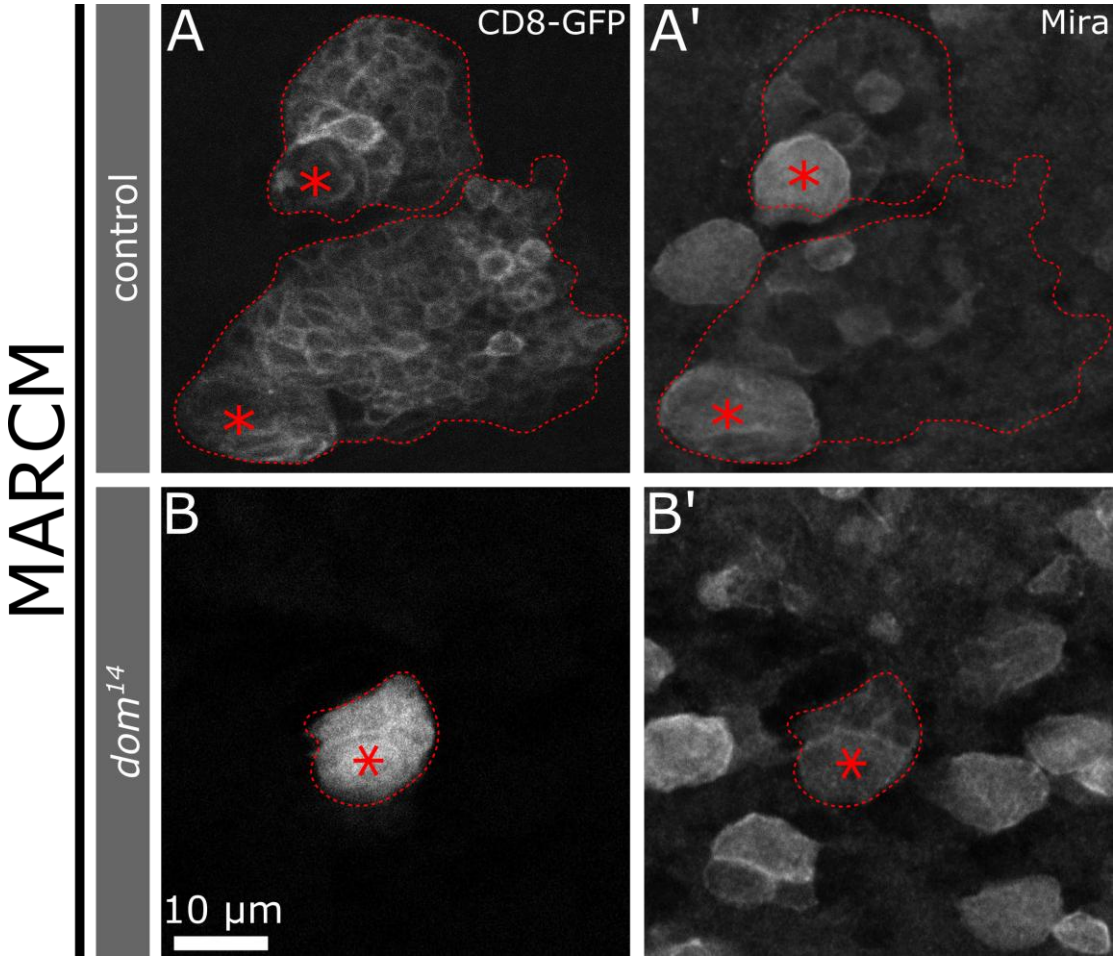

Figure 27: *dom*^{14} MARCM clones are smaller than control clones

MARCM CD8-GFP positive mitotic clones (marked with dotted lines) were induced in larval NBs in a wild type control (A) and for the *dom*^{14} allele (B). The mother NBs are marked with an asterisk. Note that control clones are considerably larger than *dom*^{14} clones induced at the same time point.

NB numbers vary within the L3 stage. I therefore analyzed NB numbers in brains during prepupal stage, a short and well identifiable stage in which the vast majority of NBs in the brain lobes is still maintained (Homem et al., 2014; Maurange et al., 2008; Siegrist et al., 2010). Further, I used a specific brain region, the ventral part of the central brain lobe, in which only type I NBs reside to ensure that only NBs and no Mira positive intermediate neural precursors (INPs) are considered (Boone and Doe, 2008). I found that control brains possess 61 ± 5.9 NBs, while *dom*-RNAi brains had only 42 ± 7.6 NBs, showing that *dom* knockdown significantly reduces the NB number ($p = 3.2E-20$, Figure 28).

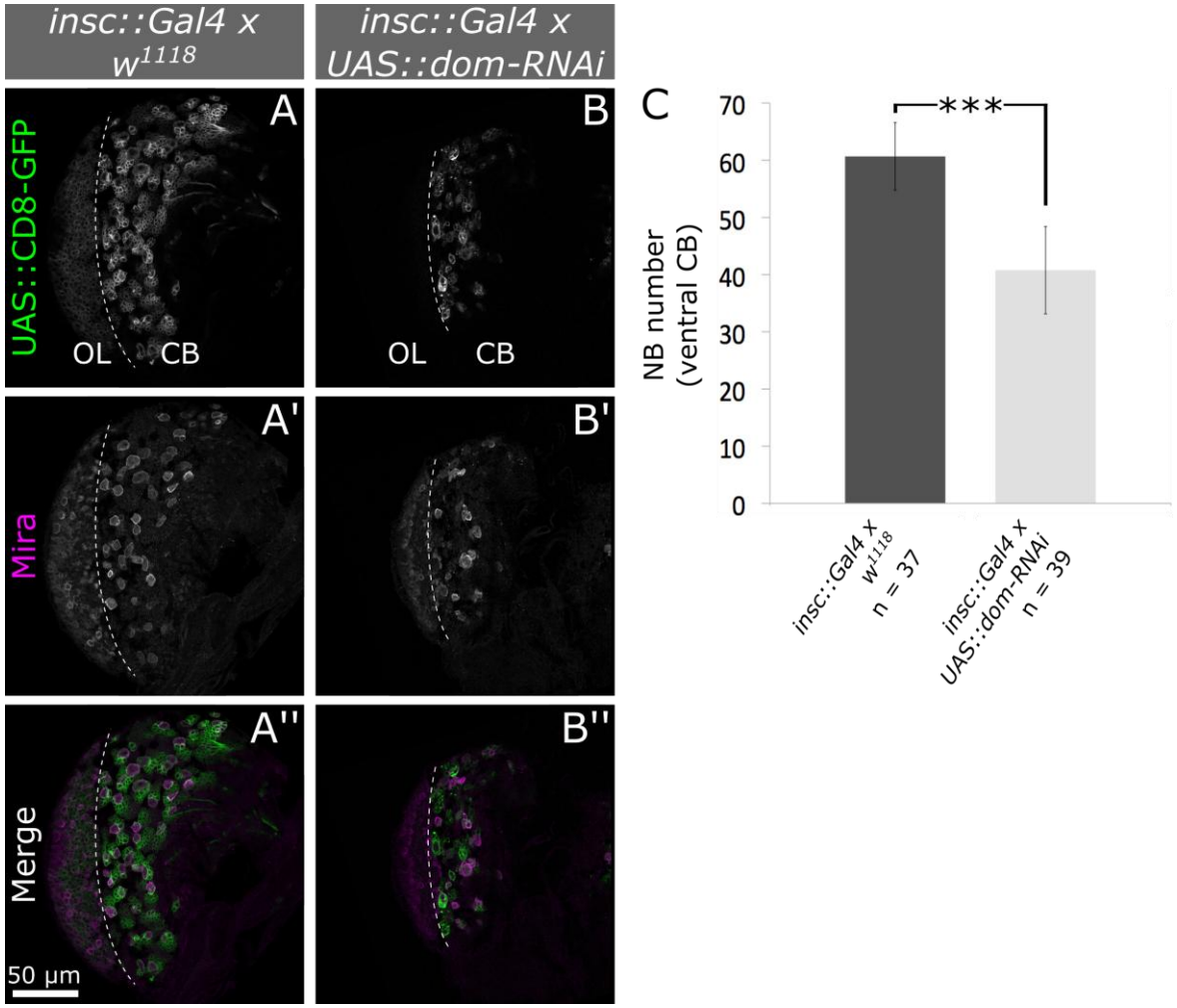

Figure 28: *domino* knockdown reduces larval neuroblast number

NB (marked by Mira) numbers were determined in ventral region of the central brain (CB) of prepupal brains. An overview is given in A and B. I: Wild type brains contain 61 ± 5.9 NBs, which are significantly more compared to *dom* knockdown with 42 ± 7.6 NBs (p = 3.2E-20). N refers to the number of quantified brain lobes. OL = optic lobe.

In view of the fact that NB and thereby neural cell lineage numbers are reduced upon *dom* knockdown, I explored whether also the cell number per lineage was decreased. The smaller sized cell clones in *dom*^{14} MARCM clones already suggest that this is the case. Additionally, staining of NB offspring cells with the marker Pros can provide further insight. A reduction of neural cell lineages would be marked by fewer Pros positive clusters alone while I rather expected less clusters together with less Pros positive cells per cluster upon *dom* knockdown. Immunostaining shows less Pros positive cells which are not arranged in clusters upon *dom* knockdown in comparison to the control (Figure 29). Together with the shorter lineages observed in MARCM analysis, this suggests that not only NB numbers but also the number of offspring cells are reduced. Further, staining for the neuron marker FasIII confirmed that also terminal differentiated neurons are reduced upon *dom* knockdown (Figure 30).

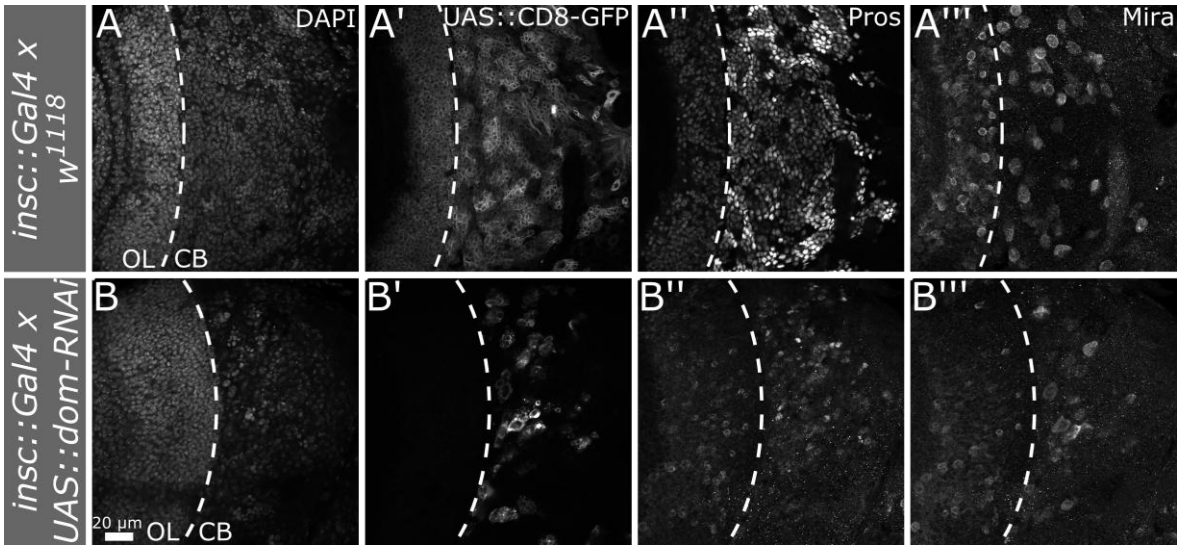

Figure 29: Neuroblast offspring cells are reduced in number upon *domino* knockdown

Confocal microscopy pictures of ventral L3 brain lobes stained for Mira as NB marker. Nuclear Pros staining marks NB offspring cells undergoing neurogenesis. (A): In the wild type Pros positive cells lie in clusters, representing offspring from the same mother NB. (B): Pros positive cells are fewer and more scattered rather than clustered upon *dom* knockdown. CB = central brain, OL = optic lobe.

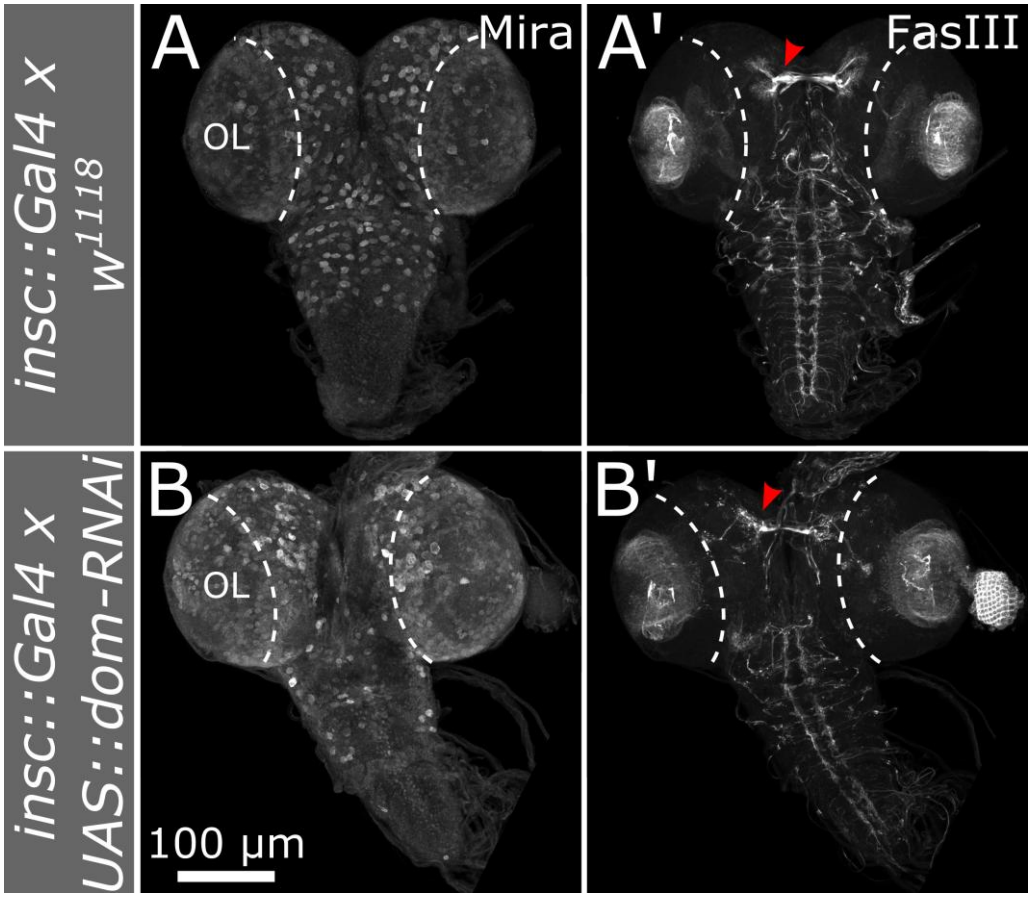

Figure 30: *domino* knockdown decreases neuron numbers in larval brains

Maximum intensity projections of L3 larval brains of the *insc* driver crossed with the wild type w^{1118} allele (A) or *UAS::dom-RNAi* (B). Mira staining marks NBs, which are reduced in number upon *dom* knockdown. FasIII stains neurons. Knockdown of *dom* reduces neurons in the larval brain, which is most severe in the ventral nerve cord. Additionally, the mushroom bodies (arrowhead) are smaller.

Dom functions in the Tip60 chromatin remodeling complex together with various other proteins (Kusch et al., 2004). To find out whether Dom is required within the Tip60 complex or functions independently in larval neurogenesis, I investigated knockdown of other Tip60 components in larval neural lineages. I found that the knockdown of several other Tip60 complex subunits reduced the number of neural cells (Figure 31). Although the GFP fluorescence was not elevated upon knockdown of all of these components, the phenotypes are remarkably similar to *dom* knockdown, indicating that the Tip60 complex or a sub-complex of it is indispensable for larval neurogenesis (see Appendix Table S 2).

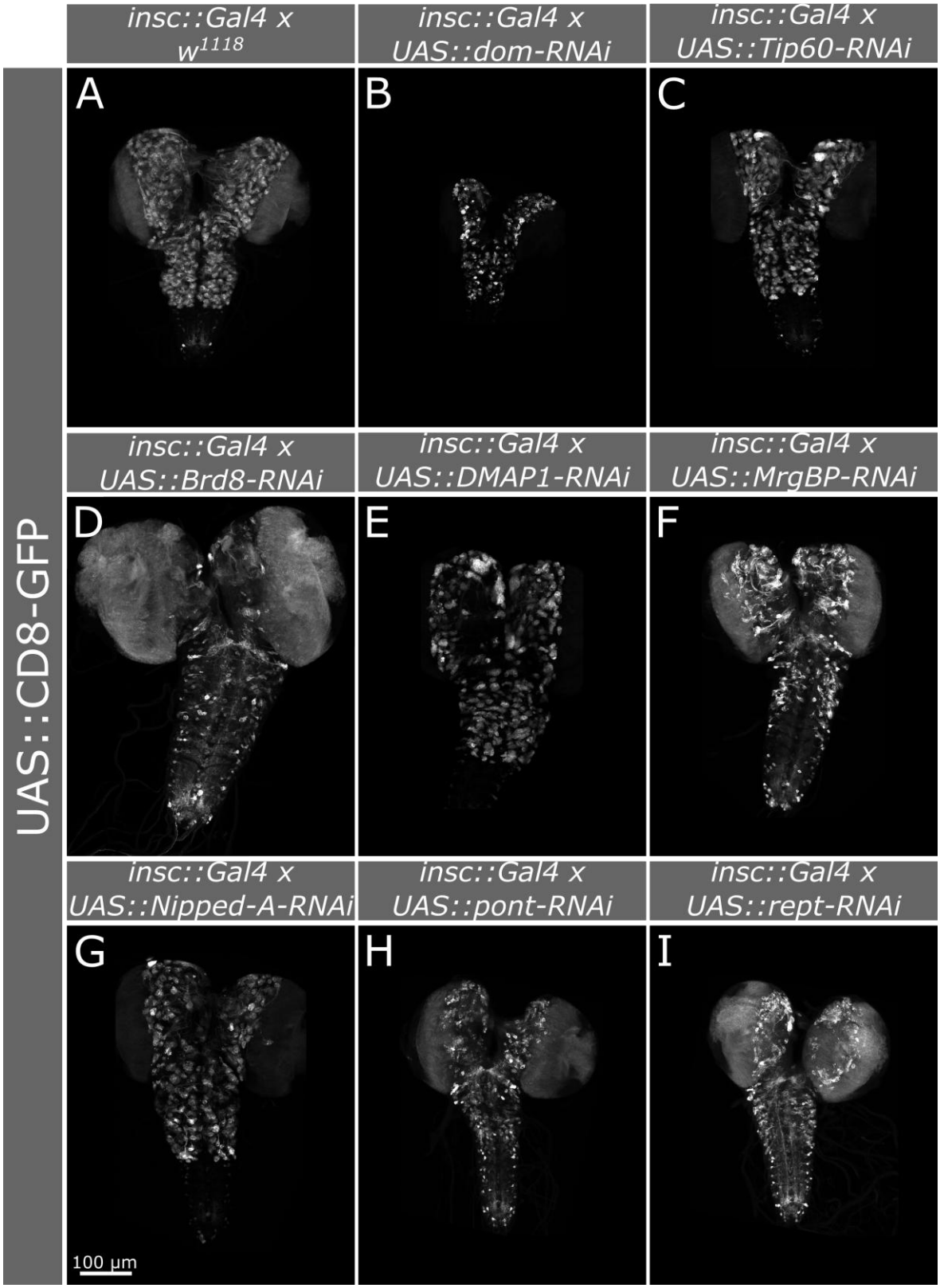

Figure 31: Members of the Tip60 complex are required for larval neural cell lineages

Maximum intensity projections of larval brains with CD8-GFP marked neural lineages. Neural knockdown of Tip60 complex members reduces the number of GFP positive cells (B – I) in comparison to the wild type (A).

Several studies carried out in mammalian systems suggest that the Tip60 HAT and the Dom homolog p400 can antagonize their function in certain cellular contexts (Mattera et al., 2009; Park et al., 2010; Tyteca et al., 2006). To elucidate whether Dom and Tip60 function together or antagonistically in Drosophila larval NBs, I knocked down *Tip60* in *dom*-RNAi larval brains under the *insc* driver. *dom*-RNAi was lethal prior to the L3 larval stage in combination with three different *Tip60*-RNAis (*UAS>tip60-RNAi* Zhu et al., 2007, v22231, v110617). Overexpression of Tip60 in *insc* driven *dom*-RNAi could not restore neural cells (Figure 32). This indicates, that the Tip60 and Dom function together in the Tip60 complex to regulate neural cell number.

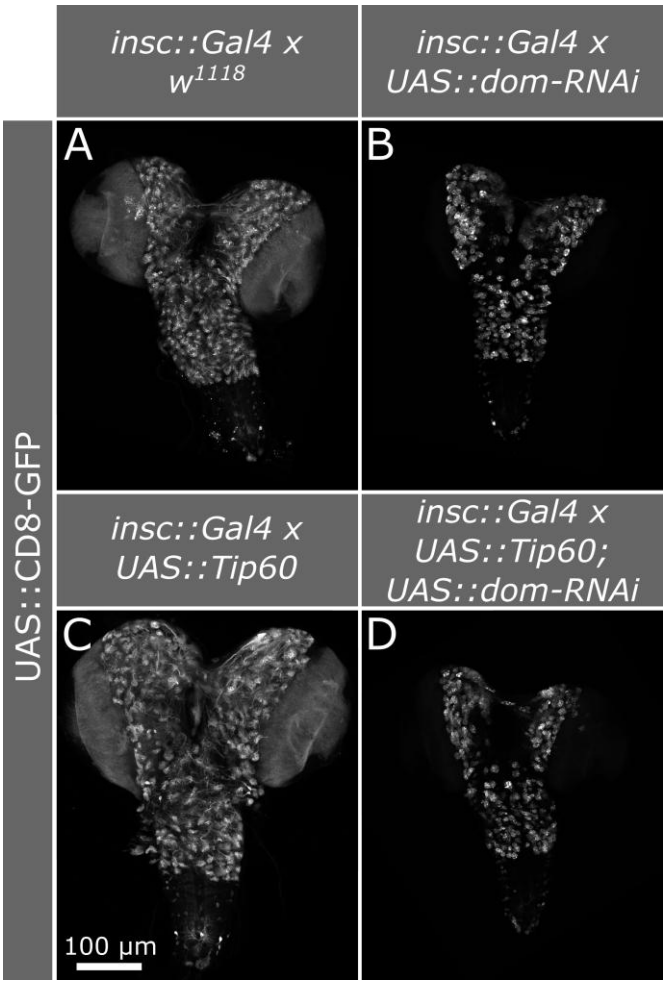

Figure 32: Tip60 overexpression does not rescue *domino* knockdown in larval neural cells

Maximum intensity projections of larval brains using the *insc* driver to express CD8-GFP in neural cells. (C): Tip60 overexpression is phenotypically normal and resembles wild type brains (A). Overexpression of Tip60 cannot rescue *dom* knockdown (D), which is marked by a reduction in CD8-GFP positive cells (B).

3.3.3. Lack of neuroblasts upon *domino* knockdown is independent of apoptosis

To examine whether *dom* knockdown decreases NB numbers by inducing apoptosis, I exploited the baculovirus P35 protein, which is a potent inhibitor of apoptosis in *Drosophila* (Hay et al., 1994). Overexpression of P35 alone in neural cells increases the NB number by approximately 12 NBs to 73 ± 5.9 in the ventral central brain of the prepupal brain lobe in comparison to 61 ± 5.9 NBs in the wild type control (Figure 33 E). This indicates that P35 is capable of restoring NBs that undergo apoptotic cell death. Maximum intensity projection of a P35 overexpressing brain illustrates that these brains are bigger and contain more GFP marked neural cells in comparison to wild type brains (Figure 33 A and B). Please note the ectopic neural lineages in the abdominal ventral nerve cord, which harbors a NB population that normally undergoes apoptosis early in the L3 instar (Bello et al., 2003).

Overexpression of P35 in *dom*-RNAi expressing brains scores 55 ± 10.1 NBs in average, thus restoring roughly 13 NBs in comparison to the 42 ± 7.6 NBs in *dom*-RNAi brains (Figure 33 E). This phenomenon is also visible in larval brain maximum intensity projections (Figure 33 C and D). P35 overexpression in *dom*-RNAi leads to significantly reduced NB numbers in comparison to the wild type control and P35 overexpression alone. The number of restored NBs (≈13) is nearly the number of NBs that can be restored by P35 overexpression in comparison to the wild type (≈12). Importantly, the ability of P35 to maintain additional NBs in *dom* knockdown proves, that P35 is able to prevent apoptosis also in the absence of Dom. Altogether, apoptosis is unlikely to be the cause for the reduced NB numbers upon *dom* knockdown.

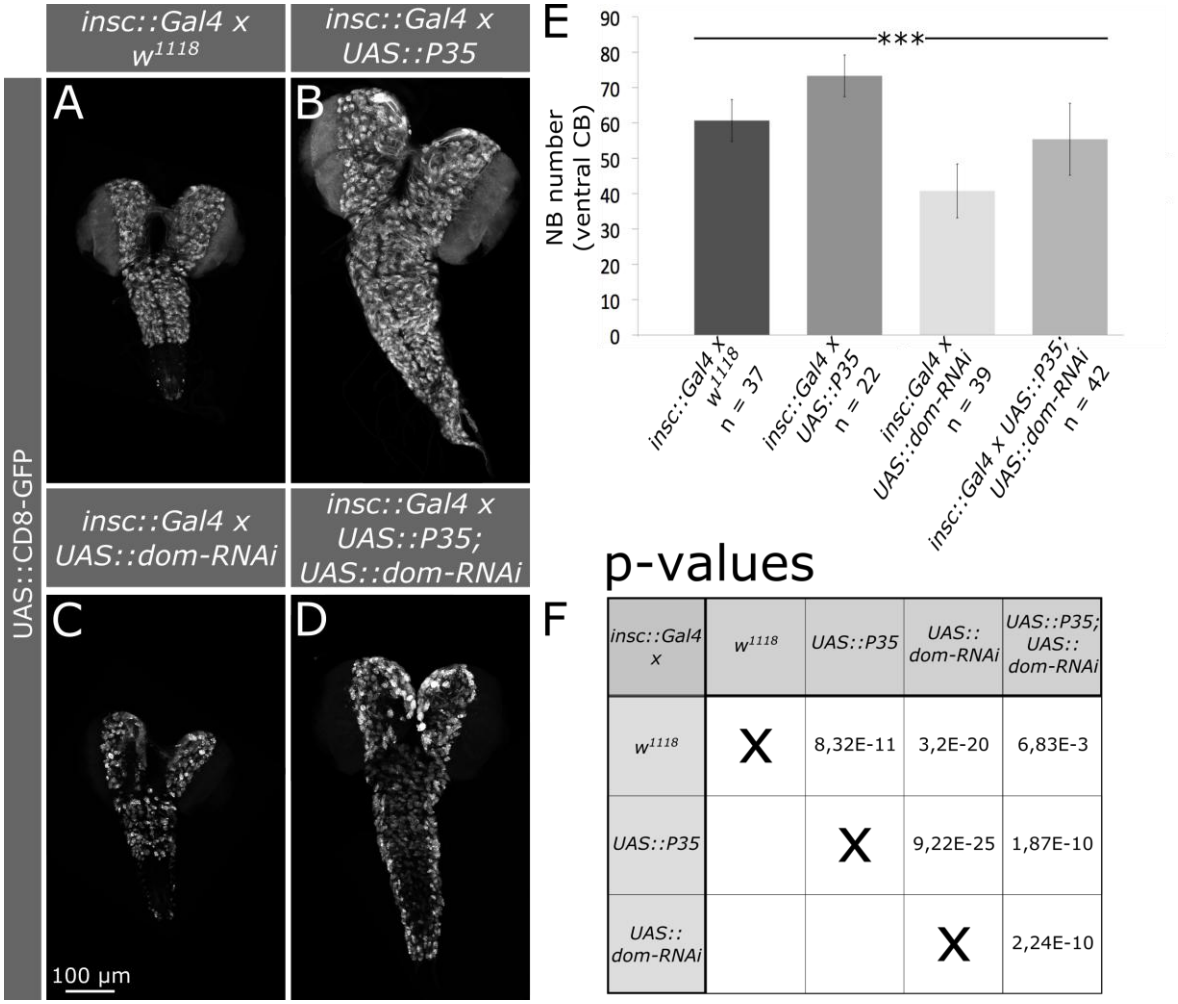

insc::Gal4 x	w^{1118}	UAS::P35	UAS:: dom-RNAi	UAS::P35; UAS:: dom-RNAi
w^{1118}	X	8,32E-11	3,2E-20	6,83E-3
UAS::P35		X	9,22E-25	1,87E-10
UAS:: dom-RNAi			X	2,24E-10

Figure 33: Inhibition of apoptosis does not restore neuroblasts lacking upon *domino* knockdown

(A – D): Maximum intensity projections of brains with CD8-GFP marked neural lineages. P35 overexpression increases neural cells in comparison to the wild type. Overexpression of P35 in *dom*-RNAi likewise increases the cell number in comparison to *dom*-RNAi alone but cannot fully restore all neural cells. (E): NB number quantification confirms that P35 maintains NBs in comparison to the wild type. P35 overexpression in *dom*-RNAi does not restore NB number to the full extent. N refers to the number of brain lobes used for quantification. (F) gives p-values from student's t-test comparison of the NB numbers.

3.3.4. *domino* knockdown leads to polarity defects in larval neuroblasts

Since apoptosis is not the reason for the lack of NBs in *dom* knockdown, other causes had to be considered. One of the most important features of NBs is their asymmetric division. Polarized localization of cell fate determinants enables the NB to self-renew and give rise to a differentiated daughter cell, the ganglion mother cell (GMC). Disturbances in the

asymmetry of the NB can lead to tumor formation or to loss of the stem cell (Knoblich, 2010).

I used the MARCM system to stain the apically localized polarity marker Baz and Mira, which is basally localized, and found that these polarity determinants are mislocalized in *dom* mutant NBs (Figure 34, M.Sc. Thesis Katja Rust, 2013). Albeit, the number of mitotic NBs in dom^{14} MARCM clones was too small to achieve reliable data for quantification.

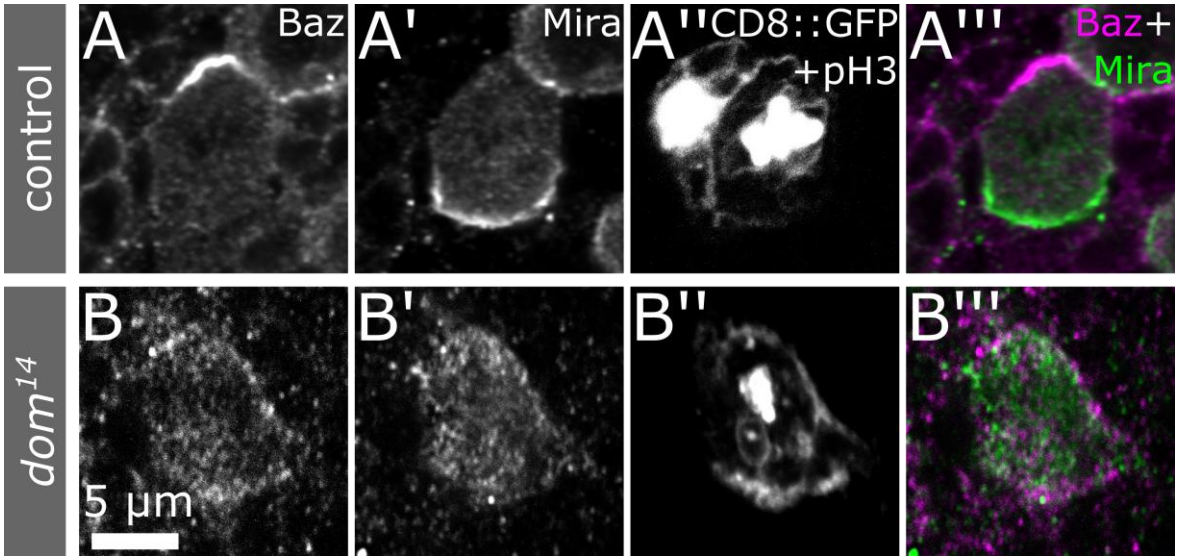

Figure 34: Neuroblast polarity is disturbed in *domino* null mutant cell clones

Polarity of dividing NBs in MARCM clones was analyzed by immunostaining and confocal microscopy. pH3 marks mitotic nuclei and is distinguishable from the CD8-GFP signal, which localizes to membranes and marks MARCM clones. Baz and Mira localize to opposite crescents in dividing wild type NBs (A) but are cytoplasmic in dom^{14} NBs (B).

For this reason, I investigated the localization of Baz as well as downstream effectors like aPKC (for aPKC see Appendix: Figure S 3, see also M.Sc. Thesis Katja Rust, 2013) and Mira in *dom*-RNAi NBs and confirmed that ≈ 24 ± 18.6% of all NBs with *dom* knockdown exhibited polarity defects during mitosis (Figure 35). While Baz and Mira localized to opposing wild type NB sides (Figure 35 A), in *dom*-RNAi NBs polarity markers were mislocalized to the cytoplasm or then whole cortex of the cell (Figure 35 C) and in some cases I observed double crescents (Figure 35 B). Investigation of NB polarity in knockdown of other Tip60 complex members showed that knockdown of several components including *rept*, *pont* and *DMAP1* also leads to severe polarity defects (data not shown).

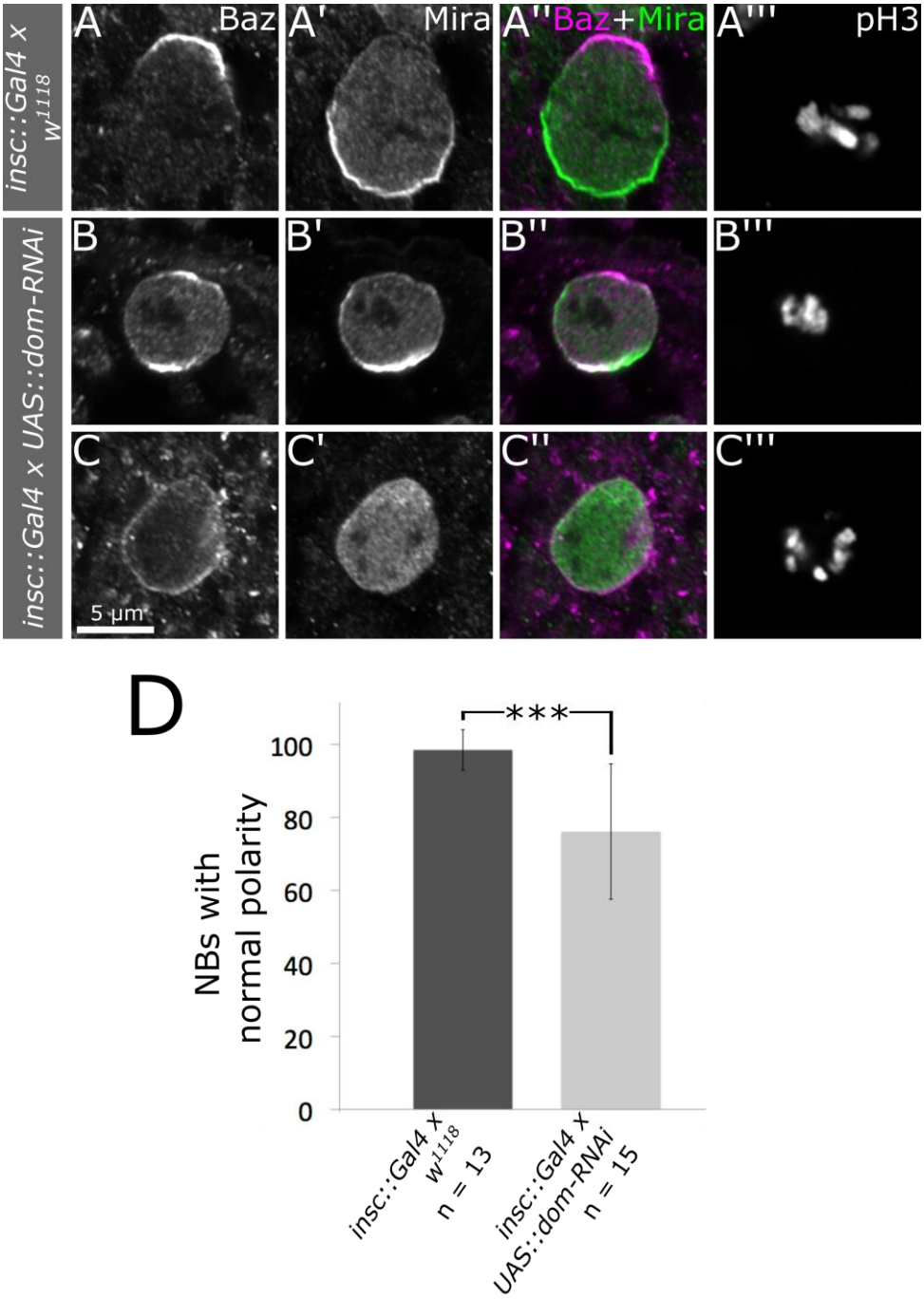

Figure 35: *domino* knockdown disturbs neuroblast polarity in the larval brain

(A – C): Airyscan pictures of mitotic (pH3 positive), larval NBs. (A): Wild type NBs localize Baz and Mira into crescents on opposing sides of the NB. *dom* knockdown occasionally leads to the formation of overlapping double crescents (B) or, more frequently, a complete mislocalization of polarity determinants (C). (D): Quantification of NBs with correct polarity shows that significantly less NBs are properly polarized upon *dom* knockdown (p = 2.96E-4). N refers to the number of analyzed brains. A minimum of 5 NBs were analyzed per brain.

3.3.5. *domino* deficient larval neuroblasts display features of termination of neurogenesis

Assuming that NBs with incorrect polarity might not be capable of producing NB daughter cells with self-renewing capacity, the observed polarity defects in *dom* knockdown NBs could be a cause for the lack of NBs. During termination of neurogenesis NBs exit the cell cycle and differentiate. Thereby, they first decrease their size until Pros, a transcription factor that activates neurogenesis, enters the NB nucleus during the interphase preceding the terminal division (Maurange et al., 2008).

I analyzed the NB radius of L3 mitotic NBs prior to cytokinesis as described in 2.2.5.2. In L3 larval stage NBs increase their size after every division, thus NB size should be most uniform immediately prior to cell division (Homem et al., 2013; Ito and Hotta, 1992). Figure 36 shows that *dom* deficient NBs are significantly smaller than wild type NBs (3.84 ± 0.28 µm wild type radius versus 3.18 ± 0.36 µm *dom*-RNAi radius, p = 3.68E-11).

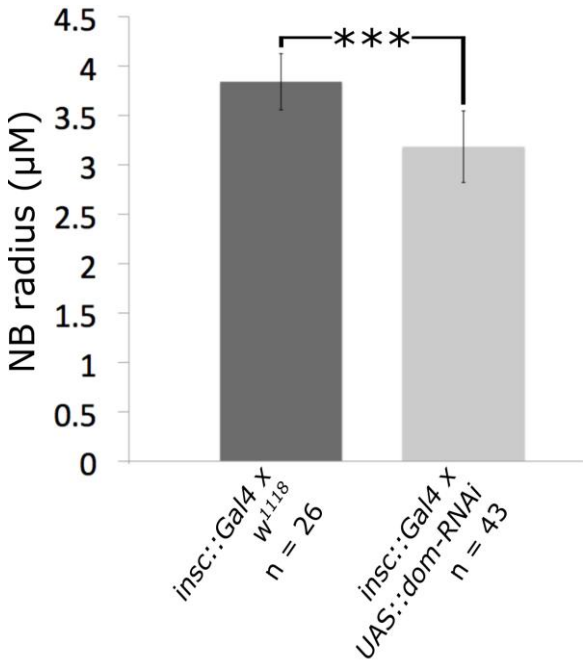

Figure 36: *domino* knockdown reduces neuroblast size

Cell size of L3 mitotic NBs before cytokinesis was measured and is indicated as NB radius. Wild type NBs are significantly bigger than NBs in which *dom* was downregulated.

The size decrease of NBs undergoing termination of neurogenesis is caused by NBs ending to increase size after each division (Homem et al., 2014). I therefore compared NB sizes of interphase NBs (NBs after division) and mitotic NBs (NBs before cytokinesis of a division). While wild type NBs are slightly bigger during mitosis (3.84 ± 0.28 µM in radius during mitosis, 3.57 ± 0.26 µM during interphase), *dom* deficient NBs are similarly small during mitosis (3.18 ± 0.36 µM) and interphase (3.23 ± 0.44 µM) (Figure 37).

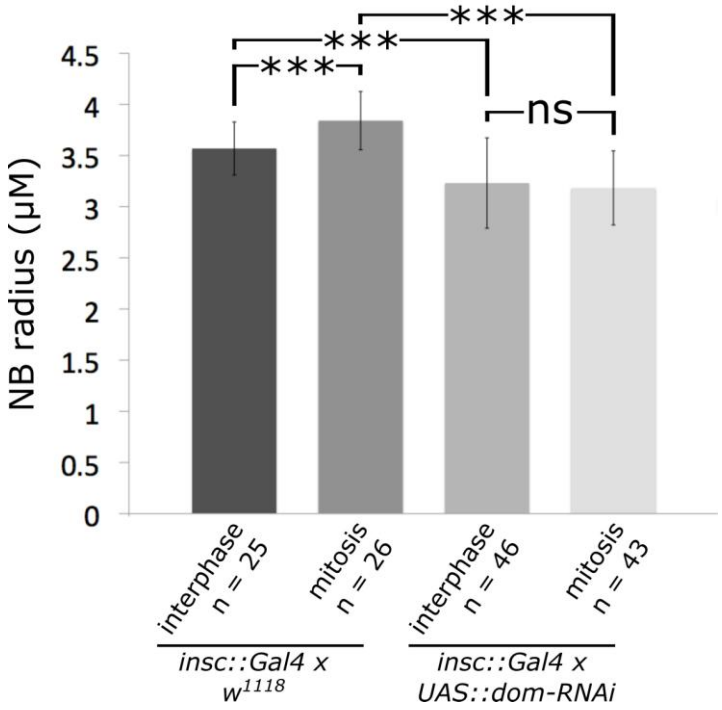

Figure 37: *domino* depleted neuroblasts are inable to increase size after division

NB radii of L3 mitotic and interphase NBs in a wild type control and upon *dom*-RNAi are compared. *dom* depleted NBs are significantly smaller than wild type NBs (p(WT mitosis/*dom* mitosis) = 3.68E-11, p(WT interphase/*dom* interphase) = 8.05E-4, p(WT interphase/*dom* mitosis) = 1.54E-5, p(WT mitosis/*dom* mitosis) = 1.99E-8). During mitosis wild type NBs are significantly bigger than during interphase (p = 8.1E-4). *dom* depleted NBs are similar in size during both cell cycle phases (p = 0.58).

Besides a reduction in size NBs also slow down their cell cycle in the end of neurogenesis (Homem et al., 2014). I thus expected to find less mitotic NBs upon knockdown of *dom.* Determination of the mitotic index of larval NBs proved that *dom*-RNAi NBs are less probable in the mitotic phase (28.28 ± 5.8%) than wild type NBs (39.02 ± 8.7%, p = 5.75E-4) (Figure 38).

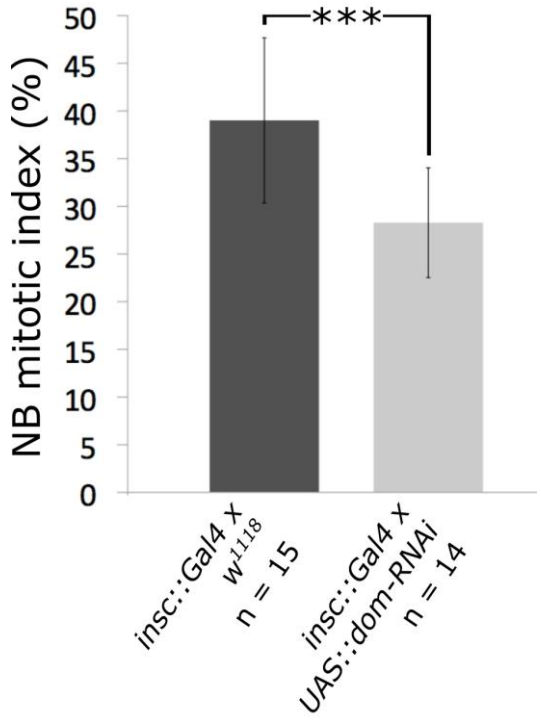

Figure 38: *domino* knockdown reduces the proportion of mitotic neuroblasts

The mitotic index (proportion of mitotic cells) of L3 NBs was analyzed in a wild type control and upon *dom*-RNAi. NBs were identified by Mira expression. pH3 was used to mark mitotic cells. N refers to the number of quantified brain lobes.

Size decrease and slowing down of the cell cycle during termination of neurogenesis is accompanied by nuclear entry of Pros into the interphase nucleus of NBs (Homem et al., 2014; Maurange et al., 2008). I immunostained *dom*-RNAi L3 NBs against Pros and analyzed the subcellular localization during the interphase. Remarkably, while Pros was cytoplasmic in 100% of NBs in the wild type control, only 53.36 ± 23.46% of *dom* depleted interphase NB showed Pros exclusively in the cytoplasm without any nuclear staining (Figure 39). Notably, I excluded 20% of *dom*-RNAi NBs from the analysis in which it was impossible to determine whether Pros was cytoplasmic or rather nuclear. However, no such case was observed in the wild type.

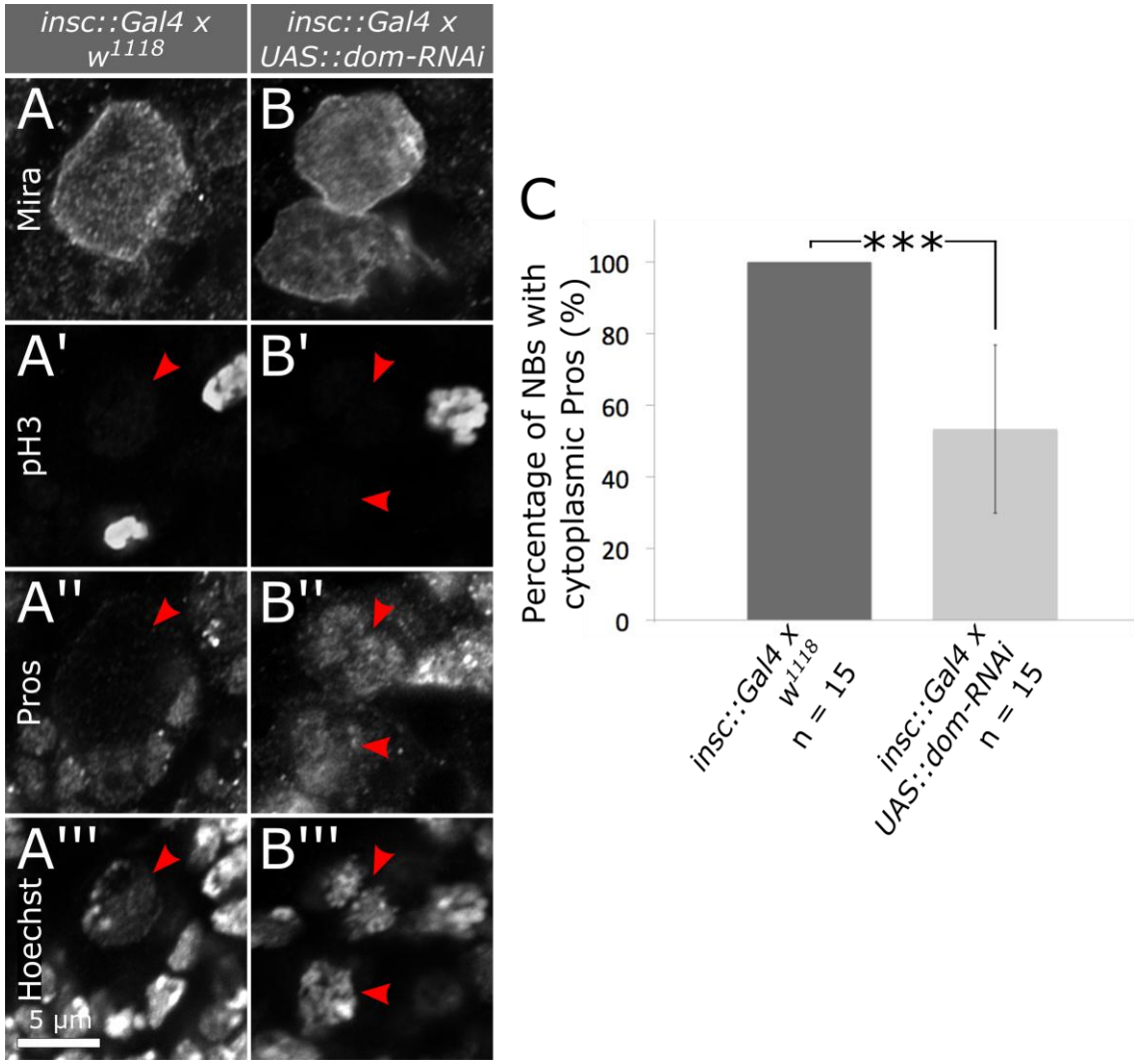

Figure 39: Prospero enters the interphase neuroblast nucleus upon *domino* knockdown

Airyscan pictures show interphase (pH3 negative) NBs in the L3 brain. (A): In the wild type control Pros is cytoplasmic and not visible in comparison to the brightly labeled nuclei of offspring cells. (B): In *dom*-RNAi NBs Pros can be observed in the nucleus, which was stained with Hoechst. (C): Quantification of NBs with normal, cytoplasmic Pros localization shows that significantly less NBs display correct localization of Pros upon *dom* knockdown than in the control (p = 2.19E-8). N = number of brains used for quantification. Per brain at least 5 NBs were analyzed.

In order to define whether the premature Pros nuclear entry is specifically dependent on *dom* knockdown alone or depends on reduced functionality of the Tip60 complex, I checked the Pros localization upon knockdown of other Tip60 members. As shown in Figure 40, Pros also enters interphase NB nuclei upon knockdown of several Tip60 components including *DMAP1*, *Nipped*-A, *pont* and *rept*.

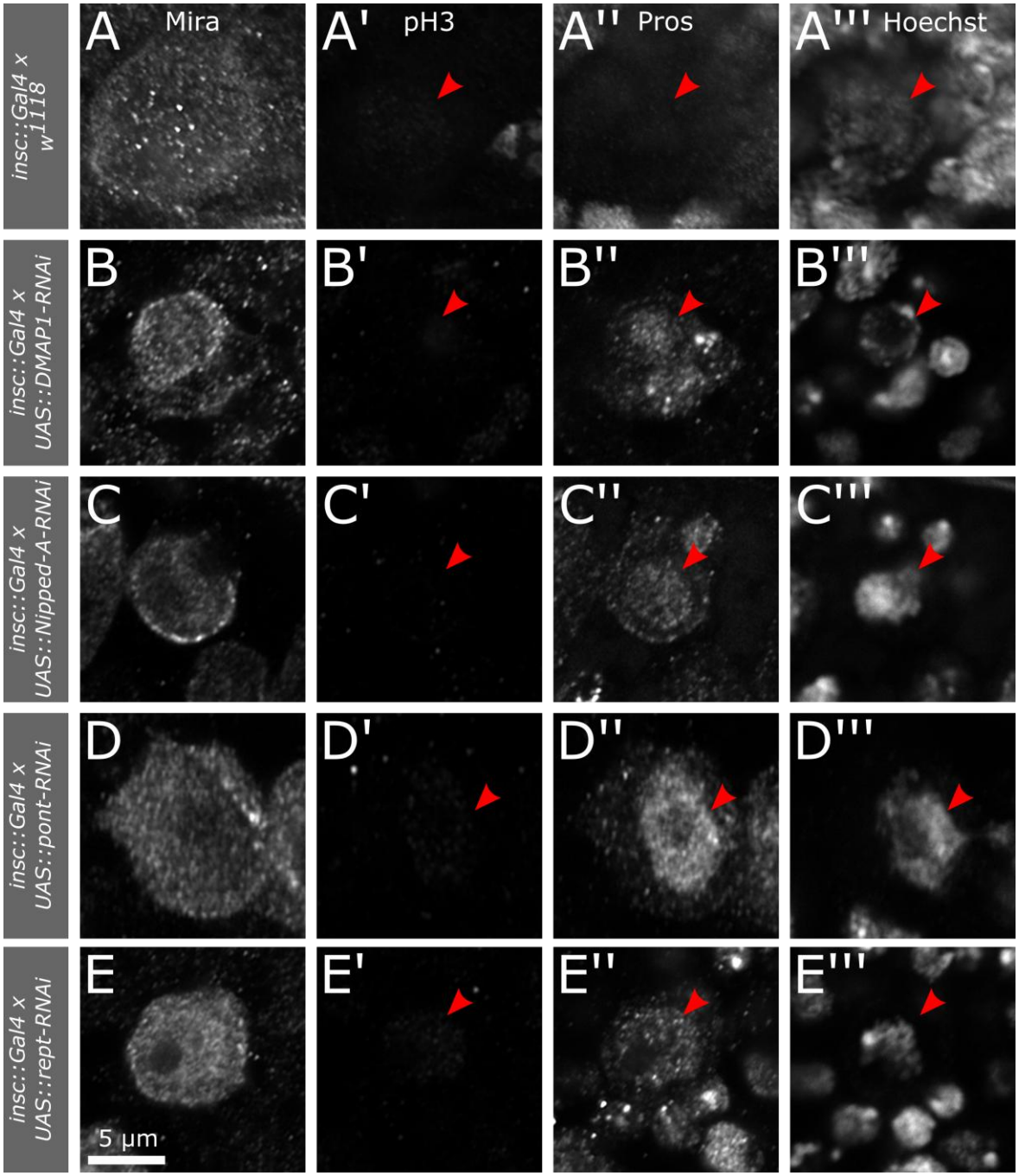

Figure 40: Knockdown of Tip60 members leads to premature Prospero nuclear localization in neuroblasts

Airyscan pictures show immunostained L3 interphase NBs marked by Mira and the absence of pH3 staining. (A): Cytoplasmic staining of Pros in the wild type NB is weak compared to neighbouring cells undergoing neurogenesis. (B – E): Interphase nuclei of NB in which Tip60 members have been knocked down show nuclear Pros staining. Arrow indicates NB nuclei.

3.3.6. Neuroblast division and its asymmetry is disturbed upon *domino* knockdown

A decreased NB size, slower cell cycle and nuclear entry of the transcription factor Pros have been reported to mark the termination of most NBs (Homem et al., 2014; Maurange et al., 2008). Nonetheless, the polarity determinant Mira was reported to localize properly in the last NB division (Maurange et al., 2008). To understand better how the polarity defects and the features of NB termination observed upon *dom* knockdown are connected, I decided to image NB divisions *in vivo*. Using CD8-GFP expressed under the *insc* driver, larval NBs can easily be identified by position, shape and size and their division can be followed by 4D confocal microscopy.

I determined the cell sizes of mother NBs and the resulting daughter cells for wild type and *dom* depleted NBs (Figure 41). Although mother and daughter NB cells are significantly smaller when *dom* is depleted (p = 3E-3 for mother NB in comparison to mother NB of w^{1118}, p = 1.3E-6 for daughter NB in comparison to daughter NB of w^{1118}) the resulting GMC is not significantly decreased in size (p = 0.072 in comparison to GMC of w^{1118}) (Figure 41 C). I thus calculated the ratio of the smaller GMC daughter cell to the bigger NB daughter (dc2/dc1) for each division (Figure 41 E). For the wild type NB divisions this ratio was 0.52 $\pm$ 0.05, confirming that the GMC daughter cell is almost half the size of the resulting NB daughter cell. For *dom* depleted NB divisions the average ratio was 0.68 $\pm$ 0.16, indicating that the size difference between the daughter cells was less dramatic. Considering the ratios for the single divisions I noted that for 20% of the *dom* depleted NB divisions the ratio was almost 1, meaning that the daughter cells are roughly similar in size. Comparing sizes of the cells from these symmetric divisions to wild type cell sizes it became obvious that the symmetrically dividing mother cell NBs in the *dom*-RNAi are equally big compared to the wild type mother cells (p = 0.144). The resulting daughter cells, however, are similarly sized such that the slightly bigger daughter cell is significantly smaller than the a wild type NB daughter cell (p = 2.2-E8) and the smaller *dom* depleted daughter cell is significantly bigger than a wild type GMC (p = 1.6E-7) (Figure 41 D).

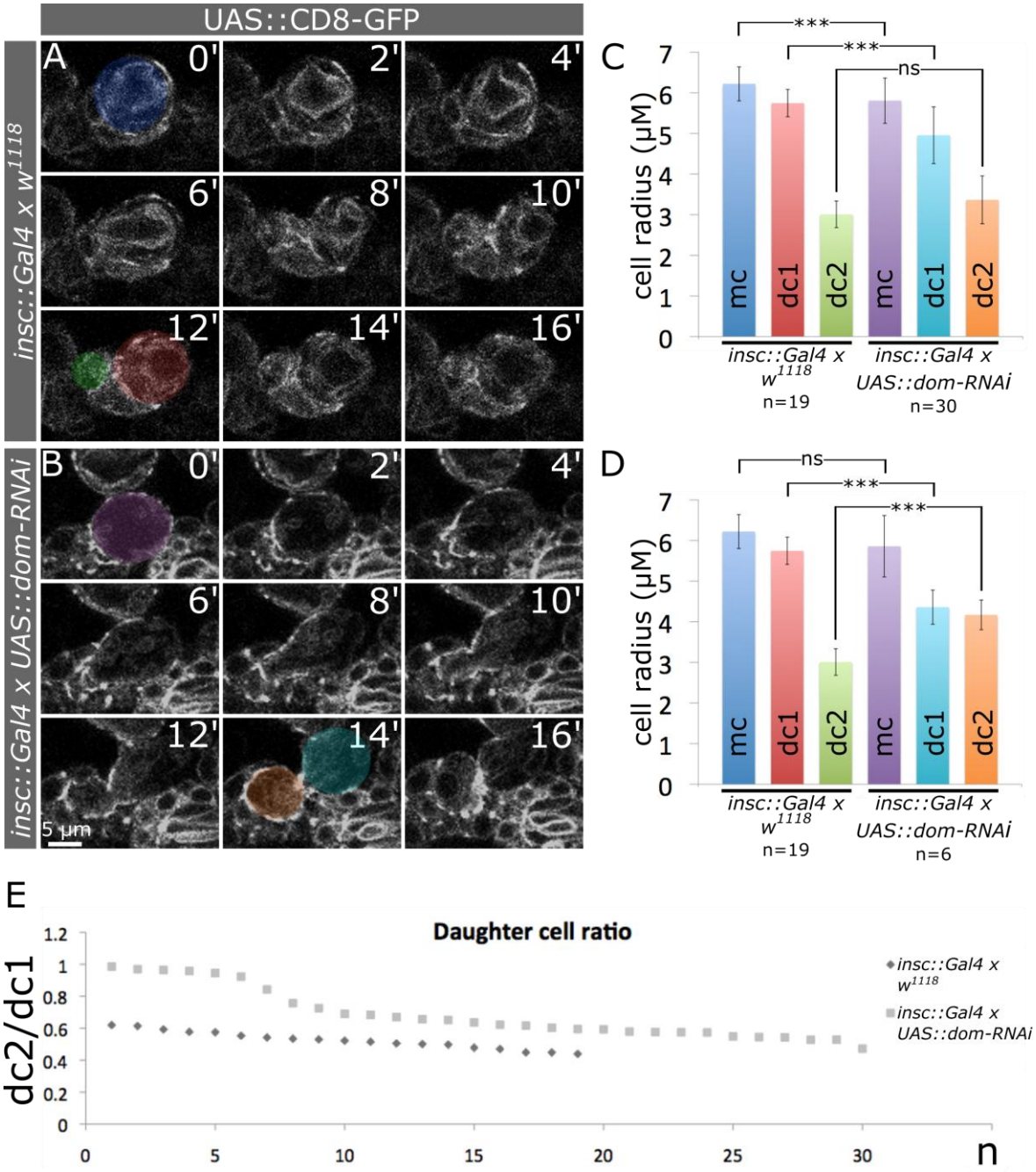

Figure 41: A subset of *domino* depleted neuroblasts divides symmetrically

(A, B): Time lapse series of a wild type NB division (A) and a *dom*-RNAi NB division (B). Numbers indicate time points in minutes. NBs and offspring cells were marked with CD8-GFP to identify and measure the cells. The mother cell (mc) NBs and the resulting daughter cells (dc) were false colored respective to the bars in the statistics for cell size (C, D). dc1 refers to the bigger, dc2 to the smaller daughter cell. Cell sizes were measured before onset (mc) and after end (dc1 & dc2) of cytokinesis. (C): Comparison of cell sizes from wild type and *dom*-RNAi NB divisions. (D): Statistics including only symmetrically dividing *dom*-RNAi NBs (dc2/dc1 ≥ 0.92). (E): Daughter cell ratio (dc2/dc1) for each NB divisions.

Live imaging analysis showed that *dom* deficient NBs undergo less asymmetric division than required to produce two distinct daughter cells, namely a big NB and a small GMC. Moreover, my results reveal that some NBs in *dom*-RNAi brains are equal in size to wild type NBs (Figure 41 D) whereas the average NB size is reduced (Figure 36, Figure 37). This indicates heterogeneity within the NB population. To examine whether the polarity defects and the Pros nuclear entry in *dom*-RNAi NBs are cause or consequence of the near-symmetric divisions, I determined whether the defects are features of bigger or rather smaller NBs. I measured NB sizes of *dom*-RNAi NBs with polarity defects or Pros nuclear entry respectively and compared them to the size of phenotypically normal *dom*-RNAi and wild type NBs. Figure 42 shows that for both features, polarity defects and Pros nuclear entry, the NBs displaying the phenotype are similarly sized with phenotypically normal *dom*-RNAi NBs (p = 0.139 for polarity defects, p = 0.089 for Pros nuclear entry). Thus, both bigger and smaller NBs similarly display polarity defects and Pros nuclear entry.

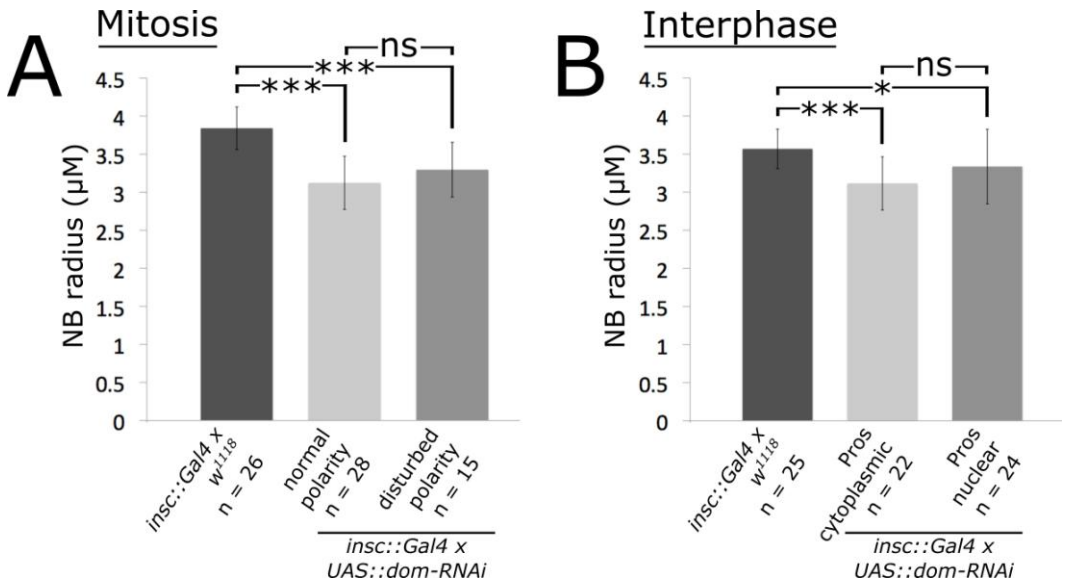

Figure 42: ***domino* depleted neuroblasts with mislocalization of fate determinants are equally sized with phenotypically normal neuroblasts**

NB sizes of wild type NBs (w^{1118}) and *dom*-RNAi NBs during mitosis (A) or interphase (B). (A): *dom*-RNAi NBs were differentiated into NBs with correct and disturbed polarity during mitosis. P(w^{1118}/*dom* normal polarity) = 6.81E-11; p(w^{1118}/*dom* disturbed polarity) = 4.09E-6; p(*dom* normal/disturbed polarity) = 0.139. (B) Interphase *dom*-RNAi NBs have been separated into NBs with cytoplasmic and nuclear Pros. P(w^{1118}/*dom* Pros cytoplasmic) = 7.35E-6; p(w^{1118}/*dom* Pros nuclear) = 0.044; p(*dom* Pros cytoplasmic/Pros nuclear) = 0.09.

3.4. Myc interacts with the Tip60 complex to maintain larval neuroblasts

3.4.1. Identification of potential Domino interactors in the maintenance of *Drosophila* larval neuroblasts

Domino and the Tip60 complex interact with various genes and proteins in different cellular contexts and organisms (see 1.3.2). To better understand how the Tip60 complex regulates NB division, I conducted a screen on potential interactors, upstream regulators and downstream targets. Available lines for knockdown, overexpression and expression of dominant negative variants have been screened for neural defects in the L3 larval brain using the *insc::Gal4* driver. Please note, that in few cases the availability of fly lines has limited the analysis (esp. for *dacapo*, the *Drosophila* p21 homolog).

Table 3: Potential Domino and Tip60 complex interactors and observed neural defects

Potential interactors and a short description of the putative interaction with Dom or the Tip60 complex are listed. The table indicates whether neural defects in the L3 brains have been observed when the potential interactor was manipulated with the *insc* driver.

Gene	Screened lines	Interaction with Dom /Tip60 complex	Neural defects
ash1	6	H3K4 methyltransferase	x
CBP	12	Potential interactor	yes
E2f1	7	Potential interactor	x
E2f2	4	Potential interactor	x
HDAC6	7	Potential regulator	x
mam	4	Potential interactor	x
myc	9	Potential interactor and HAT target	yes
dacapo (p21 homolog*)*	1	Potential downstream target	x
p53	15	Potential interactor and HAT target	yes
Set1	7	H3K4 methyltransferase	x
trr	3	H3K4 methyltransferase	x
trx	3	H3K4 methyltransferase	x

Table 3 shows, that I observed defects upon manipulation of three potential interactors. CBP (CREB binding protein, CG15319), a HAT, is encoded by the *nejire* gene in *Drosophila* and recruited to chromatin by interaction with Dom (Eissenberg et al., 2005). Knockdown or expression of dominant negative CBP was partially lethal (BL37489, v105115) or resulted in strong defects in neural organization (BL27724, BL3279, v46534, v102885) (Figure 43 E). Interestingly, while the number of neural cell lineages is reduced, the number

of cells per lineage appears to be increased with partly more than one Mira positive NB (data not shown). However, I could not detect NB polarity defects or Pros nuclear entry upon CBP manipulation. Moreover, knockdown or overexpression of dom in *CBP*-RNAi neural lineages did either not rescue the phenotype or was early larval lethal (see Appendix: Figure S 4).

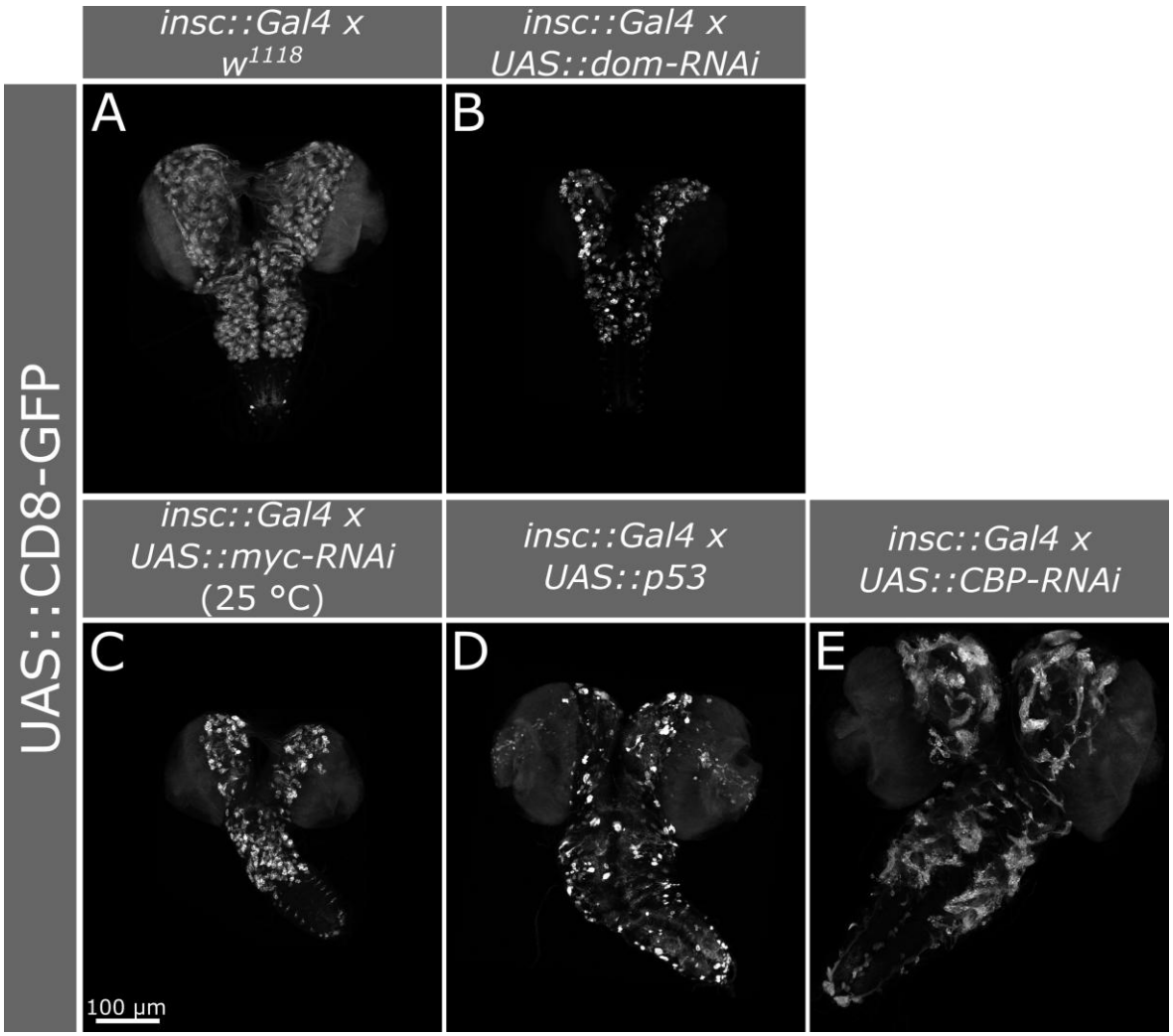

Figure 43: Potential Domino and Tip60 complex interactors affect the larval nervous system

Maximum intensity projection of larval brains expressing *insc* driven CD8-GFP in neural cells. Knockdown of *myc* (BL36123) and overexpression of p53 (BL8418) resulted in a massive decrease of neural cells (C, D). (E): Knockdown of *CBP*/*nejire* (V102885) leads to neural misorganization with less neural cell lineages but more cells per line. Please note that the knockdown of *myc* (C) was only viable at 25 °C, where the Gal4-UAS dependent knockdown is less strong, while the screen was usually carried out at 29 °C to ensure maximum induction of the Gal4-UAS system.

P53 (CG33336) is a target for the HAT activity of Tip60 and the Tip60 complex is involved in regulation of downstream p21 target expression (Chan et al., 2005; Gévry et al., 2007; Legube et al., 2004; Park et al., 2010; Tang et al., 2006; Tyteca et al., 2006). P53 can induce cell cycle arrest or apoptosis via the regulation of for example p21 (cyclin-dependent kinase inhibitor 1) or PUMA (p53 upregulated modulator of apoptosis) (Beckerman and Prives, 2010). As expected by the viability of *p53* knockout flies (Brodsky et al., 2004), expression of dominant negative p53 variants (BL8419, BL8420, BL8421, BL8422) and knockdown of *p53* by RNAi (BL29351, BL36814, BL41638, BL41720, v10692, v38235, v45138, v45139, v103001) was phenotypically normal. The overexpression of p53 (BL6584, BL8418) resulted in massively decreased neural lineages and almost complete lack of NBs (Figure 43 D and data not shown).

Since p53 is a downstream target of the Tip60 complex I depleted *p53* (v28235, v41638, v45139, v1051001) or expressed dominant negative variants (BL8419, BL8420) in *dom*-RNAi expressing neural cells. Remarkably, knockdown or manipulation of p53 function partially rescued the *dom* knockdown phenotype although not to the full degree. This suggests that the *dom* knockdown could partially rely on p53 activation. In contrast, loss of neural cells upon p53 overexpression could not be rescued by overexpression of DomB. (Figure 44). However, further experiments showed that the NB phenotype upon p53 overexpression is different from the *dom*-RNAi phenotype. The remaining NBs were unaffected in polarity and did not show Pros nuclear entry (data not shown).

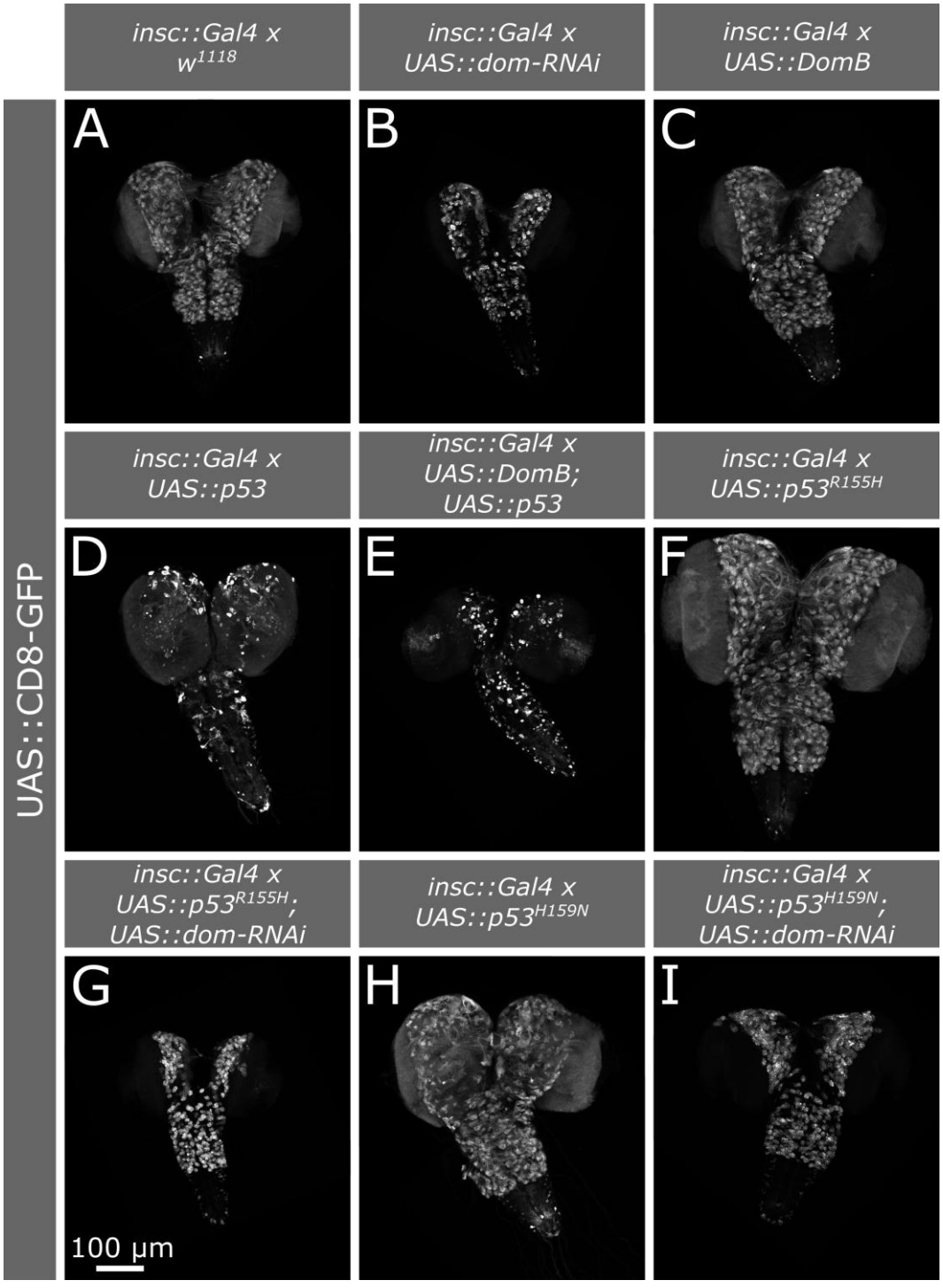

Figure 44: *domino* knockdown phenotype in neural cells is partially rescued by p53 loss of function

Maximum intensity projections of L3 instar larval brains. *insc::Gal4* drives the expression of CD8-GFP in neural cells. Like the control (A), DomB overexpression (B) and dominant negative p53 variant expression that abolish p53 DNA binding (F, H) were phenotypically normal. *dom* knockdown (B) and p53 overexpression (D) result in a reduction of neural cells. Loss of neural cells upon p53 overexpression is not rescued by upregulation of DomB expression (E). The expression of p53 variants without DNA-binding activity in *dom* depleted neural cells restores some but not all cells lacking upon *dom* knockdown (G, I).

Myc (*diminutive*, CG10798) is an important regulator of cell cycle, cell growth and tumorigenesis and was shown to recruit the Tip60 complex to target gene promoters to regulate gene expression (Frank et al., 2003). Furthermore, Myc is a target of the histone acetyltransferase activity of Tip60, which can stabilize the transcription factor by acetylation (Patel et al., 2004). Knockdown of *myc* (BL36123, BL25784, v51454, v106066) resulted in severe loss of neural cells (Figure 43 C).

3.4.2. *myc* depleted neuroblasts exhibit polarity defects and resemble neuroblasts undergoing terminal differentiation

Next, I proceeded to compare the neural phenotype resulting from *myc* knockdown with the *dom*-RNAi phenotype. Strikingly, *myc* knockdown NBs were only able to maintain normal polarity in 85.51 ± 10.69% of NBs in comparison to 98.46 ± 5.55% in the control (p = 3.48E-3) (Figure 45). Notably, it was only possible to use a *myc*-RNAi line that leads to a rather weak phenotype (V51454, from here on refered to as weak *myc*-RNAi) since stronger *myc*-RNAi (BL36123, from here on refered to as strong *myc*-RNAi) made it impossible to find enough mitotic NBs for quantification. Please note, that both RNAi lines have been used successfully used to knockdown *myc* in previous publications (Atkins et al., 2016; Song and Lu, 2011).

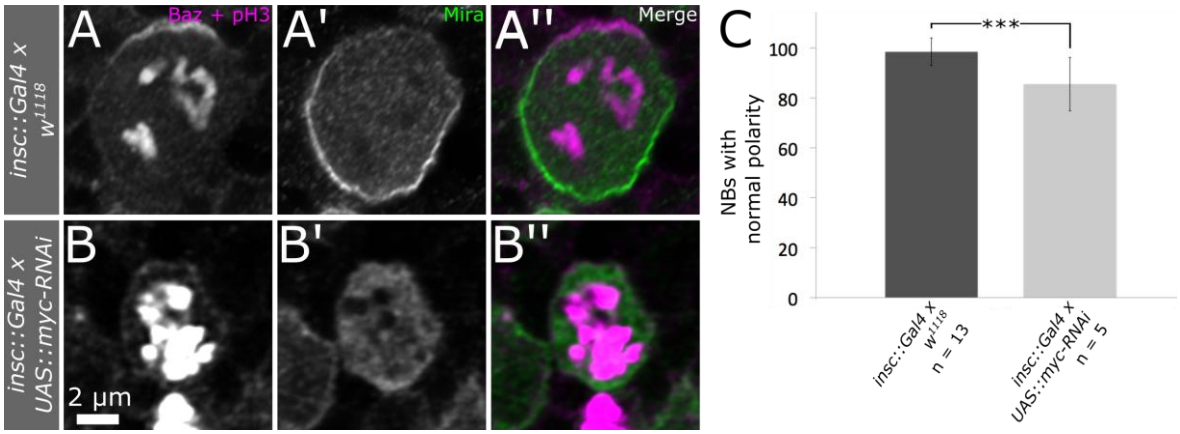

Figure 45: Knockdown of *myc* in larval neuroblasts affects polarity

The *insc* driver was used to knockdown *myc* in larval NBs. Airyscan pictures of immunostained brains reveal that the polarity markers Baz and Mira are mislocalized in dividing (pH3 positive) NBs upon *myc* knockdown (B) while the localization to opposing sides of the NB was normal in the wild type control (A). (C): Quantification of NBs with normal polarity shows a significantly smaller amount of *myc* knockdown NBs with proper polarity in comparison to the wild type.

In addition, measurement of NB size upon *myc* knockdown showed that *myc* deficient NBs are significantly smaller than wild type NBs (3.14 ± 0.49 µM *myc*-RNAi NB radius, 3.84 ± 0.28 µM wild type NB radius, p = 1.31E-8) (Figure 46).

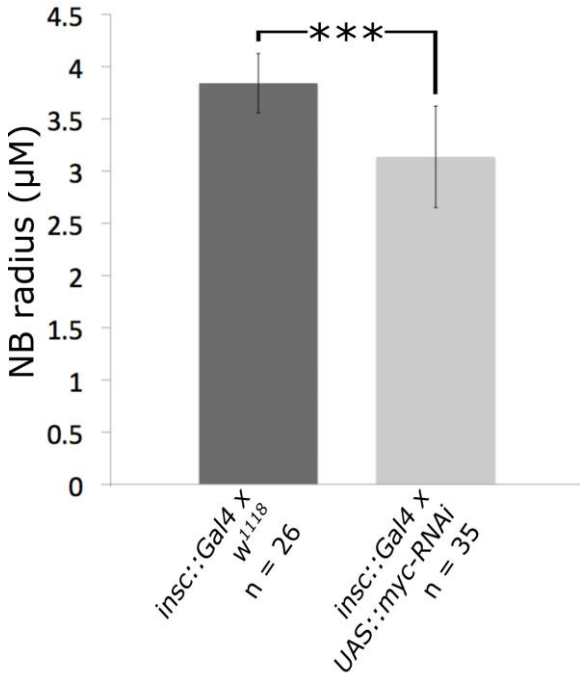

Figure 46: *myc* deficient neuroblasts are smaller

Sizes of mitotic L3 NBs before onset of cytokinesis were measured in wild type and upon *myc* depletion. *myc*-RNAi NBs are significantly smaller than wild type NBs.

Subsequently, I analyzed whether Pros enters the nucleus upon *myc* knockdown like upon downregulation of Tip60 complex subunits. Figure 47 shows that *myc* depleted interphase NB nuclei are positive for Pros and the number of NBs in which Pros is restricted from the nucleus is significantly reduced (40.73 ± 18.52% in *myc*-RNAi, 100% in WT, p = 1.49E-10).

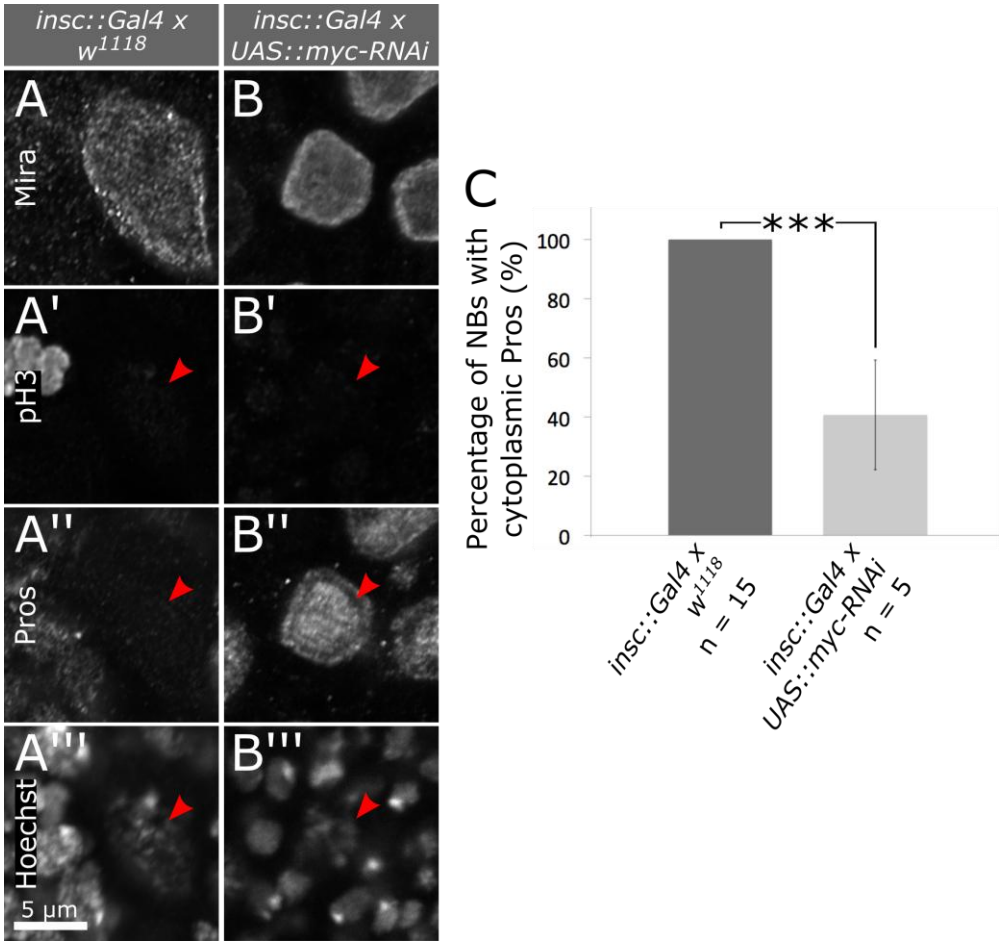

Figure 47: Prospero enters the nucleus upon *myc* knockdown

(A, B): Airyscan pictures of immunostained interphase (pH3 negative) L3 NBs. Pros is cytoplasmic and only weakly visible in the control (A) but can be detected in the nucleus of *myc*-RNAi NBs (B). (C): Quantification of NBs with cytoplasmic Pros. No cases of Pros entry were identified in the wild type while only 40.73% of *myc*-RNAi NBs show Pros exclusively in the cytoplasm.

3.4.3. Myc interacts genetically with the Tip60 complex in larval neuroblasts

The presented results indicate considerable similarities between *myc* knockdown and knockdown of *dom* and other members of the Tip60 complex. I therefore hypothesized that Myc and the Tip60 complex act together to regulate NB behaviour. Interactors of the same pathway may not only interact physically but genetically by regulating each other's expression. Since Myc is a transcription factor, I examined whether Myc influences Tip60 complex members. Staining of Dom in NBs depleted of *myc* and showed that *myc*-RNAi NB nuclei lack Dom staining (Figure 48 B).

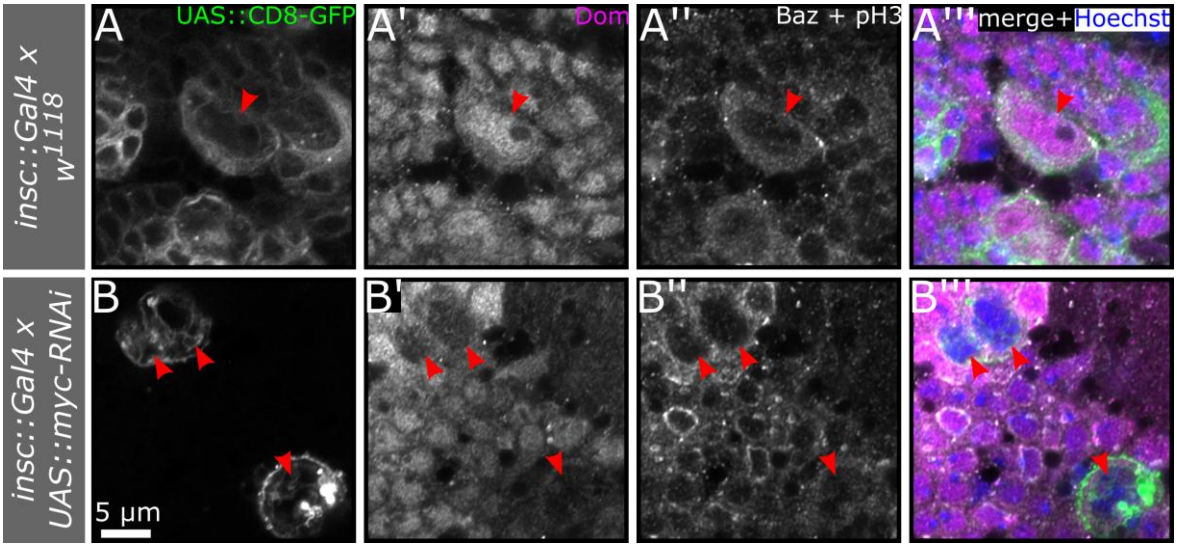

Figure 48: Neuroblasts deficient for *myc* lose Domino staining

Airyscan pictures of larval NBs (stained with Baz) in the interphase (pH3 negative). Arrowheads point at nuclei of interphase NBs. (A): Wild type NBs show Dom nuclear staining. (B): Upon *myc*-RNAi Dom staining is absent in the nucleus. Please note that the Dom antibody staining produces cytoplasmic background staining in NBs.

Subsequently, I performed rescue and epistasis experiments to gain further insight into the relationship between Myc and Dom. As expected, Myc overexpression (BL9674) did not modify the *dom*-RNAi phenotype, suggesting that Dom acts downstream or together with Myc (Figure 49). Overexpression of Dom in *myc* knockdown is likewise not expected to rescue the *myc*-RNAi phenotype, as previous studies showed that Myc recruits the Tip60 complex and thereby Dom to target gene promoters, which means that both Myc and Dom are required in the same pathway (Frank et al., 2003). Nonetheless, overexpression of DomB in *myc*-RNAi rescued the resulting L3 larvae to viability at 29 °C with the *insc* driver, which is lethal when only *myc* is depleted. The nervous system yet displays severe defects, meaning that Dom overexpression cannot fully rescue the *myc* knockdown phenotype (Figure 49). Since DomB (to date annotated as DomE) appears to be the only isoform expressed in larval NBs it is unlikely that other isoforms are required for a full rescue of *myc* knockdown (see 3.3.1). Instead, the partial rescue speaks for a regulation of *dom* expression by Myc, while both proteins are additionally required for regulating NB behaviour.

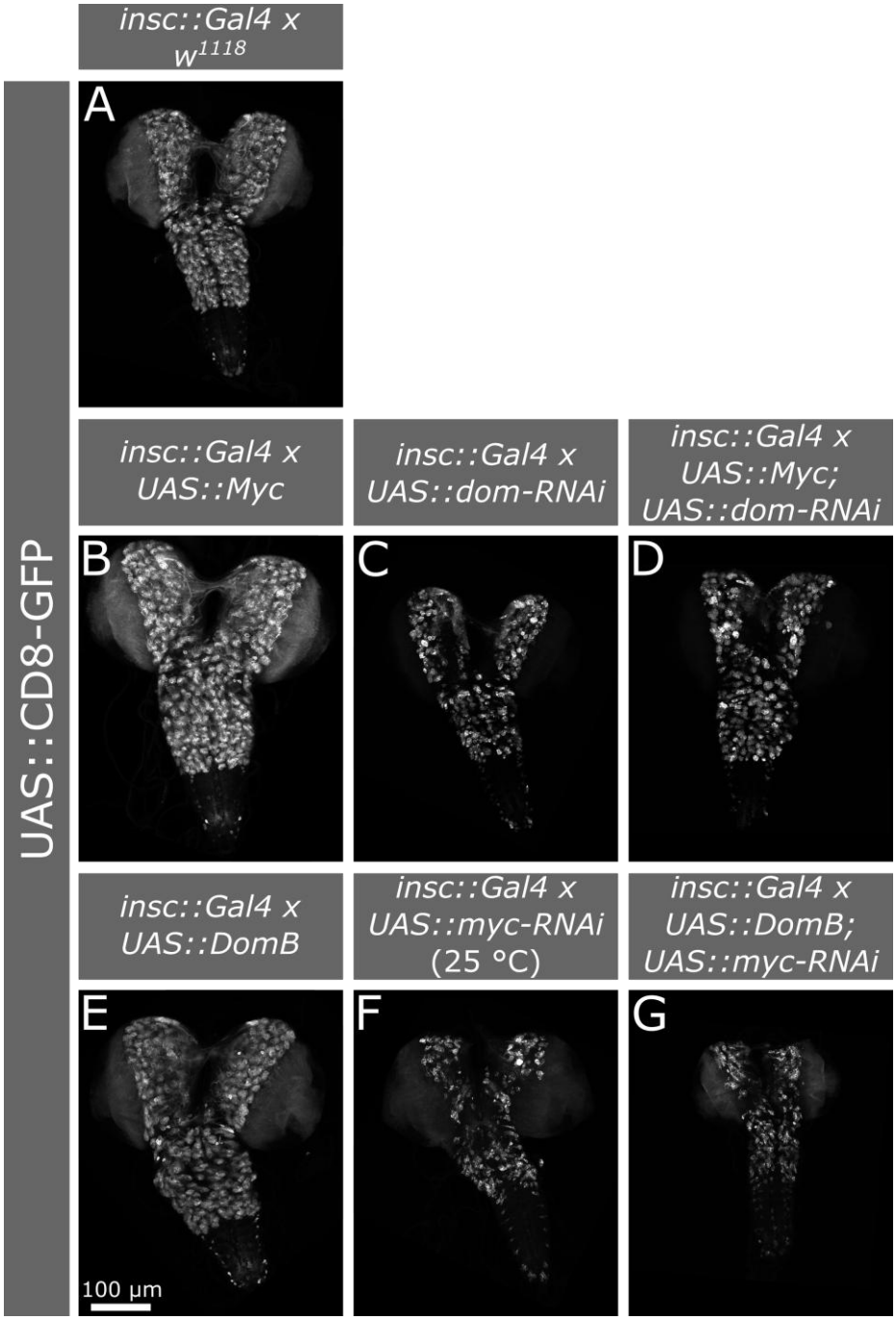

Figure 49: Rescue experiments in larval brains elucidate interaction between Myc and Domino

Maximum intensity projections of *insc::CD8-GFP* marked larval brains. (A): Wild type brain. (B): Overexpression of Myc is phenotypically normal. (C): *dom* knockdown reduces neural cell number, which is not rescued by Myc overexpression (D). (E): DomB overexpression does not alter neural cell number. (F): Knockdown of *myc* is only viable at 25 °C and decreases neural cell numbers. (G): Overexpression of DomB partially rescues *myc* knockdown to viability of the L3 stage at 29 °C but does not fully restore neural cell numbers.

3.4.4. Tip60 histone substrates in larval neuroblasts

Tip60 and its conserved homologs acetylate several lysines on H4 (K5, K8, K12) as well as lysine 5 on H2A and H2A variants *in vivo* (Squatrito et al., 2006). Histone acetylation is generally believed to increase chromatin accessibility (Görisch et al., 2005). Frank et al. (2003) postulated that Myc recruits the Tip60 complex to target gene promoters to induce histone acetylation and facilitate gene expression.

I hypothesized that knockdown of *dom* might reduce the histone acetylation by the Tip60 complex in larval NBs and used a commercially available antibody for one of the major Tip60 substrates H4K8Ac to test this hypothesis. Remarkably, the knockdown of *dom* reduces the staining for H4K8Ac in many NB nuclei. In severe cases no H4K8Ac staining was detected (Figure 50 B).

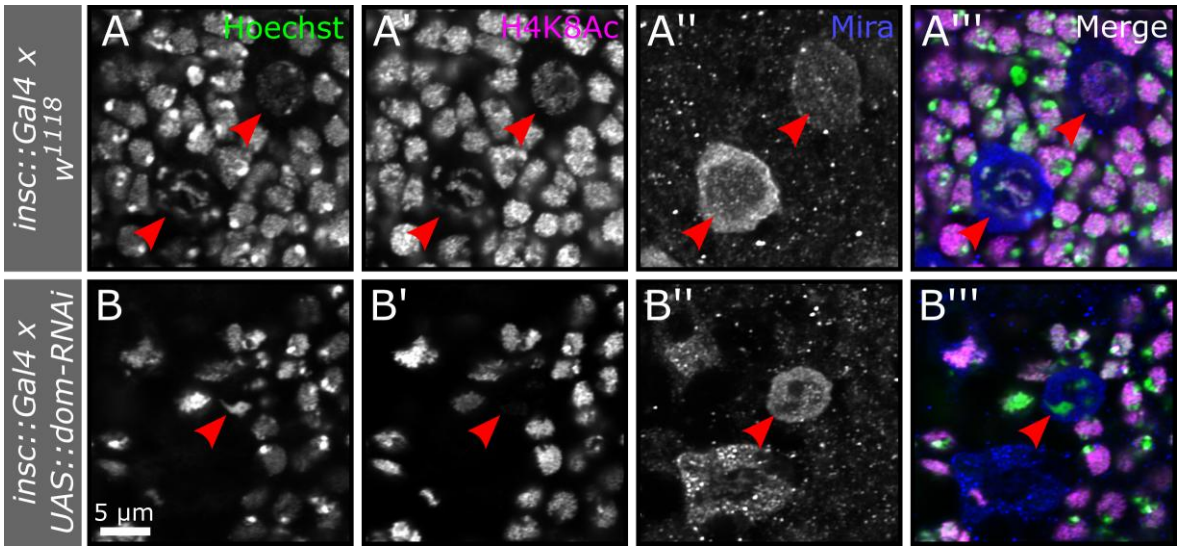

Figure 50: H4 acetylation on lysine 8 is reduced upon *domino* knockdown.

Airyscan pictures of immunostained L3 NBs. (A): H4K8Ac staining is visible in all Hoechst positive nuclei including NB nuclei (arrowhead) in the wild type. (B): Knockdown of *dom* reduces the H4K8Ac staining in many but not all NB nuclei.

Besides aceylation of histones, the Tip60 complex incorporates H2A variants. The only H2A variant in *Drosophila* is H2Av, which is incorporated and acetylated by the Tip60 complex in the chromatin of regulated promoters and during DNA break repair but not globally during endoreplication (Börner and Becker, 2016; Kusch et al., 2004; Kusch et al.,

2014). Further, H2Av incorporation by Dom was previously shown to maintain stem cells in the *Drosophila* germline (Börner and Becker, 2016; Morillo Prado et al., 2013). Taking these facts into account, I speculated that H2Av might be required for larval NBs. I knocked down *H2Av* by RNAi using the *insc* driver in larval neural lineages and analyzed L3 brains for phenotypic features observed upon *dom* depletion. Neural cells were slightly reduced in number and importantly, Pros enters the nucleus of interphase NBs upon *H2Av* knockdown (Figure 51 and Appendix: Figure S 5), indicating the importance of H2Av in larval NBs.

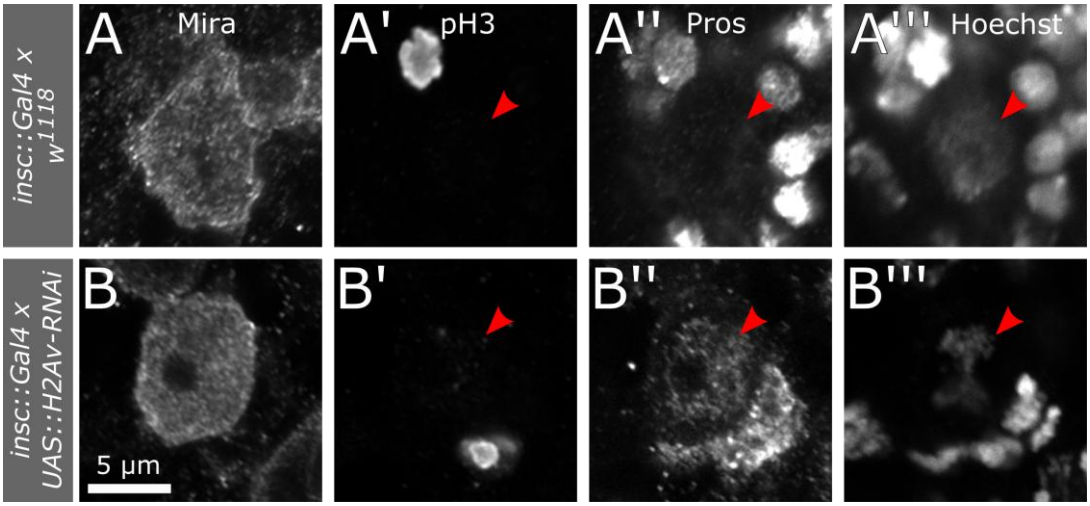

Figure 51: Larval neuroblasts require H2Av to maintain Prospero cytoplasmic

Airyscan pictures of wild type and *H2Av*-RNAi L3 NBs. NBs were immunostained with Mira. Interphase NBs were identified by absence of pH3 staining. (A): Wild type NBs keep Pros cytoplasmic, which is less well visible than nuclear staining in neighbouring cells undergoing neurogenesis. (B): *H2Av*-deficient NBs fail to hold Pros cytoplasmic and show nuclear Pros staining. Arrowheads point at interphase NB nuclei.

3.5. Overexpression of single components of the Myc/Tip60 network does not maintain neuroblasts

Drosophila NBs are not maintained until adulthood and a many NBs undergoes termination of neurogenesis by slowing down the cell cycle, reducing cell size and finally Pros nuclear entry (Homem et al., 2014; Maurange et al., 2008). These features of NBs are strikingly similar to NBs lacking Myc, components of the Tip60 complex or H2Av. It thus appears possible that these factors could be downregulated or otherwise inactivated

during naturally occurring NB termination. In that case, elevated levels of proteins in the network might be able to block NB termination.

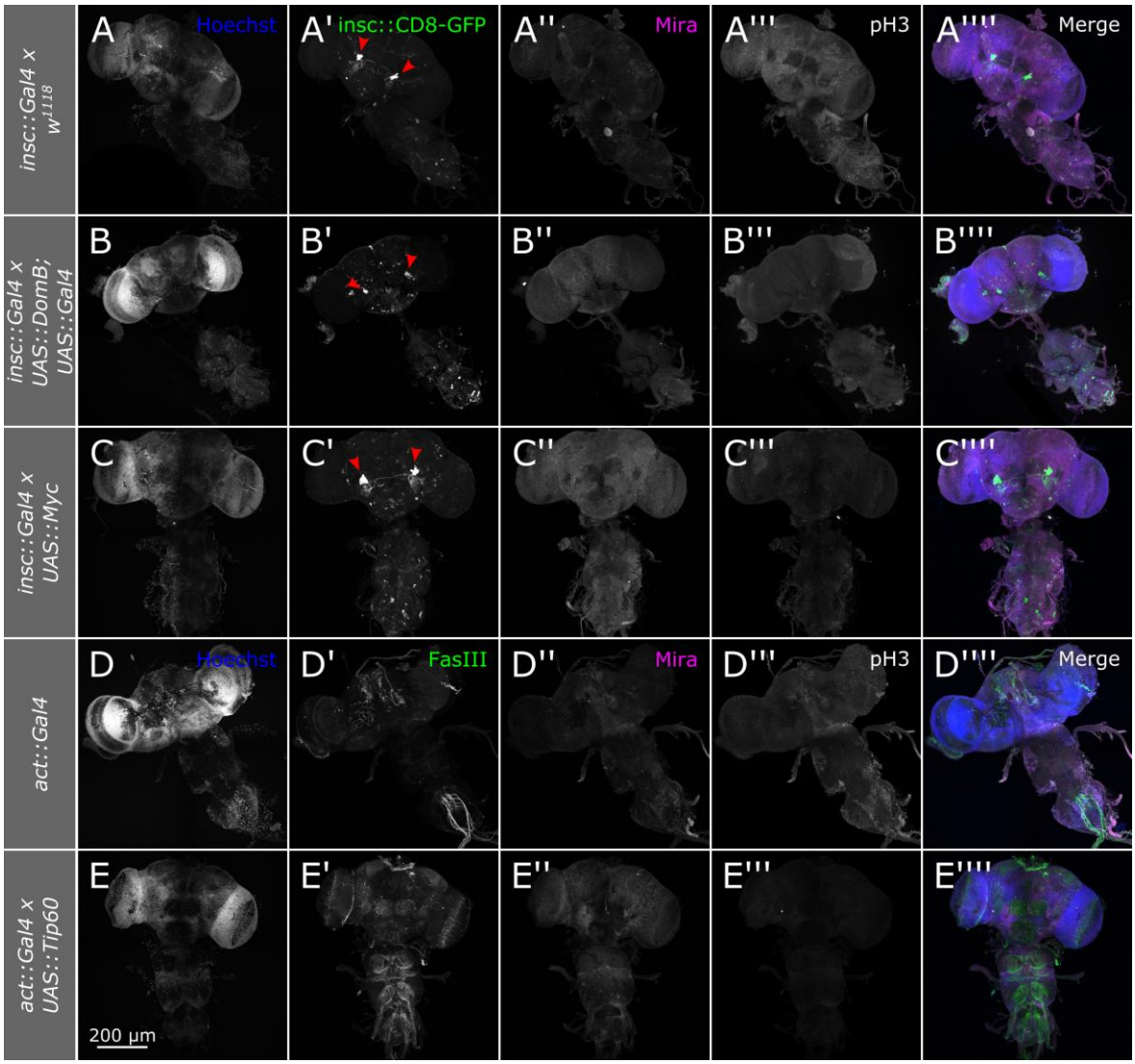

Figure 52: Overexpression of DominoB, Tip60 or Myc does not maintain neuroblasts until adulthood

Maximum intensity projections of young (< 1 day old) adult brains reveal no NBs (marked by Mira) or mitotic cells (marked by pH3) in the control driver brains (A and D). Also upon overexpression of DomB (additionally boosted by *UAS::Gal4*) (B), Myc (C) or Tip60 (E) no adult mitotic cells or NBs could be detected. Mushroom bodies are visible as two spots in brains positive for *insc* driven CD8-GFP and are marked with arrowheads. FasIII stains neurons and was used as a staining control if possible (D', E').

I used Gal4 driver lines, which are active in larval NBs to overexpress DomB, Tip60 or Myc (for validation of *act::Gal4* expression in larval NBs see Appendix: Figure S 6). For Tip60 overexpression the strong *act* driver could be used, which was lethal with DomB or Myc overexpression. Therefore, for the latter ones *insc::Gal4* was used.

Previous studies which investigated factors for NB maintenance analyzed young adult brains (Homem et al., 2014) and attempts of NB staining on pupal brains showed variation even upon precise staging. Therefore, I investigated adult brains from newly hatched flies to check whether the overexpression of DomB, Tip60 or Myc could maintain NBs until adulthood. In none of the controls, NBs or any dividing cells could be identified. Similarly, overexpression of DomB, Tip60 or Myc could not maintain NBs (Figure 52).

3.6. Domino regulates the expression of a large set of target genes

One of the well-established functions of the Tip60 complex especially in stem cells is regulation of gene expression. Moreover, Dom and Tip60 have been shown to regulate a large set of target genes in *Drosophila* (Ellis et al., 2015; Fazzio et al., 2008b; Lorbeck et al., 2011). H4K8 acetylation is reduced in *dom* deficient NBs and functional analyses have demonstrated the importance of H2Av in NB maintenance. This indicates that Dom and the Tip60 complex regulate gene expression via histone modification and incorporation in larval NBs to regulate self-renewal, polarity and division. To gain a better understanding of key regulators of NB maintenance I investigated the genes regulated by Dom in larval neural cells.

Since Dom is ubiquitously expressed, its target genes might strongly vary depending on the cellular context. I was exclusively interested in target genes in cells of the larval nervous system. *Dom* null mutants are early larval lethal, thus larval *dom* null mutant brains are not available for analysis. Homozyogus mutant cell clones can be induced but are not frequent and very small, consequently do not provide enough material for gene expression studies. I decided to use the previously validated *dom*-RNAi line v7787 for conducting a transcriptome-wide analysis (Figure 53).

In short, the neural driver line *insc::Gal4* was used to mark neural cells with CD8-GFP and for knockdown of *dom* by RNAi (for details see 2.2.6). For a wild type control the same Gal4 driver was crossed to w^{1118}. Larval brains were dissected and committed for

fluorescence activated cell sorting (FACS) based on GFP expression. Previous studies have used similar setups to sort NBs based on their larger size (Berger et al., 2012). However, due to the NB size decrease upon *dom* knockdown this was not possible. Thus, neural cells were sorted. Figure 54 shows the conditions and gates set for sorting neural, CD8-GFP positive cells. For each sort, a GFP-negative sample of brain cells was used to determine the gate for the GFP-expressing cell population (R2). Furthermore, cells were sorted by absence of propidium iodide staining (PI) to retain only living cells. For each replicate between 1.4 and 2.2 million GFP^{high} PI^{low} cells were sorted. FACS was conducted together with Christoph Göttlinger, University of Cologne, Institute for Genetics.

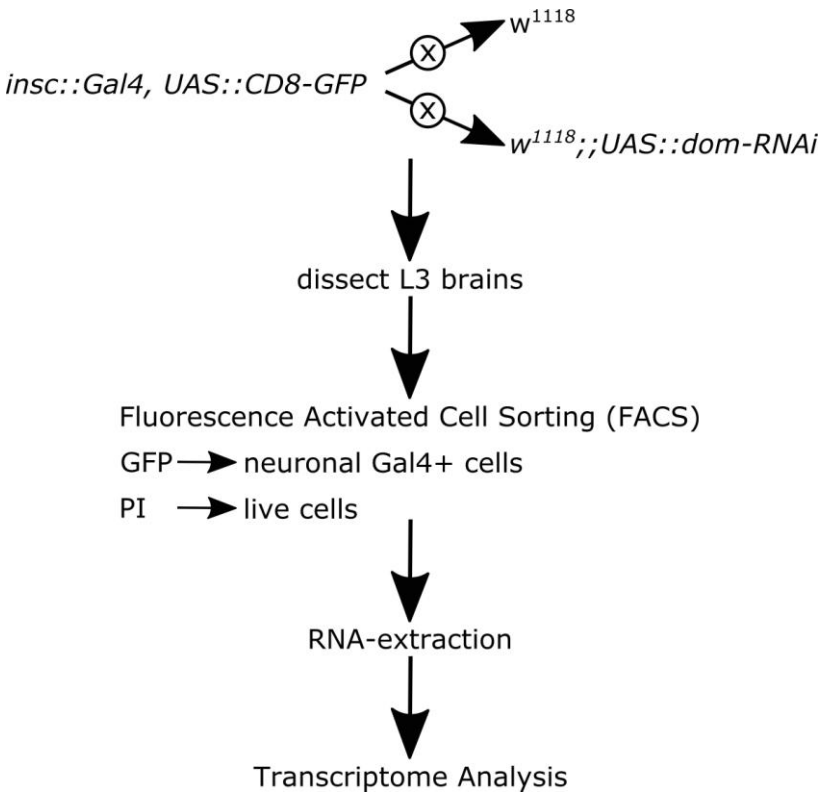

Figure 53: Experimental setup for the transcriptome-wide analysis

Stepwise procedure for the transcriptome analysis included rearing of larvae of the indicated phenotypes at 25 °C to exclude activation of heat shock genes. Larval brains were dissected and single cell suspensions were sorted by FACS, based on GFP expression and absence of propidium iodide (PI) staining to obtain live neural cells (together with Christoph Göttlinger). After RNA extraction, library preparation and RNA-sequencing was done at the Cologne Center for Genomics. Subsequent bioinformatic analysis was kindly conducted by Dr. Manu Tiwari.

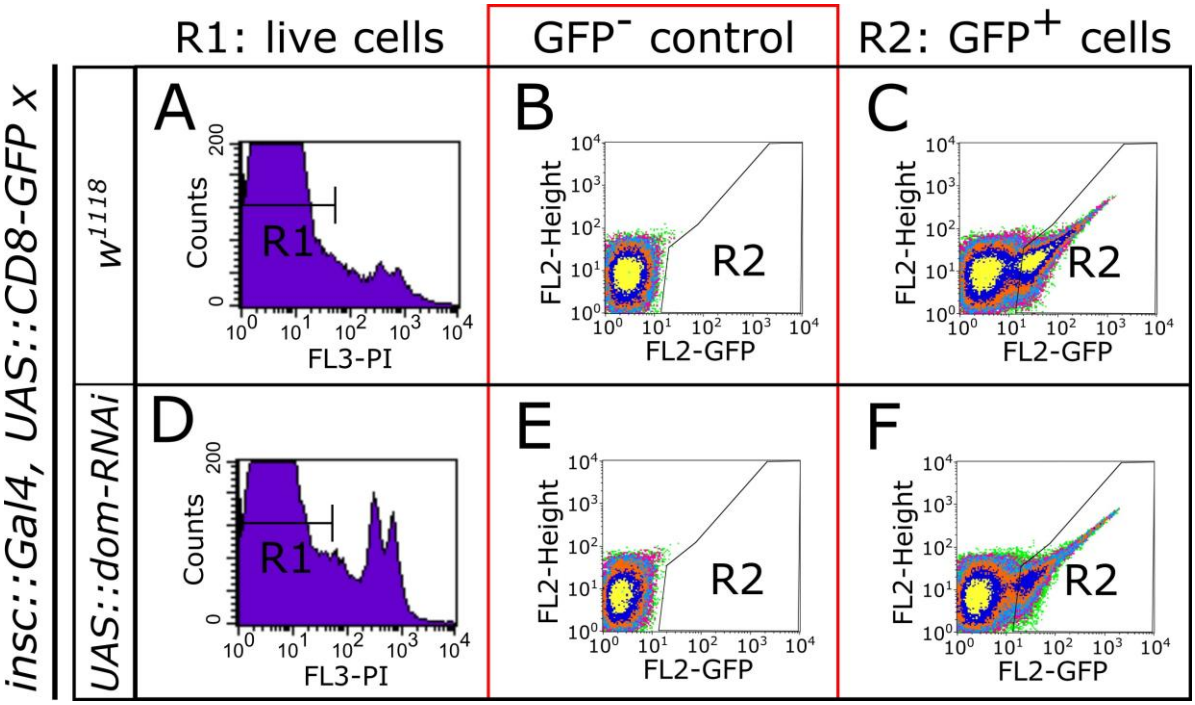

Figure 54: FACS conditions for sorting of live neural larval cells

FACS conditions for sorting of neural cells for subsequent transcriptome were based on low PI for live cells (R1) and positive GFP fluorescence (R2). A GFP-negative sample was used to discriminate between GFP^{low} and GFP^{high} conditions (Christoph Göttlinger).

A small fraction of the sorted cells was immunostained to confirm that the desired cell population was obtained. FAC-sorted cells were GFP positive and expressed correct neural markers (Figure 55).

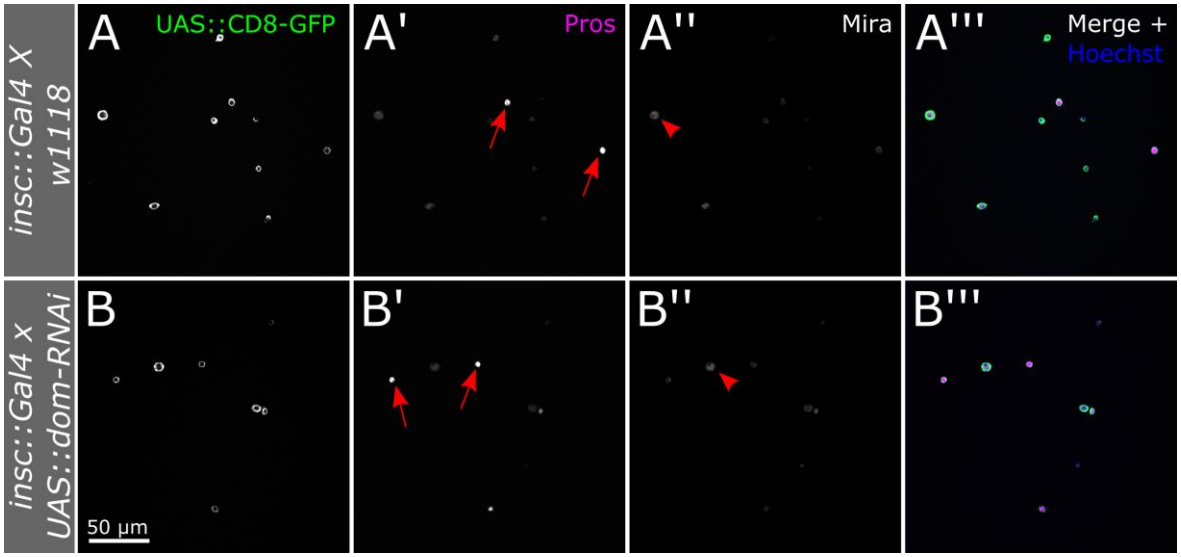

Figure 55: *insc::CD8-GFP* L3 brain cells sorted by GFP express neural markers.

GFP-positive cells were sorted by FACS from L3 brains expressing CD8-GFP with the neural driver *insc::Gal4*. For the wild type control, the driver was crossed to w^{1118} (A). For *dom* depletion the *dom*-RNAi line v7787 was used (B). Immunostaining of GFP-sorted cells confirmed that nearly all sorted cells expressed GFP (A, B). Most cells expressed high levels of Pros (arrows, A' and B'). Fewer bigger cells were positive for Mira (arrowheads), reflecting the smaller amount of NBs versus cells undergoing neurogenesis.

I extracted RNA from FACS-sorted neural cells and forwarded it to the Cologne Center for Genomics for further downstream processing and RNA-sequencing. Subsequent bioinformatic analysis to identify differentially expressed genes was done by Dr. Manu Tiwari (University of Cologne, Anatomy I, Molecular Cell Biology). Principal component analysis indicated that similar samples cluster together, showing similar variances. No outliers were identified (Figure 56).

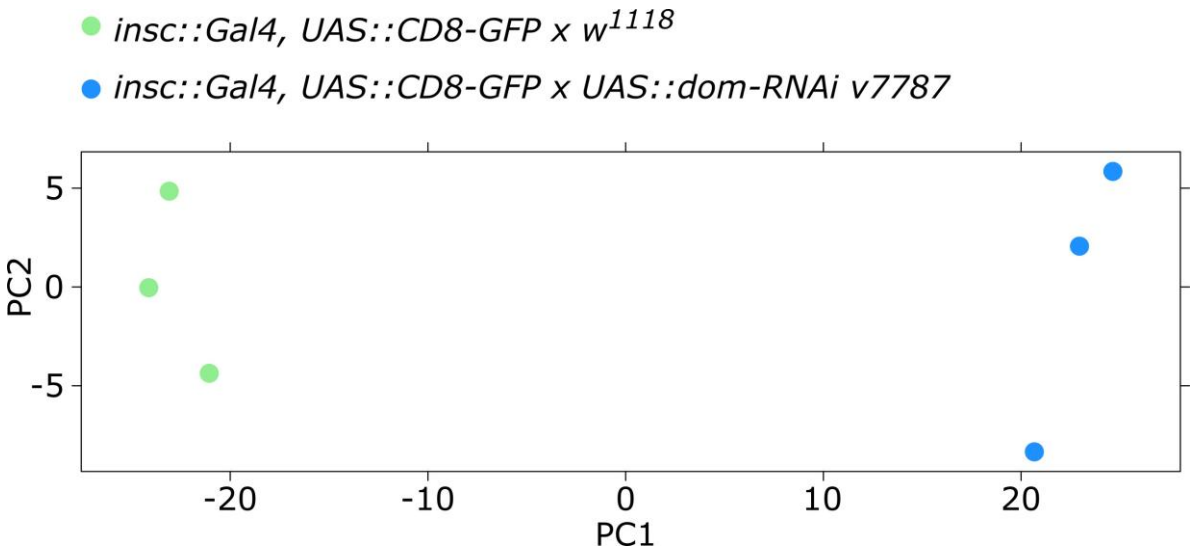

Figure 56: Principal Component Analysis

Principal Component Analysis (PCA) analysis was used to visualize sample variances. Samples clustering together indicate similar variances, suggesting that they represent comparable gene sets. Importantly, the triplicates of the wild type and the triplicates of the *dom* knockdown are present in two different clusters.

Having confirmed that all replicates pass the quality controls, differentially expressed genes in the *dom* knockdown neural cells were identified by following the pipeline described in the methods section (2.2.6.5). The MA plot, an indicator of reproducibility between experimental samples, exhibited good fit across the samples (Figure 57). In total, 3326 genes were found to be differentially expressed at FDR $\leq$ 0.05.

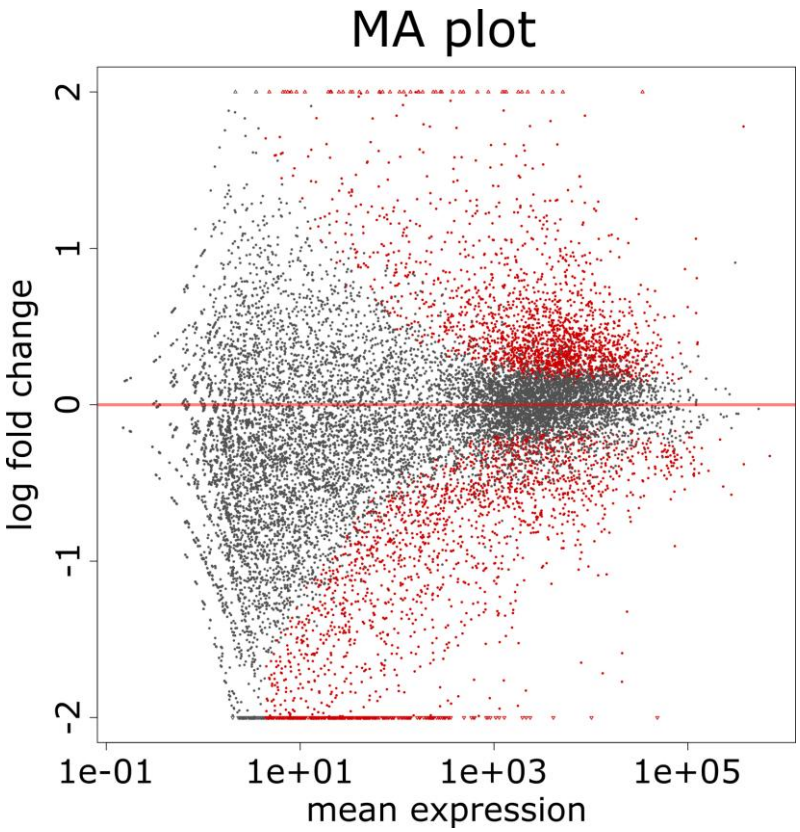

Figure 57: MA plot showing differential gene expression

Visualization of all differentially expressed genes in a mean average (MA) plot by DEseq2 analysis. Dots represent genes. Red dots mark differentially expressed genes (FDR ≤ 0.05). Genes with negative log fold change are downregulated upon *dom*-RNAi.

Importantly, *dom* is present in the downregulated genes (log_2FC = 0.576; FDR = 7.88E-7). The rather slight downregulation of *dom* might be due to the low efficiency of the RNAi and lower induction of the Gal4-UAS system at 25 °C. Alternatively, it is possible that cells with high *dom* knockdown are underrepresented, as loss of *dom* functions results in a loss of the affected cells (Ruhf et al., 2001).

Interestingly, *p53* (log2FC = 0.652; FDR = 1.9E-4) and its downstream target *dacapo* (log2FC = 0.645; FDR = 5.9E-5) were upregulated upon *dom* knockdown, indicating that *dom* is usually required for their repression. In addition, also Myc was upregulated upon *dom* knockdown (log2FC = 0.474; FDR = 9.5E-3). Importantly, if Dom can induce Myc expression, this can explain the partial rescue of *myc* knockdown by DomB overexpression (Figure 49).

3.6.1. Domino target genes regulate neuroblast fate

To identify major pathways regulated by *dom* I chose significantly regulated (FDR ≤ 0.05) target genes with -0.75 ≥ log2FC ≤ +0.75 (1355 genes) and performed Database for Annotation, Visualization and Integrated Discovery (DAVID) functional annotation of gene ontology (GO)-terms. Table 4 lists clusters of GO-terms that were significantly enriched in the *dom* target genes (enrichtment score ≥ 1.5).

Table 4: Database for Annotation, Visualization and Integrated Discovery (DAVID) functional annotation: GO-term analysis of Domino target genes

I performed DAVID functional annotation to identify enriched GO-term clusters in *dom* differentially regulated genes. Clusters represented in red color predominantly comprise upregulated genes, while those in green comprise predominantly downregulated genes. Grey clusters contain roughly equal portions of down- and upregulated genes.

Pathway	GO-Term	p-value	Count
Annotation Cluster 1, Enrichment Score 5.01			
G-protein Coupled Receptor Protein Signaling Pathway	GOTERM_BP_FAT	2.5E-10	54
Sensory Perception	GOTERM_BP_FAT	8.8E-5	37
Annotation Cluster 2, Enrichment Score 3.58			
Homeobox	INTERPRO	2.2E-7	26
Transcription Factor Activity	GOTERM_MF_FAT	9.2E-6	56
Annotation Cluster 3, Enrichment Score 2.84			
Neurotransmitter Binding	GOTERM_MF_FAT	8.8E-4	15
Annotation Cluster 4, Enrichment Score 2.34			
Heme Binding	GOTERM_MF_FAT	2.6E-5	27
Microsome	GOTERM_CC_FAT	2.3E-3	15
Annotation Cluster 5, Enrichment Score 2.32			
Sensory Perception of Chemical Stimulus	GOTERM_BP_FAT	1.2E-3	26
Annotation Cluster 6, Enrichment Score 1.85			
Gastrulation	GOTERM_BP_FAT	9.0E-4	14
Mesoderm Formation	GOTERM_BP_FAT	1.3E-3	8
Annotation Cluster 7, Enrichment Score 1.79			
Cell Fate Determination	GOTERM_BP_FAT	5.6E-3	18
Ganglion Mother Cell Fate Determination	GOTERM_BP_FAT	1.3E-2	4
NB Fate Determination	GOTERM_BP_FAT	2.3E-2	6
NB Fate Commitment	GOTERM_BP_FAT	3.2E-2	6
NB Differentiation	GOTERM_BP_FAT	3.7E-2	6
Annotation Cluster 8, Enrichment Score 1.75			
Plasma Membrane Part	GOTERM_CC_FAT	1.4E-2	40

I found that many highly enriched clusters (clusters 1, 3 and 5), representing mostly upregulated genes, contained GO-terms implicated in function of neurons. This substantiates the previously presented results pointing towards cells undergoing differentiation upon *dom* knockdown. Two clusters (cluster 4 and 8) consist of GO-terms containing genes connected to plasma membrane or the ER, which produces the plasma membrane. The misregulation of genes in these clusters could explain the elevated CD8-GFP fluorescence upon *dom* knockdown, as CD8-GFP is a membrane tethered marker.
Importantly, cluster 7 contains GO-terms implicated in regulation of NB and offspring cell behavior, which supports the premise that *dom* is required for the expression of genes modifying NB division and fate.

3.7. Domino maintains adult midgut precursors

The presented results illustrate the importance of Dom and the Tip60 complex in larval NBs of the fruit fly. However, Dom was described to be also required for various other stem cell populations in *Drosophila* (Börner and Becker, 2016; Morillo Prado et al., 2013; Xi and Xie, 2005; Yan et al., 2014). Having a fairly clear understanding of how Myc and the Tip60 complex interact to maintain larval NBs, I asked whether this knowledge can be transferred to other stem cell populations of *Drosophila* and decided to investigate the influence of Dom on adult midgut precursors (AMPs). AMPs reside in the larval midgut and start producing differentiating offspring cells during metamorphosis to replace the larval gut cells with adult gut cells. They are the progenitors of adult intestinal stem cells, yet are much easier to differentiate from other cell types in the gut than their adult homologs. AMPs are present in cell clusters making it easy to identify AMPs by morphology and do not produce differentiating offspring cells, which could inherit Gal4 and associated markers. Thus, Gal4 driver activity is restricted to AMPs specifically (Mathur et al., 2010; Micchelli et al., 2011).
In an initial experiment, I knocked down or overexpressed Dom in AMPs using the *insc::Gal4* driver, in which Gal4 positive cells are marked with CD8-GFP expression. We have confirmed that *insc::Gal4* can be used as a driver in larval AMPs (M.Sc. Thesis Nguyen, 2016). In the wild type control larval midgut, GFP positive cell clusters represent the AMPs positive for Gal4 driver activity (Figure 58 A). Remarkably, upon *dom* knockdown,

these AMP islands disappear. Instead, polyploid enterocytes, one type of differentiated gut cells that are produced by AMPs during metamorphosis and by ISCs in the adult midgut, are positive for GFP expression (Figure 58 B). Overexpression of DomB results in a slightly milder phenotype, in which AMP islands could still be identified but also GFP positive enterocytes are present (Figure 58 C).

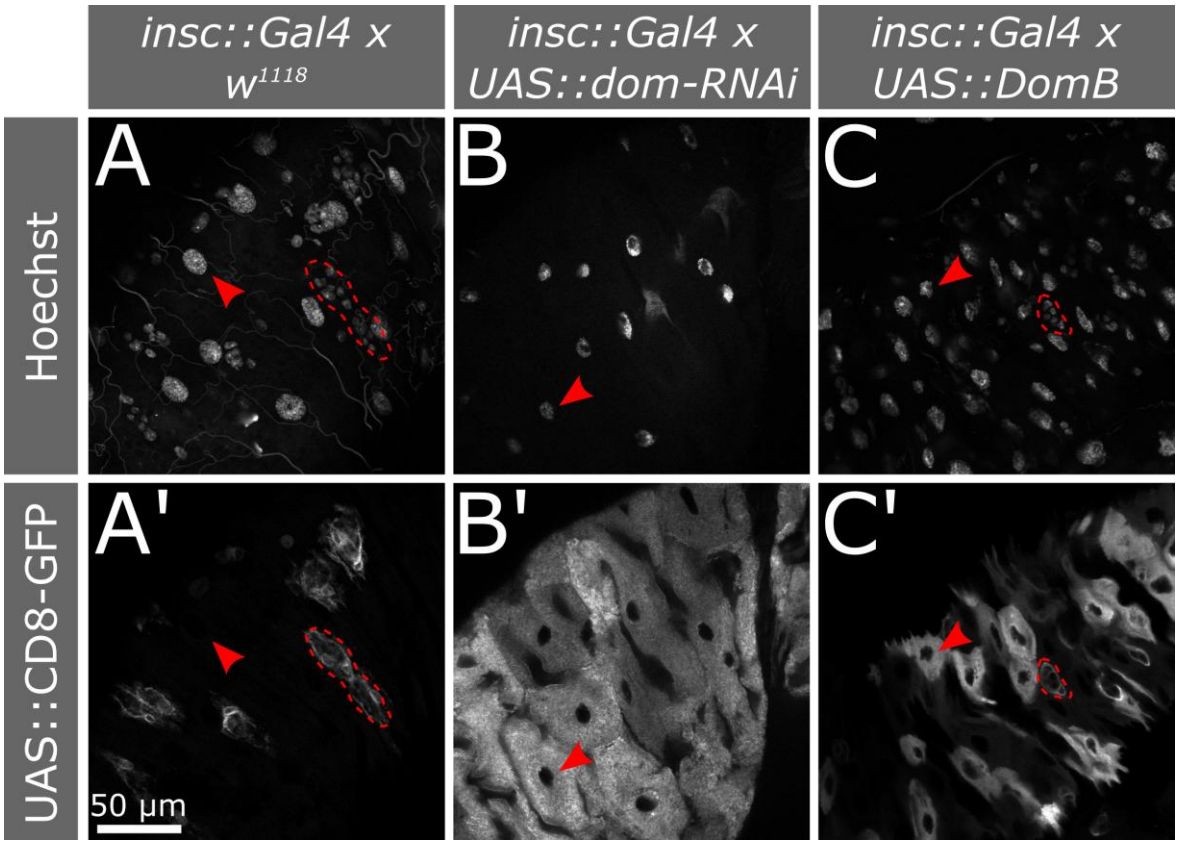

Figure 58: Domino is required in specific levels to maintain adult midgut precursors

Confocal microscopy pictures of L3 larval guts. The *insc* driver was used to express Gal4 and the CD8-GFP marker in adult midgut precursor (AMP) islands, which can also be identified by Hoechst staining as a cluster of small nuclei (marked by dotted line). Arrowheads point at polyploid enterocyte nuclei. (B, C): Upon *dom* knockdown or overexpression, AMP islands yield to GFP positive enterocytes, which are never marked by GFP in the wild type (A).

I went on to investigate the phenotypes upon loss of function of additional Tip60 subunits as well as *myc* in AMPs by screening for additional GFP positive cells in larval midguts upon knockdown with the *insc::Gal4, UAS::CD8-GFP* driver. I found that Myc as well as the Tip60 subunits Dom, Tip60, Brd8, DMAP1, E(Pc), Gas41, MrgBP, Nipped-A, Pont and Rept appear to be required to prevent ectopic GFP positive ECs and to maintain AMPs.
Subsequent experiments on the function of Dom in AMPs have been conducted together with Hong Nhung Ngyuen and will be summarized shortly for comprehension (M.Sc. Thesis Nguyen, 2016). Dom is required especially in the posterior region of the larval midgut to maintain AMP islands by an apoptosis-independent mechanism. Misregulation of Dom results in an excess of GFP positive enterocytes, most probably by premature differentiation of AMPs. Moreover, electron microscopy analysis revealed that the intestinal morphology is disturbed. Enterocytes display morphological defects and occlude the intestinal lumen. Misregulation of other Tip60 members results in similar phenotypes. Likewise, knockdown of *myc* and *H2Av* lead to loss of AMPs and generates GFP positive enterocytes.

4. Discussion

The regulation of stem cell maintenance and differentiation is a growing field of research as implications for stem cell therapies as well as generation of pluripotent stem cells are increasingly important. Additionally, factors for stem cell self-renewal are likely to be misregulated in tumors (Shackleton, 2010). Although our knowledge has greatly increased over the past years, the regulatory network in stem cells is far from being completely understood. Chromatin remodeling has emerged as one of the fundamental processes in stem cell maintenance and many stem cell factors influence epigenetic modifications. Yet, the exact interplay within this network as well as the regulated target genes remains poorly understood (Orkin and Hochedlinger, 2011). Here I have investigated the function of the chromatin remodeler Dom as well as the associated chromatin remodeling complex in *Drosophila* NB self-renewal. I provide evidence that Dom interacts with Myc to regulate genes for NB maintenance, among which the p53/Dacapo pathway might play a central role.

4.1. Domino acts in the Tip60 complex to maintain *Drosophila* neural stem cells

The importance of Dom for *Drosophila* stem cells has been demonstrated in different cell populations, including different stem cell types in the male and female germlines and NBs (Börner and Becker, 2016; Morillo Prado et al., 2013; Neumüller et al., 2011; Xi and Xie, 2005; Yan et al., 2014). In mammals it is well established that several subunits of the Tip60 complex maintain stem cells (Chen et al., 2011; Fazzio et al., 2008a; Fazzio et al., 2008b; Lu et al., 2015). However, which Tip60 subunits exactly play roles in stem cells has not been analyzed in a comprehensive manner. In *Drosophila* only Dom has been implicated in stem cell maintenance. Additionally, as Dom functions in the Tip60 and SRCAP complex, the associated chromatin remodeling complex has to be determined for each process in which Dom is involved (Eissenberg et al., 2005; Kusch et al., 2004).

In the present study I found that Dom as well as several Tip60 subunits, including the Tip60 HAT, Brd8, DMAP1, MrgBP, Nipped-A, Pontin and Reptin are likewise required for the maintenance of larval NBs (see 3.3.2, 3.3.5). Although the subunit composition of the

SRCAP and Tip60 complexes are predicted to overlap, the Tip60 HAT as well as Brd8, MrgBP and Nipped-A are present only in the Tip60 complex (Clapier and Cairns, 2009). However, knockdown of the Tip60 members *Act87E*, *Bap55*, *Eaf6*, *E(Pc)*, *Gas41* and *MRG15* did not lead to neural defects (see Appendix Table S 2). Possibly, the RNAi lines used for this purpose were ineffective. However, in yeast Yaf6, the homolog of Gas41, acts functionally redundant with Brd1, the Brd8-homolog (Bianchi et al., 2004). Therefore, knockdown could potentially be compensated by other subunits.

Moreover, the presence and functional importance of sub-complexes of the Tip60 complex has been suggested and was described in some cases. Thus, only a sub-complex of the Tip60 complex might be required for NB maintenance (Boudreault et al., 2003; Fuchs et al., 2001; Tyteca et al., 2006). In mammals, especially the homologs of Dom, Tip60, Bap55, DMAP1, Gas41, MRG15, Nipped-A, Reptin and Pontin are linked to stem cell maintenance, which highly overlaps with my findings (see 3.3.2, 3.3.5) (Chen et al., 2011; Fazzio et al., 2008b; Lu et al., 2015). Although additional evidence is required to irrefutably show this, I postulate that only a sub-complex of the Tip60 complex acts in NB maintenance, which might moreover be conserved in mammalian stem cells.

Eissenberg et al. (2005) have postulated, that the DomE isoform acts as a SRCAP homolog, while DomA is believed to function as a p400 homolog in the Tip60 complex (Kusch et al., 2004). Expression analysis as well as rescue experiments together with results from previous studies suggest that DomE is the isoform expressed and required in larval NBs (see 3.3.1, Figure 26, Ruhf et al., 2001). Thus, my data strongly argue against DomE functioning solely as a SRCAP homolog but indicate its relevance as a p400 homolog in the Tip60 complex.

In unstressed cellular contexts, p400 and Tip60 can function antagonistically, where p400 inhibits Tip60 in the absence of DNA damage (Park et al., 2010; Tyteca et al., 2006). The likewise requirement of Dom and Tip60 for the maintenance for neural cells and the lack of rescue of the *dom* knockdown phenotype by Tip60 overexpression strongly suggest, that in larval NBs Tip60 and Dom do not function antagonistically but together (see Figure 31, Figure 32).

To summarize, although the importance of Dom in *Drosophila* stem cells is well established (Börner and Becker, 2016; Morillo Prado et al., 2013; Neumüller et al., 2011;

Xi and Xie, 2005; Yan et al., 2014), this study is the first to show that Dom, most probably specifically the isoform DomE, functions with other subunits of the Tip60 complex to maintain *Drosophila* stem cells.

4.2. The Tip60 complex interacts with Myc to regulate neuroblast self-renewal

The interaction between the Tip60 complex and Myc has been well established in mammals and was recently also demonstrated to play a role in mouse embryonic stem cells (Frank et al., 2003; Fuchs et al., 2001; Gévry et al., 2007; Patel et al., 2004; Ravens et al., 2015). In *Drosophila* the interaction between Myc and the Tip60 complex is not proven. Myc regulates cellular growth and proliferation by interaction with Reptin and Pontin, two subunits of the Tip60 complex (Bellosta et al., 2005). However, as Reptin and Pontin also function in several other complexes, the relevance of this interaction for a relationship between Myc and the Tip60 complex is speculative (Grigoletto et al., 2011).

In this study, I provide evidence that Myc, like the Tip60 complex, maintains NBs by regulating asymmetric cell division and preventing Pros dependent premature differentiation (see 3.4). The reduction of cell size and the smaller mitotic index caused by *dom* as well as *myc* knockdown are typical phenotypic outcomes of *myc* loss of function (Figure 36, Figure 38, Figure 46, Bellosta and Gallant, 2010). Additionally, Myc maintains Dom expression and induction of Myc expression partially rescues the *dom* knockout phenotype (Figure 48, Figure 49). Dom itself appears to negatively regulate *myc* expression as determined by RNA-sequencing, thus Myc provides negative feedback on its own expression via regulation of *dom* (see 3.6). This regulatory feedback loop seems to be conserved in human, as c-Myc upregulates p400 in human cell lines (Chan et al., 2005; Koh et al., 2015). Moreover, data from mammalian systems have postulated the presence of specific Tip60 subunits including p400, Tip60, TRRAP, Tip48 and Tip49 and the absence of E(Pc) in Myc-interacting complexes (Frank et al., 2003; Fuchs et al., 2001; McMahon et al., 1998; Park et al., 2002; Wood et al., 2000). Interestingly, knockdown of all listed homologous Myc interactors but not *E(Pc)* results in loss of neural cells (see 3.3). Together, Myc appears to interact with the Tip60 complex in the same pathway to maintain larval NBs. Here, the sub-complex of the Tip60 complex interacting with Myc is apparently conserved with the mammalian composition. The fact that *E(Pc)* knockdown,

which does not interact with Myc (Fuchs et al., 2001), does not affect NB maintenance, supports that only Tip60 subunits that interact with Myc are required. As *E(Pc)*-RNAi works well in other cell types (Table S 2), it is very unlikely that the RNAi is ineffective in NBs. Therefore, the relevance of the Myc-interacting Tip60 subcomplex points to a functional relevance of the Tip60 complex which solely relies on interaction with Myc.

Myc was also shown to influence several types of mammalian and *Drosophila* stem cells and its function is highly dependent on the cellular context (Quinn et al., 2013). Considering that the interaction between the Tip60 complex and Myc appears to be important for NB maintenance, the Tip60 complex might be one of the factors determining how Myc functions in particular stem cells. As the function of the Tip60 complex and the interaction with Myc both are highly conserved in mammals and *Drosophila*, it might be worthwhile to investigate the importance of the Tip60 complex in the diverse stem cell types which are influenced by Myc in mammals.

4.2.1. Myc and the Tip60 complex potentially interact to regulate gene expression in larval neuroblasts

Previous studies in mammalian systems strongly suggest that the Tip60 complex is recruited by Myc to target promoters to regulate gene expression (Frank et al., 2003; Ravens et al., 2015). Reduced H4-acetylation on lysine 8 upon *dom* knockdown and the influence of H2Av on NB maintenance supports the requirement of the Tip60 complex for regulation of transcription, as both histone marks are used for regulation of gene expression (see 3.4.4) (Kusch et al., 2014; Wang et al., 2008). Additionally, Dom binds to DNA and influences the expression of a large set of target genes as investigated by RNA-sequencing among which are mainly genes for neural differentiation as well as NB fate and differentiation (see Figure 9, 3.6). This suggests that in the *Drosophila* NB, like in mouse ESCs, the Tip60 complex is required to repress genes for differentiation (Fazzio et al., 2008b). In mouse ESCs the Tip60 complex is recruited to target promoters by Myc. Further, the NB phenotype upon *myc* knockdown is strikingly similar to the *dom* loss of function phenotype. Therefore, I speculate that the regulation of Dom target genes could greatly depend on the recruitment of the Tip60 complex to promoters by Myc (Ravens et al., 2015). The hypothesis that the deregulation of a set of Myc/Tip60 complex influenced

target genes leads to the loss of larval NBs upon knockdown of *dom,* would also explain why animals with DomB overexpression are phenotypically normal. As Myc is downregulated by Brat in GMCs, it would not lead to recruitment of DomB to target promoters, thus GMCs would differentiate normally (Betschinger et al., 2006).

Myc is believed to mostly act as a transcriptional activator and the influence of Dom on H4 acetylation indicates a role in activation of gene expression (Figure 50) (Kress et al., 2015; Wang et al., 2008). Also H2Av incorporation by the Tip60 complex plays an activatory role in gene expression (Kusch et al., 2014). Moreover, the target promoters to which Myc recruits the Tip60 complex in ESCs are mainly active (Ravens et al., 2015) and in addition I found that Dom localizes to euchromatic regions in polytene chromosome preparations (Figure 7). Interestingly, Dom also colocalizes with the transcriptional activator Repo (Yuasa et al., 2003) (Figure 23). However, loss of *dom* leads to upregulation of genes for differentiation, suggesting a repressive effect on transcription (Table 4). Previous studies have linked the Tip60 complex to repression of genes for differentiation in cooperation with the pluripotency factor Nanog in mouse ESC (Fazzio et al., 2008b). Therefore, it is possible that the Tip60 complex interacts with additional transcriptional regulators other than Myc to repress target genes in NBs. However, although not demonstrated in stem cells, Myc is able to repress gene expression together with the Tip60 complex, which was shown by c-Myc/Tip60 complex induced incorporation of H2A.Z to the promoter of p21 (Gévry et al., 2007).

Although most gene clusters in *dom* target genes are derepressed upon *dom* knockdown, one cluster represented predominantly downregulated genes, meaning that Dom is required to activate their expression (Table 4). These Dom-activated genes possess transcription factor activity, thus in turn are able to regulate gene expression. Hence, it is possible that the direct set of activated Myc/Tip60 target genes is relatively small and then indirectly leads to the regulation of additional genes. Further chromatin immunoprecipitation experiments are required to specify a set of directly regulated target genes of Myc and the Tip60 complex.

Target genes with transcription factor activity are furthermore interesting candidates, as they could potentially have a large effect on NB maintenance. A gene that is downregulated in response to *dom* knockdown is *charlatan* (*chn,* CG1179, log2FC = -

1.188, FDR = 2.8E-9). Chn can act as a transcriptional repressor, thus could serve to repress genes for differentiation (Tsuda et al., 2006). *Chn* was identified in a screen for mutants which affect the embryonic nervous system development and absence of *chn* leads to loss of neurons in the peripheral nervous system (Escudero et al., 2005). Interestingly, *chn* is required for ISC division and blocks ISC differentiation when overexpressed (Amcheslavsky et al., 2014). Therefore, *chn* could be one of the target genes of Dom which regulate NB division as well as AMP maintenance.

4.2.1.1. The p53/Dacapo pathway: Potential downstream targets of Myc/Tip60 regulated gene expression

The mammalian tumor suppressor p53 was shown to activate the cyclin-dependent kinase inhibitor p21, which induces cell cycle arrest or exit (Beckerman and Prives, 2010). Downregulation of this pathway facilitates the generation of pluripotent stem cells from somatic cells and forced expression of p53 or p21 leads to differentiation of murine NSCs (Hong et al., 2009; Kawamura et al., 2009; Li et al., 2009b; Marión et al., 2009; Medrano et al., 2009; Meletis et al., 2006). Interestingly, Myc and the p53 pathway need to be coordinately controlled to ensure appropriate NSC self-renewal (Nagao et al., 2008). Additionally, c-Myc overexpression is able to induce stem cell marker expression in mouse astrocytes with p53 knockout but not in the presence of p53, further indicating functional interplay between c-Myc and the p53 network (Radke et al., 2013). *c-myc* knockout in mouse hematopoietic stem cells induces high levels of p21, leading to reduced proliferation and loss of stem cells (Baena et al., 2007). The expression of p21 is repressed by c-Myc and p400 by the incorporation of H2A.Z to the promoter region and aging human cells use this pathway to induce senescence by downregulation of p400 (Gévry et al., 2007). Another subunit of the Tip60 complex MRG15 was shown to prevent p53 accumulation and repress p21 expression in mouse NSCs, thereby maintaining proliferation and stem cell self-renewal (Chen et al., 2011).

RNA-sequencing of *dom* deficient neural cells showed that *p53* and the *Drosophila p21* homolog *dacapo* are upregulated upon *dom* loss of function (see 3.6). Interestingly, strong overexpression of p53 via the Gal4-UAS system reduces neural cells and NBs (Figure 43). Additionally, overexpression of dominant negative p53 variants which block the DNA

binding of endogenous p53, can partially rescue the loss of neural cells upon *dom* knockdown, indicating a functional relevance of p53 upregulation in *dom* knockdown (Figure 44). I have clearly demonstrated that premature differentiation and not apoptosis is the cause of NB loss. Hence, p53 might influence NB fate rather by induction of *dacapo* and thereby leading to cellular senescence than by induction of apoptotic cell death (see 3.3). This hypothesis is supported by the importance of H2Av for larval NBs, whose homolog H2A.Z represses p21 expression, and the reduced mitotic index in *dom* depleted NBs, which could be due to reduced cell cycle progression by *dacapo* activation (Figure 51, Figure 38) (Gévry et al., 2007). Moreover, mammalian c-Myc, p400 and MRG15 regulate p21 expression and p21 in induces cell cycle exit and cellular senescence. Consequently, it appears likely that the p53/Dacapo pathway could at least be partially responsible for the loss of NBs upon *myc* or Tip60 complex knockdown (Chen et al., 2011; Gévry et al., 2007). However, the Tip60 HAT might not contribute to c-Myc induced p21 repression and overexpression of p53 does not lead to Pros nuclear entry or polarity defects in NBs as in *myc* or Tip60 complex knockdown (Gévry et al., 2007) (data not shown). Therefore, the derepression of the p53/Dacapo pathway is unlikely to be the only important target of the Myc/Tip60 pathway. The incomplete rescue of *dom* loss of function by p53 dominant negative variants supports this view (Figure 44). Nonetheless, the expression level of p53 can strongly influence the set of activated target genes, making p53 an important stress sensor in the cell (Bieging et al., 2014). Using the Gal4-UAS system for overexpression will most probably lead to high levels of p53 activation, as demonstrated also by an extremely strong reduction of neural cells. In contrast, *dom* knockdown leads to a 1.57 fold enrichment of p53 and a weaker phenotype. It is therefore possible that the overexpression phenotype differs from the upregulation of p53 upon *dom* knockdown due to different p53 levels, which may matter for the subset of target genes regulated. In support of this hypothesis, a previous study found that p53 overexpression in NBs restricts their growth by activating Archipelago, which in turn represses CyclinE (Ouyang et al., 2011). Both target genes were not found to be differentially expressed upon *dom* knockdown, instead, *dacapo* is upregulated, speaking for the activation of an alternative set of p53 target genes. Additionally, it has to be considered that the Tip60 complex can act as a co-activator for p53 target gene expression in mammals and the acetylation of

p53 by Tip60 regulates the choice of p53 target genes (Legube et al., 2004; Tang et al., 2006; Tyteca et al., 2006). Thus, the absence of the Tip60 complex is in fact expected to change the set of p53 regulated genes.

So far, a direct effect of Myc on *p53* expression is not known. However, loss of function of mammalian Tip60 complex members was demonstrated to lead to genome instability, which induces p53 and its target p21 (Chen et al., 2011). It is therefore possible that the induction of *p53* and *dacapo* depends on genomic instability upon *dom* knockdown rather than a direct influence on expression or by indirect regulation of a transcriptional regulator of *p53*/*dacapo*. Nevertheless, *myc* loss of function is not associated with genomic instability and in contrast was shown to be required for the p53 response upon genotoxic stress (Phesse et al., 2014). *myc* knockdown leads to a strikingly similar phenotype like Tip60 complex knockdown and Myc is further likely to interact with the Tip60 complex in NB maintenance. Additionally, H2Av was shown to localize mainly to eurchomatic regions on larval NB chromosomes, which rather points towards a main role in transcriptional regulation rather than heterochromatin formation and genome maintenance (Rong, 2008). A recent study further showed that Tip60 complex dependent H2Av incorporation maximizes gene expression, which supports the importance of H2Av in gene expression rather than genome maintenance (Kusch et al., 2014). Thus, I hypothesize that *p53* and *dacapo* activation might be independent of genomic instability but may rather be directly or indirectly regulated by combined activity of Myc and the Tip60 complex.

Interestingly, while knockdown of *myc* can counteract proliferation in *brat* mutation induced NB tumors, forced expression of p53 reduces *numb* mutant NB tumors, underlining the importance and conservation of both factors in *Drosophila* NBs (Betschinger et al., 2003; Ouyang et al., 2011). The interaction of the Tip60 complex and especially Dom with both p53 and Myc and the misregulation of many Tip60 complex members in several types of human tumors makes the Tip60 complex a promising potential tumor suppressor candidate. Although additional experiments are required to elucidate the exact relationship between Myc, the Tip60 complex and the p53/Dacapo pathway, this study strongly suggests that all these components are important for an adequate regulation of larval NB maintenance and nervous system development.

p53 and the Dacapo homolog p21 are already well established in the maintenance of stem cells, yet have not been identified as Myc/Tip60 targets in stem cells. The identification of the p53 pathway demonstrates that by the investigation of Myc/Tip60 complex targets potential new factors for stem cell maintenance can be determined. The obvious requirement of the Tip60 complex and also Myc for AMPs further suggests that the pathway might not only target NB-specific but also general key players of stem cell maintenance (3.7). Considering the high conservation of stem cell regulation as well as Tip60 complex and Myc function in *Drosophila*, this approach might have implications for mammalian stem cell research.

4.2.2. The Tip60 complex and Myc preserve neuroblast polarity and inhibit premature differentiation

Drosophila NBs possess intrinsic polarity, which is crucial for asymmetric cell division, the establishment of a differentiating daughter cell and the self-renewal of the NB. Disturbances in NB polarity result in tumorigenesis or loss of the stem cell (Knoblich, 2010). Here I have shown that loss of the Tip60 component *dom* as well as knockdown of its interactor *myc* result in loss of NB polarity and failure to divide asymmetrically (Figure 35, Figure 41, Figure 45). Importantly, NBs mutant for *aPKC*, which is also mislocalized upon *dom* knockdown (see Appendix Figure S 3) produce smaller NB lineages, show reduced proliferation and differentiate prematurely (Lee et al., 2006a; Rolls et al., 2003).

Additionally, Tip60 complex or *myc* deficient NBs fail to exclude Pros, a transcription factor repressing self-renewal and inducing differentiation, from the nucleus (Figure 39, Figure 40, Figure 47). As I could exclude apoptotic cell death as a cause for the reduction in NB numbers (Figure 33) Pros dependent premature NB differentiation appears to be the ultimate reason for NB loss. Besides Pros nuclear entry, the reduced number of neurons in *dom* knockdown larval brains supports that NBs differentiate prematurely. In addition, the NB cell cycle is slower as indicated by a smaller mitotic index altogether further leading to reduced neuron numbers (see 3.3). Although not inspected in depth the resulting neurons appear to be able to differentiate correctly as axons are visible and the nervous system is reduced but not unstructured (Figure 30).

This importance of Dom to maintain NB polarity and prevent premature differentiation is substantiated by the loss of NBs and reduced amount of offspring cells per NB as well a NB polarity defects in MARCM clones with *dom* null mutation (Figure 27, Figure 34). Please note, the low number of clones, loss of NBs in clones and the low incidence of dividing NB MARCM clones made it challenging to quantify phenotypes in *dom* null MARCM clones. In fact, I suppose that it is only possible to investigate the function of *dom* upon knockdown but not knockout, especially when considering mitotic NBs as knockout leads to the almost complete absence of mitotic NBs. The same holds true if larger amounts of affected cells are required, for example for next generation sequencing. This underlines the usually disrespected advantage of an incomplete knockdown in comparison to full knockout studies.

Interestingly, upon strong knockdown of *myc* most NBs show Pros nuclear entry, yet can be identified as NBs and are therefore not differentiated (Figure 47). This leads to the question why the NBs are still present and do not directly differentiate upon Pros nuclear entry. In this background almost no dividing NBs have been observed, which is expected since Myc induces proliferation (see 3.4.2) (Bellosta et al., 2005). Notably, during termination of neurogenesis Pros nuclear entry precedes one final division (Maurange et al., 2008). Together, this strongly suggests that nuclear Pros can induce differentiation only in NBs which proliferate. This also explains why a previous study has not found a role for Myc in NB maintenance (Song and Lu, 2011). NBs with strong *myc* knockdown display Pros nuclear entry yet they are locked in a step prior to premature differentiation as they are unable to enter mitosis (3.4.2). Thus NB numbers might not be strongly affected. Detecting the reduced number of offspring cells requires marking the offspring cells, as I have shown using *insc::CD8-GFP* (Figure 43). Weak knockdown of *myc* in contrast results in disturbance of polarity and therefore NB division in only a small percentage of NBs (Figure 45), thus requires in depth quantification of NB numbers to identify defects.

Remarkably, nuclear entry of Pros cannot only induce premature differentiation but when nuclear transiently has also been shown to induce NB quiescence (Lai and Doe, 2014). As Myc and the Tip60 complex influence Pros nuclear entry, this pathway might be an interesting candidate for the regulation of nuclear Pros levels during NB quiescence and termination of neurogenesis. Termination of neurogenesis upon high nuclear Pros shows

some striking similarities to the process by which Tip60 complex or *myc* deficient NBs get lost. Here, NBs reduce their size as they stop increasing size after divisions and Pros enters the nucleus prior to a terminal division (Homem et al., 2014; Maurange et al., 2008). However, overexpression of components of the Myc/Tip60 pathway does not maintain NBs (Figure 52). Most likely, overexpression of only one factor is not sufficient or additional factors influence NB maintenance. The termination of neurogenesis in mushroom body NBs normally depends on apoptosis. However, failure of apoptotic induction activates an alternative mechanism, which uses autophagic cell death (Siegrist et al., 2010). Therefore, several mechanisms might act independently to ensure termination of neurogenesis in other NB populations as well.

To summarize, this study for the first time links the proto-oncogene *myc* and a chromatin remodeler to the maintenance of polarity as a mechanism of stem cell maintenance. The nuclear entry of Pros as well as the loss of NBs and neural cells in response to downregulation of the Myc/Tip60 pathway furthermore provides an easy readout system for the identification of novel interactors of this pathway. Due to the high conservation but fast and sophisticated methods for manipulation in *Drosophila* this will greatly facilitate future *in vivo* studies of the Myc/Tip60 pathway.

4.2.2.1. A model for the loss of neuroblasts upon Tip60 complex and *myc* knockdown

Knowing that NBs lose polarity and differentiate prematurely leads to the question of the timewise order of the phenotypes. One possibility is that NBs upon Tip60 complex or *myc* knockdown behave like pupal NBs ceasing neurogenesis by differentiating terminally. In this case NBs would first lose the capability to increase their size after a division (Homem et al., 2014). This is apparently the case upon *dom* knockdown (Figure 37). Next, small NBs would display Pros nuclear entry (Maurange et al., 2008). However, Pros enters the nucleus of smaller as well as bigger NBs upon *dom* knockdown (Figure 42), which argues against this scenario. Also, terminally differentiating NBs do not display polarity defects and only the last NB division produces two daughter cells of similar size (Maurange et al., 2008). Therefore, Tip60 complex and *myc* depleted NBs do not simply behave like pupal NBs undergoing terminal differentiation.

Alternatively, could the loss of polarity cause Pros nuclear entry? Polarity defects have been observed in small as well as big NBs (Figure 42), thus loss of polarity has to be considered as the earliest phenotype and cause of additional defects. Pros is held cytoplasmic by interaction with Mira, which I have demonstrated to be mislocalized (Figure 34, Figure 45). The interaction of Pros with Mira holds it cytoplasmic in wild type NBs and Pros nuclear entry is enabled by Mira degradation in the GMC (Fuerstenberg et al., 1998; Ikeshima-Kataoka et al., 1997). Yet, Tip60 complex and *myc* deficient NBs are Mira positive even when Pros is present in the nucleus (Figure 39, Figure 40, Figure 47), thus premature Mira degradation is not the cause of Pros nuclear entry in Tip60 complex and *myc* depleted NBs. However, Pros has been shown to enter the nucleus even in the presence of Mira in terminally differentiating NBs (Maurange et al., 2008). Interestingly, also *aPKC* mutant NBs are Mira positive and these NBs have been shown to differentiate prematurely, proving that polarity defects can result in premature differentiation and thus most probably also Pros nuclear localization in NBs (Lee et al., 2006a). Nonetheless, aPKC as well as Baz can still be detected in *dom* knockdown and knockout as well as *myc* knockdown NBs (Figure 34, Figure 35, Figure 45, Figure S 3). Although the loss of aPKC or Baz is therefore not the cause of Pros nuclear entry, disturbances in polarity might contribute to premature differentiation.

Nonetheless, it has to be considered that polarity defects occur in mitotic NBs, while Pros nuclear entry was monitored in interphase NBs in which the nuclear membrane is intact (Figure 34, Figure 35, Figure 39, Figure 40, Figure 45, Figure 47). If Pros would enter the nucleus of each daughter NB resulting from a division of a mother NB with disturbed polarity, it would be expected that the percentage of polarity defective NBs and Pros nuclear entry NBs are similar. Knockdown of *dom* was performed with the same RNAi line to quantify polarity defects and Pros nuclear entry, however while ≈ 24% of NBs showed polarity defects ≈ 45% displayed Pros nuclear entry (Figure 35, Figure 39). Although not quantified with the same RNAi line, *myc* knockdown shows a similar tendency, with 16% of NBs with polarity defects and 58% of NBs with nuclear Pros (Figure 45, Figure 47). This rather argues that Pros nuclear entry occurs prior to loss of polarity.

Could Pros nuclear entry in the interphase cause polarity defects in the subsequent mitosis? The fact that Pros nuclear entry and polarity defects are observed in bigger and

smaller NBs upon *dom* knockdown (Figure 42) supports the hypothesis that Pros nuclear entry precedes polarity defects. As the interphase with Pros nuclear entry would directly lead to a mitosis with disturbed polarity, the phenotypes would be expected in similarly sized NBs. However, more NBs show Pros nuclear entry than polarity defects. Interestingly, the levels of nuclear Pros have been suggested to influence whether a NB enters a quiescent state or differentiates (Lai and Doe, 2014). Notably, quantification of NBs with Pros nuclear entry unveiled a population of NBs in which Pros appeared to be present in the cytoplasm as well as the nucleus (see 3.3.5), suggesting that Pros levels slowly increase in the nucleus rather than Pros entering the nucleus in an all or nothing manner. It thus seems probable, that the amount of nuclear Pros influences whether polarity is properly established during NB division or not. However, terminally dividing NBs with Pros nuclear entry are still able to segregate Mira asymmetrically, thus Pros nuclear alone does not lead to disturbances in the polarity network (Maurange et al., 2008). Hence, although Pros nuclear entry and loss of polarity might be timely coordinated, Myc and the Tip60 complex are likely to influence NB polarity independently of Pros.

Do the nuclear levels of Pros influence the ability of NBs to enter mitosis? Pros nuclear entry was shown to induce quiescence in embryonic NBs, thus preventing them to enter mitosis (Lai and Doe, 2014). *dom* knockdown reduces the NB mitotic index (Figure 38) and upon strong knockdown of *myc* a quantification of mitotic NBs was impossible due to low numbers of dividing NBs. It therefore seems likely that low levels of nuclear Pros prevent NB division upon *dom* and *myc* knockdown as in embryonic NBs. NBs with high levels of nuclear Pros are cabable of dividing, as it has been demonstrated in pupal NBs during the terminal division (Maurange et al., 2008). Strong *myc* knockdown leads to a high number of NBs with nuclear Pros (Figure 47) but no NBs with similar levels of cytosplasmic and nuclear Pros were identified like upon *dom* knockdown. This could be due to higher efficiency of *myc* knockdown in comparison to *dom* knockdown. Notably, almost no dividing NBs were observed upon strong *myc* knockdown, although nuclear levels of Pros were apparently high. Therefore, nuclear Pros levels do not seem to regulate the ability of NBs to enter mitosis upon *myc* knockdown. As the Tip60 complex appears to act together with *myc* to regulate target genes, this is likely also true for Tip60 complex knockdown.

Altogether, Myc and the Tip60 complex appear to influence the ability of the NB to enter mitosis independently of Pros nuclear entry. This is supported by various studies, which showed that Myc regulates the cell cycle in various cell types without Pros expression (Bretones et al., 2015).

Do Pros nuclear levels influence the ability of the NB to divide asymmetrically? *dom* depleted NBs divide less asymmetric and in severe cases establish two daughter cells of similar size. Importantly, divisions show a gradient between asymmetric, less asymmetric and symmetric (Figure 41). Therefore, the nuclear levels of Pros might influence the ability of the NB to establish two differently sized daughter cells. It will be one of the future tasks to investigate whether Pros influences the ability of the daughter centrosome to accumulate pericentriolar mass and to organize microtubules to enable the establishment of a bigger daughter NB. Interestingly, the centrosome can induce Par complex localization, therefore disturbances in centrosome asymmetry might lead to polarity defects (Januschke and Gonzalez, 2010). As mentioned above, Pros is unlikely to directly influence NB polarity, therefore the Tip60 complex and Myc might also regulate asymmetry of NB division independent of Pros.

The interaction between the polarity network and the centrosome is mutual. So, do NBs first lose polarity or the ability to divide asymmetrically? The polarity network regulates spindle orientation via Pins, Gαi and Mud, while the centrosome establishes Par complex localization (Bergstralh and St Johnston, 2014; Januschke and Gonzalez, 2010). As polarity defects and less asymmetric or symmetric divisions were observed in bigger NBs (Figure 42, Figure 41), is seems likely that the NBs lose the ability to establish polarity and to divide asymmetrically at the same time.

The daughter cells that are established upon NB divisions are most likely not able to properly segregate fate determinants into daughter cells. Together with Pros nuclear entry, which represses self-renewal and induces differentiation, the resulting daughter cells might directly lose stem cell identity. The presence of smaller dividing NBs (Figure 36, Figure 37, Figure 46) indicates, that dependent on the degree of asymmetric division and Pros nuclear levels, the NB daughter cell might still have sufficient amounts of stem cell determinants for an additional division.

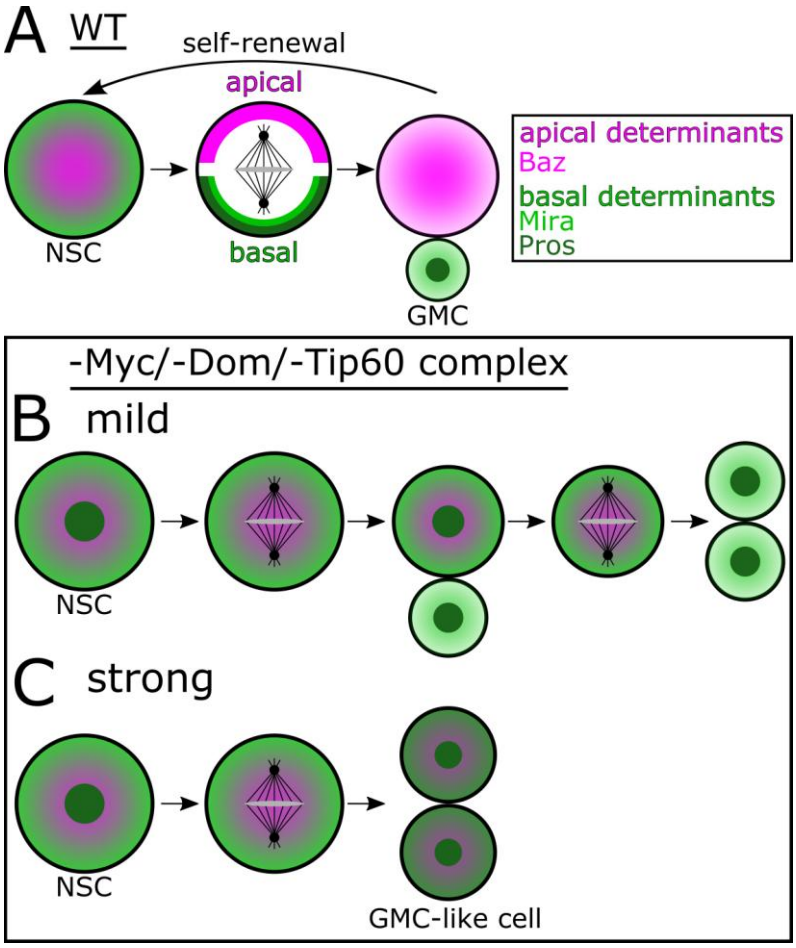

Figure 59: Myc and the Tip60 complex are required for asymmetric NB division and to prevent premature differentiation.

(A): WT NBs possess intrinsic polarity, a prerequisite for asymmetric cell division and establishment of a GMC and self-renewal. (B): Upon loss of the Myc/Tip60 pathway NBs lose polarity and Pros enters the NB nucleus. Cell divisions produce offspring cells that are less different or in severe cases almost similar in size (C). Daughter cells undergoing further divisions due to inheritance of sufficient amount of stem cell factors are unable to increase cell size. Ultimately, NBs are lost due to premature differentiation.

Altogether, the Tip60 complex and Myc appear to regulate Pros nuclear entry and NB polarity independent of each other and both defects are early onset phenotypes, as they are seen in bigger NBs (Figure 42). At the same time, the Tip60 complex and Myc ensure the entry of NBs into mitosis. The ability of NBs to divide asymmetrically is probably linked to polarity and unlikely to be caused by the observed NB size reduction. The same holds true for the loss of polarity and Pros nuclear entry (Figure 36, Figure 46). The size reduction is rather a consequence of less asymmetric or symmetric divisions than a cause

of polarity loss or Pros nuclear entry (Figure 41). Further, the inability of NBs to increase their size after division promotes size decrease (Figure 37), which is in accordance with the well-known function of Myc to activate cell growth (Bellosta and Gallant, 2010). Additionally, Pros is a repressor of self-renewal and could therefore contribute to inhibition of cell growth (Choksi et al., 2006; Chu-Lagraff et al., 1991; Doe et al., 1991; Matsuzaki et al., 1992; Vaessin et al., 1991). Finally, Pros induces differentiation of NBs upon *myc* or Tip60 complex knockdown (Figure 59).

4.2.3. Links between the Myc/Tip60 network and neuroblast division

Asymmetric cell division in the *Drosophila* NB, as well as the Myc and p53/p21 pathways are well-investigated fields of research. Interestingly, previous studies have elucidated several Myc-, Tip60 complex- or p53-regulated factors in mammals that are important for *Drosophila* NB division. One such example is the lipid phosphatase PTEN, which interacts and is colocalized with Baz in NBs. PTEN organizes the actin cytoskeleton as a feature of cell polarity and is predicted to regulate the activity of aPKC (von Stein et al., 2005). Several studies in mammalian systems have established the mutual regulation of Myc and PTEN (Ghosh et al., 1999; Kaur and Cole, 2013). Moreover, PTEN regulates p21 activity for example to regulate mouse NSC proliferation (Groszer et al., 2008; Lin et al., 2007). Thus, PTEN is potentially a Myc target in NBs, which could further link the Myc/Tip60 pathway with Dacapo regulation.

A recent study has shown that NBs upon the pupal ecdysone pulse change their metabolism from mainly glycolysis to more oxidative phosphorylation. This metabolic change is believed to contribute to uncoupling the NB cell cycle from cell growth, thus leads to size reduction prior to termination of neurogenesis (Homem et al., 2014). Remarkably, the so-called “Warburg effect”, which is induced by p53 activation, describes the p53-mediated repression of glycolysis and promotion of oxidative phosphorylation (Vousden and Ryan, 2009). Thus, the p53 activation by *myc* and Tip60 complex knockdown could contribute to premature differentiation by changing the metabolism in the NB. Moreover, the importance of the p53 pathway in induction of NB termination in the pupal stage should be considered.

Genes from the temporal transcription factor cascade as well as Hox genes, whose expression is regulated by the Polycomb group (PcG), have been shown to contribute to the timely regulation of termination of neurogenesis and also embryonic NB quiescence (Bello et al., 2003; Chai et al., 2013; Maurange, 2012; Maurange et al., 2008; Tsuji et al., 2008). Importantly, PcG and Hox genes are well known key factors in larval NB and mammalian stem cell maintenance (Bello et al., 2007; Kashyap et al., 2009; Seifert et al., 2015). Several members of the Tip60 complex, including also Dom, Reptin and Pontin, are known to contribute to the PcG-mediated repressed chromatin state to regulate Hox gene expression in *Drosophila* and mammals (Diop et al., 2008; Qi et al., 2006; Ruhf et al., 2001; Sinclair et al., 1998; Ueda et al., 2007). In murine ESCs H2A.Z is incorporated to PcG promoters and influences differentiation (Creyghton et al., 2008). Interestingly, also p53 is thought do be repressed by PcG (Solà et al., 2011). Moreover, several genes from the temporal transcription factor cascade, as well as Hox genes are targeted by Dom in neural cells (see Appendix Table S 3). Thus, the question arises whether a Tip60 complex dependent misregulation of the temporal transcription factor cascade as well as Hox gene expression, potentially regulated together with PcG, leads to the observed loss of NBs when Tip60 complex members are depleted.

4.2.4. The Myc/Tip60 pathway: A general key player of stem cell maintenance?

Besides NBs, Dom has been shown to be required in other *Drosophila* stem cells, especially in stem cells of the germline (Börner and Becker, 2016; Morillo Prado et al., 2013; Neumüller et al., 2011; Xi and Xie, 2005; Yan et al., 2014). For germline cells the ability of Dom to incorporate H2Av is crucial, supporting a potentially similar mechanism as in NBs (Börner and Becker, 2016; Morillo Prado et al., 2013). Together with Hong Nhung Nguyen, we have found that Dom, Tip60 complex members, Myc and H2Av are required for maintenance of AMPs in the larval midgut (see 3.7). Like NBs, AMPs appear to undergo premature differentiation upon disturbances in the Myc/Tip60 complex network. Remarkably, similar to NBs, AMPs express Par complex members and Insc. Thus, the Myc/Tip60 network might influence similar players of polarity in NBs and AMPs.

Myc was shown to regulate proliferation and maintenance of adult ISCs in *Drosophila* (Ren et al., 2013). Our findings indicate that this function of Myc is conserved in AMPs.

Additionally, it will be one of the future tasks to investigate the function of the Tip60 complex in adult ISCs, especially as a cofactor of Myc.

Interestingly, the Tip60 complex subunits that are required for NB and AMP maintenance overlap remarkably. Furthermore, the subunits found to influence NB and AMP maintenance match largely those subunits binding to Myc and subunits shown to maintain mammalian stem cells (see Appendix Table S 2). This strongly points to a conserved composition and function of the Myc/Tip60 network in *Drosophila* NBs and AMPs as well as mammalian stem cells.

However, unlike in NBs, AMPs also differentiate upon Dom overexpression (Figure 58). Moreover, knockdown of not only the Tip60 members that are required in NBs leads to AMP differentiation, but additionally Gas41 and E(Pc) are necessary in AMPs (see Appendix Table S 2). Especially E(Pc) is not a member of the Myc-interacting complex (Fuchs et al., 2001). This points towards an additional function of the Tip60 complex in AMPs.

Importantly, the functions of the Tip60 complex differ between cellular contexts and cell types. One prominent difference between AMPs and NBs is the importance of Notch signaling. In type I NBs, on which I have focused in this study, disturbances in Notch signaling have little to no effect (Song and Lu, 2011). AMPs establish their own niche by the production of a peripheral cell via Notch signaling (Mathur et al., 2010). Moreover, AMPs as well as mature ISCs have been shown to require active Notch signaling to be maintained and they differentiate upon knockdown of Notch signaling (Guo and Ohlstein, 2015; Ohlstein and Spradling, 2007; Takashima et al., 2011). Importantly, Dom and Nipped-A have been found to modulate Notch signaling (Eissenberg et al., 2005; Ellis et al., 2015; Gause et al., 2006; Hall et al., 2004; Kwon et al., 2013). Thus, the Tip60 complex could potentially regulate Notch signaling in larval AMPs. Misregulation was shown to regulate AMP maintenance and would result in the absence of a niche, which could not maintain AMPs undifferentiated (Mathur et al., 2010; Takashima et al., 2011).

Taken together, our findings suggest that the Tip60 complex has overlapping functions in NBs and AMPs which might be directed by interaction with Myc. In AMPs the Tip60 complex appears to have additional functions, potentially the regulation of Notch signaling. The importance of the Myc/Tip60 network in both stem cell types and the

conservation of the subunits in mammalian stem cell maintenance lead to the hypothesis that this pathway might be a general requirement in many *Drosophila* and mammalian stem cell types.

4.3. Domino is potentially required for various processes in *Drosophila* development

Considering that Dom is crucial for stem cell maintenance and further that the functions of Dom partly differ between AMPs and NBs, it is not surprising that Dom also influences *Drosophila* embryogenesis and imaginal disc development. Like AMPs, imaginal disc cells are differentially influenced by *dom* knockdown or overexpression (3.2). The role of Myc in imaginal discs cells is quite well understood. Myc levels influence cell size, whereas proliferation rates are not markedly changed (Pierce et al., 2004). However, when Myc is manipulated in a mosaic, cellular competition induces apoptosis of the cells with lower Myc levels (de la Cova et al., 2004; Moreno et al., 2004). Considering the phenotype of imaginal discs with *dom* knockdown in the posterior compartment, it will be interesting to analyze the role of apoptosis for the given effect (Figure 20). It can be hypothesized that upon the lack of *dom,* Myc target genes might not be expressed, which then could lead to the induction of apoptotic cell death in these cells by the surrounding wild type cells. In previous studies on *dom* knockdown or overexpression of *dom* in the complete disc led to morphological defects in the wing but not to a complete loss of cells. Hence, the elimination of *dom* knockdown cells by neighbouring wild type cells appears even more likely (Eissenberg et al., 2005; Ellis et al., 2015; Hall et al., 2004; Kwon et al., 2013).

In contrast to the knockdown phenotype, overexpression of DomE, the major isoform of *dom* expressed in wing discs (Ruhf et al., 2001) in the posterior compartment leads to morphologically defective wing discs, thus rather not pointing towards a cell competition mediated loss of cells (Figure 22). The morphological effects of *dom* manipulation in complete wing discs have been shown to depend on the ability of Dom to modulate Notch signaling (Eissenberg et al., 2005; Hall et al., 2004). Notch signaling regulates imaginal disc growth and patterning, thus the DomE overexpression phenotype could depend on misregulation of Notch signaling (Estella and Baonza, 2015). Taken together, the different phenotypes upon *dom* knockdown and overexpression in imaginal discs might be results of the interaction with two different cofactors: Myc and Notch signaling.

Dom null mutants embryos display a very remarkable nuclear phenotype with nuclear membrane invaginations. This phenotype resembles overexpression phenotypes of proteins that structure the nuclear envelope (Brandt et al., 2006; Brandt et al., 2008; Pilot et al., 2005). Interestingly, the nuclear envelope is linked to chromatin and morphological changes in the nuclear membrane influence gene expression, a mechanism which is for example used during maternal to zygotic transition (Hampoelz et al., 2011). The link between the nuclear envelope and chromatin is established by the heterochromatin protein 1 (HP1) and the Brahma associated factor (BAF) (Polychronidou et al., 2010; Ye et al., 1997). As the incorporation of H2Av by Dom into chromatin is required to prevent heterochromatin spreading and acts upstream to HP1 incorporation, excess HP1 could theoretically lead to the membrane invaginations (Baldi and Becker, 2013). Remarkably, the chromatin state has never been reported to influence the nuclear membrane organization, but informational flow is thought to work in the opposite direction (Polychronidou and Großhans, 2011). Although the nuclear phenotype observed in *dom* null mutant embryos will require additional thorough analyses, the results of this study question this theory.

In addition to causing an abnormal nuclear shape, *dom* mutation has a great impact on the embryonic ectodermal epithelium (3.1.3). Epithelial cells are bigger than wild type cells of the same stage, indicating difficulties in the cell cycle as embryonic cells do not increase in size but get smaller with each division. As *myc* mutants undergo normal embryogenesis (Johnston et al., 1999b; Pierce et al., 2004), Dom might interact with other key regulators of cell cycle progression in the embryo. An obvious candidate for this would be the E2F family, as they have been shown to be vital for the cell cycle in the *Drosophila* embryo and because the Tip60 complex has been linked to the E2F network in mammals and *Drosophila* (Duronio et al., 1995; Lu et al., 2007; Taubert et al., 2004). Alternatively, considering the nuclear phenotype and the bright staining of nuclei by Hoechst in *dom* mutant embryos (Figure 10, Figure 17), it is possible that Dom is required in embryonic nuclei to prevent heterochromatin spreading by H2Av incorporation, which would be crucial for genome maintenance (Rong, 2008). Misregulation of this could lead to the activation of cell cycle checkpoints, thus reduced or totally stalled cell division and consequently bigger embryonic cells.

Dom mutant embryos further display polarity defects in the epithelium. Although electron microscopy demonstrated that AJs are formed, the localization of polarity determinants appears to be affected, especially in processes requiring extensive cell shape changes, like dorsal closure. This also explains the inability of *dom* mutant embryos to form head and dorsal cuticle (3.1.3). So far no maternal *dom* null mutants have been investigated for epithelial polarity, thus one could speculate that the importance of *dom* in epithelial polarity could be even more fundamental as the maternally provided Dom protein might be sufficient for the establishment of AJs and maintenance of parts of the polarity. I did not detect extraordinary amounts of apoptotic cells and blocking apoptosis did not restore the *dom* mutant phenotype (Figure 18, Figure 19). Therefore, the cells observed to leave the tissue might reorient due to polarity defects and might be unable to maintain appropriate positioning of AJs. Considering the role of Dom in the maintenance of larval NB polarity, Dom might have a central function in regulating polarity. It will also be interesting to investigate the function of *dom* for the polarity of imaginal disc epithelial cells, as misregulation leads to defects. However, the intrinsic polarity of embryonic NBs is surprisingly unaffected, suggesting that the impact of Dom on cellular polarity might be cell-type and thus cofactor specific (Figure 11, Figure 13). The NB cell orientation is most likely defective as a secondary effect due to epithelial misorganization and subsequent defects in communication between the epithelium and the NBs (Yoshiura et al., 2012).

Notably, embryonic NBs, in contrast to larval NBs, get smaller with each division (Ito and Hotta, 1992). The importance of Dom to enable cell growth in NBs is therefore restricted to larval NBs and not required in embryonic NBs. Therefore, the growth inducing capability of Myc is also not required in embryonic NBs. Further, Myc has been shown to be dispensable for successful embryogenesis (Johnston et al., 1999b; Pierce et al., 2004). It is thus possible that Dom is required solely in NBs that depend on Myc. Additionally, considering that Dom does not maintain embryonic NB polarity and maintenance, this strongly argues against a role of the Tip60 complex in larval NBs apart from regulation of Myc-responsive genes.

Taken together, Dom functions in diverse processes and highly dependent on the cellular context. The defects observed upon dom loss of function and overexpression in this study

could depend on various cofactors like Myc, E2F and Notch signaling. The chromatin remodeling complexes in which Dom functions have been shown to vary between different cell types. Also the functions appear to vary between activation of proliferation, self-renewal and possibly cellular competition. To completely understand the processes in which Dom is involved it will be required to study which cofactors interact with Dom and in which chromatin remodeling complexes Dom executes its diverse functions.

5. Conclusion and Perspectives

The chromatin remodeler ATPase Dom and its mammalian homologs have been implicated in diverse processes including DNA repair, cell cycle regulation, stem cell maintenance and regulation of Notch signaling. This study shows that the function of *Drosophila* Dom highly depends on the cellular context and is defined by specific interactors like Myc. The subunit composition of the participating chromatin remodeling complex is variable and highly depends on the regulated process and thus might be influenced by the interacting cofactor. This demonstrates the importance of studying chromatin remodeling complexes in a comprehensive manner to understand in which processes they are involved and suggests that the complex composition could hint towards the required interactor.

The present study unravels a previously unknown interaction of Myc and the Tip60 complex in larval NBs and elucidates the mechanism by which this network functions to maintain NBs. This could further help to understand the process by which NBs terminate neurogenesis during metamorphosis.

Previous studies have shown that Myc recruits the Tip60 complex to target promoters to regulate gene expression. The presented data strongly suggest that this is the underlying process for the maintenance of NBs. However, additional experiments investigating the physical interaction between Myc and the Tip60 complex could substantiate this hypothesis. Additionally, to analyze whether Myc and the Tip60 complex indeed target an overlapping set of target genes and to identify directly regulated genes, chromatin immunoprecipitation experiments for Myc and Dom would be beneficial.

The p53/Dacapo pathway is a potential downstream target of the Myc/Tip60 network in NBs. The interplay between Myc, the Tip60 complex and the p53/Dacapo pathway is well established in mammals. However, this study is the first to suggest the p53 pathway as a Myc/Tip60 target in stem cells. Future analyses will help to understand the nature of this interplay in *Drosophila* and can provide insight into the function of p53 and Dacapo in NB maintenance.

Altogether, the factors that have been identified as key players of NB maintenance in this study as well as their interaction with each other is highly conserved between the

Drosophila NB and mammalian stem cells and especially ESCs. This underlines the power of the *Drosophila* NB as a model for stem cell research. Due to the importance of Myc, the Tip60 complex and also p53/p21 for pluripotent stem cells and human tumor formation, this might be highly advantageous for mammalian stem cell research and for implications in cancer treatment.

6. Bibliography

Abbott, D. W., Ivanova, V. S., Wang, X., Bonner, W. M. and Ausió, J. (2001). Characterization of the stability and folding of H2A.Z chromatin particles: Implications for transcriptional activation. *J. Biol. Chem.* **276**, 41945–41949.

Albertson, R. and Doe, C. Q. (2003). Dlg, Scrib and Lgl regulate neuroblast cell size and mitotic spindle asymmetry. *Nat. Cell Biol.* **5**, 166–170.

Altaf, M., Auger, A., Monnet-Saksouk, J., Brodeur, J., Piquet, S., Cramet, M., Bouchard, N., Lacoste, N., Utley, R. T., Gaudreau, L., et al. (2010). NuA4-dependent acetylation of nucleosomal histones H4 and H2A directly stimulates incorporation of H2A.Z by the SWR1 complex. *J. Biol. Chem.* **285**, 15966–15977.

Amcheslavsky, A., Nie, Y., Li, Q., He, F., Tsuda, L., Markstein, M. and Ip, Y. T. (2014). Gene expression profiling identifies the zinc-finger protein Charlatan as a regulator of intestinal stem cells in Drosophila. *Development* **141**, 2621–2632.

Anders, S., Pyl, P. T. and Huber, W. (2015). HTSeq-A Python framework to work with high-throughput sequencing data. *Bioinformatics* **31**, 166–169.

Arnold, I. and Watt, F. M. (2001). c-Myc activation in transgenic mouse epidermis results in mobilization of stem cells and differentiation of their progeny. *Curr. Biol.* **11**, 558–568.

Ashburner, M. (1989). *Drosophila: A Laboratory Handbook and Manual.*

Atkins, M., Potier, D., Romanelli, L., Jacobs, J., Mach, J., Hamaratoglu, F., Aerts, S. and Halder, G. (2016). An Ectopic Network of Transcription Factors Regulated by Hippo Signaling Drives Growth and Invasion of a Malignant Tumor Model. *Curr. Biol.* **26**, 2101–2113.

Atwood, S. X. and Prehoda, K. E. (2009). aPKC Phosphorylates Miranda to Polarize Fate Determinants during Neuroblast Asymmetric Cell Division. *Curr. Biol.* **19**, 723–729.

Baena, E., Ortiz, M., Martínez-A, C. and Moreno de Alborán, I. (2007). c-Myc is essential for hematopoietic stem cell differentiation and regulates Lin-Sca-1+c-Kit- cell generation through p21. *Exp. Hematol.* **35**, 1333–1343.

Baldi, S. and Becker, P. B. (2013). The variant histone H2A.V of Drosophila - Three roles, two guises. *Chromosoma* **122**, 245–258.

Banin, S., Moyal, L., Shieh, S.-Y., Taya, Y., Anderson, C. W., Chessa, L., Smorodinsky, N. I., Prives, C., Reiss, Y., Shiloh, Y., et al. (1998). Enhanced Phosphorytation of p53 by ATM in Response to DNA Damage. *Science* **281**, 1674–1677.

Beckerman, R. and Prives, C. (2010). Transcriptional Regulation by p53. *J. Biol. Chem.* **2**, a000935.

Beira, J. V and Paro, R. (2016). The legacy of Drosophila imaginal discs. *Chromosoma* **125**, 573–592.

Bello, B. C., Hirth, F. and Gould, A. P. (2003). A pulse of the Drosophila Hox protein Abdominal-A schedules the end of neural proliferation via neuroblast apoptosis. *Neuron* **37**, 209–219.

Bello, B., Reichert, H. and Hirth, F. (2006). The brain tumor gene negatively regulates neural progenitor cell proliferation in the larval central brain of Drosophila. *Development* **133**, 2639–2648.

Bello, B., Holbro, N. and Reichert, H. (2007). Polycomb group genes are required for neural stem cell survival in postembryonic neurogenesis of Drosophila. *Development* **134**, 1091–1099.

Bello, B. C., Izergina, N., Caussinus, E. and Reichert, H. (2008). Amplification of neural stem cell proliferation by intermediate progenitor cells in Drosophila brain development. *Neural Dev.* **3**, 5.

Bellosta, P. and Gallant, P. (2010). Myc Function in Drosophila. *Genes Cancer* **1**, 542–546.

Bellosta, P., Hulf, T., Diop, S. B., Usseglio, F., Pradel, J., Aragnol, D. and Gallant, P. (2005). Myc interacts genetically with Tip48¯Reptin and Tip49¯Pontin to control growth and proliferation during Drosophila development. *PNAS* **102**, 11799–11804.

Benton, R. and St Johnston, D. (2003). Drosophila PAR-1 and 14-3-3 inhibit Bazooka/PAR-3 to establish complementary cortical domains in polarized cells. *Cell* **115**, 691–704.

Berger, C., Harzer, H., Burkard, T. R., Steinmann, J., van der Horst, S., Laurenson, A.-S., Novatchkova, M., Reichert, H. and Knoblich, J. A. (2012). FACS purification and transcriptome analysis of drosophila neural stem cells reveals a role for Klumpfuss in self-renewal. *Cell Rep.* **2**, 407–418.

Bergstralh, D. T. and St Johnston, D. (2014). Seminars in Cell & Developmental Biology Spindle orientation : What if it goes wrong ? *Semin. Cell Dev. Biol.* **34**, 140–145.

Bergstralh, D. T., Haack, T. and St Johnston, D. (2013). Epithelial polarity and spindle orientation: intersecting pathways. *Philos. Trans. R. Soc. Lond. B. Biol. Sci.* **368**, 20130291.

Berta, M. A., Baker, C. M., Cottle, D. L. and Watt, F. M. (2010). Dose and context dependent effects of Myc on epidermal stem cell proliferation and differentiation. *EMBO Mol. Med.* **2**, 16–25.

Betschinger, J., Mechtler, K. and Knoblich, J. A. (2003). The Par complex directs asymmetric cell division by phosphorylating the cytoskeletal protein Lgl. *Nature* **422**, 326–330.

Betschinger, J., Eisenhaber, F. and Knoblich, J. A. (2005). Phosphorylation-Induced Autoinhibition Regulates the Cytoskeletal Protein Lethal (2) giant larvae. *Curr. Biol.* **15**, 276–282.

Betschinger, J., Mechtler, K. and Knoblich, J. A. (2006). Asymmetric Segregation of the Tumor Suppressor Brat Regulates Self-Renewal in Drosophila Neural Stem Cells. *Cell* **124**, 1241–1253.

Bianchi, M. M., Costanzo, G., Chelstowska, A., Grabowska, D., Mazzoni, C., Piccinni, E., Cavalli, A., Ciceroni, F., Rytka, J., Slonimski, P. P., et al. (2004). The bromodomain-containing protein Bdf1p acts as a phenotypic and transcriptional multicopy suppressor of YAF9 deletion in yeast. *Mol. Microbiol.* **53**, 953–968.

Bieging, K. T., Mello, S. S. and Attardi, L. D. (2014). Unravelling mechanisms of p53-mediated tumour suppression. *Nat. Rev. Cancer* **14**, 359–70.

Boone, J. Q. and Doe, C. Q. (2008). Identification of Drosophila type II neuroblast lineages containing transit amplifying ganglion mother cells. *Dev. Neurobiol.* **68**, 1185–1195.

Börner, K. and Becker, P. B. (2016). Splice variants of the SWR1-type nucleosome remodeling factor Domino have distinct functions during *Drosophila melanogaster* oogenesis. *Development* **143**, 3154–3167.

Boudreault, A. A., Cronier, D., Selleck, W., Lacoste, N., Utley, R. T., Allard, S., Savard, J., Lane, W. S., Tan, S. and Côté, J. (2003). Yeast Enhancer of Polycomb defines global Esa1-dependent acetylation of chromatin. *Genes Dev.* **17**, 1415–1428.

Bowman, S. K., Neumüller, R. A., Novatchkova, M., Du, Q. and Knoblich, J. A. (2006). The Drosophila NuMA Homolog Mud Regulates Spindle Orientation in Asymmetric Cell Division. *Dev. Cell* **10**, 731–742.

Bowman, S. K., Rolland, V., Betschinger, J., Kinsey, K. a, Emery, G. and Knoblich, J. A. (2008). The tumor suppressors Brat and Numb regulate transit-amplifying neuroblast lineages in Drosophila. *Dev. Cell* **14**, 535–546.

Brand, A. H. and Perrimon, N. (1993). Targeted gene expression as a means of altering cell fates and generating dominant phenotypes. *Development* **118**, 401–415.

Brandt, A., Papagiannouli, F., Wagner, N., Wilsch-Bräuninger, M., Braun, M., Furlong, E. E., Loserth, S., Wenzl, C., Pilot, F., Vogt, N., et al. (2006). Developmental control of nuclear size and shape by kugelkern and kurzkern. *Curr. Biol.* **16**, 543–552.

Brandt, A., Krohne, G. and Großhans, J. (2008). The farnesylated nuclear proteins KUGELKERN and LAMIN B promote aging-like phenotypes in Drosophila flies. *Aging Cell* **7**, 541–551.

Branzei, D. and Foiani, M. (2008). Regulation of DNA repair throughout the cell cycle. *Nat. Rev. Mol. Cell Biol.* **9**, 297–308.

Braun, A., Lemaitre, B., Lanot, R., Zachary, D. and Meister, M. (1997). Drosophila Immunity: Analysis of larval hemocytes by P-element-mediated enhancer trap. *Genetics* **147**, 623–634.

Braun, A., Hoffmann, J. A. and Meister, M. (1998). Analysis of the Drosophila host defense in domino mutant larvae, which are devoid of hemocytes. *PNAS* **95**, 14337–14342.

Brenner, C., Deplus, R., Line Didelot, C., Loriot, A., Viré, E., De Smet, C., Gutierrez, A., Danovi, D., Bernard, D., Boon, T., et al. (2005). Myc represses transcription through recruitment of DNA methyltransferase corepressor. *EMBO J.* **247600509**, 336–346.

Bretones, G., Delgado, M. D. and León, J. (2015). Myc and cell cycle control. *Biochim. Biophys. Acta* **1849**, 506–516.

Broadus, J., Fuerstenberg, S. and Doe, C. Q. (1998). Staufen-dependent localization of prospero mRNA contributes to neuroblast daughter-cell fate. *Nature* **391**, 792–795.

Brodsky, M. H., Weinert, B. T., Tsang, G., Rong, Y. S., McGinnis, N. M., Golic, K. G., Rio, D. C. and Rubin, G. M. (2004). Drosophila melanogaster MNK/Chk2 and p53 regulate multiple DNA repair and apoptotic pathways following DNA damage. *Mol. Cell. Biol.* **24**, 1219–1231.

Burma, S., Chen, B. P., Murphy, M., Kurimasa, A. and Chen, D. J. (2001). ATM Phosphorylates Histone H2AX in Response to DNA Double-strand Breaks. *J. Biol. Chem.* **276**, 42462–42467.

Burnette, W. N. (1981). "Western Blotting": Electrophoretic transfer of proteins from sodium dodecyl sulfate-polyacrylamide gels to unmodified nitrocellulose and radiographic detection with antibody and radioiodinated protein A. *Anal. Biochem.* **112**, 195–203.

Busso, D., Delagoutte-Busso, B. and Moras, D. (2005). Construction of a set Gateway-based destination vectors for high-throughput cloning and expression screening in Escherichia coli. *Anal. Biochem.* **343**, 313–321.

Buszczak, M., Paterno, S., Lighthouse, D., Bachman, J., Planck, J., Owen, S., Skora, A. D., Nystul, T. G., Ohlstein, B., Allen, A., et al. (2007). The carnegie protein trap library: a versatile tool for Drosophila developmental studies. *Genetics* **175**, 1505–1531.

Cai, Y., Jin, J., Gottschalk, A. J., Yao, T., Conaway, J. W. and Conaway, R. C. (2006). Purification and assay of the human INO80 and SRCAP chromatin remodeling complexes. *Methods* **40**, 312–317.

Canman, C. E., Lim, D.-S., Cimprich, K. A., Taya, Y., Tamai, K., Sakaguchi, K., Appella, E., Kastan, M. B. and Siliciano, J. D. (1998). Activation of the ATM Kinase by Ionizing Radiation and Phosphorylation of p53. *Science* **281**, 1677–1679.

Cao, X. and Südhof, T. C. (2001). A Transcriptionally Active Complex of APP with Fe65 and Histone Acetyltransferase Tip60. *Science* **293**, 115–120.

Cenci, C. and Gould, A. P. (2005). Drosophila Grainyhead specifies late programmes of neural proliferation by regulating the mitotic activity and Hox-dependent apoptosis of neuroblasts. *Development* **132**, 3835–3845.

Chai, P. C., Liu, Z., Chia, W. and Cai, Y. (2013). Hedgehog signaling acts with the temporal cascade to promote neuroblast cell cycle exit. *PLoS Biol.* **11**, e1001494.

Chan, H. M., Narita, M., Lowe, S. W. and Livingston, D. M. (2005). The p400 E1A-associated protein is a novel component of the p53 → p21 senescence pathway. *Genes Dev.* **19**, 196–201.

Chell, J. M. and Brand, A. H. (2010). Nutrition-responsive glia control exit of neural stem cells from quiescence. *Cell* **143**, 1161–1173.

Chen, T. and Dent, S. Y. R. (2014). Chromatin modifiers and remodellers: regulators of cellular differentiation. *Nat. Rev. Genet.* **15**, 93–106.

Chen, M., Pereira-Smith, O. M. and Tominaga, K. (2011). Loss of the chromatin regulator MRG15 limits neural stem/progenitor cell proliferation via increased expression of the p21 Cdk inhibitor. *Stem Cell Res.* **7**, 75–88.

Chen, P. B., Hung, J.-H., Hickman, T. L., Coles, A. H., Carey, J. F., Weng, Z., Chu, F. and Fazzio, T. G. (2013). Hdac6 regulates Tip60-p400 function in stem cells. *Elife* **2**, e01557.

Cheng, X. and Côté, J. (2014). A new companion of elongating RNA Polymerase II: TINTIN, an independent sub-module of NuA4/TIP60 for nucleosome transactions. *Transcription* **5**, e995571.

Choksi, S. P., Southall, T. D., Bossing, T., Edoff, K., de Wit, E., Fischer, B. E., van Steensel, B., Micklem, G. and Brand, A. H. (2006). Prospero acts as a binary switch between self-renewal and differentiation in Drosophila neural stem cells. *Dev. Cell* **11**, 775–789.

Chu-Lagraff, Q., Wright, D. M., McNeil, L. K. and Doe, C. Q. (1991). The prospero gene encodes a divergent homeodomain protein that controls neuronal identity in Drosophila. *Development* **Suppl 2**, 79–85.

Clapier, C. R. and Cairns, B. R. (2009). The biology of chromatin remodeling complexes. *Annu. Rev. Biochem.* **78**, 273–304.

Clarke, A. S., Lowell, J. E., Jacobson, S. J. and Pillus, L. (1999). Esa1p is an essential histone acetyltransferase required for cell cycle progression. *Mol Cell Biol* **19**, 2515–2526.

Cobb, L. (2013). Cell Based Assays: the Cell Cycle, Cell Proliferation and Cell Death. *Mater Methods* **3**, ISSN : 2329-5139.

Creyghton, M. P., Markoulaki, S., Levine, S. S., Hanna, J., Lodato, M. A., Sha, K., Young, R. A., Jaenisch, R. and Boyer, L. A. (2008). H2AZ Is Enriched at Polycomb Complex Target Genes in ES Cells and Is Necessary for Lineage Commitment. *Cell* **135**, 649–661.

de la Cova, C., Abril, M., Bellosta, P., Gallant, P., Johnston, L. A. and Street, W. (2004). Size by Inducing Cell Competition. *Cell* **117**, 107–116.

del Valle Rodríguez, A., Didiano, D. and Desplan, C. (2012). Power tools for gene expression and clonal analysis in Drosophila. *Nat. Methods* **9**, 47–55.

Diop, S. B., Bertaux, K., Vasanthi, D., Sarkeshik, A., Goirand, B., Aragnol, D., Tolwinski, N. S., Cole, M. D., Pradel, J., Yates, J. R., et al. (2008). Reptin and Pontin function antagonistically with PcG and TrxG complexes to mediate Hox gene control. *EMBO Rep.* **9**, 260–266.

Dobin, A., Davis, C. A., Schlesinger, F., Drenkow, J., Zaleski, C., Jha, S., Batut, P., Chaisson, M. and Gingeras, T. R. (2013). STAR: Ultrafast universal RNA-seq aligner. *Bioinformatics* **29**, 15–21.

Doe, C. Q., Chu-LaGraff, Q., Wright, D. M. and Scott, M. P. (1991). The prospero gene specifies cell fates in the Drosophila central nervous system. *Cell* **65**, 451–464.

Downs, J. A., Allard, S., Jobin-Robitaille, O., Javaheri, A., Auger, A., Bouchard, N., Kron, S. J., Jackson, S. P. and Côté, J. (2004). Binding of chromatin-modifying activities to phosphorylated histone H2A at DNA damage sites. *Mol. Cell* **16**, 979–990.

Dubois, N. C., Adolphe, C., Ehninger, A., Wang, R. A., Robertson, E. J. and Trumpp, A. (2008). Placental rescue reveals a sole requirement for c-Myc in embryonic erythroblast survival and hematopoietic stem cell function. *Development* **135**, 2455–2465.

Duronio, R. J., O'Farrell, P. H., Xie, J.-E., Brook, A. and Dyson, N. (1995). The transcription factor E2F is required for S phase during Drosophila embryogenesis. *Genes Dev.* **9**, 1445–1455.

Egger-Adam, D. (2005). Identifikation neuer Interaktionspartner des Bazooka Proteins in Drosophila melanogaster. (Doctoral Thesis).

Eissenberg, J. C., Wong, M. and Chrivia, J. C. (2005). Human SRCAP and Drosophila melanogaster DOM Are Homologs That Function in the Notch Signaling Pathway. *Mol. Cell. Biol.* **25**, 6559–6569.

Ellis, K., Friedman, C. and Yedvobnick, B. (2015). Drosophila domino Exhibits Genetic Interactions with a Wide Spectrum of Chromatin Protein-Encoding Loci. *PLoS One* **10**, e0142635.

Escudero, L. M., Caminero, E., Schulze, K. L., Bellen, H. J. and Modolell, J. (2005). Charlatan, a Zn-finger transcription factor, establishes a novel level of regulation of the proneural achaete/scute genes of Drosophila. *Development* **132**, 1211–1222.

Estella, C. and Baonza, A. (2015). Cell proliferation control by Notch signalling during imaginal discs development in Drosophila. *AIMS Genet.* **2**, 70–96.

Fang, L., Wang, Y., Du, D., Yang, G., Tak Kwok, T., Kai Kong, S., Chen, B., Chen, D. J. and Chen, Z. (2007). Cell polarity protein Par3 complexes with DNA-PK via Ku70 and regulates DNA double-strand break repair. *Cell Res.* **17**, 100–116.

Fazzio, T. G., Huff, J. T. and Panning, B. (2008a). Chromatin regulation Tip(60)s the balance in embryonic stem cell self-renewal. *Cell cycle* **7**, 3302–3306.

Fazzio, T. G., Huff, J. T. and Panning, B. (2008b). An RNAi Screen of Chromatin Proteins Identifies Tip60-p400 as a Regulator of Embryonic Stem Cell Identity. *Cell* **134**, 162–174.

Fernández-Hernández, I., Rhiner, C. and Moreno, E. (2013). Adult neurogenesis in Drosophila. *Cell Rep.* **3**, 1857–1865.

Frank, S. R., Parisi, T., Taubert, S., Fernandez, P., Fuchs, M., Chan, H.-M., Livingston, D. M. and Amati, B. (2003). MYC recruits the TIP60 histone acetyltransferase complex to chromatin. *EMBO Rep.* **4**, 575–580.

Fu, Y., Sinha, M., Peterson, C. L. and Weng, Z. (2008). The insulator binding protein CTCF positions 20 nucleosomes around its binding sites across the human genome. *PLoS Genet.* **4**, e1000138.

Fuchs, M., Gerber, J., Drapkin, R., Sif, S., Ikura, T., Ogryzko, V., Lane, W. S., Nakatani, Y. and Livingston, D. M. (2001). The p400 complex is an essential E1A transformation target. *Cell* **106**, 297–307.

Fuerstenberg, S., Peng, C., Alvarez-Ortiz, P., Hor, T. and Doe, C. Q. (1998). Identification of Miranda Protein Domains Regulating Asymmetric Cortical Localization, Cargo Binding, and Cortical Release. *Mol Cell Neurosci* **12**, 325–339.

Fujii, T., Ueda, T., Nagata, S. and Fukunaga, R. (2010). Essential role of p400/mDomino chromatin-remodeling ATPase in bone marrow hematopoiesis and cell-cycle progression. *J. Biol. Chem.* **285**, 30214–30223.

Gandarillas, A. and Watt, F. M. (1997). c-Myc promotes differentiation of human epidermal stem cells. *Genes Dev.* **11**, 2869–2882.

Gartel, A. L., Ye, X., Goufman, E., Shianov, P., Hay, N., Najmabadi, F. and Tyner, A. L. (2001). Myc represses the p21(WAF1/CIP1) promoter and interacts interacts with Sp1 Sp3. *PNAS* **98**, 4510–4515.

Gause, M., Eissenberg, J. C., Macrae, A. F., Dorsett, M., Misulovin, Z. and Dorsett, D. (2006). Nipped-A, the Tra1/TRRAP Subunit of the Drosophila SAGA and Tip60 Complexes, Has Multiple Roles in Notch Signaling during Wing Development. *Mol. Cell. Biol.* **26**, 2347–2359.

Gentleman, R., Carey, V., Bates, D., Bolstad, B., Dettling, M., Dudoit, S., Ellis, B., Gautier, L., Ge, Y., Gentry, J., et al. (2004). Bioconductor: open software development for computational biology and bioinformatics. *Genome Biol.* **5**, R80.

Gévry, N., Ho, M. C., Laflamme, L., Livingston, D. M. and Gaudreau, L. (2007). p21 transcription is regulated by differential localization of histone H2A.Z. *Genes Dev.* **21**, 1869–1881.

Gheghiani, L. and Gavet, O. (2016). E2F Transcription Factors Control the Roller Coaster Ride of Cell Cycle Gene Expression. In *Cell Cycle Oscillators: Methods and Protocols*, pp. 157–171.

Ghosh, A. K., Grigorieva, I., Steele, R., Hoover, R. G. and Ray, R. B. (1999). PTEN transcriptionally modulates c-myc gene expression in human breast carcinoma cells and is involved in cell growth regulation. *Gene* **235**, 85–91.

Golic, K. G. and Lindquist, S. (1989). The FLP recombinase of yeast catalyzes site-specific recombination in the drosophila genome. *Cell* **59**, 499–509.

Görisch, S. M., Wachsmuth, M., Tóth, K. F., Lichter, P. and Rippe, K. (2005). Histone acetylation increases chromatin accessibility. *J. Cell Sci.* **118**, 5825–5834.

Goulas, S., Conder, R. and Knoblich, J. A. (2012). The Par complex and integrins direct asymmetric cell division in adult intestinal stem cells. *Cell Stem Cell* **11**, 529–540.

Grawe, F., Wodarz, A., Lee, B., Knust, E. and Skaer, H. (1996). The Drosophila genes crumbs and stardust are involved in the biogenesis of adherens junctions. *Development* **122**, 951–959.

Grigoletto, A., Lestienne, P. and Rosenbaum, J. (2011). The multifaceted proteins Reptin and Pontin as major players in cancer. *Biochim. Biophys. Acta - Rev. Cancer* **1815**, 147–157.

Groszer, M., Groszer, M., Erickson, R., Zack, J. a, Kornblum, H. I. and Liu, X. (2008). Negative Regulation of Neural Stem / Progenitor Cell Proliferation by the Pten Tumor Suppressor Gene in Vivo. *Science* **294**, 2186–2190.

Guo, Z. and Ohlstein, B. (2015). Bidirectional Notch signaling regulates Drosophila intestinal stem cell multipotency. *Science* **350**, aab0988.

Halbsgut, N., Linnemannstöns, K., Zimmermann, L. I. and Wodarz, A. (2011). Apical-basal polarity in Drosophila neuroblasts is independent of vesicular trafficking. *Mol. Biol. Cell* **22**, 4373–4379.

Hall, L. E., Alexander, S. J., Chang, M., Woodling, N. S. and Yedvobnick, B. (2004). An EP overexpression screen for genetic modifiers of Notch pathway function in Drosophila melanogaster. *Genet. Res.* **83**, 71–82.

Hampoelz, B., Azou-Gros, Y., Fabre, R., Markova, O., Puech, P.-H. and Lecuit, T. (2011). Microtubule-induced nuclear envelope fluctuations control chromatin dynamics in Drosophila embryos. *Development* **138**, 3377–3386.

Harris, T. J. C. (2012). Adherens junction assembly and function in the Drosophila embryo. In *International Review of Cell and Molecular Biology*, pp. 45–83.

Harris, T. J. C. and Peifer, M. (2004). Adherens junction-dependent and -independent steps in the establishment of epithelial cell polarity in Drosophila. *J. Cell Biol.* **167**, 135–147.

Harris, T. J. C. and Peifer, M. (2005). The positioning and segregation of apical cues during epithelial polarity establishment in Drosophila. *J. Cell Biol.* **170**, 813–823.

Hartenstein, V. and Wodarz, A. (2013). Initial neurogenesis in Drosophila. *Wiley Interdiscip. Rev. Dev. Biol.* **2**, 701–721.

Hay, B. A., Wolff, T. and Rubin, G. M. (1994). Expression of baculovirus P35 prevents cell death in Drosophila. *Development* **120**, 2121–2129.

Homem, C. C. F., Reichardt, I., Berger, C., Lendl, T. and Knoblich, J. A. (2013). Long-term live cell imaging and automated 4D analysis of Drosophila neuroblast lineages. *PLoS One* **8**, e79588.

Homem, C. C. F., Steinmann, V., Burkard, T. R., Jais, A., Esterbauer, H. and Knoblich, J. A. (2014). Ecdysone and Mediator Change Energy Metabolism to Terminate Proliferation in Drosophila Neural Stem Cells. *Cell* **158**, 874–888.

Hong, H., Takahashi, K., Ichisaka, T., Aoi, T., Kanagawa, O., Nakagawa, M., Okita, K. and Yamanaka, S. (2009). Suppression of induced pluripotent stem cell generation by the p53-p21 pathway. *Nature* **460**, 1132–1135.

Hurov, J. B., Watkins, J. L. and Piwnica-Worms, H. (2004). Atypical PKC Phosphorylates PAR-1 Kinases to Regulate Localization and Activity. *Curr. Biol.* **14**, 736–741.

Ikeshima-Kataoka, H., Skeath, J. B., Nabeshima, Y., Doe, C. Q. and Matsuzaki, F. (1997). Miranda directs Prospero to a daughter cell during Drosophila asymmetric divisions. *Nature* **390**, 625–629.

Ikura, T., Ogryzko, V. V, Grigoriev, M., Groisman, R., Wang, J., Horikoshi, M., Scully, R., Qin, J. and Nakatani, Y. (2000). Involvement of the TIP60 histone acetylase complex in DNA repair and apoptosis. *Cell* **102**, 463–473.

Ito, K. and Hotta, Y. (1992). Proliferation pattern of postembryonic neuroblasts in the brain of Drosophila melanogaster. *Dev. Biol.* **149**, 134–148.

Izumi, H. and Kaneko, Y. (2012). Evidence of asymmetric cell division and centrosome inheritance in human neuroblastoma cells. *Proc. Natl. Acad. Sci.* **109**, 18048–18053.

Izumi, Y., Ohta, N., Hisata, K., Raabe, T. and Matsuzaki, F. (2006). Drosophila Pins-binding protein Mud regulates spindle-polarity coupling and centrosome organization. *Nat. Cell Biol.* **8**, 586–593.

Januschke, J. and Gonzalez, C. (2010). The interphase microtubule aster is a determinant of asymmetric division orientation in Drosophila neuroblasts. *J. Cell Biol.* **188**, 693–706.

Januschke, J., Llamazares, S., Reina, J. and Gonzalez, C. (2011). Drosophila neuroblasts retain the daughter centrosome. *Nat. Commun.* **2**, doi: 10.1038.

Januschke, J., Reina, J., Llamazares, S., Bertran, T., Rossi, F., Roig, J. and Gonzalez, C. (2013). Centrobin controls mother-daughter centriole asymmetry in Drosophila neuroblasts. *Nat. Cell Biol.* **15**, 241–248.

Jha, S. and Dutta, A. (2009). RVB1/RVB2: Running Rings around Molecular Biology. *Mol. Cell* **34**, 521–533.

Jiang, H. and Edgar, B. A. (2011). Intestinal stem cells in the adult Drosophila midgut. *Exp. Cell Res.* **317**, 2780–2788.

Jin, C. and Felsenfeld, G. (2007). Nucleosome stability mediated by histone variants H3.3 and H2A.Z. *Genes Dev.* **21**, 1519–1529.

Jin, J., Cai, Y., Yao, T., Gottschalk, A. J., Florens, L., Swanson, S. K., Gutiérrez, J. L., Coleman, M. K., Workman, J. L., Mushegian, A., et al. (2005). A mammalian chromatin remodeling complex with similarities to the yeast INO80 complex. *J. Biol. Chem.* **280**, 41207–41212.

Jin, Z., Kirilly, D., Weng, C., Kawase, E., Song, X., Smith, S., Schwartz, J. and Xie, T. (2008). Differentiation-Defective Stem Cells Outcompete Normal Stem Cells for Niche Occupancy in the Drosophila Ovary. *Cell Stem Cell* **2**, 39–49.

Johnston, H., Kneer, J., Chackalaparampil, I., Yaciuk, P. and Chrivia, J. (1999a). Identification of a Novel SNF2/SWI2 Protein Family Member, SRCAP, Which Interacts with CREB-binding Protein. *J. Biol. Chem.* **274**, 16370–16376.

Johnston, L. A., Prober, D. A., Edgar, B. A., Eisenman, R. N. and Gallant, P. (1999b). Drosophila myc Regulates Cellular Growth during Development. *Cell* **98**, 779–790.

Judes, G., Rifaï, K., Ngollo, M., Daures, M., Bignon, Y.-J., Penault-Llorca, F. and Bernard-Gallon, D. (2015). A bivalent role of TIP60 histone acetyl transferase in human cancer. *Epigenomics* **7**, 1351–1363.

Kaltschmidt, J. A., Davidson, C. M., Brown, N. H. and Brand, A. H. (2000). Rotation and asymmetry of the mitotic spindle direct asymmetric cell division in the developing central nervous system. *Nat. Cell Biol.* **2**, 7–12.

Kashyap, V., Rezende, N. C., Scotland, K. B., Shaffer, S. M., Persson, J. L., Gudas, L. J. and Mongan, N. P. (2009). Regulation of stem cell pluripotency and differentiation involves a mutual regulatory circuit of the NANOG, OCT4, and SOX2 pluripotency transcription factors with polycomb repressive complexes and stem cell microRNAs. *Stem Cells Dev.* **18**, 1093–1108.

Kaur, M. and Cole, M. D. (2013). MYC acts via the PTEN tumor suppressor to elicit autoregulation and genome-wide gene repression by activation of the Ezh2 methyltransferase. *Cancer Res.* **73**, 695–705.

Kawamura, T., Suzuki, J., Wang, Y. V, Menendez, S., Morera, L. B., Raya, A., Wahl, G. M. and Izpisúa Belmonte, J. C. (2009). Linking the p53 tumour suppressor pathway to somatic cell reprogramming. *Nature* **460**, 1140–1144.

Kehrer, M., Beckmann, A., Wyduba, J., Finckh, U., Dufke, A., Gaiser, U. and Tzschach, A. (2014). Floating-Harbor syndrome: SRCAP mutations are not restricted to exon 34. *Clin. Genet.* **85**, 498–499.

Keogh, M., Mennella, T. A., Sawa, C., Berthelet, S., Krogan, N. J., Wolek, A., Podolny, V., Carpenter, L. R., Greenblatt, J. F., Baetz, K., et al. (2006). The Saccharomyces cerevisiae histone H2A variant Htz1 is acetylated by NuA4 The Saccharomyces cerevisiae histone H2A variant Htz1 is acetylated by NuA4. *Genes Dev.* **20**, 660–665.

Kim, M.-Y., Ann, E.-J., Kim, J.-Y., Mo, J.-S., Park, J.-H., Kim, S.-Y., Seo, M.-S. and Park, H.-S. (2007). Tip60 histone acetyltransferase acts as a negative regulator of Notch1 signaling by means of acetylation. *Mol. Cell. Biol.* **27**, 6506–6519.

Knoblich, J. A. (2010). Asymmetric cell division: recent developments and their implications for tumour biology. *Nat. Rev. Mol. Cell Biol.* **11**, 849–860.

Knoepfler, P. S. (2008). Why Myc? An Unexpected Ingredient in the Stem Cell Cocktail. *Cell Stem Cell* **2**, 18–21.

Knoepfler, P. S., Cheng, P. F. and Eisenman, R. N. (2002). N- myc is essential during neurogenesis for the rapid expansion of progenitor cell populations and the inhibition of neuronal differentiation. *Genes Dev.* **16**, 2699–2712.

Kobor, M. S., Venkatasubrahmanyam, S., Meneghini, M. D., Gin, J. W., Jennings, J. L., Link, A. J., Madhani, H. D. and Rine, J. (2004). A protein complex containing the conserved Swi2/Snf2-related ATPase Swr1p deposits histone variant H2A.Z into euchromatin. *PLoS Biol.* **2**, E131.

Koh, C. M., Bezzi, M., Low, D. H. P., Ang, W. X., Teo, S. X., Gay, F. P. H., Al-Haddawi, M., Tan, S. Y., Osato, M., Sabò, A., et al. (2015). MYC regulates the core pre-mRNA splicing machinery as an essential step in lymphomagenesis. *Nature* **523**, 96–100.

Krahn, M. P., Egger-Adam, D. and Wodarz, A. (2009). PP2A antagonizes phosphorylation of Bazooka by PAR-1 to control apical-basal polarity in dividing embryonic neuroblasts. *Dev. Cell* **16**, 901–908.

Krahn, M. P., Bückers, J., Kastrup, L. and Wodarz, A. (2010). Formation of a Bazooka–Stardust complex is essential for plasma membrane polarity in epithelia. *J. Cell Biol.* **190**, 751–760.

Kramps, C., Strieder, V., Sapetschnig, A., Suske, G. and Lutz, W. (2004). E2F and Sp1/Sp3 Synergize but Are Not Sufficient to Activate the MYCN Gene in Neuroblastomas. *J. Biol. Chem.* **279**, 5110–5117.

Kraut, R., Chia, W., Jan, L. Y., Jan, Y. N. and Knoblich, J. A. (1996). Role of inscuteable in orienting asymmetric cell divisions in Drosophila. *Nature* **383**, 50–55.

Kress, T. R., Sabò, A. and Amati, B. (2015). MYC: connecting selective transcriptional control to global RNA production. *Nat. Rev. Cancer* **15**, 593–607.

Krogan, N. J., Keogh, M. C., Datta, N., Sawa, C., Ryan, O. W., Ding, H., Haw, R. A., Pootoolal, J., Tong, A., Canadien, V., et al. (2003). A Snf2 Family ATPase Complex Required for Recruitment of the Histone H2A Variant Htz1. *Mol. Cell* **12**, 1565–1576.

Kurooka, H. and Honjo, T. (2000). Functional interaction between the mouse Notch1 intracellular region and histone acetyltransferases PCAF and GCN5. *J. Biol. Chem.* **275**, 17211–17220.

Kusch, T., Florens, L., Macdonald, W. H., Swanson, S. K., Glaser, R. L., Yates, J. R., Abmayr, S. M., Washburn, M. P. and Workman, J. L. (2004). Acetylation by Tip60 Is Required for Selective Histone Variant Exchange at DNA Lesions. *Science* **306**, 2084–2087.

Kusch, T., Mei, A. and Nguyen, C. (2014). Histone H3 lysine 4 trimethylation regulates cotranscriptional H2A variant exchange by Tip60 complexes to maximize gene expression. *Proc. Natl. Acad. Sci. U. S. A.* **111**, 4850–4855.

Kwon, M. H., Callaway, H., Zhong, J. and Yedvobnick, B. (2013). A targeted genetic modifier screen links the SWI2/SNF2 protein domino to growth and autophagy genes in Drosophila melanogaster. *G3 (Bethesda).* **3**, 815–825.

Laemmli, U. K. (1970): (1970). Cleavage of Structural Proteins during Assembly of Head of Bacteriophage-T4. *Nature* **227**, 680–685.

Lai, S.-L. and Doe, C. Q. (2014). Transient nuclear Prospero induces neural progenitor quiescence. *Elife* **3**, doi: 10.7554.

Laurenti, E., Varnum-Finney, B., Wilson, A., Ferrero, I., Blanco-Bose, W. E., Ehninger, A., Knoepfler, P. S., Cheng, P. F., MacDonald, H. R., Eisenman, R. N., et al. (2008). Hematopoietic Stem Cell Function and Survival Depend on c-Myc and N-Myc Activity. *Cell Stem Cell* **3**, 611–624.

Lee, T. and Luo, L. (1999). Mosaic analysis with a repressible cell marker for studies of gene function in neuronal morphogenesis. *Neuron* **22**, 451–461.

Lee, T. and Luo, L. (2001). Mosaic analysis with a repressible cell marker (MARCM) for Drosophila neural development. *Trends Neurosci.* **24**, 251–254.

Lee, C.-Y., Robinson, K. J. and Doe, C. Q. (2006a). Lgl, Pins and aPKC regulate neuroblast self-renewal versus differentiation. *Nature* **439**, 594–598.

Lee, C.-Y., Wilkinson, B. D., Siegrist, S. E., Wharton, R. P. and Doe, C. Q. (2006b). Brat is a Miranda cargo protein that promotes neuronal differentiation and inhibits neuroblast self-renewal. *Dev. Cell* **10**, 441–449.

Lee, K., Lau, Z. Z., Meredith, C. and Park, J. H. (2012). Decrease of p400 ATPase complex and loss of H2A.Z within the p21 promoter occur in senescent IMR-90 human fibroblasts. *Mech. Ageing Dev.* **133**, 686–694.

Legube, G., Linares, L. K., Lemercier, C., Scheffner, M., Khochbin, S. and Trouche, D. (2002). Tip60 is targeted to proteasome-mediated degradation by Mdm2 and accumulates after UV irradiation. *EMBO J.* **21**, 1704–1712.

Legube, G., Linares, L. K., Tyteca, S., Caron, C., Scheffner, M., Chevillard-Briet, M. and Trouche, D. (2004). Role of the histone acetyl transferase Tip60 in the p53 pathway. *J. Biol. Chem.* **279**, 44825–44833.

Lessard, J. a and Crabtree, G. R. (2010). Chromatin regulatory mechanisms in pluripotency. *Annu. Rev. Cell Dev. Biol.* **26**, 503–532.

Li, H. (2011a). Improving SNP discovery by base alignment quality. *Bioinformatics* **27**, 1157–1158.

Li, H. (2011b). A statistical framework for SNP calling, mutation discovery, association mapping and population genetical parameter estimation from sequencing data. *Bioinformatics* **27**, 2987–2993.

Li, H. and Jasper, H. (2016). Gastrointestinal stem cells in health and disease: from flies to humans. *Dis. Model. Mech.* **9**, 487–499.

Li, H., Handsaker, B., Wysoker, A., Fennell, T., Ruan, J., Homer, N., Marth, G., Abecasis, G. and Durbin, R. (2009a). The Sequence Alignment/Map format and SAMtools. *Bioinformatics* **25**, 2078–2079.

Li, H., Collado, M., Villasante, A., Strati, K., Ortega, S., Cañamero, M., Blasco, M. a and Serrano, M. (2009b). The Ink4/Arf locus is a barrier for iPS cell reprogramming. *Nature* **460**, 1136–1139.

Li, S., Wang, H. and Groth, C. (2014). Drosophila neuroblasts as a new model for the study of stem cell self-renewal and tumor formation. *Biosci. Rep.* **34**, 401–414.

Lin, P.-Y., Fosmire, S. P., Park, S.-H., Park, J.-Y., Baksh, S., Modiano, J. F. and Weiss, R. H. (2007). Attenuation of PTEN increases p21 stability and cytosolic localization in kidney cancer cells: a potential mechanism of apoptosis resistance. *Mol. Cancer* **6**, 16.

Lin, C.-H., Jackson, A. L., Guo, J., Linsley, P. S. and Eisenman, R. N. (2009). Myc-regulated microRNAs attenuate embryonic stem cell differentiation. *EMBO J.* **28**, 3157–3170.

Llanos, S., Efeyan, A., Monsech, J., Dominguez, O. and Serrano, M. (2006). A high-throughput loss-of-function screening identifies novel p53 regulators. *Cell Cycle* **5**, 1880–1885.

Lorbeck, M., Pirooznia, K., Sarthi, J., Zhu, X. and Elefant, F. (2011). Microarray analysis uncovers a role for Tip60 in nervous system function and general metabolism. *PLoS One* **6**, e18412.

Lu, B., Rothenberg, M., Jan, L. Y. and Jan, Y. N. (1998). Partner of Numb colocalizes with numb during mitosis and directs numb asymmetric localization in Drosophila neural and muscle progenitors. *Cell* **95**, 225–235.

Lu, J., Ruhf, M.-L., Perrimon, N. and Leder, P. (2007). A genome-wide RNA interference screen identifies putative chromatin regulators essential for E2F repression. *PNAS* **104**, 9381–9386.

Lu, W., Fang, L., Ouyang, B., Zhang, X., Zhan, S., Feng, X., Bai, Y., Han, X., Kim, H., He, Q., et al. (2015). Actl6a protects embryonic stem cells from differentiating into primitive endoderm. *Stem Cells* **33**, 1782–1793.

Lye, C. M. and Sanson, B. (2011). Tension and Epithelial Morphogenesis in Drosophila Early Embryos. In *Current Topics in Developmental Biology*, pp. 145–187.

Manfruelli, P., Arquier, N., Hanratty, W. P. and Sémériva, M. (1996). The tumor suppressor gene, lethal(2)giant larvae (l(2)gl), is required for cell shape change of epithelial cells during Drosophila development. *Development* **122**, 2283–2294.

Marión, R. M., Strati, K., Li, H., Murga, M., Blanco, R., Ortega, S., Fernandez-Capetillo, O., Serrano, M. and Blasco, M. A. (2009). A p53-mediated DNA damage response limits reprogramming to ensure iPS cell genomic integrity. *Nature* **460**, 1149–1153.

Mathur, D., Bost, A., Driver, I. and Ohlstein, B. (2010). A Transient Niche Regulates the Specification of Drosophila Intestinal Stem Cells. *Science* **327**, 210–213.

Matsuzaki, F., Koizumi, K., Hama, C., Yoskioka, T. and Nabeshima, Y. (1992). Cloning of the Drosophila Prospero Gene and its Expression in Ganglion Mother Cells. *Biochem. Biophys. Res. Commun.* **182**, 1326–1332.

Mattera, L., Escaffit, F., Pillaire, M.-J., Selves, J., Tyteca, S., Hoffmann, J.-S., Gourraud, P.-A., Chevillard-Briet, M., Cazaux, C. and Trouche, D. (2009). The p400/Tip60 ratio is critical for colorectal cancer cell proliferation through DNA damage response pathways. *Oncogene* **28**, 1506–1517.

Mattera, L., Courilleau, C., Legube, G., Ueda, T., Fukunaga, R., Chevillard-Briet, M., Canitrot, Y., Escaffit, F. and Trouche, D. (2010). The E1A-associated p400 protein modulates cell fate decisions by the regulation of ROS homeostasis. *PLoS Genet.* **6**, e1000983.

Maurange, C. (2012). Temporal Specification of Neural Stem Cells. Insights from Drosophila Neuroblasts. *Curr. Top. Dev. Biol.* **98**, 199–228.

Maurange, C., Cheng, L. and Gould, A. P. (2008). Temporal transcription factors and their targets schedule the end of neural proliferation in Drosophila. *Cell* **133**, 891–902.

Mavrich, T. N., Jiang, C., Ioshikhes, I. P., Li, X., Venters, B. J., Zanton, S. J., Tomsho, L. P., Qi, J., Glaser, R. L., Schuster, S. C., et al. (2008). Nucleosome organization in the Drosophila genome. *Nature* **453**, 358–362.

Maya, R., Balass, M., Kim, S.-T., Shkedy, D., Leal, J.-F. M., SHifman, O., Moas, M., Buschmann, T., Ronai, Z., Shiloh, Y., et al. (2001). ATM-dependent phosphorylation of Mdm2 on serine 394: role in p53 activation by DNA damage. *Genes Dev.* **15**, 1067–1077.

Mazumdar, A. and Mazumdar, M. (2002). How one becomes many: Blastoderm cellularization in Drosophila melanogaster. *BioEssays* **24**, 1012–1022.

McGill, M. A., McKinley, R. F. A. and Harris, T. J. C. (2009). Independent cadherin-catenin and Bazooka clusters interact to assemble adherens junctions. *J. Cell Biol.* **185**, 787–796.

McMahon, S. B., Van Buskirk, H. A., Dugan, K. A., Copeland, T. D. and Cole, M. D. (1998). The novel ATM-related protein TRRAP is an essential cofactor for the c- Myc and E2F oncoproteins. *Cell* **94**, 363–374.

Medrano, S., Burns-Cusato, M., Atienza, M. B., Rahimi, D. and Scrable, H. (2009). Regenerative capacity of neural precursors in the adult mammalian brain is under the control of p53. *Neurobiol. Aging* **30**, 483–497.

Meletis, K., Wirta, V., Hede, S. M., Nister, M., Lundeberg, J. and Frisen, J. (2006). P53 Suppresses the Self-Renewal of Adult Neural Stem Cells. *Development* **133**, 363–369.

Meneghini, M. D., Wu, M. and Madhani, H. D. (2003). Conserved histone variant H2A.Z protects euchromatin from the ectopic spread of silent heterochromatin. *Cell* **112**, 725–736.

Meshorer, E. (2007). Chromatin in embryonic stem cell neuronal differentiation. *Histol. Histopathol.* **22**, 311–319.

Micchelli, C. A., Sudmeier, L., Perrimon, N., Tang, S. and Beehler-Evans, R. (2011). Identification of adult midgut precursors in Drosophila. *Gene Expr. Patterns* **11**, 12–21.

Mitchell, L., Lambert, J.-P., Gerdes, M., Al-Madhoun, A. S., Skerjanc, I. S., Figeys, D. and Baetz, K. (2008). Functional dissection of the NuA4 histone acetyltransferase reveals its role as a genetic hub and that Eaf1 is essential for complex integrity. *Mol. Cell. Biol.* **28**, 2244–2256.

Mizuguchi, G., Shen, X., Landry, J., Wu, W.-H., Sen, S. and Wu, C. (2004). ATP-Driven Exchange of Histone H2AZ Variant Catalyzed by SWR1 Chromatin Remodeling Complex. *Science* **303**, 343–348.

Morais-de-Sá, E., Mirouse, V. and St Johnston, D. (2010). aPKC phosphorylation of Bazooka defines the apical/lateral border in Drosophila epithelial cells. *Cell* **141**, 509–523.

Moreno, E., Basler, K. and Zu, C.- (2004). dMyc Transforms Cells into Super-Competitors. *Cell* **117**, 117–129.

Morillo Prado, J. R., Srinivasan, S. and Fuller, M. T. (2013). The histone variant His2Av is required for adult stem cell maintenance in the Drosophila testis. *PLoS Genet.* **9**, e1003903.

Moumen, M., Chiche, A., Deugnier, M.-A., Petit, V., Gandarillas, A., Glukhova, M. A. and Faraldo, M. M. (2012). The Proto-Oncogene Myc Is Essential for Mammary Stem Cell Function. *Stem Cells* **30**, 1246–1254.

Müller, H. A. J. and Wieschaus, E. (1996). armadillo, bazooka, and stardust are critical for early stages in formation of the zonula adherens and maintenance of the polarized blastoderm epithelium in Drosophila. *J. Cell Biol.* **134**, 149–163.

Muñoz-Espín, D. and Serrano, M. (2014). Cellular senescence: from physiology to pathology. *Nat. Rev. Mol. Cell Biol.* **15**, 482–496.

Murphy, M. J., Wilson, A. and Trumpp, A. (2005). More than just proliferation: Myc function in stem cells. *Trends Cell Biol.* **15**, 128–137.

Nagao, M., Campbell, K., Burns, K., Kuan, C.-Y., Trumpp, A. and Nakafuku, M. (2008). Coordinated control of self-renewal and differentiation of neural stem cells by Myc and the p19ARF-p53 pathway. *J. Cell Biol.* **183**, 1243–1257.

Nagasaki, K., Asami, T., Sato, H., Ogawa, Y., Kikuchi, T., Saitoh, A., Ogata, T. and Fukami, M. (2014). Long-term follow-up study for a patient with Floating-Harbor syndrome due to a hotspot SRCAP mutation. *Am. J. Med. Genet. A* **164A**, 731–735.

Nair, S. S. and Kumar, R. (2012). Chromatin remodeling in Cancer: A Gateway to regulate gene Transcription. *Mol. Oncol.* **6**, 611–619.

Nekrasov, M., Amrichova, J., Parker, B. J., Soboleva, T. A., Jack, C., Williams, R., Huttley, G. A. and Tremethick, D. J. (2012). Histone H2A.Z inheritance during the cell cycle and its impact on promoter organization and dynamics. *Nat Struct Mol Biol* **19**, 1076–1083.

Neumüller, R. A., Richter, C., Fischer, A., Novatchkova, M., Neumüller, K. G. and Knoblich, J. A. (2011). Genome-wide analysis of self-renewal in Drosophila neural stem cells by transgenic RNAi. *Cell Stem Cell* **8**, 580–593.

Nguyen, H. N. (2016). The Function of Chromatin Remodeler domino in Drosophila Intestinal Stem Cells. (M.Sc. Thesis).

Ohlstein, B. and Spradling, A. (2007). Multipotent Drosophila intestinal stem cells specify daughter cell fates by differential notch signaling. *Science* **315**, 988–992.

Ohshiro, T., Yagami, T., Zhang, C. and Matsuzaki, F. (2000). Role of cortical tumour-suppressor proteins in asymmetric division of Drosophila neuroblast. *Nature* **408**, 593–596.

Orkin, S. H. and Hochedlinger, K. (2011). Chromatin connections to pluripotency and cellular reprogramming. *Cell* **145**, 835–850.

Ouyang, Y., Song, Y. and Lu, B. (2011). dp53 Restrains ectopic neural stem cell formation in the Drosophila brain in a non-apoptotic mechanism involving Archipelago and cyclin E. *PLoS One* **6**, e28098.

Pampalona, J., Januschke, J., Sampaio, P. and Gonzalez, C. (2015). Time-lapse recording of centrosomes and other organelles in Drosophila neuroblasts. In *Methods in Cell Biology*, pp. 301–315.

Park, J. H. and Roeder, R. G. (2006). GAS41 is required for repression of the p53 tumor suppressor pathway during normal cellular proliferation. *Mol. Cell. Biol.* **26**, 4006–4016.

Park, J., Wood, M. A. and Cole, M. D. (2002). BAF53 forms distinct nuclear complexes and functions as a critical c-Myc-interacting nuclear cofactor for oncogenic transformation. *Mol. Cell. Biol.* **22**, 1307–1316.

Park, J. H., Sun, X. J. and Roeder, R. G. (2010). The SANT Domain of p400 ATPase Represses Acetyltransferase Activity and Coactivator Function of TIP60 in Basal p21 Gene Expression. *Mol. Cell. Biol.* **30**, 2750–2761.

Park, J. H., Smith, R. J., Shieh, S. Y. and Roeder, R. G. (2011). The GAS41-PP2Cbeta complex dephosphorylates p53 at serine 366 and regulates its stability. *J. Biol. Chem.* **286**, 10911–10917.

Parmentier, M. L. (2000). Rapsynoid/Partner of Inscuteable controls asymmetric division of larval neuroblasts in Drosophila. *J. Neurosci.* **20**, RC84.

Patel, J. H., Du, Y., Ard, P. G., Phillips, C., Carella, B., Chen, C.-J., Rakowski, C., Chatterjee, C., Lieberman, P. M., Lane, W. S., et al. (2004). The c-MYC oncoprotein is a substrate of the acetyltransferases hGCN5/PCAF and TIP60. *Mol. Cell. Biol.* **24**, 10826–10834.

Peng, C. Y., Manning, L., Albertson, R. and Doe, C. Q. (2000). The tumour-suppressor genes lgl and dlg regulate basal protein targeting in Drosophila neuroblasts. *Nature* **408**, 596–600.

Petronczki, M. and Knoblich, J. A. (2001). DmPAR-6 directs epithelial polarity and asymmetric cell division of neuroblasts in Drosophila. *Nat. Cell Biol.* **3**, 43–49.

Phesse, T. J., Myant, K. B., Cole, A. M., Ridgway, R. A., Pearson, H., Muncan, V., van den Brink, G. R., Vousden, K. H., Sears, R., Vassilev, L. T., et al. (2014). Endogenous c-Myc is essential for p53-induced apoptosis in response to DNA damage in vivo. *Cell Death Differ.* **21**, 956–966.

Pierce, S. B., Yost, C., Britton, J. S., Loo, L. W. M., Flynn, E. M., Edgar, B. A. and Eisenman, R. N. (2004). dMyc is required for larval growth and endoreplication in Drosophila. *Development* **131**, 2317–2327.

Pilot, F., Philippe, J., Lemmers, C., Chauvin, J. and Lecuit, T. (2005). Developmental control of nuclear morphogenesis and anchoring by charleston , identified in a functional genomic screen of Drosophila cellularisation. *Development* **133**, 711–723.

Pirooznia, S. K., Sarthi, J., Johnson, A. A., Toth, M. S., Chiu, K., Koduri, S. and Elefant, F. (2012). Tip60 HAT activity mediates APP induced lethality and apoptotic cell death in the CNS of a Drosophila Alzheimer's disease model. *PLoS One* **7**, e41776.

Podhorecka, M., Skladanowski, A. and Bozko, P. (2010). H2AX Phosphorylation: Its Role in DNA Damage Response and Cancer Therapy. *J. Nucleic Acids* **2010**, doi: 10.4061.

Polychronidou, M. and Großhans, J. (2011). Determining nuclear shape: the role of farnesylated nuclear membrane proteins. *Nucleus* **2**, 17–23.

Polychronidou, M., Hellwig, A. and Großhans, J. (2010). Farnesylated Nuclear Proteins Kugelkern and Lamin Dm0 Affect Nuclear Morphology by Directly Interacting with the Nuclear Membrane. *Mol. Biol. Cell* **21**, 3409–3420.

Pradhan, S. K., Su, T., Yen, L., Jacquet, K., Huang, C., Côté, J., Kurdistani, S. K. and Carey, M. F. (2016). EP400 Deposits H3.3 into Promoters and Enhancers during Gene Activation. *Mol. Cell* **61**, 27–38.

Pressman, S., Reinke, C. A., Wang, X. and Carthew, R. W. (2012). A Systematic Genetic Screen to Dissect the MicroRNA Pathway in Drosophila. *G3 (Bethesda).* **2**, 437–448.

Qi, D., Jin, H., Lilja, T. and Mannervik, M. (2006). Drosophila reptin and other TIP60 complex components promote generation of silent chromatin. *Genetics* **174**, 241–251.

Quinn, L. M., Secombe, J. and Hime, G. R. (2013). Myc in Stem Cell Behaviour: Insights from Drosophila. In *Transcriptional and Translational Regulation of Stem Cells*, pp. 269–285.

Radke, J., Bortolussi, G. and Pagenstecher, A. (2013). Akt and c-Myc Induce Stem-Cell Markers in Mature Primary p53-/- Astrocytes and Render These Cells Gliomagenic in the Brain of Immunocompetent Mice. *PLoS One* **8**, e56691.

Ravens, S., Yu, C., Ye, T., Stierle, M. and Tora, L. (2015). Tip60 complex binds to active Pol II promoters and a subset of enhancers and co-regulates the c-Myc network in mouse embryonic stem cells. *Epigenetics Chromatin* **8**, 45.

Rebollo, E., Sampaio, P., Januschke, J., Llamazares, S., Varmark, H. and Gonzalez, C. (2007). Functionally Unequal Centrosomes Drive Spindle Orientation in Asymmetrically Dividing Drosophila Neural Stem Cells. *Dev. Cell* **12**, 467–474.

Rebollo, E., Roldán, M. and Gonzalez, C. (2009). Spindle alignment is achieved without rotation after the first cell cycle in Drosophila embryonic neuroblasts. *Development* **136**, 3393–3397.

Ren, F., Shi, Q., Chen, Y., Jiang, A., Ip, Y. T., Jiang, H. and Jiang, J. (2013). Drosophila Myc integrates multiple signaling pathways to regulate intestinal stem cell proliferation during midgut regeneration. *Cell Res.* **23**, 1133–1146.

Reynolds, E. S. (1963). The use of lead citrate at high pH as an electron-opaque stain in electron microscopy. *J. Cell Biol.* **17**, 208–212.

Riley, T., Sontag, E., Chen, P. and Levine, A. (2008). Transcriptional control of human p53-regulated genes. *Nat. Rev. Mol. Cell Biol.* **9**, 402–412.

Robinson, J. T., Thorvaldsdóttir, H., Winckler, W., Guttman, M., Lander, E. S., Getz, G. and Mesirov, J. P. (2011). Integrative genomics viewer. *Nat. Biotechnol.* **29**, 24–26.

Rolls, M. M., Albertson, R., Shih, H.-P., Lee, C.-Y. and Doe, C. Q. (2003). Drosophila aPKC regulates cell polarity and cell proliferation in neuroblasts and epithelia. *J. Cell Biol.* **163**, 1089–1098.

Rong, Y. S. (2008). Loss of the histone variant H2A.Z restores capping to checkpoint-defective telomeres in Drosophila. *Genetics* **180**, 1869–1875.

Rountree, M. R., Bachman, K. E. and Baylin, S. B. (2000). DNMT1 binds HDAC2 and a new co-repressor, DMAP1, to form a complex at replication foci. *Nat. Genet.* **25**, 269–277.

Ruhf, M. L., Braun, A., Papoulas, O., Tamkun, J. W., Randsholt, N. and Meister, M. (2001). The domino gene of Drosophila encodes novel members of the SWI2/SNF2 family of DNA-dependent ATPases, which contribute to the silencing of homeotic genes. *Development* **128**, 1429–1441.

Rusan, N. M. and Peifer, M. (2007). A role for a novel centrosome cycle in asymmetric cell division. *J. Cell Biol.* **177**, 13–20.

Rust, K. (2013). Analysis of domino , a Potential Bazooka Binding Partner in Drosophila Neuroblasts. (M.Sc. Thesis).

Saiki, R., Scharf, S., Faloona, F., Mullis, K., Horn, G., Erlich, H. and Arnheim, N. (1985). Enzymatic amplification of beta-globin genomic sequences and restriction site analysis for diagnosis of sickle cell anemia. *Science* **230**, 1350–1354.

Saini, N. and Reichert, H. (2012). Neural stem cells in Drosophila: molecular genetic mechanisms underlying normal neural proliferation and abnormal brain tumor formation. *Stem Cells Int.* **2012**, 486169.

Saksouk, N., Avvakumov, N., Champagne, K. S., Hung, T., Doyon, Y., Cayrou, C., Paquet, E., Ullah, M., Landry, A. J., Côte, V., et al. (2009). HBO1 HAT Complexes Target Chromatin throughout Gene Coding Regions via Multiple PHD Finger Interactions with Histone H3 Tail. *Mol. Cell* **33**, 257–265.

Sapountzi, V., Logan, I. R. and Robson, C. N. (2006). Cellular functions of TIP60. *Int. J. Biochem. Cell Biol.* **38**, 1496–1509.

Sato, T., Russell, M. A. and Denell, R. E. (1983). Homoeosis in Drosophila: a new enhancer of polycomb and related homoeotic mutations. *Genetics* **105**, 357–370.

Satoh, Y., Matsumura, I., Tanaka, H., Ezoe, S., Sugahara, H., Mizuki, M., Shibayama, H., Ishiko, E., Ishiko, J., Nakajima, K., et al. (2004). Roles for c-Myc in self-renewal of hematopoietic stem cells. *J. Biol. Chem.* **279**, 24986–24993.

Schaefer, M., Shevchenko, A. and Knoblich, J. A. (2000). A protein complex containing Inscuteable and the Galpha-binding protein Pins orients asymmetric cell divisions in Drosophila. *Curr. Biol.* **10**, 353–362.

Schindelin, J., Arganda-Carreras, I., Frise, E., Kaynig, V., Longair, M., Pietzsch, T., Preibisch, S., Rueden, C., Saalfeld, S., Schmid, B., et al. (2012). Fiji: an open-source platform for biological-image analysis. *Nat. Methods* **9**, 676–682.

Schirling, C., Heseding, C., Heise, F., Kesper, D., Klebes, A., Klein-Hitpass, L., Vortkamp, A., Hoffmann, D., Saumweber, H. and Ehrenhofer-Murray, A. E. (2010). Widespread regulation of gene expression in the Drosophila genome by the histone acetyltransferase dTip60. *Chromosoma* **119**, 99–113.

Schober, M., Schaefer, M. and Knoblich, J. A. (1999). Bazooka recruits Inscuteable to orient asymmetric cell divisions in Drosophila neuroblasts. *Nature* **402**, 548–551.

Schwartz, D. C. and Cantor, C. R. (1984). Separation of yeast chromosome-sized DNAs by pulsed field gradient gel electrophoresis. *Cell* **37**, 67–75.

Seifert, A., Werheid, D. F., Knapp, S. M., Tobiasch, E., Seifert, A., Werheid, D. F. and Knapp, S. M. (2015). Role of Hox genes in stem cell differentiation. *World J. Stem Cells* **7**, 583–595.

Seoane, J., Le, H.-V. and Massague, J. (2002). Myc suppression of the p21 Cip1 Cdk inhibitor influences the outcome of the p53 response to DNA damage. *Nature* **419**, 729–734.

Shackleton, M. (2010). Normal stem cells and cancer stem cells: Similar and different. *Semin. Cancer Biol.* **20**, 85–92.

Siddall, N. A., Lin, J. I., Hime, G. R. and Quinn, L. M. (2009). Myc-What we have learned from flies. *Curr Drug Targets* **10**, 590–601.

Siegrist, S. E. and Doe, C. Q. (2005). Microtubule-induced pins/Galphai cortical polarity in Drosophila neuroblasts. *Cell* **123**, 1323–1335.

Siegrist, S. E., Haque, N. S., Chen, C. H., Hay, B. A. and Hariharan, I. K. (2010). Inactivation of Both foxo and reaper Promotes Long-Term Adult Neurogenesis in Drosophila. *Curr. Biol.* **20**, 643–648.

Siller, K. H., Cabernard, C. and Doe, C. Q. (2006). The NuMA-related Mud protein binds Pins and regulates spindle orientation in Drosophila neuroblasts. *Nat. Cell Biol.* **8**, 594–600.

Sinclair, D. A. R., Clegg, N. J., Antonchuk, J., Milne, T. A., Stankunas, K., Ruse, C., Grigliatti, T. A., Kassis, J. A. and Brock, H. W. (1998). Enhancer of Polycomb is a suppressor of position-effect variegation in Drosophila melanogaster. *Genetics* **148**, 211–220.

Skeath, J. B. and Doe, C. Q. (1998). Sanpodo and Notch act in opposition to Numb to distinguish sibling neuron fates in the Drosophila CNS. *Development* **125**, 1857–1865.

Słomnicki, Ł. P. and Leśniak, W. (2008). A putative role of the Amyloid Precursor Protein Intracellular Domain (AICD) in transcription. *Acta Neurobiol. Exp. (Wars).* **68**, 219–228.

Solà, S., Xavier, J. M., Santos, D. M., Aranha, M. M., Morgado, A. L., Jepsen, K. and Rodrigues, C. M. P. (2011). p53 interaction with JMJD3 results in its nuclear distribution during mouse neural stem cell differentiation. *PLoS One* **6**, e18421.

Song, Y. and Lu, B. (2011). Regulation of cell growth by Notch signaling and its differential requirement in normal vs. tumor-forming stem cells in Drosophila. *Genes Dev.* **25**, 2644–2658.

Sousa-Nunes, R., Yee, L. L. and Gould, A. P. (2011). Fat cells reactivate quiescent neuroblasts via TOR and glial insulin relays in Drosophila. *Nature* **471**, 508–512.

Spana, E. P. and Doe, C. Q. (1996). Numb antagonizes Notch signaling to specify sibling neuron cell fates. *Neuron* **17**, 21–26.

Squatrito, M., Gorrini, C. and Amati, B. (2006). Tip60 in DNA damage response and growth control : many tricks in one HAT. *Trends Cell Biol.* **16**, 433–442.

Su, W. H., Mruk, D. D., Wong, E. W. P., Lui, W. Y. and Cheng, C. Y. (2013). Polarity protein complex scribble/lgl/dlg and epithelial cell barriers. *Adv. Exp. Med. Biol.* **763**, 149–170.

Sun, Y., Jiang, X., Chen, S., Fernandes, N. and Price, B. D. (2005). A role for the Tip60 histone acetyltransferase in the acetylation and activation of ATM. *PNAS* **102**, 13182–13187.

Takahashi, K. and Yamanaka, S. (2006). Induction of Pluripotent Stem Cells from Mouse Embryonic and Adult Fibroblast Cultures by Defined Factors. *Cell* **126**, 663–676.

Takashima, S., Adams, K. L., Ortiz, P. A., Ying, C. T., Moridzadeh, R., Younossi-Hartenstein, A. and Hartenstein, V. (2011). Development of the Drosophila entero-endocrine lineage and its specification by the Notch signaling pathway. *Dev. Biol.* **353**, 161–172.

Tang, Y., Luo, J., Zhang, W. and Gu, W. (2006). Tip60-Dependent Acetylation of p53 Modulates the Decision between Cell-Cycle Arrest and Apoptosis. *Mol. Cell* **24**, 827–839.

Taty-Taty, G. C., Chailleux, C., Quaranta, M., So, A., Guirouilh-Barbat, J., Lopez, B. S., Bertrand, P., Trouche, D. and Canitrot, Y. (2015). Control of alternative end joining by the chromatin remodeler p400 ATPase. *Nucleic Acids Res.* **44**, 1657–1668.

Taubert, S., Gorrini, C., Frank, S. R., Parisi, T., Fuchs, M., Chan, H.-M., Livingston, D. M. and Amati, B. (2004). E2F-dependent histone acetylation and recruitment of the Tip60 acetyltransferase complex to chromatin in late G1. *Mol. Cell. Biol.* **24**, 4546–4556.

Tea, J. S. and Luo, L. (2011). The chromatin remodeling factor Bap55 functions through the TIP60 complex to regulate olfactory projection neuron dendrite targeting. *Neural Dev.* **6**, 5.

Tepass, U. (1996). Crumbs, a component of the apical membrane, is required for zonula adherens formation in primary epithelia of Drosophila. *Dev. Biol.* **177**, 217–225.

Tepass, U. (2012). The apical polarity protein network in Drosophila epithelial cells: regulation of polarity, junctions, morphogenesis, cell growth, and survival. *Annu. Rev. Cell Dev. Biol.* **28**, 655–685.

Tepass, U., Gruszynski-DeFeo, E., Haag, T. A., Omatyar, L., Török, T. and Hartenstein, V. (1996). shotgun encodes Drosophila E-cadherin and is preferentially required during cell rearrangement in the neurectoderm and other morphogenetically active epithelia. *Genes Dev.* **10**, 672–685.

Tepass, U., Tanentzapf, G., Ward, R. and Fehon, R. (2001). Epithelial Cell Polarity and Cell Junctions in Drosophila. *Annu. Rev. Cell Dev. Biol.* **16**, 423–457.

Thorvaldsdóttir, H., Robinson, J. T. and Mesirov, J. P. (2012). Integrative Genomics Viewer (IGV): High-performance genomics data visualization and exploration. *Brief. Bioinform.* **14**, 178–192.

Tsuda, L., Kaido, M., Lim, Y.-M., Kato, K., Aigaki, T. and Hayashi, S. (2006). An NRSF/REST-like repressor downstream of Ebi/SMRTER/Su(H) regulates eye development in Drosophila. *EMBO J.* **25**, 3191–3202.

Tsuji, T., Hasegawa, E. and Isshiki, T. (2008). Neuroblast entry into quiescence is regulated intrinsically by the combined action of spatial Hox proteins and temporal identity factors. *Development* **135**, 3859–3869.

Tyteca, S., Vandromme, M., Legube, G., Chevillard-Briet, M. and Trouche, D. (2006). Tip60 and p400 are both required for UV-induced apoptosis but play antagonistic roles in cell cycle progression. *EMBO J.* **25**, 1680–1689.

Ueda, T., Watanabe-fukunaga, R., Ogawa, H., Fukuyama, H., Higashi, Y., Nagata, S. and Fukunaga, R. (2007). Critical role of the p400/mDomino chromatin-remodeling ATPase in embryonic hematopoiesis. *Genes to Cells* **12**, 581–592.

Ullah, M., Pelletier, N., Xiao, L., Zhao, S. P., Wang, K., Degerny, C., Tahmasebi, S., Cayrou, C., Doyon, Y., Goh, S.-L., et al. (2008). Molecular architecture of quartet MOZ/MORF histone acetyltransferase complexes. *Mol. Cell. Biol.* **28**, 6828–6843.

Vaessin, H., Grell, E., Wolff, E., Bier, E., Jan, L. Y. and Jan, Y. N. (1991). prospero is expressed in neuronal precursors and encodes a nuclear protein that is involved in the control of axonal outgrowth in Drosophila. *Cell* **67**, 941–953.

van Attikum, H. and Gasser, S. M. (2005). The histone code at DNA breaks: a guide to repair? *Nat. Rev. Mol. Cell Biol.* **6**, 757–765.

Van Den Broeck, A., Nissou, D., Brambilla, E., Eymin, B. and Gazzeri, S. (2012). Activation of a Tip60/E2F1/ERCC1 network in human lung adenocarcinoma cells exposed to cisplatin. *Carcinogenesis* **33**, 320–325.

Varlakhanova, N. V., Cotterman, R. F., deVries, W. N., Morgan, J., Donahue, L. R., Murray, S., Knowles, B. B. and Knoepfler, P. S. (2010). Myc maintains embryonic stem cell pluripotency and self-renewal. *Differentiation* **80**, 9–19.

Vastenhouw, N. L. and Schier, A. F. (2012). Bivalent histone modifications in early embryogenesis. *Curr. Opin. Cell Biol.* **24**, 374–386.

von Stein, W., Ramrath, A., Grimm, A., Müller-Borg, M. and Wodarz, A. (2005). Direct association of Bazooka/PAR-3 with the lipid phosphatase PTEN reveals a link between the PAR/aPKC complex and phosphoinositide signaling. *Development* **132**, 1675–1686.

von Trotha, J. W., Egger, B. and Brand, A. H. (2009). Cell proliferation in the Drosophila adult brain revealed by clonal analysis and bromodeoxyuridine labelling. *Neural Dev.* **4**, 9.

Vousden, K. H. and Ryan, K. M. (2009). P53 and Metabolism. *Nat. Rev. Cancer* **9**, 691–700.

Waikel, R. L., Kawachi, Y., Waikel, P. a, Wang, X. J. and Roop, D. R. (2001). Deregulated expression of c-Myc depletes epidermal stem cells. *Nat. Genet.* **28**, 165–168.

Walther, R. F. and Pichaud, F. (2010). Crumbs/DaPKC-dependent apical exclusion of Bazooka promotes photoreceptor polarity remodeling. *Curr. Biol.* **20**, 1065–1074.

Wang, S. L., Hawkins, C. J., Yoo, S. J., Müller, H. A. J. and Hay, B. A. (1999). The Drosophila caspase inhibitor DIAP1 is essential for cell survival and is negatively regulated by HID. *Cell* **98**, 453–463.

Wang, H., Ouyang, Y., Somers, W. G., Chia, W. and Lu, B. (2007). Polo inhibits progenitor self-renewal and regulates Numb asymmetry by phosphorylating Pon. *Nature* **449**, 96–100.

Wang, Z., Zang, C., Rosenfeld, J. A., Schones, D. E., Barski, A., Cuddapah, S., Cui, K., Roh, T.-Y., Peng, W., Zhang, M. Q., et al. (2008). Combinatorial patterns of histone acetylations and methylations in the human genome. *Nat. Genet.* **40**, 897–903.

Weng, M., Golden, K. L. and Lee, C.-Y. (2010). dFezf/Earmuff maintains the restricted developmental potential of intermediate neural progenitors in Drosophila. *Dev. Cell* **18**, 126–135.

White, K., Grether, M. E., Abrams, J. M., Young, L., Farrell, K. and Steller, H. (1994). Genetic Control of Programmed Cell Death in Drosophila. *Science* **264**, 677–683.

Wilson, A., Murphy, M. J., Oskarsson, T., Kaloulis, K., Bettess, M. D., Oser, G. M., Pasche, A.-C., Knabenhans, C., MacDonald, H. R. and Trumpp, A. (2004). c-Myc controls the balance between hematopoietic stem cell self-renewal and differentiation. *Genes Dev.* **18**, 2747–2763.

Wirtz-Peitz, F., Nishimura, T. and Knoblich, J. A. (2008). Linking Cell Cycle to Asymmetric Division: Aurora-A Phosphorylates the Par Complex to Regulate Numb Localization. *Cell* **135**, 161–173.

Wodarz, A. and Näthke, I. (2007). Cell polarity in development and cancer. *Nat. Cell Biol.* **9**, 1016–1024.

Wodarz, A., Ramrath, A., Kuchinke, U. and Knust, E. (1999). Bazooka provides an apical cue for Inscuteable localization in Drosophila neuroblasts. *Nature* **402**, 544–547.

Wodarz, A., Ramrath, A., Grimm, A. and Knust, E. (2000). Drosophila atypical protein kinase C associates with Bazooka and controls polarity of epithelia and neuroblasts. *J. Cell Biol.* **150**, 1361–1374.

Wood, M. a, McMahon, S. B. and Cole, M. D. (2000). An ATPase/helicase complex is an essential cofactor for oncogenic transformation by c-Myc. *Mol. Cell* **5**, 321–330.

Xi, R. and Xie, T. (2005). Stem cell self-renewal controlled by chromatin remodeling factors. *Science* **310**, 1487–1489.

Xu, T. and Rubin, G. M. (1993). Analysis of genetic mosaics in developing and adult Drosophila tissues. *Development* **117**, 1223–1237.

Yamada, H. Y. (2012). Human Tip60 (NuA4) Complex and Cancer. In *Colorectal Cancer Biology - From Genes to Tumor*, pp. 217–240.

Yan, D., Neumüller, R. A., Buckner, M., Ayers, K., Li, H., Hu, Y., Yang-Zhou, D., Pan, L., Wang, X., Kelley, C., et al. (2014). A regulatory network of Drosophila germline stem cell self-renewal. *Dev. Cell* **28**, 459–473.

Ye, Q., Callebaut, I., Pezhman, A., Courvalin, J. and Worman, H. J. (1997). Domain-specific Interactions of Human HP1-type Chromodomain Proteins and Inner Nuclear Membrane Protein LBR. *J. Biol. Chem.* **272**, 14983–14989.

Yoshiura, S., Ohta, N. and Matsuzaki, F. (2012). Tre1 GPCR signaling orients stem cell divisions in the Drosophila central nervous system. *Dev. Cell* **22**, 79–91.

Yu, F., Morin, X., Cai, Y., Yang, X. and Chia, W. (2000). Analysis of partner of inscuteable, a Novel Player of Drosophila Asymmetric Divisions, Reveals Two Distinct Steps in Inscuteable Apical Localization. *Cell* **100**, 399–409.

Yuasa, Y., Okabe, M., Yoshikawa, S., Tabuchi, K., Xiong, W.-C., Hiromi, Y. and Okano, H. (2003). Drosophila homeodomain protein REPO controls glial differentiation by cooperating with ETS and BTB transcription factors. *Development* **130**, 2419–2428.

Zhang, H., Richardson, D. O., Roberts, D. N., Utley, R., Erdjument-Bromage, H., Tempst, P., Côté, J. and Cairns, B. R. (2004). The Yaf9 component of the SWR1 and NuA4 complexes is required for proper gene expression, histone H4 acetylation, and Htz1 replacement near telomeres. *Mol. Cell. Biol.* **24**, 9424–9436.

Zhu, X., Singh, N., Donnelly, C., Boimel, P. and Elefant, F. (2007). The cloning and characterization of the histone acetyltransferase human homolog Dmel\TIP60 in Drosophila melanogaster: Dmel\TIP60 is essential for multicellular development. *Genetics* **175**, 1229–1240.

7. List of Figures

8. List of Tables

9. Abbreviations

Abbreviation	Meaning
::	Promoter
α	alpha
Act	Actin
Ada2	Adenosine deaminase 2
AF	Alexa Fluor
APS	Ammonium persulfate
Arp	Actin-related protein
Ash1	Absent, small, or homeotic discs 1
ATP	Adenosine triphosphate
β	beta
β-Gal	β-galactosidase
Bap55	Brahma associated protein 55 kDa
BAF53a	BRG1-associated factor 53A
Bdf1	Bromodomain-containing factor 1
bp	Base pair
Brd8	Bromodomain containing 8
BRG1	Brahma related gene 1
BSA	Bovine serum albumin
γ	gamma
°C	Degree Celsius
CD8	Cluster of differentiation 8
CDK	Cyclin-dependen kinase
CHD	Chromodomain-helicase-DNA binding
c-Myc	Cellular Myc
CREB	cAMP response element-binding protein
CTX	Citrate Triton X-100 medium
Cy	Cyanine
CyO	Curly of Oster
Da	Dalton
DAPI	4',6-diamidino-2-phenylindole
dcr	Dicer
ddH_2O	Double distilled water
DMAP1	DNA methyltransferase 1-associated protein 1
DNA	Deoxyribonucleic acid
dNTP	Deoxyribonucleotide triphosphate
DTT	Dithiothreitol
dUTP	Deoxyuridine triphosphate
E1A	Early region 1A
Eaf	Esa1-associated factor

Abbreviation	Meaning
EDTA	Ethylenediaminetetraacetic acid
EGTA	Ethylene glycol-bis(β-aminoethyl ether)-N,N,N',N'-tetraacetic acid
elav	embryonic lethal abnormal vision
Esa1	Essential Sas2-related acetyltransferase-1
et al.	*et alii* (and colleagues)
E(Pc)	Enhancer of Polycomb
Epl1	Enhancer of Polycomb-like protein 1
FasIII	Fasciclin III
FM	First multiple
Foxo	Forkhead box, sub-group O
g	Gram
Gαi	G protein α i subunit
Gal	Galactokinase synthesis
Gas41	Glioma-amplified sequence 41
Gcn5	General control of aminoacid biosynthesis 5
GFP	Green fluorescent protein
h	Hour
H	Histone
H3K4me3	H3 methylated on lysine 4
H4K8Ac	H4 acetylated on lysine 8
Hid	Head involution defective
Hox	Homeobox gene
HRP	Horseradish peroxidase
Htz1	Histone *Thermococcus zilligii* 1
Ing3	Inhibitor of growth-3
INO80	Inositol requiring mutant 80
ISWI	Imitation switch
k	kilo
KCM	KCl medium
L	liter
LB	Lysogeny broth
L-Myc	Lung cancer cell line Myc
µ	micro
m	milli
M	Molar (mol/L)
MDM2	Mouse double minute 2
Min	Minute
Miz-1	Myc-interacting zinc finger protein 1
MORF	Mortality factor
MRG15	MORF-related gene 15
MrgBP	MRG/MORF4L binding protein
mRNA	Messenger RNA
Myb	Myeoblastosis proto-oncogene
Myc	Myelocytomatosis proto-oncogene

Abbreviation	Meaning
n	nano
NcoR	Nuclear receptor co-repressor 1
NHS	Normal horse serum
N-Myc	Neuronal myc
ns	Not significant
NuA4	Nucleosome acetyltransferase of H4
p21	21 kDa, also CDK-inhibitor 1
P35	Early 35 kDa protein
p400	E1A-binding protein 400 kDa
p53	53 kDa protein
PAGE	Polyacrylamide gel electrophoresis
Par	Partitioning-defective
PBS	Phosphate buffered saline
PBSTw	Phosphate buffered saline with Tween-20
PBSTx	Phosphate buffered saline with Triton X-100
Repo	Reversed polarity
Rpr	Reaper
pH	*potentia Hydrogenii*
RNA	Ribonucleic acid
rpm	Rounds per minute
RT	Room temperature (21 °C)
s	Second
SANT	Swi3-Ada2-NcoR-TFIIIB
SDS	Sodium dodecyl sulfate
SET	Supressor of variegation 3-9, Enhancer of Zeste and Trithorax
Set1	SET domain containing 1
SM	Second multiple
Sp	Specificity protein
SRCAP	Snf2-related CREBBP activator protein
Swi/Snf	Switching defective/sucrose-non fermenting
Swr1	Swi2 ATPase domain-related-1
TBS	Tris-buffered saline
TBST	Tris-buffered saline with Tween-20
TEMED	Tetramethylethylenediamine
TFIIIB	Transcription factor IIIB
Tip	Tat-interactive protein
TM	Third multiple
TNT	Tris-NaCl-Triton
Tra1	Transcription-associated protein 1
Tris	Tris(hydroxymethyl)aminomethane
Trr	Trithorax-related
TRRAP	Transformation/transcription domain-associated protein
Trx	Trithorax
Twi	Twist

Abbreviation	Meaning
U	Units
UV	Ultraviolet
v/v	Volume per volume
V	Volt
Vps72	Vacuolar protein sorting 72
w/v	Weight per volume
WT	Wild type
YT	Yeast tryptone medium

10. Appendix

Table S 1: Additional fly lines used in this study

BL = Bloomington Drosophila Stock Center, V = Vienna Drosophila RNAi Center (VDRC).

Stock	Genotype	Description / Application	Source/Reference
Gal4 driver lines			
ase::Gal4	*ase::Gal4*	NB specific driver	Andrew Jarman
elav::Gal4	*elav::Gal4*	NB specific driver	BL8760
pros::Gal4	*pros::Gal4*	NB specific driver	Fumio Matsuzaki
sca::Gal4	*sca::Gal4*	NB specific driver	Christian Klämbt
wor::Gal4	*wor::Gal4*	NB specific driver	Chris Doe
wor::Gal4, UAS::CD8-GFP	*UAS-dcrII,wor::Gal4, UAS::CD8-GFP/ CyO;UAS::dcrII*	NB specific driver	Neumüller et al., 2011
Fly lines for the manipulation of Tip60 complex members			
UAS::Act87E-RNAi	*UAS::Act87E-RNAi*	Act87E-RNAi	V102480
UAS::Act87E-RNAi	*UAS::Act87E-RNAi/ TM6B*	Act87E-RNAi	BL42652
UAS::Bap55-RNAi	*UAS::Bap55-RNAi/ CyO(twi::GFP)*	Bap55-RNAis	V24703, V24704
UAS::Bap55-RNAi	*UAS::Bap55-RNAi/ TM6B*	Bap55-RNAi	BL31708
UAS::Brd8-RNAi	*UAS::Brd8-RNAi*	Brd8-RNAis	V41530, V41531, BL42658
UAS::Brd8-RNAi	*UAS::Brd8-RNAi/CyO(twi::GFP)*	Brd8-RNAi	V49989
UAS::Eaf6-RNAi	*UAS::Eaf6-RNAi*	Eaf6-RNAis	V31761, V42321, V101457, BL33904, BL33905, BL50518
UAS::E(Pc)-RNAi	*UAS::E(Pc)-RNAi*	E(Pc)-RNAi	v35268, BL28686
UAS::E(Pc)-RNAi	*UAS::E(Pc)-RNAi/ CyO(twi::GFP)*	E(Pc)-RNAi	V35271
UAS::E(Pc)-RNAi	*UAS::E(Pc)-RNAi/ TM6B*	E(Pc)-RNAi	BL35271
UAS:Gas41-RNAi	*UAS:Gas41-RNAi*	Gas41-RNAis	V12616, V106922
UAS::Ing3-RNAi	*UAS::Ing3-RNAi/ CyO(twi-GFP)*	Ing3-RNAi	V52510
UAS::Ing3-RNAi	*UAS::Ing3-RNAi*	Ing3-RNAi	V109799
UAS::MRG15-RNAi	*UAS::MRG15-RNAi/ TM6B*	MRG15-RNAis	V43800, BL35241
UAS::MRG15-RNAi	*UAS::MRG15-RNAi*	MRG15-RNAis	V43802, V110618,

Stock	Genotype	Description / Application	Source/Reference
UAS::MrgBP-RNAi	*UAS::MrgBP-RNAi*	MrgBP-RNAis	V41403
UAS::Nipped-A-RNAi	*UAS::Nipped-A-RNAi/ TM6B*	Nipped-A-RNAi	V40789, V44781
UAS::Nipped-A-RNAi	*UAS::Nipped-A-RNAi/ CyO(twi::GFP)*	Nipped-A-RNAi	V40790
UAS::Nipped-A-RNAi	*UAS::Nipped-A-RNAi*	Nipped-A-RNAis	V52486, BL31255, BL34849, BL35595
UAS::rept-RNAi	*UAS::rept-RNAi*	rept-RNAis	V103483
UAS::rept-RNAi	*UAS::rept-RNAi/TM6B*	rept-RNAi	BL32415
UAS::pont-RNAi	*UAS::pont-RNAi/ SM6-TM6B*	pont-RNAi	BL50972
UAS::Tip60^{E431Q}	*UAS::Tip60^{E431Q}*	Expresses HAT deficient Tip60	Lorbeck et al., 2011
UAS::Tip60-RNAi	*UAS::Tip60-RNAi*	Tip60-RNAi	V22231, V22233, V110617, BL28563, BL35243, Schirling et al., 2010
UAS::YL-1-RNAi	*UAS::YL-1-RNAi/TM6B*	YL-1-RNAi	V21903
UAS::YL-1-RNAi	*UAS::YL-1-RNAi/ CyO(twi::GFP)*	YL-1-RNAi	V107951
UAS::YL-1-RNAi	*UAS::YL-1-RNAi*	YL-1-RNAi	BL31938
Fly lines for the manipulation of potential Dom/Tip60 complex interactors			
UAS::ash1-RNAi	*UAS::ash1-RNAi/TM6B*	ash1-RNAis	V28982, BL33705
UAS::ash1-RNAi	*UAS::ash1-RNAi*	ash1-RNAis	V108832, BL31050, BL36130, BL36803
UAS::dap-RNAi	*UAS::dap-RNAi*	dap-RNAi	BL36720
UAS::E2F1	*UAS::E2F1,UAS-Dp/ TM6B*	Expresses E2F1 and the E2F1 interacting transcription factor Dp	BL4770
UAS::E2F1-RNAi	*UAS::E2F1-RNAi*	E2F1-RNAi	V15886, V15887, V108837, BL27564, BL31214, BL36126
UAS::E2F2-RNAi	*UAS::E2F2-RNAi*	E2F2-RNAi	V45743, V100990, BL27995, BL36674
UAS::HDAC6	*UAS::HDAC6*	HDAC6 overexpression	BL51181

Stock	Genotype	Description / Application	Source/Reference
UAS-HDAC6^{H237A}	*UAS-HDAC6^{H237A}/ CyO(twi::GFP)*	Expresses HDAC6 with amino acid exchange in one of the histone deacetylase domains	BL51183
UAS::HDAC6	*UAS::HDAC6^{H664A}/ CyO(twi::GFP)*	Expresses HDAC6 with amino acid exchange in one of the histone deacetylase domains	BL51184
UAS:: HDAC6^{H237A,H664A}	*UAS-HDAC6^{H237A,H664A}; MKRS/TM6B*	Expresses HDAC6 with amino acid exchange in both histone deacetylase domains	BL51185
UAS::HDAC6-RNAi	*UAS::HDAC6-RNAi*	HDAC6-RNAi	V108831, BL31053
UAS::HDAC6-RNAi	*UAS::HDAC6-RNAi/ SM6-TM6B*	HDAC6-RNAi	BL34072
UAS::mam	*UAS::mam*	Mam overexpression	BL27743
UAS::mam^{N}	*UAS::mam^{N}*	Expresses truncated Mam	BL26672
UAS::mam-RNAi	*UAS::mam-RNAi*	mam-RNAi	V48690, V102091
UAS::Set1-RNAi	*UAS::Set1-RNAi*	Set1-RNAi	V40682, V40683, BL33704, BL38368
UAS::Set1-RNAi	*UAS::Set1-RNAi/TM6B*	Set1-RNAis	V45267, V10833
UAS::Set1-RNAi	*UAS::Set1-RNAi/ CyO(twi::GFP)*	Set1-RNAi	BL40931
UAS::trr-RNAi	*UAS::trr-RNAi*	trr-RNAi	V10749, BL36916
UAS::trr-RNAi	*UAS::trr-RNAi/ CyO(twi::GFP)*	trr-RNAi	V110276
UAS::trx-RNAi	*UAS::trx-RNAi*	trx-RNAi	V37715, V108122, BL31092

Stock	Genotype	Description / Application	Source/Reference
Fly lines for manipulation of potential Dom interactors together with *dom*			
UAS::CBP^{2161A}; UAS::dom-RNAi	*UAS::CBP^{2161A}; UAS::dom-RNAi/TM6B*	Expression of HAT deficient CBP and *dom* knockdown	CBP: BL32579, dom: V7787
UAS::CBP-RNAi; UAS::dom-RNAi	*UAS::CBP-RNAi; UAS::dom-RNAi/TM6B*	Knockdown of *CBP* and *dom*	CBP: V46534, V102885, V105115, dom: V7787
Fly lines for marker expression			
UAS::CD8-GFP	*UAS::CD8-GFP*	For Gal4-driven expression of membrane tethered GFP	BL32184

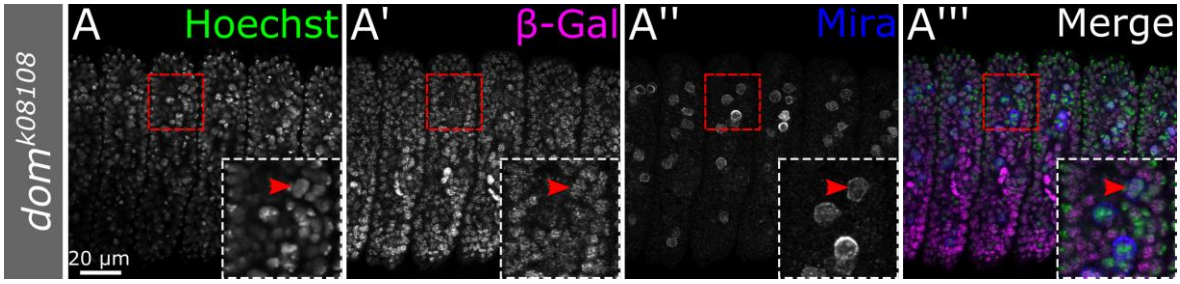

Figure S 1: domino is expressed in all cell types in the *Drosophila* embryo

Embryos of the β-Gal reporter line *dom*^{k08108} were immunostained to investigate dom expression. β-Gal is expressed in all cells including Mira positive NBs (arrowhead).

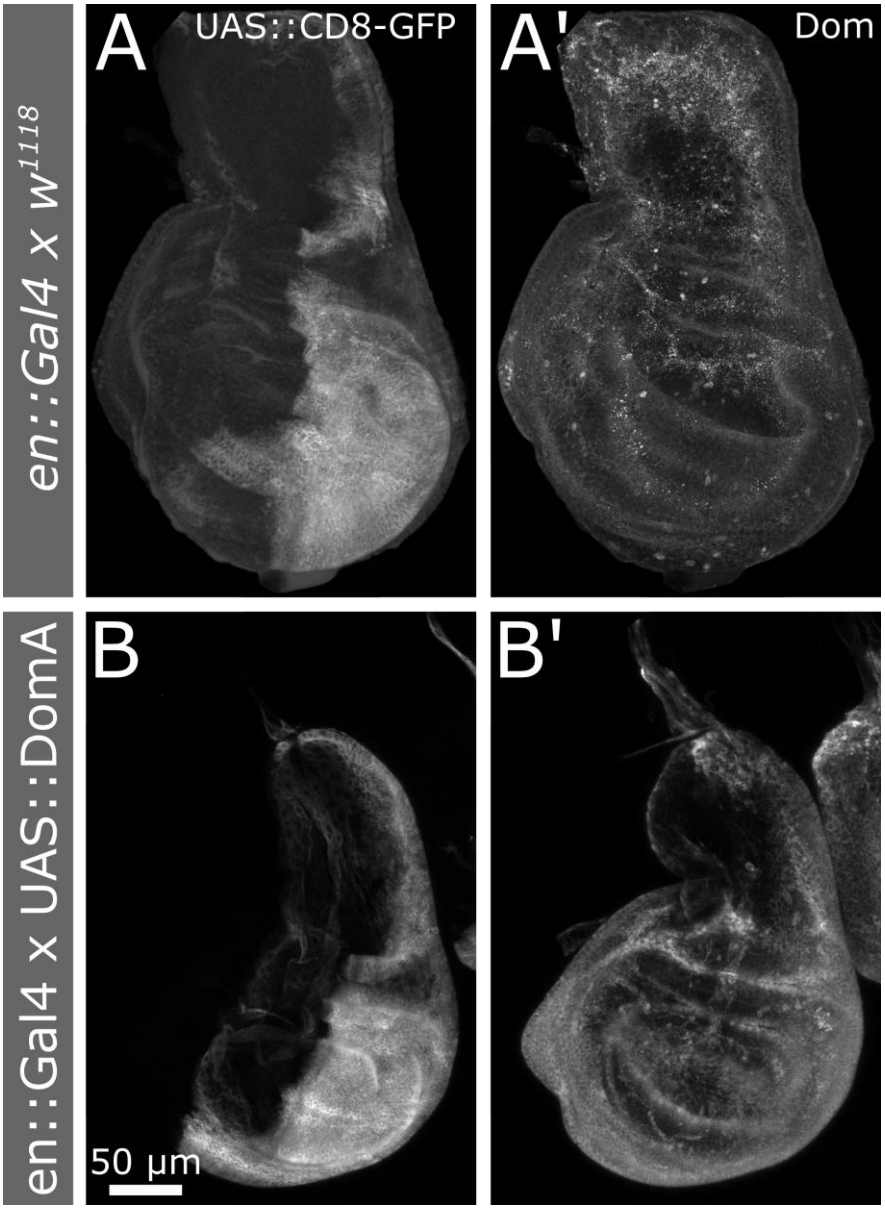

Figure S 2: DominoA overexpression was not detected in wing imaginal discs

The *en* driver was used to express CD8-GFP together with DomA in the posterior L3 wing disc compartment. Overexpression of DomA does not lead to enhanced Dom levels as determined by Dom antibody staining (B) in comparison to a wild type control (A).

Table S 2: Tip60 complex subunits in neuroblast and adult midgut precursor maintenance

Tip60 complex subunits have been knocked down in NBs and AMPs by the Gal4-UAS system with the *insc::Gal4* driver. Subunits functioning in NB and AMP maintenance are marked with "yes". It is indicated which subunits have been implicated in stem cell maintenance in *Drosophila* or mammals and which components are known to interact with Myc. x marks the subunits which have not been co-purified but which were not further investigated. E(Pc) was shown to not interact with Myc ("no").

Tip60 subunit	NB phenotype	AMP phenotype	Maintenance of stem cells	Co-purifies with Myc
dom	yes	yes	yes	yes
Tip60	yes	yes	yes	yes
Act87E	x	x	x	yes
Bap55	x	x	yes	yes
Brd8	yes	yes	x	x
DMAP1	yes	yes	yes	x
Eaf6	x	x	x	x
E(Pc)	x	yes	x	no
Gas41	x	yes	yes	x
Ing3	x	x	x	x
MrgBP	yes	yes	x	x
MRG15	x	x	yes	x
Nipped-A	yes	yes	yes	yes
Pontin	yes	yes	yes	yes
Reptin	yes	yes	yes	yes
YL-1	x	x	x	x

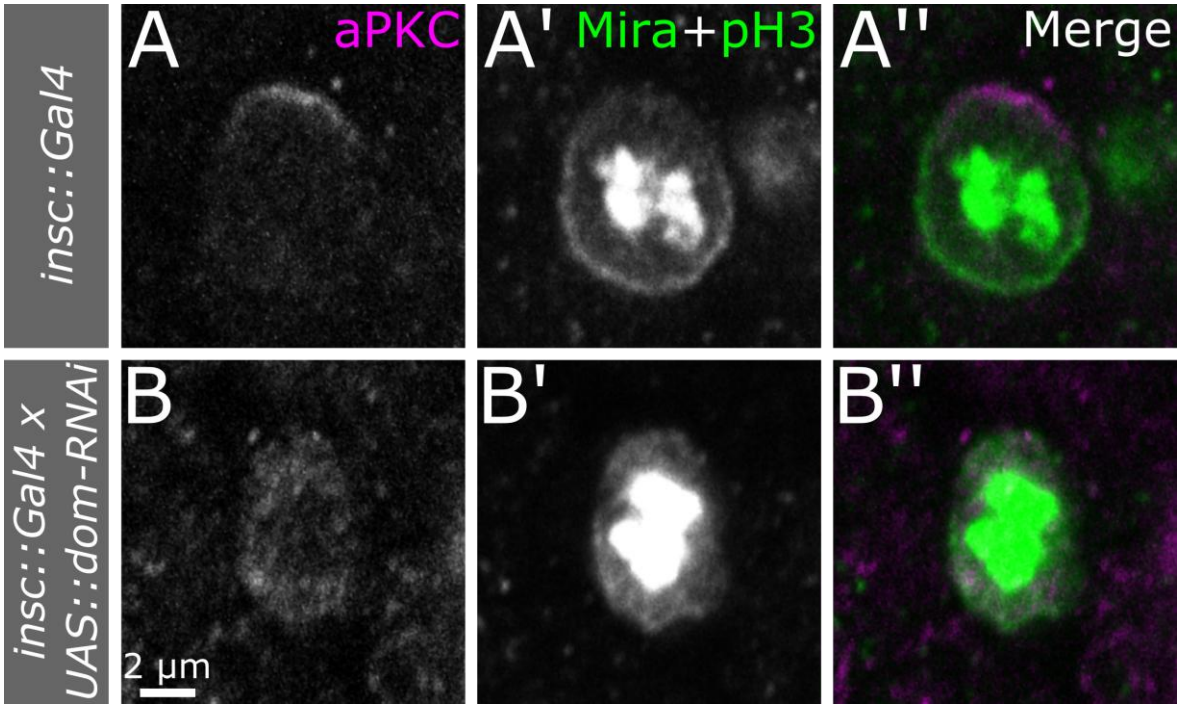

Figure S 3: aPKC and Miranda are mislocalized upon *domino* knockdown

Confocal images of immunostained L3 NBs undergoing mitosis as identified by nuclear pH3 staining. (A): Wild type NBs show apical aPKC staining and basal Mira localization. (B): *dom* depleted NBs show mislocalized aPKC and Mira.

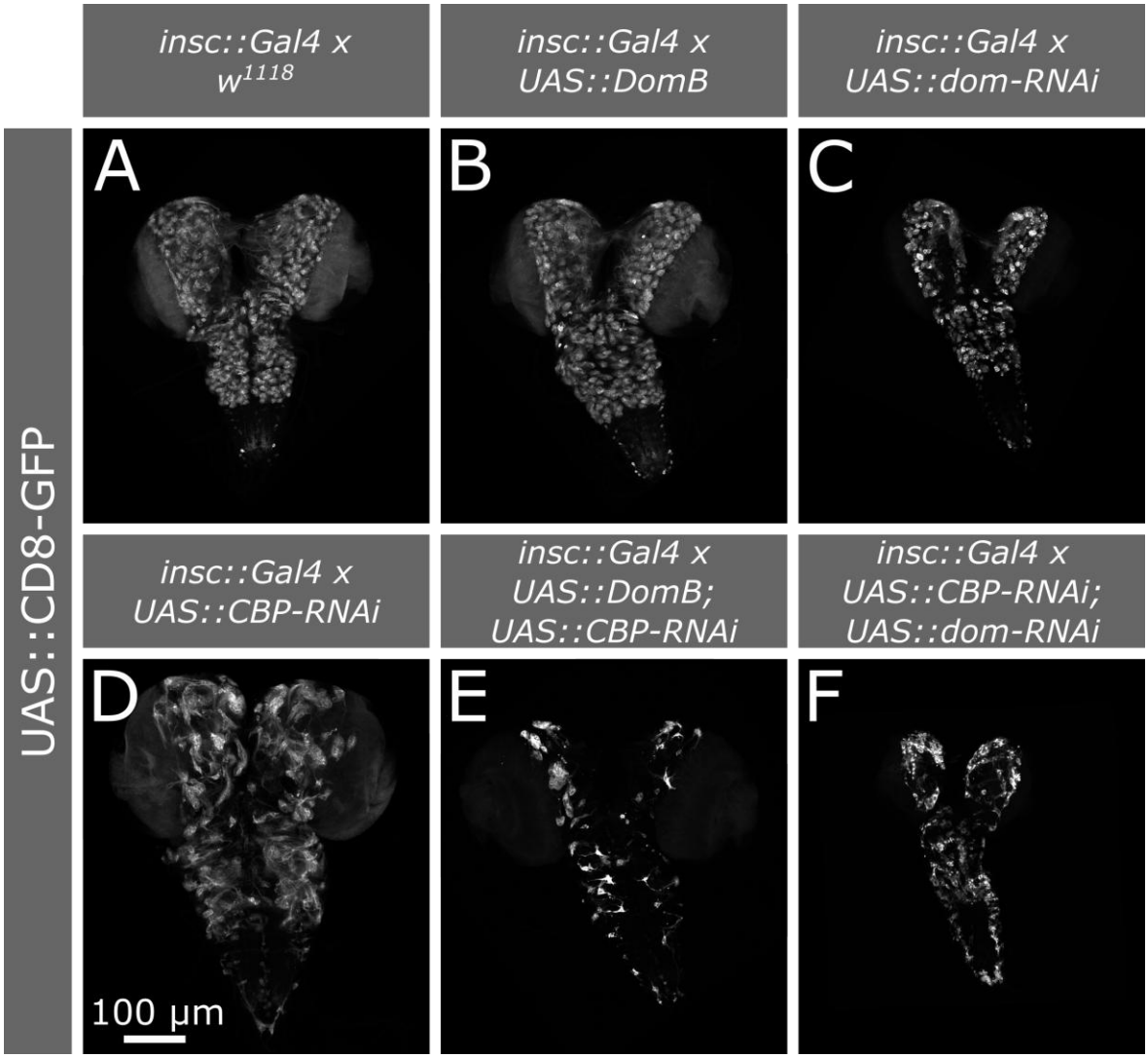

Figure S 4: Knockdown of *domino* and *CBP* impairs neural cell lineages

Maximum intensity projections of L3 brains expression with CD8-GFP marked neural cells. (A): Wild type brain. (B): DomB overexpression does not change neural cell numbers. (C): Knockdown of *dom* reduces neural cells. (D): Knockdown of *CBP* leads to neural misorganization. (E): Overexpression of DomB aggravates the *CBP* knockdown phenotype and further reduces cell numbers. (F): Co-knockdown of *CBP* and *dom* amplifies both single phenotypes or is lethal dependent on the strength of *CBP* knockdown by different RNAi-lines.

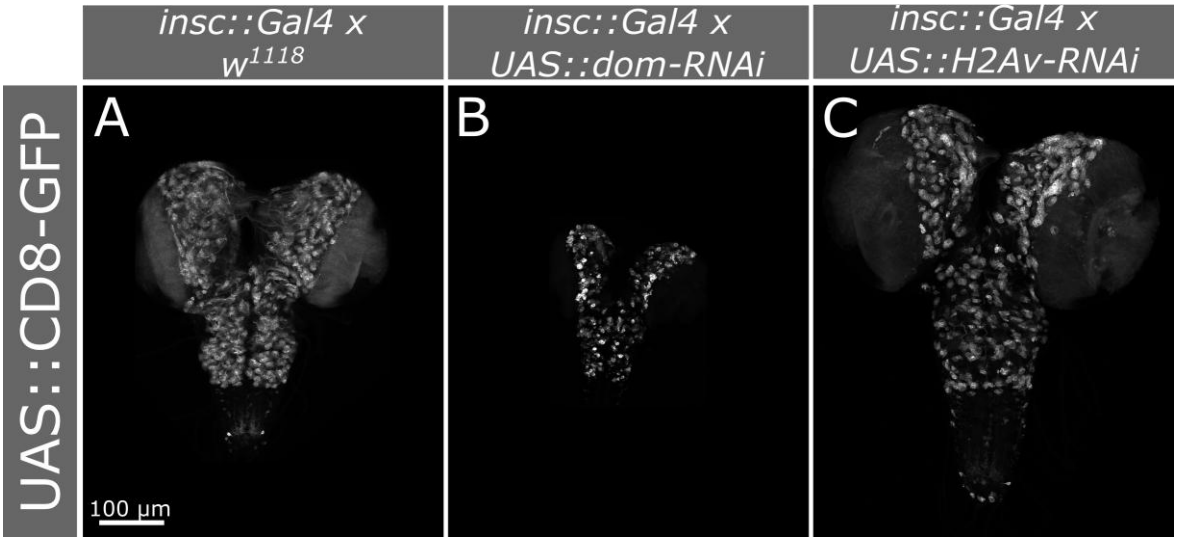

Figure S 5: H2Av is required to maintain larval neural cells

Maximum intensity projections of L3 brains. Neural cells are marked with CD8-GFP. The wild type brain (A) harbors more neural cells than upon knockdown of *dom* (V7787) (B) or *H2Av* (BL34844) (C). Note that the bigger brain size for H2Av-RNAi was inconsistent and is most likely due to slightly older larvae.

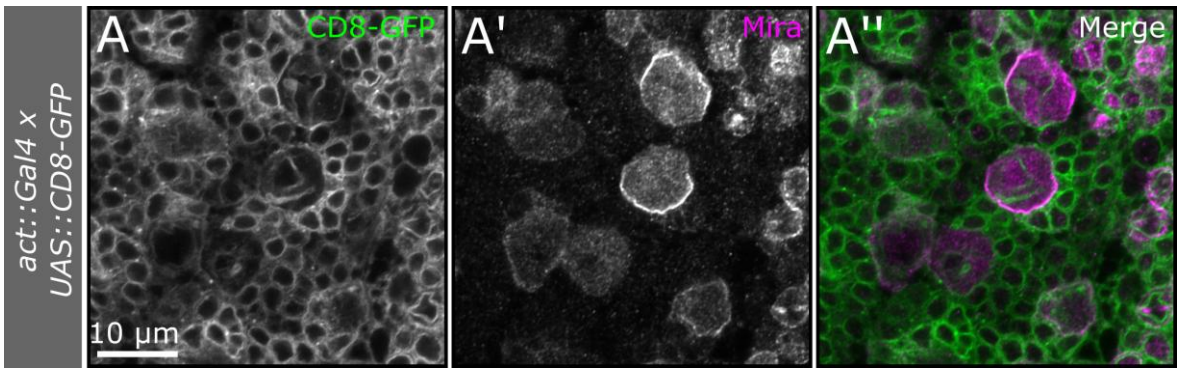

Figure S 6: The *act::Gal4* driver is active in larval neuroblasts

Confocal microscopy pictures of larval brains expressing CD8-GFP (A) driven by *act::Gal4* confirm that the driver is active in NBs. Mira labels NBs.

Table S 3: Domino targets several factors from the temporal transcription factor cascade and Hox genes

Genes from the temporal transcription factor (TF) cascade, also in the optic lobe (OL), and Hox genes (grouped in Antennapedia complex = ANT-C or the Bithorax complex = BX-C) are listed. Genes differentially regulated by Dom are indicated by log2 Foldchange (FC, positive when upregulated in *dom*-RNAi) and false discorey rate (FDR).

Gene	Annotation	Log2FC	FDR	Gene group
hunchback	CG9786	-2.023	2.1E-12	NB TF cascade
Krüppel	CG3340	1.072	4.5E-05	NB TF cascade
pdm1	CG34395	-	-	NB TF cascade
pdm2	CG12287	-	-	NB TF cascade
castor	CG2102	-	-	NB TF cascade
seven up	CG11502	0.377	4E-5	NB TF cascade
grainy head	CG42311	-0.794	3.7E-2	NB TF cascade
homothorax	CG17117	-0.943	6.4E-07	NB TF cascade (OL)
eyeless	CG1464	-	-	NB TF cascade (OL)
sloppy paired 1	CG16738	0.783	1.4E-3	NB TF cascade (OL)
sloppy paired 2	CG2939	0.709	1.5E-2	NB TF cascade (OL)
Dichaete	CG5893	0.524	2.1E-3	NB TF cascade (OL)
tailless	CG1378	0.767	5E-10	NB TF cascade (OL)
Antennapedia	CG1028	-	-	Hox gene (ANT-C)
Deformed	CG2189	-0.593	4.8E-2	Hox gene (ANT-C)
fushi tarazu	CG2047	3.625	1.08E-44	Hox gene (ANT-C)
labial	CG1264	-	-	Hox gene (ANT-C)
proboscipedia	CG31481	-0.492	3.9E-2	Hox gene (ANT-C)
Sex combs reduced	CG1030	-0.555	5E-2	Hox gene (ANT-C)
zerknüllt	CG1046	-	-	Hox gene (ANT-C)
zerknüllt-related	CG1048	-	-	Hox gene (ANT-C)
abdominal A	CG10325	-	-	Hox gene (BX-C)
Abdominal B	CG11648	0.727	1.3E-3	Hox gene (BX-C)
Ultrabithorax	CG10388	-1.055	1.2E-3	Hox gene (BX-C)

Acknowledgements

I am grateful to Prof. Dr. Andreas Wodarz for his support and advice during this project. Thank you for your trust in my decisions and helping me to develop my own ideas and for being there in moments of doubt.

Prof. Dr. Tomas Pieler and PD Dr. Halyna Shcherbata have been very supportive. Your input during thesis committee meetings has been a great help.

I would like to thank the members of my extended committee, Prof. Dr. Matthias Dobbelstein for having an open ear during the lab rotation and also during my PhD time, Dr. Roland Dosch, who has accompanied me since bachelor times and Prof. Dr. Ernst Wimmer, whose tremendous enthusiasm in *Drosophila* greatly contributed to my research interest.

I would like to thank Prof. Dr. Arno Müller, Prof. Dr. Jörg Großhans and Prof. Dr. Thomas Klein for discussing my project with me, the useful suggestions and for providing fly stocks.

I am grateful to Dr. Jens Januschke who was a great teacher for live imaging and my work has definetly benefited from that.

It was very helpful that Vinodh Ilangovan from the lab of Prof. Dr. Gregor Eichele and Dr. Felice Elefant shared fly stocks for Tip60.

I would further like to thank the GGNB for funding me.

Steffen und Kerstin, thank you for the amazing organization of the IMPRS for Molecular Biology. It was so helpful that you always spared some time for any questions and concerns.

I am thankful to everyone from the Göttingen lab and all the adopted lab members of the coffee round for all the good (now old) times in the lab. Especially, I thank Karen and Hamze whose advice was a great guidance particularly in the beginning.

Moving the lab to cologne made me get to know many great people and I would like to express my gratitude to the whole lab for their support and help in the last two years. I want to thank Olaf and Christian for their computer support and never giving up of

convincing me of Mac versus Windows, Jolanta, for being the good soul of the lab, Monique and Soya for their organizational talents and Steffi and Bharath for all the fun times. A big thanks goes to Hong for being an interested and dedicated student. Manu, thank you not only for your help with the project but also going through the first few lonely weeks with me in this big, big city. Ferdinand Antonius, I really enjoy working with you and I appreciate your enthusiasm. Julia, Irina and Theresa, thank you for not only being colleagues but friends, for listening and talking, for shopping and makeup, for celebrating and workout.

Dear friends, you guys are simply amazing. Anita, without you this time would have been much harder and sharing runs over runs and walks over walks with you always comes with the guarantee of happiness for me.
Annika and Kirsten, whenever we meet and should it be just on skype I will surely have a big grin on my face for the rest of the day.
All of you going climbing with me and taking chalk baths with or because of me, I cannot say how much I enjoyed spending these countless hours in the hall with you during the past years: Lena, Juliane, Bernie and Natalie, Manuel and Jens.
Spending the evening in the kitchen with Theresa after a long day in the lab and wishing each other some “Wohlsein” before we “schlafen im Liegen” is always great to relax.

My family has been a great help during my entire studies. I could always rely on you and I will never be able to express my love for you. My grandmother’s care (packages) and all the positive energy from my brother (Let’s build it, I have potatoes, alu foil and a bike!) helped me to keep going.
I am thankful to my beloved parents for raising me to always believe in my abilities and their imperturbable trust in me. Without your encouragement I would not be where I am today and I will always be grateful for that.
Finally and certainly not least, I would like to thank Vivek for being by my side and lighting up my days. You have been there for me to celebrate the highs and help me get through the lows and I appreciate that you always support and have faith in me.

Curriculum Vitae

Katja Rust
* 04.12.1988 in Hanover, Germany

Personal Address
Rochusstraße 67-69
D-50827 Cologne, Germany
Tel.: +49-0170-4340542

Working Address
Molecular Cell Biology/AG Wodarz
Anatomy I
University of Cologne
Kerpener Straße 62, Building 37
D-50937 Cologne, Germany
Tel.: +49-221-478-32278

e-mail: **krust@gwdg.de**
katja.rust_@uk-koeln.de

Education

From Sept 2011 - present	IMPRS M.Sc./PhD program Molecular Biology at the Georg-August-University Göttingen
2013	Master of Science, grade 1.15
Oct 2008 – June 2011	Bachelor course of Biology at the Georg-August-University Göttingen with focus on Molecular Life Sciences, grade 1.4
2008	Graduation at the Hölty-Gymnasium Wunstorf with general qualification for university entrance (Abitur), grade 1.6

Practical Training

Nov 2014 - present	Continuation of PhD Thesis: "The Tip60 chromatin remodeling complex is required for maintenance and polarity of *Drosophila* neural stem cells", Supervisor: Prof. Dr. Andreas Wodarz, University of Cologne
Oct 2012 – Oct 2014	PhD Thesis: "The Tip60 chromatin remodeling complex is required for maintenance and polarity of *Drosophila* neural stem cells", Supervisor: Prof. Dr. Andreas Wodarz, Georg-August-University Göttingen
Aug 2015	Internship for live imaging methods on *Drosophila* neuroblasts with Dr. Jens Januschke, University of Dundee
Okt 2012 – Mar 2013	M.Sc. Thesis: "Analysis of *domino*, a potential Bazooka binding partner in *Drosophila* neuroblasts", Supervisor: Prof. Dr. Andreas Wodarz, Georg-August-University Göttingen

Jan – Feb 2012	Lab rotation: "Analysis of miR-449 and its host gene CDC20B", Supervisor: Prof. Dr. Matthias Dobbelstein, Georg-August-University Göttingen
Feb - April 2012	Lab rotation: "Analysis of the function of potential PAR/Bazooka interactors in *Drosophila* stem cells", Supervisor: Prof. Dr. Andreas Wodarz, Georg-August-University Göttingen
April – June 2012	Lab rotation: "Biology of odiferous defensive stink glands of the red flour beetle *Tribolium castaneum*", Supervisor: Prof. Dr. Ernst Wimmer, Georg-August-University Göttingen
Oct 2010 – April 2011	B.Sc. Thesis: "Analysis of the contribution of SYNCRIP towards RNA-localization in *Xenopus laevis* oocytes", Supervisor: Prof. Dr. Tomas Pieler, Georg-August-University Göttingen

Teaching

Nov 2015 – Aug 2016	Supervision of M.Sc. Thesis: Hong Nhung Nguyen in the M.Sc. program Life and Medical Sciences, University of Bonn "The Function of Chromatin Remodeler *domino* in *Drosophila* Intestinal Stem Cells"
Okt 2013	Supervision of the practical course "*Drosophila* Neurogenesis" in the M.Sc. program Neuroscience, Georg-August-University of Göttingen
Aug – Okt 2013	Supervision of lab rotation: Ninett Wolfram in the M.Sc. program Developmental, Neural and Behavioral Biology, Georg-August-University of Göttingen "Functional analysis of Skittles in *Drosophila* neuroblasts"
April 2011	Supervision of practical course: Biochemistry for medical students, Georg-August-University of Göttingen

Awards

Jan 2013 – Sept 2016	Excellence Stipend from the Göttingen Graduate School for Neurosciences, Biophysic und Molecular Biosciences (GGNB)
Oct 2011 – Sept 2012	International Max Planck Research School support

Talk

Sept 2016	"The Tip60 chromatin remodeler complex interacts with Myc to maintain *Drosophila* neural stem cells" German *Drosophila* Meeting, 2016, Cologne, Germany

Poster presentations

Sept 2015	"The chromatin remodeler Domino is required for maintenance and polarity of *Drosophila* neural stem cells", Ernst Klenk Symposium in Molecular Medicine, Cologne, Germany
Jan 2015	"The chromatin remodeler Domino is required for maintenance and polarity of *Drosophila* neural stem cells", Joint Meeting of the German and French Societies of Developmental Biologists, Nuremberg, Germany
Sept 2014	"Analysis of the chromatin remodeler Domino in *Drosophila* neural stem cells", Horizons in Molecular Biology, Göttingen, Germany
Mar 2014	"Analysis of the chromatin remodeler Domino in *Drosophila* neural stem cells", International Meeting of the German Society for Cell Biology (DGZ), Regensburg, Germany
Mar 2013	"A potential new Bazooka binding partner is required for asymmetric stem cell division", International Joint Meeting of the German Society for Cell Biology (DGZ) and the German Society for Developmental Biology (GfE), Heidelberg, Germany

Transferable skills

2013	Organization of the 10th Horizons in Molecular Biology
2013	Organization of the GZMB (Göttingen Center for Molecular Biosciences) Symposium